



Titre: Analyse biomécanique de l'articulation de genou durant la bipédie humaine
Title:

Auteur: Malek Adouni
Author:

Date: 2014

Type: Mémoire ou thèse / Dissertation or Thesis

Référence: Adouni, M. (2014). Analyse biomécanique de l'articulation de genou durant la bipédie humaine [Ph.D. thesis, École Polytechnique de Montréal]. PolyPublie.
Citation: <https://publications.polymtl.ca/1458/>

 **Document en libre accès dans PolyPublie**
Open Access document in PolyPublie

URL de PolyPublie: <https://publications.polymtl.ca/1458/>
PolyPublie URL:

Directeurs de recherche: Aboulfazl Shirazi
Advisors:

Programme: Génie mécanique
Program:

UNIVERSITÉ DE MONTRÉAL

ANALYSE BIOMÉCANIQUE DE L'ARTICULATION DE GENOU DURANT
LA BIPÉDIE HUMAINE

MALEK ADOUNI

DÉPARTEMENT DE GÉNIE MÉCANIQUE
ÉCOLE POLYTECHNIQUE DE MONTRÉAL

THÈSE PRÉSENTÉE EN VUE DE L'OBTENTION
DU DIPLÔME DE PHILOSOPHIAE DOCTOR
(GÉNIE MÉCANIQUE)

JUILLET 2014

UNIVERSITÉ DE MONTRÉAL

ÉCOLE POLYTECHNIQUE DE MONTRÉAL

Cette thèse intitulée:

ANALYSE BIOMÉCANIQUE DE L'ARTICULATION DE GENOU DURANT
LA BIPÉDIE HUMAINE

présentée par : ADOUNI Malek

en vue de l'obtention du diplôme de : Philosophiae Doctor

a été dûment accepté par le jury d'examen constitué de :

M. LAKIS Aouni A, Ph.D, président

M. SHIRAZI-ADL Aboulfazl, Ph.D, membre et directeur de recherche

M. SAVARD Pierre, Ph.D, membre

M. MOGLO Kodjo, Ph.D, membre

DÉDICACE

À mes parents

À ma femme et mon fils

À mes frères et sœurs

À toutes les personnes qui j'aime

À mes amis

REMERCIEMENTS

Je voudrais exprimer ma reconnaissance à tous ceux qui m'ont donné la possibilité pour accomplir ce travail.

Mes premiers remerciements vont d'abord à mon directeur de thèse, le professeur A. Shirazi, qui a été l'initiateur de ce projet. Je le remercie, sincèrement, pour les fructueuses discussions que nous avons eues et pour tout l'appui qu'il a manifesté tout au cours de mon doctorat.

Je remercie également la mission universitaire de Tunisie en Amérique du Nord (MUTAN) et le conseil de recherches en sciences naturelles et en génie (CSRNG) pour leurs apports financiers à la réalisation de ladite étude.

Je remercie également Monsieur Aouni Lakis, professeur au département de génie mécanique, Monsieur Pierre Savard, professeur à l'Institut de génie biomédical et Monsieur Kodjo Moglo, professeur adjoint au département de génie mécanique Royal Military College of Canada, pour avoir accepté de faire partie de mon jury d'examen de thèse.

Je voudrais remercier M.Z. Bendjaballah, K.E. Moglo, W. Mesfar et R Shirazi, pour leurs efforts antérieurs dans le développement du modèle de genou.

J'exprime aussi une grande gratitude à tous les membres de section de mécanique appliquée, particulièrement, Hafedh Marouane, Zakaria El Ouaid, Ali Shahvarpour, Stephen okoth olala.

RÉSUMÉ

Les activités de la vie quotidienne comme la marche et la montée d'escaliers imposent des charges et des mouvements relativement importants sur l'articulation du genou humain. Cette charge mécanique augmente dans de nombreuses tâches professionnelles et récréatives entraînant des blessures et des dégénérescences dans les ligaments, les ménisques, le cartilage et l'os. Toute faiblesse ou modification par rapport à la structure native qui conduit à la dégénérescence dans l'un de ces composants influencent la réponse de l'ensemble du joint et augmente le risque d'autres perturbations. Les gestions efficaces, non-opératoires et post-opératoires des désordres affectant le joint du genou humain exigent une bonne connaissance des distributions des contraintes et des déformations dans les différentes composantes constituant le joint, dans les situations intacte et altérée. Ces valeurs, à leur tour, dépendent fortement non seulement des charges extérieures et des forces d'inertie, mais aussi des activités musculaires à travers le joint. De ce fait la précision dans l'estimation des forces musculaires a une incidence directe sur la fiabilité des contraintes et des déformations prédites dans le joint. Les mesures directes *in vivo* des contraintes tissulaires et des forces musculaires restent invasives. Par contre la modélisation numérique est reconnue comme un outil complémentaire indispensable pour estimer plusieurs variables d'intérêt. Ainsi, les difficultés techniques rencontrées dans les mesures de mouvements et la considération plus réaliste des charges physiologiques rendent les tests *in vitro* également limités surtout quand on regarde des variables internes comme les contraintes et les déformations dans les ligaments et le cartilage.

Pour atteindre ces objectifs, un modèle éléments finis itératif, contrôlé par les données cinématique et cinétique collectées durant la marche humaine, qui tient compte des structures passives du joint du genou et l'ensemble de la musculature active de l'extrémité inférieure a été utilisé. Dans ce modèle les articulations de la hanche et de la cheville ont été considérées comme des joints rigides simplement sphériques (3D pour la hanche et 2D pour la cheville), alors que l'articulation de genou est représentée sous la forme d'un modèle déformable d'éléments finis non linéaire. Les cartilages et les ménisques constituant le joint ont été modélisés comme des structures composites formées d'une matrice hyper-élastique renforcée par des réseaux non-homogènes de fibre de collagène avec des propriétés mécanique non linéaires. Les ligaments présentant des propriétés non linéaires et des déformations initiales distinctes. Des mesures

cinématique et cinétique in vivo collectées chez des sujets asymptomatiques et des sujets atteints de l'ostéoarthrite sévère du genou, pendant la phase d'appui sont utilisées pour modéliser séparément les deux groupes. Les analyses sont effectuées pour six instances de temps correspondant au début 0% (initiation de la phase de réception), 5%, 25%, 50%, 75% et 100% (fin de la phase de propulsion), de la phase d'appui. L'estimation des forces musculaires passe par une technique d'optimisation en résolvant les équations d'équilibre obtenues à chaque niveau de la phase d'appui. Le minimum de la somme des contraintes musculaires élevée à la puissance 3, a été considéré comme la fonction objectif dans le problème d'optimisation. Des contraintes d'inégalités obligeant les contraintes musculaires à demeurer supérieures aux contraintes passives et inférieures aux contraintes maximales, complètent le problème d'optimisation. La réponse de l'articulation du genou est ensuite analysée par la réactualisation des forces musculaires qui équilibrent le moment induit par les forces de poids et de réaction du pied, ceci va faire tendre ce moment, au niveau du joint, vers zéro, après un nombre d'itérations bien défini. Notre investigation initiale s'est concentrée sur la réponse du joint du genou humain dans le cas de la marche à cadence normale sur des sujets sains et l'effet de la modélisation globale et locale du membre inférieur. Ensuite, les mêmes étapes d'analyse ont été considérées pour étudier l'effet de l'ostéoarthrite sévère sur les réponses active et passive du joint du genou. Un volet consiste à étudier la réponse du genou à 50% de la phase d'appui sous l'effet d'un changement de rotation et de moment dans le plan frontal. Cette dernière servira, à minimiser la charge supportée par le plateau tibial médial durant la phase d'appui lors de la marche. À noter que cette approche est originale et elle est très peu présente dans la littérature. Finalement, les contradictions rapportées et le faible nombre d'études dans la littérature, ont motivé notre intérêt pour l'étude de la relation entre le muscle *gastrocnemius* et le ligament croisé antérieur (LCA) durant la marche et durant une contraction isolée de ce muscle sur le joint tibiofemoral en flexion.

Avec la technique d'optimisation locale, un modèle où on néglige les équations d'équilibre de la hanche, une prédiction remarquable a été obtenue pour les modifications subies par les forces musculaires et la réponse passive du joint du genou durant la phase d'appui. Ces prédictions concordent avec les résultats des études antérieures sur la marche humaine. Effectuer les analyses sur 6 périodes du début à la fin de la phase d'appui (0%, 5%, 25%, 50%, 75% et 100%) montre une activité maximale de trois groupes musculaires principaux entourant le joint à 5% pour les muscles du *Ischio-jambiers*, à 25% pour le quadriceps et à 75% pour le muscle

jumeau. Le ligament croisé antérieur a atteint son maximum de 343 N à 25% de la phase d'appui, et cette valeur a diminué par la suite. Les forces de contact atteignent leurs maximums de 1908 N, 2467 N et 2238 N à 5%, 25% et 75% de la phase d'appui, respectivement, où la majorité de la charge passe à travers le compartiment médial causant une déformation et une concentration de contraintes plus importante par rapport au compartiment latéral. Les valeurs maximales de pression de contact sont égales à 8.1 MPa et 7.5 MPa à 25% et 75% de la phase d'appui, respectivement. Cependant, l'inclusion de l'équilibre de l'articulation de la hanche dans l'optimisation, le long des articulations du genou et de la cheville, a légèrement influencé les réponses musculaires globales autour de l'articulation du genou ($< 10\%$). En conséquence, les différences sont encore plus petites entre les forces ligamentaires, les forces de contact, et les contraintes/déformations du cartilage au cours de la phase d'appui durant la marche. Par contre, la répartition des forces totales entre les composantes musculaires uni-et bi-articulaires dans les quadriceps et les *Ischio-jambiers*, s'est considérablement altérée durant la phase d'appui pour assurer un équilibre simultané des deux articulations (hanche et genou).

En ce qui concerne la comparaison entre les patients atteints de l'ostéoarthrite sévère du genou par rapport aux sujets normaux, les forces musculaires ont peu baissé à toutes les périodes sauf à 50% de la phase d'appui et ceci en accord général avec les travaux antérieurs. La force dans le ligament croisé antérieur est restée presque inchangée. Les forces et les contraintes de contact diminuent en moyenne d'environ 25%. Les modifications des propriétés des matériaux dues à l'ostéoarthrite ont eu un effet négligeable sur les forces musculaires, mais ont augmenté les aires de contact et les déformations du cartilage; entraînant une diminution des pressions de contact maximale et moyenne. Par exemple, la pression moyenne tibiofemorale diminue à 5% de la phase d'appui de 2.5 MPa à 1.3 MPa après la diminution de la rigidité des cartilages et des ménisques. Les réductions des contraintes moyenne et maximale du contact ainsi que l'augmentation des déformations des tissus cartilagineux et le transfert de charge via les ménisques sont partiellement dues aux changements cinétique-cinématique de la marche et aux détériorations des propriétés matérielles du cartilage chez le sujet atteint de l'ostéoarthrite sévère.

L'altération de la rotation du joint du genou dans le plan frontal de $\pm 1.5^\circ$ ou le moment d'adduction de $\pm 50\%$ par rapport à son état de référence (1.6° et 17 Nm) à 50% de la phase d'appui influencent considérablement la réponse biomécanique du joint. La diminution de l'angle d'adduction de 1.5° augmente considérablement les forces sur le quadriceps et les *Ischio-*

jambiers de 30 N et 110 N, respectivement. Par contre une diminution de l'angle d'adduction a fait diminuer les forces dans les muscles ci-mentionnés dans presque les mêmes proportions. Ces forces musculaires suivent de près la tendance de la variation du moment d'adduction. Les forces de contact tibial sont restées plus grandes toujours sur le plateau médial. Le rapport des forces de contact entre les deux plateaux, médial et latéral, a été considérablement altéré avec le changement de l'angle d'adduction. En effet ce rapport augmente grandement de 8.8 à 90 avec l'augmentation de l'angle d'adduction et diminue de 8.8 à 1.6 quand cet angle diminue. La variation du moment d'adduction a faiblement altéré le rapport des forces entre les deux plateaux d'un écart inférieur à 1. En conséquence, si l'objectif est de diminuer la force de contact interne, indépendamment de la charge latérale, une baisse de la rotation de l'adduction est beaucoup plus efficace qu'une réduction du moment d'adduction. L'altération de la résistance passive non linéaire du joint du genou, provoquée par le changement de l'angle d'adduction, peut expliquer la variation du comportement biomécanique du joint du genou. Ces résultats expliquent la faible corrélation entre le moment d'adduction et le chargement du compartiment médial lors de la marche et ceci suggère que la répartition de la charge interne est dictée par la rotation d'adduction du joint du genou.

Les altérations de l'activité du muscle *jumeau* à la fin de la phase d'appui de -36% ou de +26% influencent nettement les forces des muscles du *Ischio-jambiers*. Le muscle *jumeau* agit comme une composante antagoniste au ligament croisé antérieur en augmentant sensiblement sa force de 271 à 331 N. Nos simulations sous contraction isolée du muscle *jumeau* ont confirmé ces résultats pour tous les angles de flexion. En particulier, la force du ligament croisé antérieur a augmenté notablement avec l'augmentation des forces du muscle jumeau même à des angles de flexion très élevés. Une tendance qui n'était pas présente, même dans l'activité des quadriceps reconnue également comme un antagoniste du ligament croisé antérieur. Les muscles *Ischio-jambiers* et le muscle *jumeau* sont deux fléchisseurs de l'articulation du genou et jouent des rôles opposés soit respectivement la protection et le chargement du ligament croisé antérieur. De l'autre côté, le fait de savoir que le muscle *jumeau* est un antagoniste du ligament croisé antérieur doit contribuer à la prévention efficace des blessures post-opératoires, durant la réhabilitation après une reconstruction de ce ligament.

Un nouveau modèle d'éléments finis itératif contrôlé par des données expérimentales cinématiques et qui tient compte de la synergie entre les structures passives et la musculature

active de l'articulation du genou a été utilisée pour la première fois pour déterminer les forces musculaires, les contraintes et les déformations tissulaires simultanément au cours de la marche. Nos analyses transitoires sont validées par le faible temps d'exécutions des activités quotidiennes comme la marche. Les prédictions sur la cinématique articulaire, les forces ligamentaires et les forces et pressions de contact concordent avec les résultats rapportés dans la littérature. Les prévisions actuelles ont des implications importantes dans l'évaluation et le traitement appropriés des troubles de l'articulation du genou afin d'éviter non seulement d'autres blessures mais aussi de retrouver un fonctionnement proche de la normale pour l'ensemble du joint.

ABSTRACT

Activities of daily living such as walking and stair climbing impose relatively large loads and movements on the human knee joint. This mechanical burden increases in many occupational and recreational tasks causing injuries and degenerations in joint ligaments, menisci, cartilage and bone. Any failure, degeneration or alteration in one of these components influences the response of the entire joint and likely increases the risk of further perturbations. Effective preventive and conservative/surgical managements of joint disorders depend hence on a sound knowledge of stress and strain distributions in various components under both intact and altered conditions. These values, in turn, are heavily dependent not only on external loads and inertial forces but on muscle activities across the joint. As such, accuracy in estimation of muscle forces has a direct bearing on the reliability of stresses and strains. Since direct *in vivo* measurements of tissue stresses and muscle forces remain invasive, computational modeling is recognized as a vital complementary tool to estimate multiple variables of interest. Due to technical difficulties in measurements and consideration of physiological loads and motions, *in vitro* testing is also limited especially when looking for cartilage/meniscus stresses/strains and ligament forces.

Towards these objectives, an iterative kinematics-driven FE model that accounts for the passive structures of the knee joint and active musculature of the lower extremity is employed. This model incorporates the hip as 3D and the ankle as 2D spherical joints whereas the knee is represented as a complex FE model with nonlinear depth-dependent fibril-reinforced cartilage and menisci, ligaments with distinct nonlinear properties and initial strains, patellofemoral and tibiofemoral joints. Based on reported *in vivo* measurements, hip/knee/ankle joint rotations/moments and ground reaction forces at foot during the gait stance phase collected in asymptomatic subjects and subjects with severe knee OA are used to separately model both groups. Analyses are performed at 6 time instances corresponding to beginning 0% (heel strike), 5%, 25%, 50%, 75% and 100% (toe off) of the stance phase. At each stance period, muscle forces at the hip, knee and ankle are predicted using static optimization (sum of cubed muscle stresses) with moment equations as constraints (3 at knee, 3 at hip, and 1 at ankle). The Knee joint response is subsequently analyzed with updated muscle forces as external loads and iterations at deformed configurations continue till convergence is reached. The relative effects of the consideration of moment equations at the hip joint alongside those at the knee and ankle joints on estimated knee joint muscle forces as well as contact forces and internal stresses in ligaments,

cartilage layers, and menisci during the stance phase of gait in asymptomatic subjects were investigated. Apart from changes in input kinematics/kinetics, the OA model accounted also for likely alterations in material properties associated with the disease. The validity of certain reported strategies used in vivo to decrease the loading in the medial plateau during stance phase of gait by reducing knee adduction moment were also tested and compared with altered knee adduction angle. Finally, the effect of changes in the gastrocnemius activations, during gait and isolated contraction with free flexion, on the knee joint biomechanics and especially anterior cruciate ligament loading was also studied.

With local optimization, where moment equilibrium equations at the hip joint are neglected, predictions confirm that muscle forces and joint response alter substantially during the stance phase. Predictions are in general agreement with results of earlier studies. Performing the analyses at 6 periods from beginning to the end (0%, 5%, 25%, 50%, 75% and 100%), hamstrings forces peaked at 5%, quadriceps forces at 25% whereas gastrocnemius and bicep femoris forces at 75%. Anterior cruciate ligament force reached its maximum of 343 N at 25% and decreased thereafter. Contact forces reached maximum of 1908 N, 2467 N and 2238 N at 5%, 25% and 75% periods respectively, with the medial compartment carrying a major portion of load and experiencing larger relative movements and cartilage strains. Contact pressures reached their peak on the medial plateau of 8.1 MPa and 7.5 MPa at 25% and 75% period, respectively. Much smaller contact stresses were computed at the patellofemoral joint. However, global optimization indicates that inclusion of the hip joint in the optimization along the knee and ankle joints only slightly (<10%) influences total forces in quadriceps, lateral hamstrings and medial hamstrings. As a consequence, even smaller differences are found in predicted ligament forces, contact forces/areas, and cartilage stresses/strains during the stance phase of gait. The distribution of total forces between the uni- and bi-articular muscle components in quadriceps and in lateral hamstrings, however, substantially alter at different stance phases.

In OA patients compared to normal subjects, muscle forces dropped nearly at all stance periods except the mid-stance. Force in the anterior cruciate ligament remained overall the same. Total contact forces-stresses overall decreased by about 25%. Alterations in properties due to OA had negligible effects on muscle forces but increased contact areas and cartilage strains and reduced contact pressures. For example, the average contact pressure noticeably dropped from 2.5 MPa to 1.3 MPa at 5% stance. Reductions in contact stresses as well as increases in tissue

strains and transfer of load via menisci are partly due to the altered kinetics-kinematics of gait and partly due to deteriorations in cartilage-menisci properties in OA patients.

Changes in the knee adduction rotation of $\pm 1.5^\circ$ or the knee reference adduction moment of $\pm 50\%$ substantially affect the knee joint passive and active response at mid-stance of gait. Quadriceps and hamstrings forces substantially increased as adduction rotation dropped and diminished as adduction rotation increased and followed the trend in external adduction moment. Tibial contact forces remained larger always on the medial plateau. The ratio of the contact forces on the medial plateau to that on the lateral plateau was found unaffected by changes in moments but substantially increased from 8.8 to 90 with greater adduction rotation and diminished with smaller adduction rotation yielding a more uniform distribution. If the aim is to diminish the medial contact force irrespective of the lateral load, a drop in adduction rotation is much more effective than reducing the adduction moment. Substantial role of changes in adduction rotation is due to the associated alterations in joint nonlinear passive resistance. These findings explain the poor correlation between knee adduction moment and tibiofemoral compartment loading during gait suggesting that the internal load partitioning is dictated by the joint adduction rotation.

The effect of different gastrocnemius activation levels on the knee joint biomechanics in general and ACL forces in particular was investigated. In the lower extremity model in gait at 75% stance period, changes in gastrocnemius activity by +36% or -26% primarily altered forces in hamstrings with little effects on quadriceps. Gastrocnemius acted as ACL antagonist by substantially increasing its force. Simulations under isolated contraction of gastrocnemius confirmed these findings at all flexion angles. In particular, ACL force (anteromedial bundle) substantially increased with gastrocnemius activity at larger knee flexion angles. While hamstrings and gastrocnemius are both knee joint flexors, they play opposite roles in respectively protecting or loading ACL. Although the quadriceps is also recognized as antagonist of ACL, at larger joint flexion and in contrast to quadriceps, activity in gastrocnemius substantially increased ACL forces. The fact that gastrocnemius is an antagonist of ACL should help in effective prevention of ACL injuries, coping with an ACL injury and post ACL reconstruction periods.

To our knowledge no previous study investigated the detailed knee joint passive-active response in gait. Novel iterative kinematics-driven FE model that accounts for the synergy between passive structures and active musculature of the knee joint was used to determine muscle

forces and tissue stresses/strains during the gait. The predictions on joint kinematics, ligament forces and contact areas/pressures were in good agreement with reported results in the literature. The current predictions have important implications in proper evaluation and treatment of knee joint disorders in order to not only prevent further injuries and degenerations but to regain a near-normal function of the entire joint.

TABLE DES MATIÈRES

DÉDICACE.....	III
REMERCIEMENTS	IV
RÉSUMÉ.....	V
ABSTRACT	X
TABLE DES MATIÈRES	XIV
LISTE DES FIGURES.....	XIX
LISTE DES SIGLES ET ABRÉVIATIONS	XXVIII
LISTE DES ANNEXES.....	XXX
CHAPITRE 1 INTRODUCTION.....	1
CHAPITRE 2 ANATOMIE ET REVUE DE LA LITTÉRATURE.....	3
2.1 Anatomie fonctionnelle.....	3
2.1.1 Cartilage	4
2.1.2 Ménisque	5
2.1.3 Ligaments.....	6
2.1.4 Muscles.....	7
2.2 Revue de la Littérature	9
2.2.1 Études Expérimentales	9
2.2.2 Études Mathématiques et Numériques.....	12
2.2.3 Analyses de la bipédie humaine	16
2.3 Objectifs	24
2.4 Plan de thèse.....	26
CHAPITRE 3 ARTICLE 1: COMPUTATIONAL BIODYNAMICS OF HUMAN KNEE JOINT IN GAIT: FROM MUSCLE FORCES TO CARTILAGE STRESSES	28

3.1	Abstract	29
3.2	Introduction	29
3.3	Methods	31
3.3.1	Finite Elements Model	31
3.3.2	Material Properties	32
3.3.3	Muscle Force Estimation	33
3.3.4	Loading, Kinematics and Boundary Conditions	34
3.4	Results	35
3.5	Discussion	36
3.6	Acknowledgement	39
3.7	References	40
CHAPITRE 4 ARTICLE 2: CONSIDERATION OF EQUILIBRIUM EQUATIONS AT THE HIP JOINT ALONGSIDE THOSE AT THE KNEE AND ANKLE JOINTS HAS MIXED EFFECTS ON KNEE JOINT RESPONSE DURING GAIT		52
4.1	Abstract	53
4.2	Introduction	53
4.3	Methods	55
4.4	Results	56
4.5	Discussion	57
4.6	Acknowledgements	59
4.7	References	60
CHAPITRE 5 ARTICLE 3: EVALUATION OF KNEE JOINT MUSCLE FORCES AND TISSUE STRESSES-STRAINS DURING GAIT IN SEVERE OA VERSUS NORMAL SUBJECTS		69
5.1	Abstract	70

5.2	Introduction	70
5.3	Methods	73
5.3.1	Finite Elements Model	73
5.3.2	Material Properties	74
5.3.3	Muscle Force Estimation	75
5.3.4	Loading, Kinematics and Boundary Conditions	76
5.4	Results	76
5.5	Discussion	78
5.6	Acknowledgements	82
5.7	References	83
CHAPITRE 6 ARTICLE 4: PARTITIONING OF KNEE JOINT INTERNAL FORCES IN GAIT IS DICTATED BY THE KNEE ADDUCTION ANGLE AND NOT BY THE KNEE ADDUCTION MOMENT		98
6.1	Abstract	99
6.2	Introduction	99
6.3	Methods	102
6.3.1	Finite Elements Model	102
6.3.2	Muscle Force Estimation	103
6.3.3	Loading, Kinematics and Boundary Conditions	103
6.4	Results	104
6.5	Discussion	105
6.6	Acknowledgement	109
6.7	References	110

CHAPITRE 7	ARTICLE 5: GASTROCNEMIUS ACTS AS ACL ANTAGONIST: ANALYSIS OF THE ROLE OF GASTROCNEMIUS ACTIVATION ON KNEE BIOMECHANICS IN LATE STANCE AND IN FLEXION	124
7.1	Abstract	125
7.2	Introduction	125
7.3	Methods.....	127
7.4	Results	130
7.4.1	Gait Simulation	130
7.4.2	Knee Joint Simulations.....	130
7.5	Discussion	131
7.6	Acknowledgements	134
7.7	References	135
CHAPITRE 8	DISCUSSION	148
8.1	Généralités.....	148
8.2	Évaluation du modèle.....	149
8.2.1	Comportements structurel et mécanique	149
8.3	Simulations.....	151
8.3.1	Données cinématiques et cinétiques.....	151
8.3.2	Transformation du système d'axe	152
8.3.3	Détermination des forces musculaires.....	152
8.3.4	Simulations et études paramétriques.....	153
8.4	Analyse des résultats	154
8.4.1	Forces musculaires	154
8.4.2	Forces ligamentaires.....	159
8.4.3	Force, pression et aire de contact	161

8.4.4	Modèle raffiné et non raffiné	164
8.4.5	Limitations des modèles.....	165
CHAPITRE 9 CONCLUSION ET RECOMMANDATIONS		167
9.1	Conclusion.....	167
9.2	Recommandations.	169
BIBLIOGRAPHIE		171
ANNEXES		194

LISTE DES FIGURES

Figure 1-1: Principaux éléments constituant l'articulation du genou humain : (a) jointure Tibio-fémorale, (b) cartilages articulaires, (c) ménisques, (d) jointure patello-fémorale.	4
Figure 1-2: Courbe contrainte-déformation pour les ligaments principaux, ligaments croisé antérieur (ACL) et postérieur (PCL), ligaments collatérales médial (MCL) et latéral (LCL), et le tendon rotulien(PT) (Butler et al., 1986).	7
Figure 1-3: (a) Présentation du mécanisme extenseur, Rotule, Tendon et Quadriceps, (b) Présentation du muscle du <i>gastrocnemius</i> , (c) Présentation du muscle du <i>hamstring</i>	8
Figure 1-4: Présentation des orientations des muscles du quadriceps selon les trois modèles, anatomique, mathématique et de l'angle Q (Sakai et al., 1996).	8
Figure 1-5: Représentation de la géométrie du modèle par éléments finis de Blankevoort et Huiskes .(1991a). Ce modèle inclut les condyles fémoraux, les surfaces tibiales ainsi que les ligaments principaux.	13
Figure 1-6: Le modèle fémoro-patellaire de Heegaard et al.(1995).	15
Figure 1-7: (a) Maillages tridimensionnelles des structures osseuses, (b) Maillages tridimensionnelles de tissus mou (cartilage, ménisques, ligaments)(Ramaniraka et al., 2005).	16
Figure 1-8: Représentation schématique du cycle de marche et de ses principales phases et sous-phases. (www.observatoire-du-mouvement.com).....	17
Figure 1-9: Mouvements angulaires dans le plan sagittal de la hanche, du genou et de cheville chez des individus normaux sur un cycle de marche unique ; <i>OT</i> , <i>opposite toe off</i> ; <i>HR</i> . <i>heel rise</i> ; <i>OI</i> , <i>opposite initial contact</i> ; <i>TO</i> , <i>toe off</i> ; <i>FA</i> , <i>feet adjac TV</i> , <i>tibia vertical</i> (Whittle, 1996).	18
Figure 1-10: Force de réaction de sol mesurée par instrument expérimental (plate-forme de force) et normalisée par le poids du corps durant la phase d'appui chez des individus sains. (Hunt et al., 2001) , (+ / postérieur et latéral).	20

Figure 1-11: (a) les variations des forces et des moments dans l'articulation de genou durant la marche, (b) le système de coordonnées pour le plateau tibial instrumenté (Kutzner et al., 2010).....22

Figure 2-1: Knee joint FE model; tibiofemoral (TF) and patellofemoral (PF) cartilage layers, menisci, patellar Tendon (PT), quadriceps, hamstrings and gastrocnemius muscles (a), TF and PF cartilage layers, menisci and joint ligaments (b). Crosses indicate the reference points (RP) representing rigid bony structures that are not shown. Quadriceps components are vastus medialis obliquus (VMO), rectus femoris (RF), vastus intermedius medialis (VIM), and vastus lateralis (VL). Hamstring components include biceps femoris (BF), semimembranosus (SM), and the TRIPOD made of Sartorius (SR), gracilis (GR), and semitendinosus (ST). Gastrocnemius components are gastrocnemius medial (GM) and gastrocnemius lateral (GL). Tibialis posterior and Soleus muscles of the ankle joint are not shown. Joint ligaments include lateral patellofemoral (LPFL), medial patellofemoral (MPFL), anterior cruciate (ACL), posterior cruciate (PCL), lateral collateral (LCL), and medial collateral (MCL).....44

Figure 2-2: Knee joint rotations (a) and moments (b) reported as mean of asymptomatic subjects during the stance phase of gait (Astefan et al., 2008a) as well as vertical, anterior, and lateral ground reaction force components (c) reported during the stance phase of gait on asymptomatic subjects (Hunt et al., 2001), and mean normalized surface EMG data (d) recorded in 7 different knee joint muscles (Astefan, 2007). For muscle abbreviations, see the caption of Fig. 1. Six instances corresponding to beginning (heel strike, HS 0%), 5%, 25%, 50%, 75% and end (toe off, TO 100%) of the stance phase are indicated. Note that moments and forces are normalized to the BW=606.6 N of the female subject.....45

Figure 2-3: Predicted Muscle and TP forces at different stance phases (see Fig. 1 caption for muscle abbreviations). Ratios to body weight are given on the right axis.....46

Figure 2-4: Predicted Ligaments forces at different stance phases (see Fig. 1 caption for ligaments abbreviations). (+) Results found in the model with less-refined mesh and isotropic representation of cartilage layers. Ratios to body weight are given on the right axis.....47

Figure 2-5: Predicted total TF (covered: via menisci, uncovered: via cartilage, M: medial plateau, L: lateral) and PF contact forces at different stance phases. Ratios to body weight are given on the right axis.	48
Figure 2-6: Predicted total TF (M: Medial and L: Lateral) and PF contact areas at different stance phases. (+) Results found in the model with less-refined mesh and isotopic representation of cartilage layers.....	49
Figure 2-7: Predicted contact pressure at articular surface of lateral and medial tibial plateaus at different stance phases. Note that a common legend is used for ease in comparisons.	50
Figure 2-8: Maximum (tensile) principal strain in solid matrix at the superficial and lowermost layers of lateral and medial tibial cartilage at 25% and 75% stance phases. Note that a common legend is used for ease in comparisons.	51
Figure 3-1: (A) Schematic diagram showing the 34 muscles incorporated into the lower extremity model (taken from OpenSim(Delp et al., 2007)), framed ones indicate muscles added in this study versus the earlier one (Adouni et al., 2012). Quadriceps components are vastusmedialisobliquus (VMO), rectus femoris (RF), vastusintermidusmedialis(VIM), and vastuslateralis (VL). Hamstring components include biceps femoris long head (BFLH), biceps femoris short head (BFSH), semimembranous(SM), and the TRIPOD made of sartorius (SR), gracilis (GA), and semitendinosus (ST). Gastrocnemius components are gastrocnemius medial (GM) and gastrocnemius lateral (GL). Tibialis posterior(TP) and soleus (SO) muscles are uni-articular ankle muscles. Hip joint muscles (not all shown) include adductor, long (ADL), mag (3 components ADM) and brev (ADB); gluteus max (3 components GMAX), med (3 components GMED) and min (3 components GMIN); iliacus (ILA), iliopsoas (PSOAS), quadriceps femoris; pectineus (PECT); tensor fascia lata (TFL); periformis. (B) Knee FE model; tibiofemoral (TF) and patellofemoral (PF) cartilage layers, menisci, patellar Tendon (PT). Joint ligaments include lateral patellofemoral (LPFL), medial patellofemoral (MPFL), anterior cruciate (ACL), posterior cruciate (PCL), lateral collateral (LCL), and medial collateral (MCL). Reference points (RP) for tibia and patella bony rigid bodies are also shown.....	63

- Figure 3-2: Predicted muscle forces at different stance phases. Earlier results (Adouni et al, 2012) accounting for the knee and ankle equations only (K + A) are also shown for comparison (see Fig. 1 for muscle abbreviations).64
- Figure 3-3: Predicted muscle forces in bi-articular (BFLH, RF, ST, SR, GA) and uni-articular (BFSH, VIM) components at different phases of stance. Earlier results (Adouni et al, 2012) accounting for the knee and ankle equations only (K + A) are also shown for comparison (see Fig. 1 for muscle abbreviations).65
- Figure 3-4: Predicted Ligament forces at different stance phases. Earlier results (Adouni et al, 2012) accounting for the knee and ankle equations only (K + A) are also shown for comparison (see Fig. 1 for ligament abbreviations).66
- Figure 3-5: Predicted total TF (as well as individual components at medial and lateral plateaus) and PF contact forces. Earlier results (Adouni et al, 2012) accounting for the knee and ankle equations only (K + A) are also shown for comparison.67
- Figure 3-6: Predicted contact pressure at articular surfaces of lateral and medial tibial plateaus at 25% and 75% of stance phase. Earlier results (Adouni et al, 2012) accounting for the knee and ankle equations only (K + A) are also shown for comparison. Note that a common legend is used for ease in comparisons.68
- Figure 4-1: (A) Schematic diagram showing the 34 muscles incorporated into the lower extremity model (taken from OpenSim(Delp et al., 2007)). Quadriceps: vastus medialis obliquus (VMO), rectus femoris (RF), vastus intermedius medialis (VIM) and vastus lateralis (VL); Hamstrings: biceps femoris long head (BFLH), biceps femoris short head (BFSH), semimembranous (SM) and TRIPOD made of sartorius (SR), gracilis (GA) and semitendinosus (ST); Gastrocnemius: medial (MG) and lateral (LG). Tibialis posterior (TP) and soleus (SO) muscles are uni-articular ankle muscles. Hip joint muscles (not all shown) include adductor, long (ADL), mag (3 components ADM) and brev (ADB); gluteus max (3 components GMAX), med (3 components GMED) and min (3 components GMIN), iliacus (ILA), iliopsoas (PSOAS), quadriceps femoris, pectineus (PECT), tensor fascia lata (TFL), periformis. (B) Knee FE model; tibiofemoral (TF) and patellofemoral (PF) cartilage layers, menisci and patellar Tendon (PT). Joint ligaments: lateral/medial patellofemorals

(LPFL/MPFL), anterior/posterior cruciates(ACL/PCL) and lateral collateral/medial collaterals (LCL/MCL).	89
Figure 4-2: Knee joint rotations (R) and moments (M)reported as mean of asymptomatic (N)and severe OA (OA)subjects during the stance phase of gait.(Astephen, 2007) (a) Felxion/Extension,(b) Adduction/Abduction and(c) Internal/External, (d) vertical, anterior and lateral GRF components.(Hunt et al., 2001)Six instances corresponding to beginning (heel strike, HS 0%), 5%, 25%, 50%, 75% and end (toe off, TO 100%) of the stance phase are indicated.Loads are normalized to the BW=606.6 N for the female subject of our FE model.	90
Figure 4-3: Muscle forces at different periods, (a) quadriceps, (b) lateral hamstring, (c) medial hamstring and (d)gastrocnemius.OA: SevereOA with intact material properties, N: results(Adouni et al., 2012)inasymptomatic subjects, OA+E, OA+E+P and OA+M+C present to different degrees the OA deterioration in cartilage and menisci roperties (see text).	91
Figure 4-4:Predicted ACL forces at different stance periods (see caption of Fig.3).	92
Figure 4-5: Predicted total TF contact forces (cov: via menisci, uncov: via cartilage, M: medial plateau, L: lateral) (See caption of Fig.3).....	93
Figure 4-6: Predicted contact pressure distributions and max values at articular surfaces of tibial plateaus at different periods in normal and OA (with no change in material properties) models. Note that a common legend is used for ease in comparisons. The greater contact stresses on the medial plateau after 25% stance period and absence of articulation at the lateral plateau at TO are evident.Stresses are smaller in the OA model at all periods except at the mid-stance.	94
Figure 4-7: Predicted contact pressures distributions and max values at articular surfaces of tibial plateaus at the 50% of stance phase for normal and OA (with different material properties) models (see caption of Fig. 3). OA-associated deterioration in the articular tissues tends to increase contact areas and decrease contact pressures. Large stresses occur at the medial plateau on the cartilage-cartilage (uncovered) areas.	95

Figure 4-8: Maximum (tensile) principal strains distributions and max values at superficial and deep layers of femoral cartilage at the 50% stance phase for normal, OA (with different material properties) models (see caption of Fig. 3). Strains are much larger in the lower most layer compared to the superficial layer and on the medial condyle compared to the lateral one.96

Figure 4-9: Ensemble averaged EMG (EMG)(Astephen, 2007; Hubley-Kozey et al., 2009) and estimated muscle forces (Model) normalised to their maximum values during the stance phase for various knee muscles.97

Figure 5-1: **(A)** Schematic diagram showing the 34 muscles incorporated into the lower extremity model (taken from OpenSim (Delp et al., 2007)). Quadriceps: vastus medialis obliquus (VMO), rectus femoris (RF), vastus intermedius medialis (VIM) and vastus lateralis (VL); Hamstrings: biceps femoris long head (BFLH), biceps femoris short head (BFSH), semimembranous (SM) and TRIPOD made of sartorius (SR), gracilis (GA) and semitendinosus (ST); Gastrocnemius: medial (MG) and lateral (LG). Tibialis posterior (TP) and soleus (SO) muscles are uni-articular ankle muscles. Hip joint muscles (not all shown) include adductor, long (ADL), mag (3 components ADM) and brev (ADB); gluteus max (3 components GMAX), med (3 components GMED) and min (3 components GMIN), iliacus (ILA), iliopsoas (PSOAS), quadriceps femoris, pectineus (PECT), tensor fascia lata (TFL), periformis. **(B)** Knee FE model; tibiofemoral (TF) and patellofemoral (PF) cartilage layers, menisci and patellar Tendon (PT). Joint ligaments: lateral/medial patellofemorals (LPFL/MPFL), anterior/posterior cruciates (ACL/PCL) and lateral collateral/medial collaterals (LCL/MCL).116

Figure 5-2: Knee joint adduction rotations (a) and moments (b) reported in the literature as mean of asymptomatic subjects during the stance phase of gait. The range of values for the data from our reference study (Astephen, 2007) is also shown. Solid circle show the reference (Ref) and extreme values of $\text{Ref} \pm 1.5^\circ$ in rotation and $\text{Ref} \pm 50\%$ in moment. Note that moments are reported normalized to BW (Kg). Number of subjects used by Ref equal to 60 subjects (37 female and 23 male), 15 subjects for Gao et al.,(2010), 30 subjects (25 Female and 5 Male) for Zhang et al.,(2003), 40 subjects (28 Male and 12 Female) for Kadaba et al.,(1990), 8 subjects (6 Male and 2 Female) for Kozanek et al.,(2009), 8 subjects (Male) for

benoit et al.,(2005)-SM (used skin marker) and BP (used Bone pin), 5 subjects for Bulgeroni et al.,(1997), 1 subject for Meyre et al.,(2013) and Walter et al., (2010), 28 subjects for Winby et al.,(2013), 10 subjects (6 Male and 4 Female) for Schmalz et al.,(2006) and finally 60 subjects for Roda et al.,(2012). 117

Figure 5-3: Predicted muscle forces at midstance of stance phase. (a) Quadriceps, (b) Lateral Hamstring, (c) Medial Hamstring and (d) Gastrocnemius. R ± 1.5 ; the reference adduction rotation of 1.6° is altered by $\pm 1.5^\circ$ to 3.1° and 0.1° or M $\pm 50\%$ the knee reference adduction moment of 17 Nm is varied by $\pm 50\%$ to 25Nm and 9Nm. 118

Figure 5-4: Predicted Ligament and patellar Tendon (PT) forces at 50% of stance phase (midstance). R ± 1.5 ; the reference adduction rotation of 1.6° is altered by $\pm 1.5^\circ$ to 3.1° and 0.1° or M $\pm 50\%$ the knee reference adduction moment of 17 Nm is varied by $\pm 50\%$ to 25Nm and 9Nm. 119

Figure 5-5: Predicted total TF (c) (as well as individual components at medial (a) and lateral (b) plateaus) and ratio medial to lateral forces (d). R ± 1.5 ; the reference adduction rotation of 1.6° is altered by $\pm 1.5^\circ$ to 3.1° and 0.1° or M $\pm 50\%$ the knee reference adduction moment of 17 Nm is varied by $\pm 50\%$ to 25Nm and 9Nm. 120

Figure 5-6: Predicted total TF (M: Medial and L: Lateral) and PF contact areas at midstance. R ± 1.5 ; the reference adduction rotation of 1.6° is altered by $\pm 1.5^\circ$ to 3.1° and 0.1° or M $\pm 50\%$ the knee reference adduction moment of 17 Nm is varied by $\pm 50\%$ to 25Nm and 9Nm. 121

Figure 5-7: Predicted contact pressure at articular surface of lateral and medial tibial plateaus at midstance. R ± 1.5 ; the reference adduction rotation of 1.6° is altered by $\pm 1.5^\circ$ to 3.1° and 0.1° or M $\pm 50\%$ the knee reference adduction moment of 17 Nm is varied by $\pm 50\%$ to 25Nm and 9Nm. Note that a common legend is used for ease in comparisons. 122

Figure 5-8: Maximum (tensile) principal strain in solid matrix at the superficial and lowermost layers of lateral and medial tibial cartilage at midstance. R ± 1.5 ; the reference adduction rotation of 1.6° is altered by $\pm 1.5^\circ$ to 3.1° and 0.1° or M $\pm 50\%$ the knee reference adduction moment of 17 Nm is varied by $\pm 50\%$ to 25Nm and 9Nm. Note that a common legend is used for ease in comparisons. 123

Figure 6-1: (A) Schematic diagram showing the 34 muscles incorporated into the lower extremity model (taken from OpenSim(Delp et al., 2007)). Quadriceps: vastus-medialis-obliquus (VMO), rectus femoris (RF), vastus-intermidus-medialis (VIM) and vastus-lateralis (VL); Hamstrings: biceps femoris long head (BFLH), biceps femoris short head (BFSH), semimembranous (SM) and TRIPOD made of sartorius (SR), gracilis (GA) and semitendinosus (ST); Gastrocnemius: medial (MG) and lateral (LG). Tibialis posterior (TP) and soleus (SO) muscles are uni-articular ankle muscles. Hip joint muscles (not all shown) include adductor, long (ADL), mag (3 components ADM) and brev (ADB); gluteus max (3 components GMAX), med (3 components GMED) and min (3 components GMIN), iliacus (ILA), iliopsoas (PSOAS), quadriceps femoris, pectineus (PECT), tensor fascia lata (TFL), periformis. (B) Knee FE model; tibiofemoral (TF) and patellofemoral (PF) cartilage layers, menisci and patellar Tendon (PT). Joint ligaments: lateral/medial patellofemorals (LPFL/MPFL), anterior/posterior cruciates (ACL/PCL) and lateral collateral/medial collaterals (LCL/MCL). 140

Figure 6-2: Predicted muscle forces at 75% of stance phase. (a) Quadriceps, (b) Gastrocnemius, (c) Lateral Hamstring and (d) Medial Hamstring. Min-G: minimum activation of gastrocnemius muscle, Ref-G: reference activation of gastrocnemius muscle. Max-G: maximum activation of gastrocnemius muscle. 141

Figure 6-3: Predicted knee joint forces at 75% of stance phase. (a) Anterior cruciate ligament (ACL) force, (b) Total contact force, (c) Total contact area and (d) contact pressure. Min-G: minimum activation of gastrocnemius muscle, Ref-G: reference activation of gastrocnemius muscle. Max-G: maximum activation of gastrocnemius muscle. 142

Figure 6-4: (A) Computed force in anterior cruciate ligament (ACL) at different flexion angles and under isolated gastrocnemius force of 0N, 500N and 1000N. (B) ACL force under gastrocnemius force of 1000N at 0° and 90° in the cases Ref: reference case with free coupled rotations, V/V: varus/valgus fixed, I/E: internal/external fixed, V/V+I/E: constrained coupled rotations. 143

Figure 6-5: Computed force in ACL bundles at different flexion angles and under isolated gastrocnemius force of 1000N. ACL-am; anteromedial bundle and ACL-pl; posterolateral bundle. 144

Figure 6-6: Flexor joint moment on the tibia under gastrocnemius forces of 500 N and 1000 N at different flexion angles.....	145
Figure 6-7: Predicted total TF (M: Medial and L: Lateral) contact forces at different flexion angles and under gastrocnemius forces of 1000 N.....	146
Figure 6-8: Predicted contact pressure at articular surface of lateral and medial tibial plateaus at different flexion angles and undergastrocnemius force of 1000 N. Note that a common legend is used for ease in comparisons.	147
Figure 7-1: Référentiel non orthogonal défini par Grood et Santy., (1983), employé pour décrire la cinétique et la cinématique des articulations des membres inférieurs.....	152

LISTE DES SIGLES ET ABRÉVIATIONS

ACL	: anterior cruciate ligament.
AD	: adductor, long (+L), mag (+M) and brev (+B).
BFLH	: biceps femoris long head.
BFSH	: biceps femoris short head.
G	: gluteus max (+MAX), med (+MED) and min (+MIN).
GA	: gracilis.
GM	: gastrocnemius medial.
GL	: gastrocnemius lateral.
ILA	: iliacus.
LCA	: ligament croisé antérieur.
LCL	: lateral collateral ligament.
LCP	: ligament croisé postérieur.
LPFL	: lateral patellofemoral ligament.
MCL	: medial collateral ligament.
MPFL	: medial patellofemoral ligament.
P	: periformis.
PCL	: posterior cruciate ligament.
PECT	: pectineus.
PF	: patellofemoral.
PSOAS	: iliopsoas.
PT	: patellar Tendon.
RF	: rectus femoris.
SM	: semimembranous.

SO : soleus.
SR : Sartorius.
ST : semitendinosus.
TF : tibiofemoral.
TFL : tensor fascia lata.
TP : tibialis posterior.
VMO : vastus medialis obliquus,
VI : vastus intermidus,
VM : vastus medialis.
VL : vastus lateralis.

LISTE DES ANNEXES

ANNEXE 1 : Modèle itérative.....	194
ANNEXE 2 : Validation des propriétés matérielles.....	195
ANNEXE 3 : Modèle et Input.....	207

CHAPITRE 1 INTRODUCTION

L'analyse de la bipédie humaine est un processus important dans le domaine de l'orthopédie et la médecine. Le nombre élevé des études effectuées dans le domaine démontre l'importance de cette analyse dans la prévention, l'identification et le traitement des anomalies affectant les membres inférieurs durant les pratiques quotidiennes de l'activité de la marche. Ceci était clair par la détermination des relations complexes entre la limitation fonctionnelle et l'incapacité de l'application de l'activité et le cadre de référence normal (cas intact). En définissant ces relations, non seulement, nous serons en mesure de concevoir des études plus optimales des stratégies actuelles de traitement de réadaptation, mais également pour envisager des nouvelles stratégies de traitement de réadaptation.

Des études statistiques estiment que plus 13,9% des adultes âgés de 25 ans et plus 33,6 % de ceux de 65 ans en Amérique du Nord (Lawrence et al., 2008) souffrent de l'ostéoarthrite (OA). Cette dernière représente une incapacité permanente qui nécessite un traitement. En raison de sa structure complexe et de sa capacité élevée de portance du poids du corps humain, le genou est considéré comme l'articulation la plus souvent touchée par cette maladie (OA). L'ostéoarthrite du genou est une des cinq principales causes de limitations fonctionnelles chez les adultes non-institutionnalisés (Guccione et al., 1994). En une décennie, presque 1 million d'adultes canadiens vont être atteints par l'ostéoarthrite. En 2026, 5 millions de Canadiens seront touchés et aux États-Unis, en 2030, ce nombre sera de 41,1 millions (Reuters, 2003). Du point de vue économique, le coût annuel de l'ostéoarthrite dépasse 3,4 milliards de dollars au Canada (Santé Canada) et 13,2 milliards de dollars aux États-Unis par an (Buckwalter and Mankin, 1997). Le genou est associé à une grande partie de ce fardeau financier. L'arthroplastie totale du genou (*totale knee replacement*) représente parfois le seul traitement de cette maladie (OA). Le nombre de ces opérations ne cesse pas d'augmenter, il a atteint un pourcentage élevé aux États-Unis de 84% et 38.5% au Canada entre les années 1997 et 2009 (American Academy of Orthopedic Surgeons [AAOS]).

Les ménisques et les ligaments constituant l'articulation de genou sont très susceptibles aussi aux blessures. Ceux qui souffrent des blessures ligamentaires et/ou méniscales ont un risque significatif de générer des maladies chroniques à long terme telles que l'ostéoarthrite (OA). Les lésions ligamentaires, plus précisément dans le ligament croisé antérieur (LCA), se produisent

souvent lors des activités sportives. Ils affectent plus que 200 000 personnes aux États-Unis, avec environ 95 000 ruptures du ligament croisé antérieur (American Orthopaedic Association [AOS]). En plus, environ 50% des patients atteints par les lésions de LCA sont également atteints par des lésions méniscales. Ceci montre bien que les pathologies sont assez nombreuses au niveau de genou humain et le traitement nécessite parfois une intervention chirurgicale soit pour les réparations ou bien pour implantations.

Afin de faire face à ces problèmes qui affectent le genou et qui augmentent les plages des limitations fonctionnelles durant l'application des activités quotidiennes comme la marche, il est impératif de comprendre les mécanismes physio-biologiques qui entraînent ces anomalies suite aux sollicitations mécaniques. Dans ce contexte, notre étude propose de modéliser la biomécanique du joint du genou humain durant l'application de la marche normale et altérée.

CHAPITRE 2 ANATOMIE ET REVUE DE LA LITTÉRATURE

2.1 Anatomie fonctionnelle

L'articulation du genou est une articulation qui supporte le poids du corps, située entre l'extrémité inférieure du fémur et l'extrémité supérieure du tibia. Entre ces deux extrémités; on a les condyles fémoraux et les plateaux tibiaux qui sont recouverts de cartilage où s'interposent deux ménisques interne et externe. Les ligaments maintiennent en contact le fémur et le tibia : en périphérie ce sont les ligaments latéraux (ligament latéral interne et ligament latéral externe). Au centre du genou on trouve les ligaments croisés : ligament croisé postérieur et ligament croisé antérieur (Fig. 1.1). Une deuxième jointure de transmission de charge définie dans cette articulation est la jointure patello-fémorale, qui relie l'os fémorale à l'os de la rotule et qui est caractérisée par une couche du cartilage plus épaisse que celle décrite précédemment. Aussi elle se caractérise par deux ligaments qui sont l'aileron interne et l'aileron externe et le tendon musculaire supérieur (Quadriceps) et inférieur (Tendon rotulien) (Fig.1.1).

Dans le plan sagittal l'articulation du genou peut tourner de 135° de l'hyper-extension à l'hyper-flexion en fonction des activités. Par exemple, en marche normale, l'articulation du genou fléchit de l'extension complète à 30° de flexion et subit de la compression en appui de 2 à 4 fois le poids corporel. Cette charge peut augmenter à des valeurs plus élevées dans des activités comme la course, monte/descente d'escalier et le saut. Aussi, la compression axiale, la force antéro-postérieure, le moment varus-valgus et le couple interne-externe sont également pris en charge par l'articulation du genou.

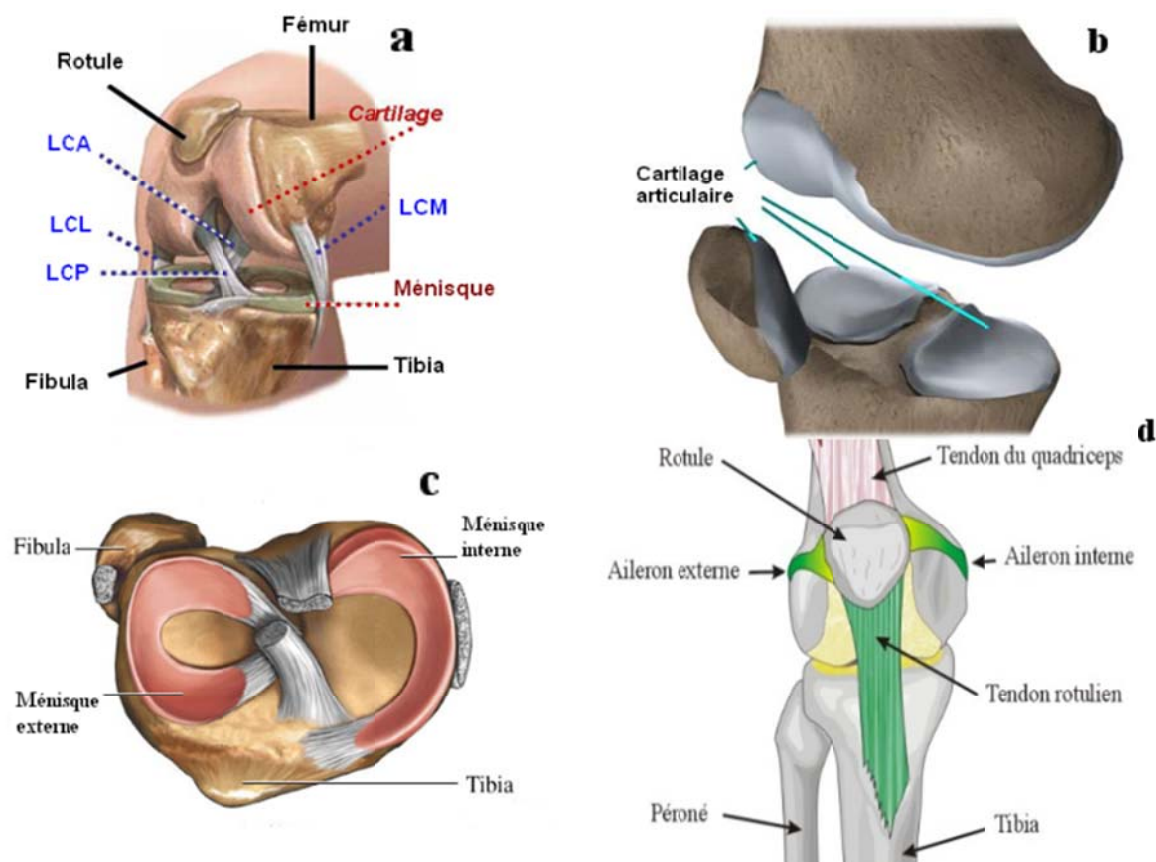


Figure 2-1: Principaux éléments constituant l'articulation du genou humain : (a) jointure Tibio-fémorale, (b) cartilages articulaires, (c) ménisques, (d) jointure patello-fémorale.

((a- health.allrefer.com), (b- www.eorthopod.com), (c- www.Biokineticist.com), (d- www.genou.com))

2.1.1 Cartilage

Le cartilage articulaire offre une surface ferme, lisse et un coefficient de frottement très faible qui aide les mobilités du joint. L'épaisseur du cartilage articulaire dans le genou n'est pas uniforme et varie de 1 à 7mm. Ses propriétés de compressibilité et d'élasticité permettent aux surfaces articulaires d'absorber les charges de compression auxquelles le genou est soumis (Fig. 1.1b). La structure du cartilage articulaire a attiré l'attention de chercheurs depuis l'année 1742 (Hunter, 1742). Des études effectuées sur cette substance dévoilent que sa composition principale est constituée par la matrice extracellulaire et les chondrocytes. Les principales composantes de cette matrice sont des fibres de collagène (principalement de type II), protéoglycannes et l'eau, dispersées avec des différentes proportions, 50-73% (de son poids sec), 15-30% (de son poids

sec) et 58-78% (de son poids) respectivement (Broom and Marra, 1986; Clarke, 1974; Mow et al., 1980).

Les compositions du cartilage articulaire changent selon la profondeur. Beaucoup de travaux histologiques et mécaniques montrent que le cartilage est formé de quatre bandes différentes, leur disposition joue un rôle primordial dans le système de chargement du cartilage. La couche superficielle représente 5-10% de la hauteur totale du cartilage et elle est en contact direct avec le fluide synovial qui sert comme une surface de glissement avec des fibres orientés horizontalement. La zone de transition représente la deuxième couche du cartilage articulaire où les fibres de collagène sont orientées d'une manière aléatoire et leur épaisseur varie entre 40 et 45% de l'épaisseur totale, La couche profonde du cartilage représente aussi 40 à 45% de l'épaisseur totale du cartilage articulaire: les fibres de collagène sont orientées orthogonalement à la surface articulaire et finalement la couche la plus dure du cartilage articulaire est la couche calcifiée et qui est en jonction directe avec la plaque osseuse. Cette couche représente 5 à 10% de la hauteur du cartilage.

2.1.2 Ménisque

Les ménisques sont des fibrocartilages en forme de demi-lune dont la section est partiellement triangulaire avec une base périphérique. Les ménisques sont des fibrocartilages semblables à celles du cartilage articulaire, dont la composition principale est formée d'eau (60 à 80% de son poids) et de chaîne des fibres de collagène (principalement de type I) qui représente 60 à 70% du poids sec de ménisque avec de la matrice extracellulaire à base de molécules de protéoglycannes (1-2% de poids sec) et de cellules (fibroblastes et chondrocytes), glycoprotéines et élastine (Adams et al., 1983; Ingman et al., 1974). Les fibres de collagène sont orientées d'une manière radiale et circonférentielle sur les zones superficielles et profondes. Ces fibres sont caractérisées par un faible diamètre par rapport à celui de la couche moyenne.

En ce qui concerne le transfert de charges, Spilker et al, (1992) ont trouvé que plus que 50% des forces sont transmises par le ménisque pendant le chargement en compression du genou. Son rôle d'amortissement est lié aux capacités viscoélastiques, où la relaxation et le fluage. La stabilité des ménisques est liée à sa forme concave ; leurs comportements mécaniques leur

permettent une large flexibilité d'adaption avec la forme du condyle et de plateau tibiale. Alors que, le rôle de lubrification est dû à une extrusion de liquide lors du chargement en compression.

2.1.3 Ligaments

Les ligaments sont des bandes fibreuses du tissu connectif reliant deux ou plusieurs structures ensemble. Quatre ligaments principaux (LCA, LCP, LCM et LCL) contrôlent le mouvement relatif de l'articulation tibiofemorale (Fig. 1.1). Deux ligaments patellofémoraux (MPFL pour « *Medial Patellofémoral Ligament* » et LPFL pour « *Lateral Patellofémoral Ligament* »), appelés également ailerons rotuliens interne et externe jouent un rôle dans la stabilité de la rotule. Selon les conditions de chargement, un ou plusieurs de ces ligaments assurent la stabilité de la jointure articulaire. Le ligament croisé antérieur (LCA) relie la zone postéro-latérale du condyle fémoral à la face antéro-interne inter-condylienne du tibia. Cette orientation permet au LCA de résister à la translation antérieure du tibia par rapport au fémur. Le ligament croisé postérieur (LCP) relie la zone inter-condylienne postérieure du tibia au condyle médial du fémur. Cette configuration permet au LCP de résister au mouvement postérieur du tibia par rapport au fémur. Le ligament collatéral médial (LCM) est situé légèrement postérieure sur la face interne de l'articulation du genou. Ce ligament résiste essentiellement les rotations valgus du joint. Le ligament collatéral latéral (LCL) s'étend le long de l'extérieur du genou, reliant le fémur au péroné. Le ligament collatéral latéral assure la stabilité contre les mouvements varus du joint.

La détermination des propriétés mécaniques d'un ligament représente un prérequis primordial dans sa modélisation numérique. Des études antérieures ont été réalisées dans ce domaine pour déterminer le comportement mécanique du ligament, c.-à-d. connaître la déformation maximale, la contrainte maximale et le module d'élasticité. Parmi ces travaux on cite celui de Butler et al. (1986) qui est présenté sur la figure ci-dessous (Fig. 1.2).

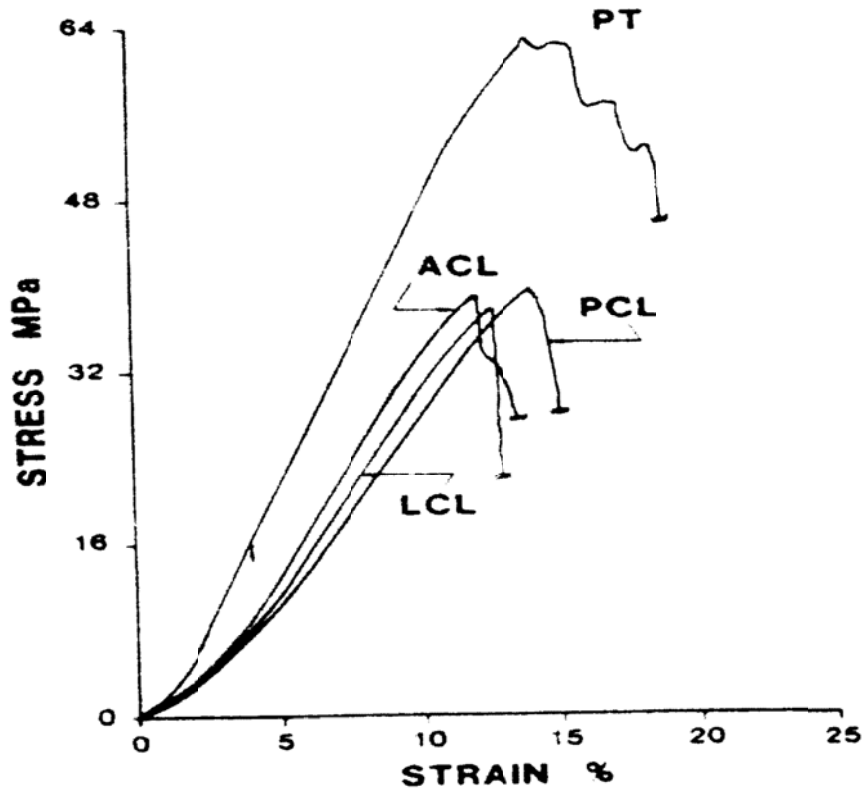


Figure 2-2: Courbe contrainte-déformation pour les ligaments principaux, ligaments croisé antérieur (ACL) et postérieur (PCL), ligaments collatérales médial (MCL) et latéral (LCL), et le tendon rotulien (PT) (Butler et al., 1986).

2.1.4 Muscles

Le mécanisme actif entourant l'articulation du genou, appelé aussi mécanisme musculaire, est constitué de deux sous mécanismes: un mécanisme extenseur (quadriceps) et un mécanisme fléchisseur (*Ischio-jambiers* et *Jumeau*) ; le premier contient les muscles droit antérieur (rectus-femoris RF), vaste externe (vastus lateralis VL), crural (vastus intermedius VI) et vaste interne (vastus medialis VM) et le deuxième contient les muscles jumeau latérale (GL), jumeau médiale (GM), biceps femoris (BF), demi-membraneux (semimembranosus SM) et une combinaison du sartorius (SR), gercilis (GR) et demi-tendineux (semitendinosus ST). Ce dernier groupe est appelé le TRIPOD (Fig. 1.3).

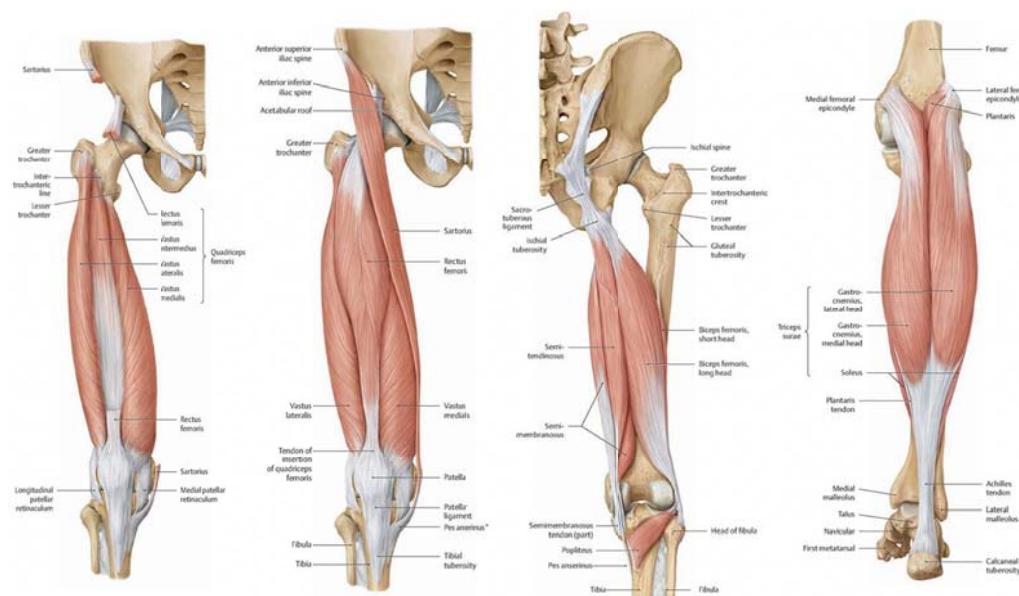


Figure 2-3: le mécanisme musculaire entourant l'articulation du genou (www.thieme.com).

L'orientation spatiale de composantes musculaires a un rôle primordial dans la prédiction des cinématiques du joint. En ce qui concerne la jointure fémoro-patellaire, le modèle d'angle Q proposé par les travaux de Sakai et al.(1996) a été considéré comme le modèle le plus fidèle dans la reconstruction de la cinématique de la rotule. En effet, ce résultat a été trouvé après une comparaison avec deux autres modèles ; à savoir le modèle anatomique (Lieb and Perry, 1971) et le modèle mathématique (Yamaguchi G et al., 1990) (Fig. 1.4).

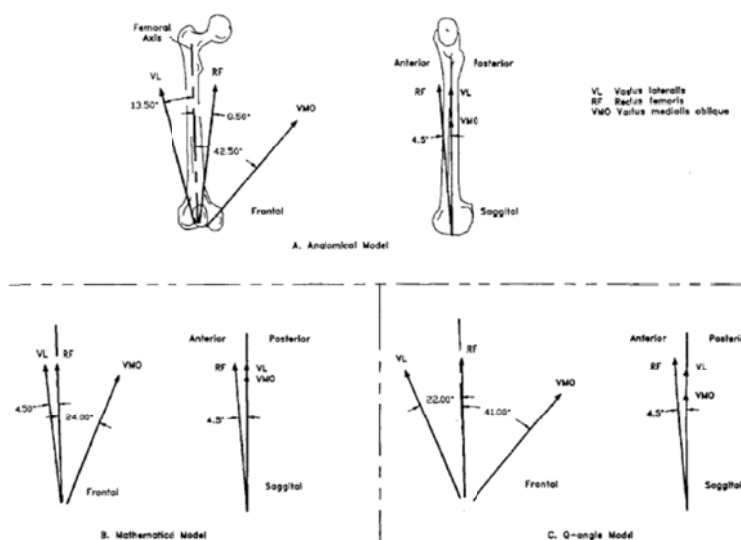


Figure 2-4: Présentation des orientations des muscles du quadriceps selon les trois modèles, anatomique, mathématique et de l'angle Q (Sakai et al., 1996).

Après cette présentation de l'anatomie du genou, nous évaluerons les différentes études expérimentales et théoriques qui ont traitées le sujet du genou humain et aussi les analyses faites sur le membre inférieur durant la bipédie humaine (la marche).

2.2 Revue de la Littérature

La revue se consacre à survoler les études qui ont prises le genou humain comme sujet et qui auront un lien avec notre travail. Pour cela, cette revue bibliographique a été divisée en trois parties: la première s'occupe de la présentation des études expérimentales, la deuxième est consacrée à la présentation des études numériques et en enfin la troisième traite des analyses de la bipédie humaine dont on va essayer de mettre plus d'accent dans cette revue de littérature.

2.2.1 Études Expérimentales

Plusieurs études expérimentales ont été faites afin de mieux comprendre la biomécanique du genou. Ces études ont visé essentiellement à déterminer le rôle de chaque composant du joint (ligaments, cartilages, ménisques, etc.), le transfert de charges, la distribution de la pression et les différentes zones de contact, les forces ligamentaires et la cinématique du joint pour divers chargements extérieurs et diverses positions du genou.

Les surfaces et les pressions moyenne et maximale de contact sur le plateau tibial ont été mesurées sous l'action d'une large force de compression allant jusqu'à 2000N en pleine extension. Des films sensibles à la pression, des capteurs du formage de couleur, des capteurs de micro-indentation en plastique, une radiologie, une radiographie ont été utilisés pour ces mesures prises sur des cadavres humains. Une gamme de pression de contact maximale moyenne pour une compression de 1000N dans les différentes études est obtenue comprise entre 1,6 à 3,2 MPa (Ahmed and Burke, 1983; Fukubayashi and Kurosawa, 1980; Inaba et al., 1990; Walker and Erkiuan, 1975). La pression de contact moyenne est rapportée comme étant de l'ordre de 0,48 à 2,2 MPa (Huang et al., 2003; Krause et al., 1976; Kurosawa et al., 1980; Seedhom and Hargreaves, 1979). La surface de contact totale des deux plateaux a été également mesurée, et elle varie de 1150 à 2084 mm² sous 1000N de compression (Ahmed and Burke, 1983; Brown and Shaw, 1984; Huang et al., 2003; Krause et al., 1976; Kurosawa et al., 1980; Maquet et al., 1975; Seedhom and Hargreaves, 1979).

Le déplacement axial du tibia par rapport au fémur dans des échantillons cadavériques humains a été également mesuré. Cette mesure est de l'ordre $\sim 0,6-0,8$ mm dans une compression uni-axiale de 1000 N (Kurosawa et al., 1980; Walker and Erkiuan, 1975). La dispersion dans les données expérimentales est due, à des différences dans les échantillons, à la durée d'application de la charge, aux conditions aux rives et aux appareils de mesure. Ces études ont tenté d'évaluer aussi la contribution du cartilage et du ménisque sur chaque compartiment dans la transmission de charges qui est subi par la jointure tibiofemorale. Sous une charge de compression de 1400 N, la contribution des ménisques médial et latéral rapportée est respectivement de 81% et 77% (Seedhom and Hargreaves, 1979), tandis qu'un pourcentage de $\sim 45\%$ a été également signalé comme la moyenne sur les deux compartiments de 16 spécimens dans les mêmes conditions de chargements (Shrive et al., 1978). La contribution relative à la charge des ménisques diminue avec l'augmentation de la charge de compression (Ahmed and Burke, 1983; Walker and Erkiuan, 1975). Par exemple, pour des valeurs de de compression de 445 et 1335 N, la partie latérale du ménisque atteint respectivement $82\pm 10\%$ et $77\pm 7\%$ alors que celle du ménisque interne est dans une proportion de $69\pm 17\%$ et $62\pm 12\%$, respectivement (Ahmed and Burke, 1983).

Dans le but d'évaluer la contribution de la structure ligamentaire lors des différents chargements appliqués sur le genou, plusieurs études *in-vitro* se sont concentrées surtout sur les ligaments croisés vu leur influence directe sur la stabilité du genou et ceci en mesurant leurs forces ou leurs déformations (Ahmed and Burke, 1983; Butler et al., 1980; Huberti et al., 1984; Li et al., 1999; Li et al., 2004; Markolf et al., 1996; Markolf et al., 2004). Une partie de ces travaux s'est concentrée sur l'étude du ligament croisé antérieur (LCA), vu la fréquence de sa déchirure lors des activités sportives ainsi que son rôle primordial dans la stabilisation du genou (Li et al., 1998; Markolf et al., 1998; Woo et al., 1998).

Une tentative pour mesurer la tension dans les ligaments entourant le joint tibiofemorale a été faite auparavant par Ahmed et al. (1987) en utilisant des jauges de déformation ' *Buckle Transducer*'. À cause d'un problème d'encombrement, les bandes antéro-interne du ligament croisé antérieur, postéro-externe du ligament croisé postérieur, superficielle du ligament latéral interne et le ligament latéral externe ont été considérées pour des angles de flexion du genou allant de 40° à 90° . Des chargements passifs, susceptibles de causer des tensions importantes dans ces bandes, sont appliqués comme une translation antérieure et une rotation axiale du tibia avec ou sans compression axiale. Dans une étude ultérieure Ahmed et al. (1992) ont présenté

cette fois-ci des résultats similaires mais pour des chargements combinés à savoir une translation antérieure appliquée à un tibia ayant subi une rotation axiale au préalable ou encore une rotation axiale appliquée au tibia après avoir subi une translation antérieure. Ces études ont montré que le ligament croisé antérieur est le frein primaire pour le mouvement de translation antérieure de tibia par rapport au fémur. Ce rôle important du ligament croisé antérieur a été également démontré par la suppression de ce ligament et en comparant le déplacement antérieur du tibia par rapport au fémur avec un cas intact (Butler et al., 1980; Fukubayashi et al., 1982; Hsieh and Walker, 1976; Kanamori et al., 2000; Markolf et al., 1976; Shoemaker and Markolf, 1985). La translation antérieure du tibia s'est doublée dans le cas du ligament déficient. Récemment, une étude effectuée par Abebe et al.(2011) a comparé l'effet de la mise en place d'une greffe de reconstruction du LCA sur la capacité de rétablissement de la mobilité normale du genou humain. Cette étude a montré que l'emplacement anatomique du côté fémorale est plus fiable dans le rétablissement de la cinématique du joint que celle à l'emplacement antéro-proximal par rapport au site de fixation du LCA.

La relation entre l'activation musculaire et le chargement ligamentaire, spécifiquement le ligament croisé antérieur, a attiré l'attention des chercheurs dans la littérature (Beynon and Fleming, 1998; Draganich and Vahey, 1990; Goss et al., 1998; Li et al., 1999; Li et al., 1998; Li et al., 2004; Markolf et al., 2004; More et al., 1993; Pandy and Shelburne, 1997). Ces travaux ont montré que l'activation du quadriceps augmente la tension du ligament croisé antérieur à des angles faibles de flexion. Par contre, la co-activation des muscles du *Ischio-jambiers* diminue considérablement la force dans ce ligament. Cette conclusion rejoint le fait que le *Ischio-jambiers* est un élément important dans la compensation des anomalies fonctionnelles du genou suite aux lésions associées au ligament croisé antérieur (Kålund et al., 1990). L'effet des forces musculaires sur le ligament croisé postérieur, a été étudié dans certaines études cadavériques telles que celles de Markolf et al.(2004), de Li et al.(2004) et de Höher et al.(1999). Ces travaux ont dévoilé la relation antagoniste entre les muscles de *Ischio-jambiers* et le ligament croisé postérieur surtout pour des grands angles de flexion. Une co-activation du quadriceps peut réduire significativement la force dans le LCP (Höher et al., 1999).

Le comportement biomécanique du joint fémoro-patellaire a été examiné dans plusieurs travaux dans la littérature. Ces travaux ont essayé de comprendre le rôle de la rotule ainsi que les charges transmises à travers elle et de vérifier l'hypothèse de l'amplification de force musculaires

à travers ce joint (Ahmed and Burke, 1983; Buff et al., 1988; Huberti et al., 1984; Hungerford and Barry, 1979; Lewallen et al., 1990; Mizuno et al., 2001; Singerman et al., 1995; Terry et al., 1986). La détermination du chargement mécanique dans le joint fémoro-patellaire a été le thème de plusieurs travaux expérimentaux. Malgré la diversité qui existe entre les procédés expérimentaux, la force et l'aire de contact augmentent presque linéairement avec l'augmentation de l'angle de flexion. Une répartition plus appropriée de la force de compression a été observée due à l'augmentation de l'aire de contact ce qui permet de diminuer la contrainte de contact (Ahmed and Burke, 1983; Huberti et al., 1984; Singerman et al., 1995).

En conclusion, nous pouvons dire que les travaux expérimentaux ont été très pertinents et leurs contributions à l'amélioration de nos connaissances sont mémorables. En effet, le but principal de ces études expérimentales est la détermination des aspects interdépendants qui décrivent la biomécanique du genou sous différents chargements externes.

2.2.2 Études Mathématiques et Numériques

Les approches mathématiques et numériques sont des outils complémentaires qui peuvent prévoir toutes les variables d'intérêt telles que les mouvements primaires et couplés, ainsi que les forces musculaires, ligamentaires et de contact. Par conséquent, un modèle théorique peut apporter une nouvelle perspective dans la compréhension du comportement biomécanique de l'articulation du genou.

Depuis les années 90, avec l'avancement technologique dans la reconstruction des géométries du joint et les nombres élevés des études expérimentales qui ont investigués les propriétés mécaniques des tissus constituant le joint, une bonne amélioration a été apportée sur la modélisation numérique du joint du genou. Plusieurs études ont développé le modèle tibiofemoral. La précision de leurs prédictions dépend essentiellement de l'intégration ou non des éléments constituant le joint. Un grand nombre de ces modèles a été développé par la méthode des éléments finis sans prendre en considération la présence des ménisques. (Atkinson et al., 2000; Blankevoort and Huiskes, 1991a; Blankevoort et al., 1991b; Crowninshield et al., 1976; Grood and Hefzy, 1982).

Les modèles de Blankvoort et al.(1991a; 1988; 1991b), Blankvoort et Huikes (1996; 1991b) ainsi de Mommersteeg et al.(1996a; 1997; 1996b) sont parmi les premiers modèles

d'éléments finis de l'articulation tibiofemorale qui ont été intensivement analysés sous différentes configurations de charges en flexion (Fig. 1.5). Des ressorts uni-axiaux élastiques non-linéaires ont été considérés pour les ligaments, alors que les cartilages articulaires ont été modélisés par un comportement déformable ayant une faible épaisseur. Les équations d'équilibre, qui tiennent compte de tous les efforts internes et externes, ont été solutionnées pour obtenir la cinématique du joint. De même, Andriacchi et al.(1983) ont développé un modèle tridimensionnel pour trouver la réponse biomécanique du joint sous des charges axiales combinées avec des moments d'adduction et d'abduction durant la flexion. Dans leur modèle, les cartilages ont été représentés par des corps rigides, tandis que, les ligaments ont été représentés par des ressorts élastiques non-linéaires. Beynnon et al.(1996) ont aussi développé un modèle bidimensionnel du joint fémoro-tibial en flexion passive.

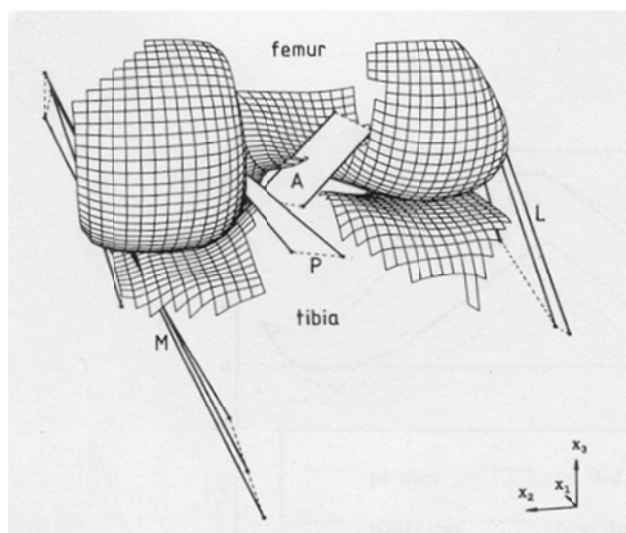


Figure 2-5: Représentation de la géométrie du modèle par éléments finis de Blankevoort et Huiskes (1991a). Ce modèle inclut les condyles fémoraux, les surfaces tibiales ainsi que les ligaments principaux.

La plupart des modèles tibiofemorale développés dans les vingt dernières années ont pris en considération les ménisques dans leurs modélisations (Bendjaballah et al., 1995; Donahue and Hull, 2002; Li et al., 2002a; Mesfar and Shirazi-Adl, 2005; Moglo and Shirazi-Adl, 2003a; Pena et al., 2005; Shirazi et al., 2008; Yang et al., 2010). Un modèle d'éléments finis développé par Li et al.(2002a) est composé par des structures osseuses (fémur, tibia et rotule), des cartilages articulaires, des ressorts non linéaires, qui simulent la résistance équivalente des ménisques et des

ligaments croisés et collatéraux. Un module d'élasticité de 5MPa et un coefficient de Poisson de 0.45 ont été considérés pour simuler le matériau du cartilage. Les ligaments sont modélisés par des éléments ressorts non linéaires, alors que, les structures osseuses sont considérées comme des corps rigides. Ce travail consiste à l'étude de la biomécanique du joint du genou avec un ligament croisé antérieur, reconstruit et blessé.

Le modèle de Pena et al.,(2005) a été employé afin d'estimer les surfaces de contact ainsi que la distribution des contraintes et des déformations au niveau du cartilage suite à une force axiale de compression dans les trois cas de joint tibiofemoral suivants : un joint sain, un avec une déchirure dans le ménisque interne et un joint qui a subi une ménisectomie totale. Ce modèle considère le cartilage articulaire et les ménisques comme des structures élastiques linéaires alors que les ligaments sont considérés comme des structures hyper-élastiques. Il est à noter que ce modèle ne tient compte que de la position de l'extension complète du genou ce qui pourrait être considéré comme une limitation majeure de ce modèle.

Le modèle tibiofemoral qui a été jugé comme le plus raffiné au niveau des modélisations anatomiques dans la littérature est celui de Bendjaballah et al.(1995, 1997, 1998) qui a été amélioré dans une étape subséquente par Moglo et Shirazi-Adl.(2003a, 2003b, 2005). Ce modèle est constitué de trois structures osseuses (tibia, fémur et rotule) et leurs cartilages articulaires, de deux ménisques médial et latéral, ainsi que des cinq principaux ligaments (collatéraux, croisés et tendon rotulien). Les comportements mécaniques assignés pour ce modèle sont: le cartilage articulaire considéré comme un matériau élastique isotrope ($E=15\text{MPa}$, $\nu=0.45$), le ménisque présenté comme un composite non homogène avec une matrice élastique isotrope ($E=10\text{Mpa}$, $\nu=0.45$) renforcé par des fibres de collagènes radiales et circonférentielles. Ce modèle a été employé par Bendjaballah et al.(1995, 1997, 1998) pour la détermination des forces transmises à travers les composants du joint ainsi que la détermination du rôle et de l'influence des ligaments et de l'état des contraintes sous l'effet des forces de compression, moments varus-valgus et la charge des forces antérieures et postérieures. Par la suite, Moglo et Shirazi-Adl.(2003a, 2003b, 2005) ont analysé la réponse du genou sous l'effet de la flexion du joint et le phénomène de couplage entre les ligaments croisés antérieur et postérieur durant la flexion passive du genou humain. Récemment une amélioration additionnelle a été faite par Shirazi et al.(2008) sur ce modèle où une implémentation de fibres de collagène avec des fractions volumique appropriées dans le cartilage articulaire a été mise en évidence. Cette dernière étude a été plus physiologique

que les études précédentes puisque elle s'est intéressée à l'effet des fibres de collagènes sur la réponse de l'articulation de genou sous un chargement pur en compression ou un chargement combiné (compression et/ou force antérieure ou postérieure).

Certains autres travaux se concentrent sur l'étude du joint patello-fémoral. Les approches mathématiques et numériques ont comme un but principal de déterminer trois aspects interdépendants qui décrivent la biomécanique du joint patello-fémoral (Fig. 1.6). Ceci inclut la détermination de la force du contact patello-fémoral, de la zone et pression de contact (Essinger et al., 1989; Heegaard et al., 1995; Heegaard et al., 2001; Hefzy et al., 1992; Hefzy and Yang, 1993; Reithmeier and Plitz, 1990; Van Eijden et al., 1986; Yamaguchi and Zajac, 1989). Des résultats décrivant le mouvement de la rotule en fonction de l'angle de flexion du genou, aussi des problèmes de contact signalés pour des degrés de flexion moins de 10° oblige que la plage de flexion du genou soit comprise entre 20° et 160° . Ces résultats ont été fournis à l'aide des modèles 3D d'éléments finis, où la géométrie du joint et les propriétés mécaniques du tendon rotulien sont pris en considération.

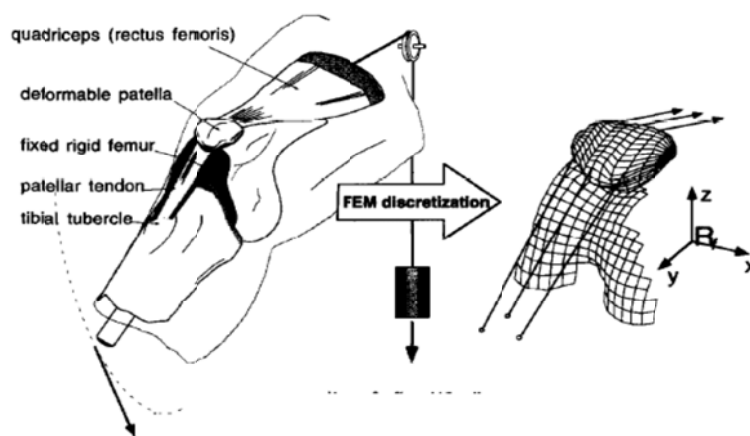


Figure 2-6: Le modèle fémoro-patellaire de Heegaard et al.(1995)

Les modèles d'éléments finis totaux qui prennent en considération les deux jointures (tibiofemorale et patello-fémorale) sont moins nombreux. On considère par exemple les travaux de Ramaniraka et al.(2005) qui ont pour but d'étudier la biomécanique du genou humain suite à une coupure du ligament croisé postérieur et suite à sa reconstruction. Pour cela ils ont conçu un modèle déformable de l'articulation du genou. Les ligaments sont considérés comme des structures hyper-élastiques. Les différentes surfaces de contact sont modélisées par des éléments de contact à grand déplacement (Fig 1.7). Le cartilage articulaire a été modélisé avec un module d'élasticité de 12MPa et un coefficient de Poisson de 0.45. Dans ce travail aucune précontrainte n'a été attribuée aux ligaments

ce qui permet d'avancer que le modèle ne pourra pas être validé. Le modèle le plus complet dans les littératures est celui de Mesfar et Shirazi-Adl.(2005, 2006a, b). Ces études sont une suite de travaux de Moglo et Shirazi-Adl.(2003a, 2003b, 2005) où une amélioration est faite par l'addition du mécanisme extenseur (rotule-tendon rotulien-groupes musculaires de quadriceps) et les muscles fléchisseurs *Ischio-jambiers*. Cette amélioration a permis de voir l'effet d'activation de ces muscles avec de magnitudes variables sous une marge de flexion de 0° à 90° sur la réponse jointure tibio-fémorale et fémoro-patellaire intacte et altérée et ainsi pour étudier la réponse de cette articulation durant l'application des exercices à chaîne cinétique ouvertes (OKC) ou fermées (CKC) (Adouni and Shirazi-Adl, 2009; Mesfar and Shirazi-Adl, 2008a, b).

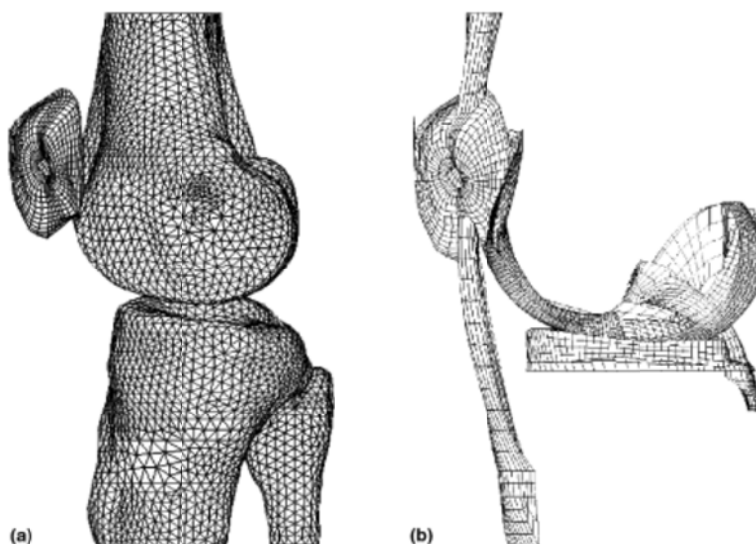


Figure 2-7: (a) Maillages tridimensionnels des structures osseuses, (b) Maillages tridimensionnels des tissus mous (cartilage, ménisques, ligaments)(Ramaniraka et al., 2005).

2.2.3 Analyses de la bipédie humaine

La bipédie (*gait*) est organisée en cycles de mouvements des membres inférieurs. Ces cycles sont reproductibles et symétriques. A l'intérieur de ces cycles, les mouvements relatifs des différentes composantes ; bassin, fémurs, tibia et pieds sont également reproductibles et symétriques. Sa description peut présenter des différences dans les détails selon les auteurs mais elle tend aujourd'hui vers une définition unique admise par tous. Par convention, le cycle de marche normale débute lorsque le talon d'un pied se pose (*heel strike*) et se termine lorsque ce

même talon se pose à nouveau de manière consécutive sur le sol; il comprend deux phases essentielles qui sont la phase d'appui (*Stance phase*) et la phase oscillante (*swing phase*). Le cycle de la marche normale dure environ 1 seconde (Bouisset, 2002; Perry, 1992; Rose et al., 1994) (Fig. 1.8).

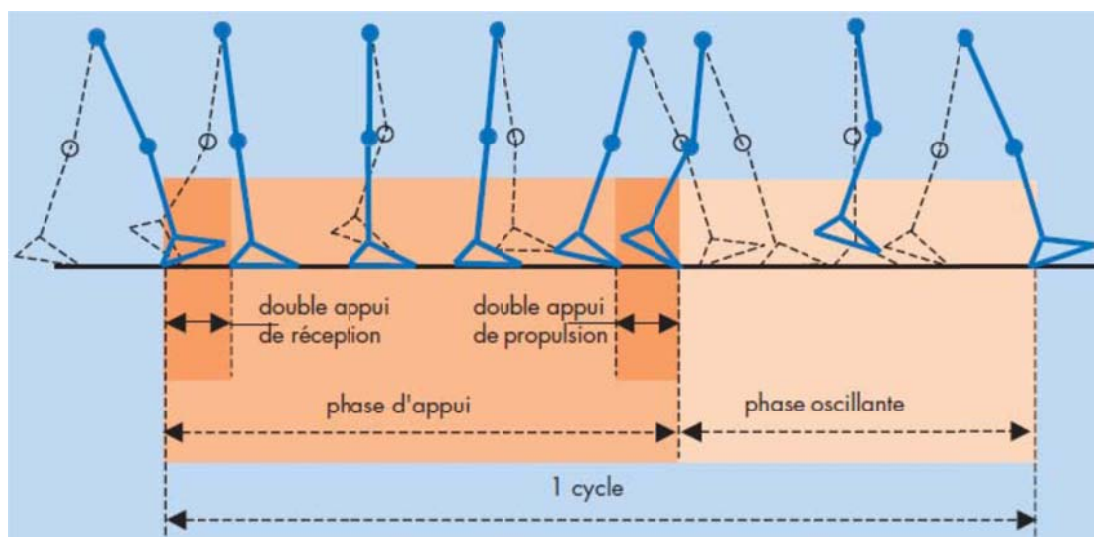


Figure 2-8: Représentation schématique du cycle de marche et de ses principales phases et sous-phases. (www.observatoire-du-mouvement.com)

Au cours des deux dernières décennies, l'analyse de la marche a été transformée à partir d'une discipline purement académique à un outil utile dans les mains des biomécaniciens et des thérapeutes. Ceci est dû à l'avancement technologique qui est mis en service pour avoir une collection précise des données cinématiques et cinétiques au cours de ce processus. Diverses tentatives expérimentales ont été faites pour décrire le mouvement des membres inférieurs durant la marche en palier normal, (Anderson and Pandy, 2001; Eng and Winter, 1995; 2006; Hunt et al., 2001; Hurwitz et al., 1998; Neptune et al., 2004; Perron et al., 2000; Whittle, 1996; Winby et al., 2009; Yu et al., 1997; Zajac et al., 2002, 2003). Ces études donnent les rotations tridimensionnelles de chacune de trois articulation inférieures (hanche, genou, cheville) presque à l'aide du même dispositif expérimental (stéréovision « caméra vidéo, marqueur»). Des travaux théoriques effectués par Anderson et Pandy.(2001) ont été traduits par une combinaison de la théorie d'optimisation dynamique et d'un modèle neuro-musculo-squelettique du corps humain (elle se concentre sur la partie du membre inférieur) qui est caractérisé par 23 degrés de

liberté et entouré par 54 unités musculaires. Le problème d'optimisation dynamique a été employé pour calculer les paramètres biomécaniques (cinématiques, cinétiques et activités musculaires) modélisant les différentes parties du cycle de marche sujet à une minimisation d'énergie métabolique qui est dépensée par une unité de distance de parcours. Tous les résultats calculés ont été comparés et validés par des résultats expérimentaux. La plupart des recherches expérimentales ou théoriques effectuées sur des individus sans pathologie ou historique pathologique ostéo-articulaires nous donne presque les même résultats cinématiques pour les différentes joints articulaires qui constituent le membre inférieur (Fig. 1.9).

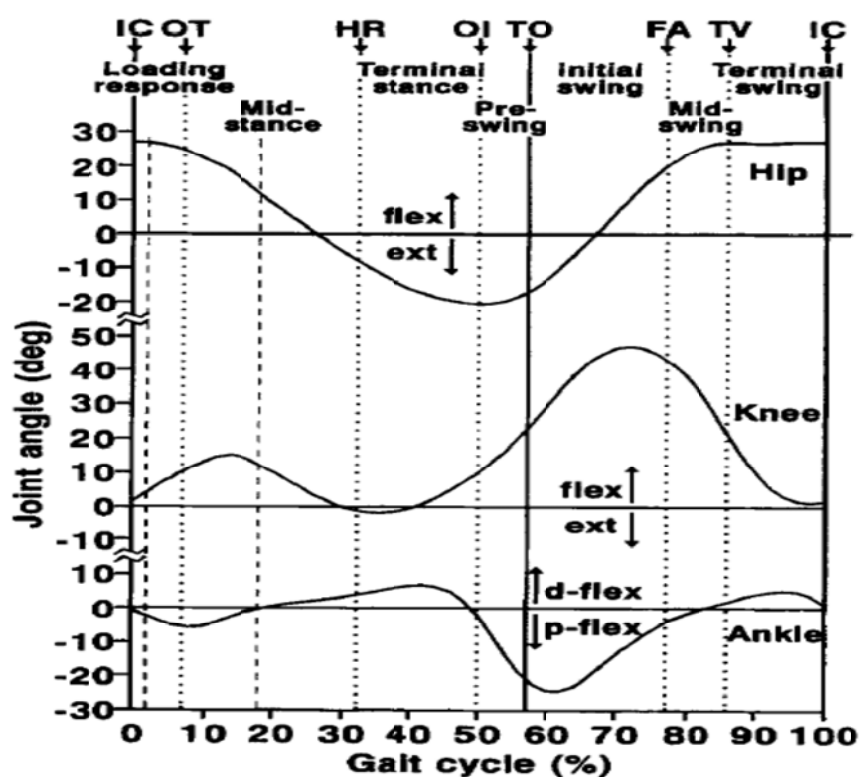


Figure 2-9: Mouvements angulaires dans le plan sagittal de la hanche, du genou et de cheville chez des individus normaux sur un cycle de marche unique ; OT, *opposite toe off*; HR, *heel rise*; OI, *opposite initial contact*; TO, *toe off*; FA, *feet adjac TV*, *tibia vertical* (Whittle, 1996).

Très peu d'études ont été effectuées pour déterminer la cinématique produite au joint tibiofemoral (déplacements relatifs du fémur par rapport au tibia). Parmi ces études, on considère les travaux de Lafortune et al.(1992) , et Li et al.(2009), qui ont mesuré à l'aide de la technique stéréovision la cinématique tridimensionnelle du joint du genou. Ils ont trouvé qu'il y a un déplacement relatif important produit entre le fémur et le tibia durant la phase de la marche

normale en palier. Ces translations sont pratiquement plus grandes du côté médial que celle du côté latéral durant la phase d'appui. L'un des problèmes les plus reconnus dans la recherche de la biomécanique de la marche est la variabilité qui est due au placement des marqueurs rétro-réfléchissants selon la peau et sur des repères anatomiques spécifiques (Gorton et al., 2009). Un placement incorrect du marqueur peut entraîner des erreurs allant de 20° à 25° dans les angles des articulations discrètes pendant la marche (Szczerbik and Kalinowska 2011; Groen et al., 2012). En plus, même si les testeurs sont très expérimentés (10 ans et plus), les différences inter-testeur vont de 2° à 6° dans les angles de pointe (Caravaggi et al., 2011; Wilken et al., 2012). Ce niveau d'erreur est inacceptable pour la recherche en biomécanique où les différences significatives peuvent être de quelques degrés seulement (McGinley et al., 2009). Ainsi, des nombreuses études dans la littérature ont montré qu'une altération majeure de la résistance passive du joint résulte en un faible changement des angles des rotations, particulièrement dans le plan frontal (Bendjaballah et al., 1997; Blankevoort et al., 1988; Markolf et al., 1981; Marouane et al., 2013).

L'outil cinématique décrit ci-dessus permet, à l'aide des techniques de mesures de forces et de moments de réaction au pied, aux cliniciens le calcul de ces moments articulaires. La force de la réaction au pied étant le sujet de plusieurs travaux. Parmi ces derniers on peut citer ceux de Hunt et al. (2006; 2001), Anderson and Pandy. (2001), McGowan et al. (2009), Shelburne et al. (2006). Par exemple, l'étude de Hunt et al. (2001) a mis l'accent sur la cinématique de joint du cheville par la comparaison de l'amplitude et les modes de déplacement du segment arrière-pied par rapport à la jambe, du segment avant-pied par rapport à l'arrière-pied et de la force de réaction du sol des mâles adultes normaux pendant la phase d'appui de la marche. Shelburne et al. (2006) ont montré que l'orientation de la force de réaction est le facteur principal du chargement de compartiment médial du plateau tibial durant la phase d'appui de la marche normale. La plupart de ces travaux montrent une évolution temporelle aléatoire périodique au cours de phase d'appui. Cette réaction augmente jusqu'à un maximum initial de réception et freinage, décroît, puis présente un second maximum de poussée et accélération. Sa valeur moyenne, lors de la phase d'appui, est de l'ordre de 9,5 N/kg du poids corporel, et l'intensité de chacune des deux maxima est plus élevée de 2,6 N/kg approximativement (Hunt et al., 2001) (Fig. 1.10).

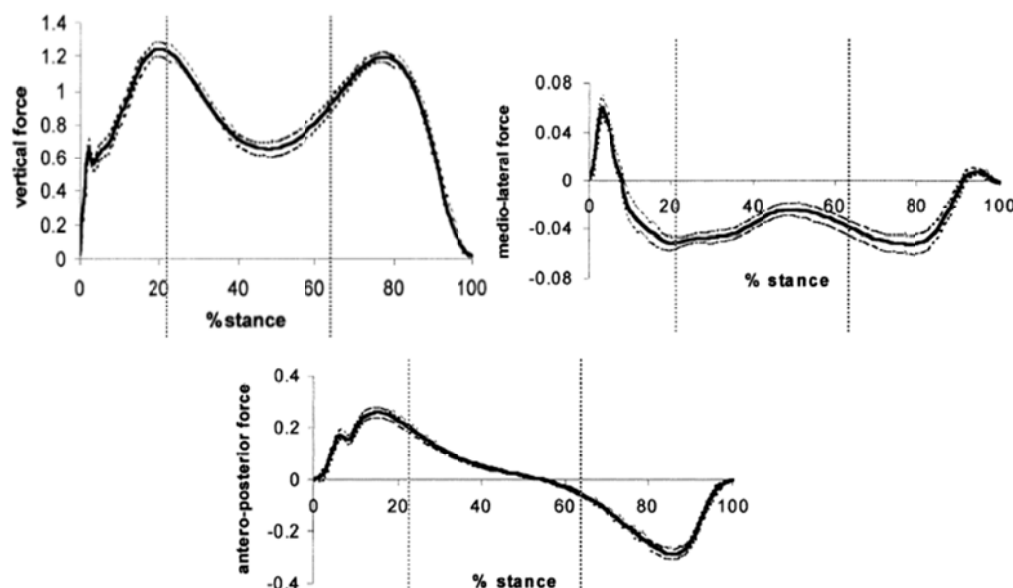


Figure 2-10: Force de réaction de sol mesurée par instrument expérimental (plate-forme de force) et normalisée par le poids du corps durant la phase d'appui chez des individus sains. (Hunt et al., 2001), (+ / postérieur et latéral).

Ces données citées précédemment sont indispensables pour implémenter un modèle de dynamique inverse. Ce modèle donne accès à une évaluation des forces et moments internes dans les articulations (cinétique). Des analyses cinétiques de membres inférieurs ont été réalisées par Eng et Winter.(1995) pendant la marche normale pour déterminer les informations complémentaires qui peuvent être acquises à partir d'un modèle de trois dimensions par rapport aux modèles planaires. Comme prévu, ils ont montré que la majeure partie du travail a été effectuée dans le plan de la progression, puisque le but de la locomotion est de soutenir le corps contre la gravité, tout en générant des mouvements qui propulsent le corps vers l'avant. De même, ils ont également montré que le seul travail important a été fait dans le plan frontal de la hanche lors de la marche (23% du travail total due à cette articulation). Ceci suggère que l'analyse cinétique en trois dimensions est nécessaire seulement pour l'articulation de la hanche à cause de la quantité importante du travail faite dans le plan frontal pour contrôler le bassin et le tronc contre les forces gravitationnelles.

Les travaux de Hurwitz et al.(1998) ont étudié la relation entre les charges dans le joint du genou et la distribution de la densité minérale dans les deux parties proximales médiale et latérale du l'os tibial. Ils ont trouvé une corrélation positive entre le moment d'adduction du genou

pendant la marche et le ratio de distribution d'os, ce qui montre que ce moment représente un outil prédictif important dans le chargement de deux compartiments du tibia. Ces prédictions sont en accord avec beaucoup de travaux qui trouvent que la plupart de la charge supportée par le joint tibio-fémoral passe par le plateau médial (Kim et al., 2009; Neptune et al., 2004; Shelburne et al., 2006; Wang et al., 1990; Weidenhielm et al., 1994; Winby et al., 2009; Yang et al., 2010). Alors qu'elles contredisent la proposition d'Eng et Winter. (1995) c.-à-d. la modélisation de joint de genou dans différents plans est obligatoire pour arriver à comprendre correctement le mécanisme de chargement de joint. Une étude effectuée par Kim et al. (2009) a testé la validité de la prévision de la charge calculée théoriquement dans le joint du genou durant la marche normale. Cette validité est basée sur la comparaison entre des mesures expérimentales sur des sujets avec des prothèses et des résultats calculés théoriquement à l'aide du modèle d'Anderson and Pandy. (2001). Un bon accord trouvé entre les forces de contacts calculées et les mesures dans les deux compartiments de plateaux tibiales avec un pourcentage d'erreur trouvé d'ordre 7%. Les recherches accentuées sur le déséquilibre des chargements, entre les deux plateaux tibiaux durant la marche normale sur des sujets sains, représente un outil explicatif de nombreuses pathologies affectant le joint de genou durant des activités quotidiennes (l'ostéoarthrite).

Un modèle d'éléments finis du joint tibiofémoral a été développé et employé pour analyser cette articulation durant la phase d'appui de la marche humaine (Mononen et al., 2013a; 2013b). Ce modèle est constitué de cartilages articulaires qui sont considérés comme des matériaux composites poroélastiques et des ménisques qui sont modélisés comme un matériau transversal isotrope élastique. La matrice et les fibres constituant les cartilages articulaires sont à la fois modélisés par un seul élément solide dans ce travail. Les objectifs de ces études sont la détermination des paramètres du contact et la répartition des contraintes et des déformations du cartilage articulaire durant la phase d'appui. Pour atteindre leurs objectifs, ils ont contrôlé le modèle du genou par la cinématique et la force axiale du joint tibiofémoral déterminées auparavant durant l'analyse de la marche. La non considération du joint patellofémoral et l'absence de composantes musculaires et ligamentaires durant les travaux de Mononen et al.(2013a;2013b) sont considérées comme des limitations majeur qui peuvent affecter leurs prédictions.

Récemment, une étude effectuée par Kutzner et al.(2010) a mesuré les composantes de forces de contact et de moments agissant sur le joint de genou chez 5 sujets in vivo par une

implémentation d'instrument sous le plateau tibial pour diverses activités quotidiennes. Ils ont trouvé que le plateau tibial durant la marche normale a une force de contact totale allant jusqu'à 261% BW (*Body Weight*) (Fig. 1.11). Cette technique a été utilisée ultérieurement pour tester la relation entre la charge excessive sur le plateau médial et le moment externe d'adduction (Meyer et al., 2013; Walter et al., 2010; Winby et al., 2013), puisque ce moment articulaire a été considéré pour certaines références (Zhao et al., 2007) comme un indicateur sur l'évolution de l'ostéoartrite.

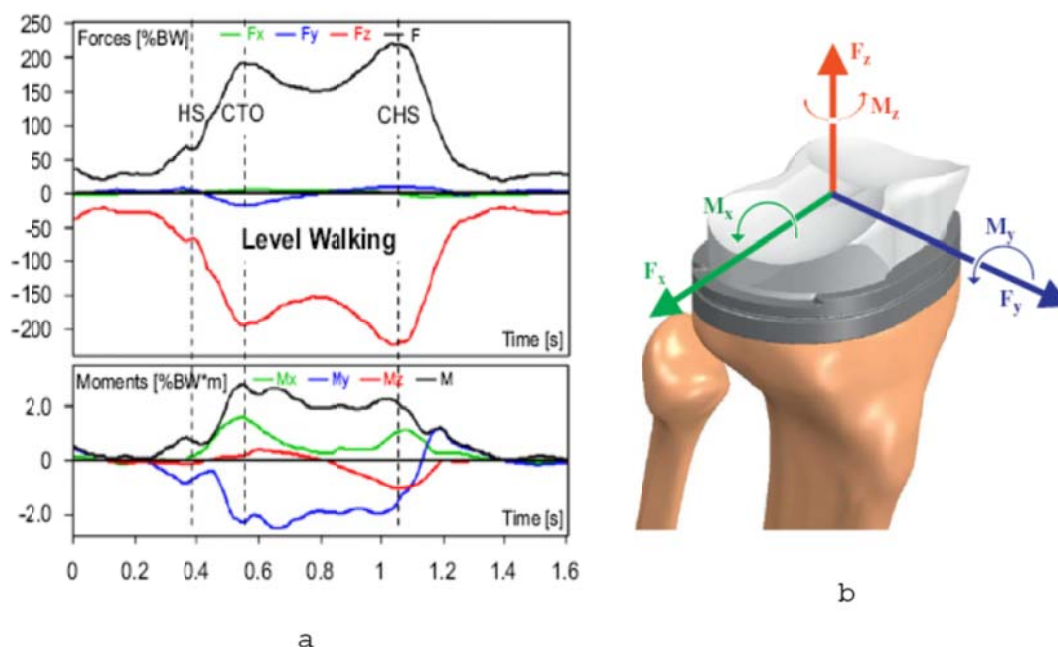


Figure 2-11: (a) les variations des forces et des moments dans l'articulation de genou durant la marche, (b) le système de coordonnées pour le plateau tibial instrumenté (Kutzner et al., 2010)

Le changement dans les tendances cinématique et cinétique du joint de genou dû à l'altération de la vitesse de la marche normale a été étudié par Holden et al. (1997) pendant la phase d'appui. Une différence remarquable produite seulement au niveau des vitesses très lentes (0.33 et 0.67 m/s), traduite par un faible angle et moment de flexion, ceci induit une puissance faible sur presque 80% de la phase d'appui. À cette vitesse, la plupart des sujets participant à cette étude ont un moment qui ne peut pas être classé principalement avec confiance comme fléchisseurs ou extenseurs.

Les activités musculaires durant la marche humaine représentent un facteur très important pour les chercheurs. Ces activités musculaires ont été évaluées soit *in vivo* avec des mesures directes de l'activité électromyographie (EMG) ou par des modèles biomécaniques utilisant l'optimisation ou les données EMG (Anderson and Pandy, 2001; Besier et al., 2009; Heiden et al., 2009; Kim et al., 2009; Neptune et al., 2004; Piazza, 2006; Shelburne et al., 2004; Shelburne et al., 2005, 2006; Zajac et al., 2002, 2003). Une étude récente effectuée par Winby et al.(2009), a utilisé un modèle *EMG-Driven* pour examiner les contributions des forces musculaires aux chargements du compartiment médial et latéral du genou pendant la marche normale. Ce modèle considère l'articulation du genou comme un joint pivot rigide. La détermination des forces de contact médial et latéral est basée sur l'équilibre de moment résiduel dans le plan frontal (différence entre le moment externe et le moment musculaires). Contrairement aux études précédentes, les résultats indiquent que le compartiment médial ne porte pas la majorité de la charge au cours de la phase d'appui. Les muscles assurent une stabilité suffisante pour contrebalancer la tendance du moment d'adduction externe (décharger le compartiment latéral). Cette stabilité est principalement fournie par les quadriceps, le *hamstring* et le *gastrocnémiens*, aussi bien par la contribution du tenseur fasciae-latae qui est significative. Les valeurs de forces musculaires trouvées ont été en bon accord avec les travaux effectués par Besier et al.(2009) qui ont utilisé la même technique de calcul, mais, cette fois juste pour étudier l'effet des forces musculaires sur des sujets qui ont de douleur dans la jointure patello-fémorale. Heiden et al.(2009) ont montré que les activités des muscles latéraux sont plus élevées pour des sujets souffrant de l'ostéoartrite par rapport aux sujets normaux. Ce résultat est corroboré par les travaux de Astephen et al.(2008a; 2008b) qui ont étudié l'effet de la sévérité de l'ostéoartrite sur les changements des facteurs biomécaniques de trois joints de membres inférieurs (hanche, genou, cheville). Cette corrélation a été claire par l'augmentation du moment d'adduction externe dans l'articulation de genou.

Un faible chargement, subi par le joint patello-fémorale durant la marche normale, est dû principalement au faible moment calculé dans le joint du genou à des angles élevés de flexion, tel que, quand la valeur maximale de ce moment est produit à 20°, alors la force de réaction dans le joint patello-fémorale est très faible. Reilly et Martens.(1972) ont arrivé à cette conclusion après une estimation de 0.5 BW en moyenne de la force de réaction patello-fémorale chez des individus normaux. Ces résultats sont en accord avec les travaux de Mason et al.,(2008) qui ont trouvés que

la force de contact dans le joint patello-fémorale varie entre 0 et 0.8BW durant la marche normale. D'autre part, la marche n'est pas une préoccupation majeure pour le joint patello-fémoral.

Un faible nombre de travaux de recherche a été effectué pour estimer la force dans le ligament croisé antérieur (LCA) durant la marche normale (Andriacchi and Dyrby, 2005; Beard et al., 1996; Liu and Maitland, 2000), par exemple les travaux de Shelburne et al.(2004). Cette étude a pour objectif le calcul et l'explication de la variation temporelle de force subite par le ligament croisé antérieur (LCA) lors de la marche normale. Le calcul est passé par deux étapes nécessaires: D'abord, le calcul des paramètres cinématiques, cinétiques et musculaires entourant le joint de genou à l'aide des techniques décrites ci-dessus (modèle musculo-squelettique, optimisation dynamique). Ensuite, ces données ont été employées comme un input pour un modèle 3D plus détaillé du joint du genou en tenant compte de la structure passive qui l'entoure. Ce modèle a permis de déterminer les positions relatives dans le joint tibiofemoral et les forces dans tous les ligaments entourant le joint de genou. Dans le début de la phase d'appui, la force de cisaillement antérieure du tendon rotulien domine sur la force de cisaillement totale appliquée sur le joint, ceci va transmettre une charge élevée dans le ligament croisé antérieur (303N). Contrairement au début de la phase d'appui, la fin de cette dernière est caractérisée par un faible chargement de ligament croisé antérieur. La considération du joint du genou comme un joint pivot rigide et le calcul séquentiel de forces ligamentaires ont représentés des limitations majeures dans ladite étude. Récemment, Yang et al.(2010) ont étudié les variations des forces ligamentaires durant la phase d'appui à l'aide d'un modèle d'éléments finis 3D du joint tibiofemoral. Une technique de réduction a été utilisée dans cette étude pour déterminer les forces musculaires qui sont considérées par la suite comme des forces externes appliquées sur le modèle du genou. Leurs résultats montrent une tendance inverse des résultats trouvés par Shelburne et al.(2004), où la force dans le ligament croisé antérieur augmente durant la phase d'appui et atteint son maximum à la fin de cette phase (500N). Cette différence est probablement due à l'absence d'une modélisation adéquate des composantes musculaires dans les travaux de Yang et al.(2010).

2.3 Objectifs

La revue de la littérature nous a permis d'avoir une vue d'ensemble sur les travaux expérimentaux et théoriques prenant comme sujet l'étude du genou humain d'une façon générale

ou durant l'exécution de la marche humaine. En effet, les études expérimentales ont pris en considération une multitude d'axes de recherche, telles que, la détermination d'activités musculaires, cinématiques du joint et la force de contact. Ces dernières ont été essentielles à l'amélioration du modèle théorique qui représente une alternative fiable afin d'étudier le phénomène de la marche normale.

Le résumé de la revue bibliographique sur la marche humaine montre l'absence d'une étude complète du genou durant l'exécution de ce type de pratique quotidien qui tient compte de tous les paramètres conduisant à le décrire fidèlement. À cause de ce manque de modélisation adéquate du genou humain durant l'application de la marche, ce travail envisage de développer un modèle valide qui prend en considération le comportement passif et actif simultanément de l'articulation du genou durant l'activité de la marche humaine. Ce modèle est développé par Bendjaballah et al.(1995) et amélioré par Moglo et Shirazi-Adl.(2003a) , Mesfar et Shirazi-Adl.(2005) et Shirazi et al.(2008). Aussi, ce travail envisage d'abord à analyser l'articulation de genou dans des conditions altérées par la maladie ostéoarticulaire (l'ostéoarthrite), ensuite, à tester la validité de technique de minimisation de la charge tibial médiale, enfin, à vérifier la relations entre les activités musculaires et les forces ligamentaires, particulièrement la relation entre les muscles de *gastrocnemius* et le LCA. Compte tenu de ces objectifs et afin de pouvoir les réaliser, le travail suit alors les grandes lignes suivantes :

1) Modifier en première étape l'état initial de propriétés de matériaux du cartilages articulaires (Shirazi et al., 2008) qui est presque incompressible à un état équivalent compressible hyper-élastique afin d'atteindre un taux de convergence acceptable.

2) Modifier le modèle existant en ajoutant les muscles de la cheville et les muscles *gastrocnemius* aux articulations du genou.

3) Étudier la réponse biodynamique complète du genou humain durant la marche normale avec des données provenant de sujets sains sans aucun historique pathologique pris de la littérature (Astephen et al., 2008a; 2008b; Hunt et al., 2001). Puis, valider les résultats avec les mesures disponibles. Deux sous étapes ont été considérées ici, (1) Étudier l'équilibre de l'articulation de cheville (considérer comme un joint sphérique) pour déterminer les forces musculaires poly-articulaires et les utiliser comme des actionnaires externe sur l'articulation de

genou. (2) faire des calculs itératifs des forces musculaires entourant l'articulation de genou par le principe de l'optimisation et l'analyse non-linéaires de la structure.

4) Étudier l'impact de considération de l'équation d'équilibre de l'articulation de la hanche simultanément avec l'articulation de genou et cheville sur la réponse globale et locale du genou humain durant la phase d'appui de la marche. Cette partie a pour but de comparer les prédictions de deux modèles au niveau de l'articulation de genou; modèle (1) est le modèle qui été utilisé pour accomplir l'objectif 3 indiqué précédemment et qui est constitué de deux articulations seulement (cheville, genou) et le modèle (2) est un modèle musculo-squelettique complet de membre inférieur du corps humain qui est constitué de deux joints sphériques rigides (cheville et hanche) est un joint déformable en comportement passif presque réel.

5) Étudier l'effet de la maladie ostéoarticulaire comme l'ostéoarthritis (en modifiant les propriétés des cartilages et des ménisques) sur les réponses musculaires et aussi sur les réponses passives d'articulations (ligaments, cartilages, ménisques).

6) Étudier la sensibilité du joint du genou sous différentes angles et moments d'adduction (varus).

7) Finalement, étudier l'effet de l'altération de l'activité des muscles de *gastrocnemius* sur les réponses active (muscles) et passive de l'articulation de genou, particulièrement le ligament croisé antérieur (LCA) durant la marche humaine, lorsque ce muscle est en plein activité et aussi durant une flexion de joint de 0° à 90° .

2.4 Plan de thèse

Les articles suivants ont été publiés ou soumis pour publication au cours de mes études doctorales:

Adouni, M., Shirazi-Adl, A., Shirazi, R., 2012. Computational biodynamics of human knee joint in gait: From muscle forces to cartilage stresses. *Journal of Biomechanics*. 45(12):2149-56.

Adouni, M., Shirazi-Adl, A., 2013. Consideration of equilibrium equations at the hip joint alongside those at the knee and ankle joints has mixed effects on knee joint response during gait. *Journal of Biomechanics*. 46(3):619-24.

Adouni, M., Shirazi-Adl, A., 2014. Evaluation of Knee Joint Muscle Forces and Tissue Stresses-Strains During Gait in Severe OA Versus Normal Subjects. *Journal of Orthopedic Research*, 32, 69-78.

Adouni, M., Shirazi-Adl, A., 2014. Partitioning of Knee joint Internal forces in Gait is dictated by the Knee Adduction Angle and not by the Knee Adduction Moment. *Journal of Biomechanics* 47:1696-1703.

Adouni, M., Shirazi-Adl, A., 2014. Gastrocnemius as ACL Antagonist: Analysis of the role of Gastrocnemius activation on knee biomechanics in gait and in flexion. Submitted in *Computer Methods in Biomechanics and Biomedical Engineering* (Février -2014).

**CHAPITRE 3 ARTICLE 1: COMPUTATIONAL BIODYNAMICS OF
HUMAN KNEE JOINT IN GAIT: FROM MUSCLE FORCES TO
CARTILAGE STRESSES**

Adouni, M¹; Shirazi-Adl, A¹; Shirazi, R²

¹Division of Applied Mechanics, Department of Mechanical Engineering

École Polytechnique, Montréal, Québec, Canada

²Department of Bioengineering and Whitaker Institute of Biomedical Engineering, University of
California–San Diego, San Diego, California

Article published in

Journal of Biomechanics 2012

Volume 45, Issue 12, Pages 2149-2156.

Keywords: Gait, Knee joint, Finite element method, Cartilage, Muscle forces, Ligaments

3.1 Abstract

Using a validated finite element model of the intact knee joint we aim to compute muscle forces and joint response in the stance phase of gait. The model is driven by reported *in vivo* kinematics-kinetics data and ground reaction forces in asymptomatic subjects. Cartilage layers and menisci are simulated as depth-dependent tissues with collagen fibril networks. A simplified model with less refined mesh and isotropic depth-independent cartilage is also considered to investigate the effect of model accuracy on results. Muscle forces and joint detailed response are computed following an iterative procedure yielding results that satisfy kinematics/kinetics constraints while accounting at deformed configurations for muscle forces and passive properties. Predictions confirm that muscle forces and joint response alter substantially during the stance phase and that a simplified joint model may accurately be used to estimate muscle forces but not necessarily contact forces/areas, tissue stresses/strains, and ligament forces. Predictions are in general agreement with results of earlier studies. Performing the analyses at 6 periods from beginning to the end (0%, 5%, 25%, 50%, 75% and 100%), hamstrings forces peaked at 5%, quadriceps forces at 25% whereas gastrocnemius forces at 75%. ACL Force reached its maximum of 343 N at 25% and decreased thereafter. Contact forces reached maximum at 5%, 25% and 75% periods with the medial compartment carrying a major portion of load and experiencing larger relative movements and cartilage strains. Much smaller contact stresses were computed at the patellofemoral joint. This novel iterative kinematics-driven model is promising for the joint analysis in altered conditions.

3.2 Introduction

Activities of daily living such as walking and stair climbing impose relatively large loads and movements on the human knee joint. This mechanical burden increases in many occupational and recreational tasks causing injuries and degenerations in joint ligaments, menisci, cartilage and bone. Any failure, degeneration or alteration in one of these components influences the response of the entire joint and likely increases the risk of further perturbations (Moglo and Shirazi-Adl, 2005). Effective preventive and conservative/surgical managements of joint disorders depend hence on a sound knowledge of stress and strain distributions in various components under both intact and altered conditions. These values, in turn, are heavily dependent not only on external loads and inertial forces but on muscle activities across the joint. As such,

accuracy in estimation of muscle forces has a direct bearing on the reliability of stresses and strains. Since direct *in vivo* measurements of tissue stresses and muscle forces remain invasive and likely impossible, computational modeling is recognized as a vital complementary tool to estimate multiple variables of interest. Due to technical difficulties in measurements and consideration of physiological loads and motions, *in vitro* testing is also limited especially when looking for cartilage/meniscus stresses/strains and ligament forces.

Using instrumented knee implants, efforts have been directed to *in vivo* measurement of loads on the knee joint of subjects in daily activities (Kutzner et al., 2010). Forces up to ~3 times body weight have been recorded in walking. These measured data, though very valuable, are however collected on implanted joints and not intact ones. Moreover, they are restricted to the load components transmitted via the implant itself. Mathematical modeling along with joint kinematics and ground reaction forces are combined with such measurements to estimate muscle, compartmental, and ligament forces (Anderson and Pandy, 2001; Delp et al., 2007; Kim et al., 2009; Lin et al., 2010; Shelburne et al., 2004; Zhao et al., 2007). To gain further insight into biomechanics of the joint during gait, some recent works have employed MRI, video motion systems and fluoroscopy to estimate changes in ACL length, contact areas and cartilage thickness (Andriacchi et al., 2009; Coleman et al., 2011; Koo et al., 2011; Taylor et al., 2011) or to identify the effect of ACL-deficiency on joint kinematics (Chen et al., 2011). The medial plateau is found to experience larger tibiofemoral movements and cartilage strains.

In parallel, other studies have used 3D link-segment models (inverse dynamics and optimization) to predict load distribution between medial and lateral compartments as well as ligament forces during simulated gait (Shelburne et al., 2004; Shelburne et al., 2005, 2006). These models, however, explicitly neglect not only the compliant cartilage layers and menisci but the knee joint passive resistance. Similarly and using measured *in vivo* load in one subject with instrumented knee, joint contact forces have been estimated during the gait (Lin et al., 2010; Zhao et al., 2007). Simulating cartilage and menisci with linear elastic properties, a recent finite element (FE) model study in gait has on the other hand neglected joint rotations, redundancy in equations, patellofemoral joint, and out-of-sagittal plane moments (Yang et al, 2010).

Despite foregoing *in vivo* measurement and model studies, a detailed musculoskeletal FE model of the entire intact knee joint with depth-dependent nonlinear cartilage/meniscus properties

remains yet to be developed. This model study should provide important data during gait on not only the muscle forces but the ligament forces, contact stresses as well as stresses/strains within the cartilage and menisci. Such is the aim of the current study that is based directly on earlier developments, validations and applications of a detailed FE model of the knee joint (Adouni and Shirazi-Adl, 2009; Bendjaballah et al., 1995; Mesfar and Shirazi-Adl, 2006b; Moglo and Shirazi-Adl, 2005; Shirazi et al., 2008). In the current study, cartilage of both tibiofemoral (TF) and patellofemoral (PF) joints along with menisci are simulated as depth-dependent non-homogeneous composites enclosing nonlinear collagen fibril networks (Shirazi and Shirazi-Adl, 2009a, b; Shirazi et al., 2008). For the sake of comparison, a less-refined model with isotropic (no fibril networks) depth-independent cartilage is also considered. Both models incorporate the mean reported *in vivo* gait data on hip/knee/ankle joint moments/rotations (Astéphen et al., 2008a) and ground reaction forces (Hunt et al., 2001) of asymptomatic subjects. In this manner, biodynamics of gait during the stance phase, at both global musculature and local tissue-level, are investigated with iterative FE models of the knee joint and lower extremity that are driven by measured *in vivo* kinetics/kinematics. We hypothesize that (1) muscle activation levels and contact stresses/areas substantially alter during the stance phase and (2) in contrast to contact stresses/areas, ligament forces and tissue stresses/strains, the muscle forces can as accurately be estimated by the less complex FE model.

3.3 Methods

3.3.1 Finite Elements Model

The FE model includes bony structures (tibia, patella, femur), TF and PF joints, major TF (ACL, PCL, LCL, MCL) and PF (MPFL, LPFL) ligaments, patellar tendon (PT), as well as quadriceps (3 distinct muscles), hamstrings (3 muscles), gastrocnemius (2 muscles), tibialis posterior and soleus (Adouni and Shirazi-Adl, 2009; Shirazi et al., 2008) (see Fig. 2.1 for details). The bony structures are represented by rigid bodies due to their much higher stiffness (Donahue and Hull, 2002).

Muscle components are modeled by uniaxial elements with orientations at full extension taken from the literature. The Q angle model ($Q = 14^\circ$, (Sakai et al., 1996)) is used for quadriceps muscles; orientations relative to the femoral axis in frontal/sagittal planes are: RF-VIM $0^\circ/4^\circ$

anteriorly, VL 22° laterally/0° and VMO 41° medially/0°. Orientations for hamstrings muscles relative to the tibial axis, respectively for BF, SM, and TRIPOD are taken (Aalbersberg et al., 2005) as 11.8° medially, 7° laterally, and 7.1° medially in the frontal plane whereas 0°, 16.1°, and 18.7° posteriorly in the sagittal plane. Gastrocnemius fascicles are parallel to the tibial axis in the sagittal plane while oriented (GM) 5.3° medially or (GL) 4.8° laterally in the frontal plane (Delp et al., 2007; Hillman, 2003). Tibialis posterior/Soleus are oriented 5.3°/4.1° laterally and 1.0°/4° anteriorly relative to the tibial axis (Delp et al., 2007). Ligaments are each modeled by a number of uniaxial elements with different initial pre-strains, non-linear (tension-only) material properties, and initial cross-sectional areas of 42, 60, 18, 25, 99, 42.7 and 28.5 mm² for ACL, PCL, LCL, MCL, PT, MPFL, and LPFL, respectively (Mesfar and Shirazi-Adl, 2005).

Articular cartilage layers and menisci are modeled as depth-dependent composites of an isotropic bulk reinforced by networks of collagen fibrils. In the cartilage superficial zone, fibrils are oriented horizontally parallel to the surface whereas they become random in the transitional zone and then turn perpendicular in the deep zone anchoring into the subchondral bone. Membrane elements are used to simulate fibril networks in the superficial and deep zones while brick elements represent the transitional zone network. In menisci, collagen fibrils are primarily oriented in the circumferential direction within the bulk but have no preferred orientation on bounding surfaces (Shirazi and Shirazi-Adl, 2009a; Shirazi et al., 2008).

3.3.2 Material Properties

Depth-dependent isotropic hyperelastic (Ogden-Compressible) material properties are considered for non-fibrillar solid matrix of cartilage layers with the elastic modulus varying linearly from 10 MPa at the surface to 18 MPa at the deep zone and a Poisson's ratio of 0.49. In the short-term stance phase loading, this model with a compressible material is initially verified by additional simulations to be equivalent to the incompressible elastic model with much smaller moduli (in the range of 0.3-1.2 MPa) used earlier (Shirazi and Shirazi-Adl, 2009a; Shirazi et al., 2008). Compressible hyperelastic model was initially also employed for the non-fibrillar menisci but due to convergence problems at contact areas, the matrix of menisci was represented, similar to our earlier studies (Mesfar and Shirazi-Adl, 2005), by a compressible elastic material with a Young's modulus of 10 MPa and a Poisson's ratio of 0.45.

For cartilage collagen fibrils volume fractions, 15% is considered in the superficial region, 18% in the transitional region, and 21% in the deep zone. Thicknesses of these zones are, respectively, 15%, 22.5%, and 62.5% of the total value at each point. In the menisci, the collagen content is 14% in the circumferential direction and 2.5% in the radial direction of the bulk region along with 12% in the outer surfaces at both directions (Shirazi and Shirazi-Adl, 2009b; Shirazi et al., 2008).

For the sake of comparison with this depth-dependent fibril reinforced model, another less-refined model with isotropic representation of cartilage layers, similar to the earlier generation of our model (Bendjaballah et al., 1995; Mesfar and Shirazi-Adl, 2006b, 2008b), is also used. The differences are limited to the less refinement of cartilage/menisci meshes as well as the depth-independent isotropic (modulus of 12 MPa and Poisson's ratio of 0.45) representation of cartilage layers.

3.3.3 Muscle Force Estimation

An optimization technique is used to evaluate unknown muscle forces at each instance of stance phase. Cost function of the sum of cubed muscle stresses (Eq. 1) (Arjmand and Shirazi-Adl, 2006) is used along with inequality equations on muscle forces remaining positive and larger than their passive forces but smaller than the sum of their passive and maximum active forces (Eq. 3). The passive forces are neglected due to the expected negligible increases in muscle lengths while the maximum active stress is taken as 0.6 MPa (Arjmand and Shirazi-Adl, 2006). Prescribed joint rotations generate 3 moment equilibrium equations that act as constraints (Eq. 2).

$$Cost\ Function = \sum_{i=1}^n \left(\frac{F_i}{PCSA_i} \right)^3 \quad (Eq.1)$$

$$\sum_{i=1}^n r_{ij} \times F_{ij} = M_{j\{1,2,3\}} \quad (Eq.2)$$

$$F_{pi} \leq F_i \leq (F_{pi} + \sigma_{i\max} \times PCSA_i) \quad (Eq.3)$$

With F_i , F_{pi} , r_{ij} , $\sigma_{i\max}$, $PCSA_i$ being the force, passive force component, lever arms in different planes, maximum stress, and physiological cross-sectional areas of muscle i (Delp et al., 2007), respectively. M_j are required moments computed in the FE model under prescribed rotations.

3.3.4 Loading, Kinematics and Boundary Conditions

The hip/knee/ankle joint rotations/moments and ground reaction forces at foot during the stance phase (Fig. 2) are taken from the mean data of *in vivo* measurements on asymptomatic subjects during gait (Astefphen et al., 2008a; Hunt et al., 2001). The location of resultant ground reaction force at each instant is determined so as to generate reported joint moments (Astefphen et al., 2008a) accounting for the leg/foot weight (29.78 N/7.98 N). Non-orthogonal local joint coordinate systems (Grood and Suntay, 1983) are considered in compliance with prescribed rotations (Astefphen et al., 2008a). Since our model was constructed based on a female knee joint, a body weight of BW=606.6 N (61.9 kg) is considered (De Leva, 1996). Analyses are carried out at 6 time instances corresponding to HS (heel strike), 5%, 25%, 50%, 75%, and TO (toe-off) of stance phase (Fig. 2.2). At each period the femur is initially fixed in its instantaneous position while the tibia and patella are completely free except for the prescribed TF rotations.

At each stance period under associated prescribed TF rotations (Fig. 2.2), ground reaction forces (Fig. 2), leg/foot weight, and GL/GM forces (already evaluated via equilibrium of moments at the ankle joint alongside tibialis posterior and soleus muscles), unknown forces in remaining muscles are iteratively estimated. This is done by initially evaluating muscle forces (Eqs. 1-3) counterbalancing required moments in the deformed configuration. These forces are subsequently applied in the model as additional external loads and the procedure is repeated (8-12 iterations) till convergence is reached; when unbalanced required moments fall below 0.1 Nm. In this manner, both kinematics and kinetics conditions are simultaneously satisfied while accounting for the penalty of muscle forces and the joint passive resistance. Matlab (R2009a Optimization Toolbox, genetic algorithms) and ABAQUS 6.10.1 (Static analysis) commercial programs are used iteratively at each phase.

3.4 Results

Muscle forces in GL and GM initiated at 25% and reached their maximum, respectively of 0.29 BW and 0.88 BW, at 75% period (Fig. 2.3). Quadriceps forces peaked at 25% (Fig. 2.3) with the RF-VI carrying the largest portion at 0.74 BW compared to 0.58 BW in VL and 0.40 BW in VM. The PT force followed similar trend reaching maximum of 1.56 BW at 25% (Fig. 2.3). While resisting the adduction moment (Fig. 2.2), BF muscle peaked at 1.00 BW at 5% (Fig. 2.3). Almost the same muscle forces were computed in the simplified (isotropic cartilage) model (max difference of 0.02 BW).

Among ligaments, ACL force was the largest followed by the LCL and MCL while PCL remained unloaded throughout and PF ligaments resisted small forces (each <20 N). ACL Force (PL bundle only) increased from 231 N at HS to its peak of 343 N at 25% and decreased thereafter (Fig. 4). The MCL was loaded only at HS and 5% period, while in contrast the LCL was primarily loaded at TO (Fig. 2.4). Use of the simplified model markedly influenced ligament forces; e.g., peak ACL force dropped to 275 N at 25% while peak LCL force increased to 238 N at TO (Fig. 4).

Except at the HS and 5% period, the medial plateau carried much larger forces than the lateral one with peaks at 25% and 75% periods (Fig. 2.5). The load was transmitted primarily through the uncovered areas (via cartilage-cartilage) (Fig. 2.5). The TF contact area reached also its maximum at 25% (922 mm²) and 75% (1017 mm²) periods (Fig. 2.6). The PF contact force and area followed the same trend as quadriceps forces and reached their peak at 25% period; 459 N and 232 mm². Large differences were computed when using the less refined model with isotropic cartilage; TF contact forces were smaller (by 5.4 % at 25%) while contact areas were larger (by 168 mm² or 18.2 % at 25% and 206 mm² or 20.2% at 75%) (Fig. 2.6).

In accordance with the compartmental loads (Fig. 2.5), contact pressures were much larger on the medial plateau where they shifted posteromedially during the stance and reached their peak of 8.1 MPa at 25% period (Fig. 2.7). Tensile strains were also larger in the cartilage of the medial plateau reaching greater values at deep fibril networks (peak of 16% at 25% period) (Fig. 2.8). The simplified isotropic model computed smaller contact pressures at TF and PF contact areas (by 19 % for mean pressure and 30 % for peak pressure).

3.5 Discussion

A novel passive-active FE model of the lower extremity is developed to predict the global-local biodynamics of the knee joint during stance phase of gait. The model accounts for major muscle groups crossing the joint and represents the cartilage and menisci as depth-dependent nonlinear non-homogeneous composites with collagen fibril networks. It is driven by in vivo measured hip/knee/ankle kinematics (Astefan et al. 2008a) and ground reaction forces (Hunt et al., 2001) reported for asymptomatic subjects. Muscle forces and joint detailed response are computed following an iterative procedure yielding results that satisfied kinematics/kinetics constraints while accounting at deformed configurations for the muscle forces as well as nonlinear passive properties. A simplified model of the joint with less refined mesh and isotropic depth-independent cartilage layers is also considered to investigate the effect of model accuracy on results. Predictions confirm the hypotheses in that (1) muscle forces and detailed joint response alter substantially during the stance phase and (2) a simplified joint model may accurately be used to estimate muscle forces but not necessarily contact forces/areas, tissue stresses/strains, and ligament forces.

In accordance with our earlier investigations (Shirazi et al., 2008), the transient response of the cartilage and menisci under higher strain rates during the gait can accurately be captured either by a biphasic analysis or equivalently by an incompressible elastic analysis using similar equilibrium moduli. In this study, however and due to convergence difficulties, a compressible model with much larger elastic moduli varying linearly from 10 MPa at the surface to 18 MPa at the deep zone and a Poisson's ratio of 0.49 are employed. These values were chosen after extensive preliminary parametric studies on the entire joint in axial compression while matching results of the model with incompressible materials for soft tissues (Shirazi et al, 2008).

Muscle forces in this work are estimated while satisfying the moment equations at both the ankle and knee joints. The knee joint muscles that cross the hip, however, should also participate in similar equations at the hip joint. To assess the extent of changes had the hip joint moment equations been considered simultaneously alongside those at the knee and ankle joints, the model was extended to account for the hip joint muscles (Delp et al., 2007) and moments (Astefan et al., 2008a). Preliminary results so far (not presented here) have shown relatively

small changes ($<10\%$) in estimated muscle forces when the hip joint is included. Presentation and discussion of these results will be the subject of a future work.

Earlier model studies of the knee joint during walking have neglected the joint passive resistance when computing muscle forces (Shelburne et al., 2005, 2006). Ligaments, menisci and articular surfaces contribute to the passive moment carrying capacity of the joint that is expected to increase in compression. These passive moments tend to support a portion of net external moments and thus reduce required muscle forces. Precise quantification of the joint passive resistance under various compression forces needs however separate studies that are currently underway. Differences between the applied moments (i.e., inverse dynamics) and moments resisted by muscles at the final converged solution indicate passive joint flexion, adduction and internal moments of, respectively, 6.5, 9.0, and 2.1 Nm at 25% period and 5.2, 10.8, and 2.0 Nm at 75% period of stance phase.

Comparison of results when using a simplified model with less refined mesh and isotropic homogeneous cartilage layers instead of a refined mesh with depth-dependent cartilage properties and collagen fibrils networks demonstrate negligible changes in estimated muscle forces (<0.02 BW). Forces in ligaments and contact forces/stresses/areas are however altered. The contact stresses and areas are naturally affected due both to the refinement and more realistic presentation of cartilage itself. Use of the simplified model is hence justified when looking for the overall response and muscle forces. Future simulations of joint disorders (i.e., ligament injuries, cartilage defects and degenerations) justify also the use of the detailed model of the joint. It is to be emphasized that alterations in the input kinematics/kinetics, material and structural properties as well as joint flexion axis considered in this study likely influence the results the extent of which can only be quantified by proper sensitivity analyses (Daher et al., 2010; Moglo and Shirazi-Adl, 2005).

Predicted activation levels in quadriceps and gastrocnemius muscles are in satisfactory agreement with values in the literature (Besier et al., 2009; Lin et al., 2010; Neptune et al., 2004; Shelburne et al., 2005; Winby et al., 2009) and follow the same relative trends as measured EMG activities (Astéphen, 2007). The computed hamstring forces peaked right after the HS at 5% period (Fig. 2.3). Reported normalized EMG activities in the superficial lateral and medial hamstrings (Astéphen et al., 2007) are also highest right at the HS and decrease thereafter (Fig.

2.2d). Additional FE analyses at 75% stance period demonstrate that had we totally neglected the soleus muscle contribution to resist flexion at the ankle joint, we would have a substantial drop in BF activity (from 381 N to 181 N) at the expense of significant increases in GL and GM forces (from 710 N to 1512 N) as well as in quadriceps forces (from 4 N to 299 N). Such drop in BF force appears to further improve agreement with reported negligible hamstrings EMG in the 2nd phase of stance (Fig. 2d). Comparisons between estimated muscle forces and recorded EMG data should however also account for the (a) absence of coactivity in the model in order to enhance joint stability and control, (b) lack of consideration for hip moment equations when computing knee muscle forces, and (c) inherent limitation of select surface electrodes in measuring EMG data especially of deeper hamstrings muscles (e.g., BF short head).

As a consequence of relatively small flexion angles during the stance, the quadriceps muscle forces remain nearly equal to PT forces with a ratio of ~ 0.95 . These PT forces, in turn and due to their anterior orientation, pull the tibia anteriorly that increases ACL force (Fig. 2.4). With the drop in PT force, the anterior shear force and hence ACL force decrease at the later periods of the stance phase. Bursts of activity in GM and GL, especially at 75% stance period, tend to markedly decrease hamstrings forces and as a result increase ACL forces. Similar variations have been reported in earlier model studies (Shelburne et al. (2004; 2005, 2006). As expected and under these conditions, PCL remain slack. The large force in the LCL at TO period is due to the joint adduction angle and activities in medial hamstrings in response to the joint small abduction moment (Fig. 2.2).

Due to the adduction moment on the joint, the medial compartment carries the major portion of compression at all instances except the HS and 5% period (Fig. 2.5). These forces, at both plateaus, are transmitted primarily at uncovered areas via cartilage-cartilage interfaces. The disproportionate partition of load between TF compartments is corroborated by earlier works (Andriacchi et al., 2009; Hurwitz et al., 1998; Kutzner et al., 2010; Neptune et al., 2004; Shelburne et al., 2006; Thambyah, 2007; Zhao et al., 2007). In comparison, relatively low contact forces are computed at the PF joint that is due to the small joint flexion angles during the stance phase. The gait loading has not indeed been identified as a major concern for the PF joint (Mason et al., 2008).

Contact stresses as well as cartilage stresses/strains are influenced by compartmental loads. Cartilage on the medial compartment experiences greater compressive stresses/strains as well as a posterior shift in the contact area (Figs 7 and 8). In corroboration, Koo et al. (2011) and Coleman et al. (2011) recorded during walking larger decreases in the cartilage thickness and greater posterior movements on the medial plateau compared with the lateral one. Noteworthy are the relatively large tensile strains computed in the deep vertical fibril networks of the medial cartilage under the contact region. These strains are even larger than those in the superficial horizontal fibril networks at the same region. The crucial role of deep fibril networks in the load bearing of the cartilage has been demonstrated (Shirazi et al., 2008). These results may explain the frequent observation of the joint osteoarthritis at the medial compartment (Engh, 2003; Sharma et al., 2000).

In summary, the current novel iterative kinematics-driven FE model that accounts for the synergy between passive structures and active musculature of the knee joint was used to determine muscle forces and tissue stresses/strains during the gait. Future works will consider gait of symptomatic subjects with ACL injury and/or OA that should shed further light on biodynamics of the joint in normal and perturbed conditions.

3.6 Acknowledgement

The work is supported by a grant from the Natural Sciences and Engineering Research Council of Canada (NSERC-Canada) and a scholarship from the University Mission of Tunisia in North America (MUTAN-Tunisia).

3.7 References

- Aalbersberg, S., Kingma, I., Ronsky, J.L., Frayne, R., van Dieen, J.H., 2005. Orientation of tendons in vivo with active and passive knee muscles. *Journal of Biomechanics* 38, 1780-1788.
- Adouni, M., Shirazi-Adl, A., 2009. Knee joint biomechanics in closed-kinetic-chain exercises. *Computer Methods in Biomechanics and Biomedical Engineering* 12, 661.
- Anderson, F.C., Pandy, M.G., 2001. Dynamic optimization of human walking. *Journal of Biomechanical Engineering* 123, 381.
- Andriacchi, T.P., Koo, S., Scanlan, S.F., 2009. Gait mechanics influence healthy cartilage morphology and osteoarthritis of the knee. *The Journal of Bone and Joint Surgery. American volume*. 91, 95.
- Arjmand, N., Shirazi-Adl, A., 2006. Sensitivity of kinematics-based model predictions to optimization criteria in static lifting tasks. *Medical engineering & physics* 28, 504-514.
- Astephen, J.L., Deluzio, K.J., Caldwell, G.E., Dunbar, M.J., 2008a. Biomechanical changes at the hip, knee, and ankle joints during gait are associated with knee osteoarthritis severity. *Journal of Orthopaedic Research* 26, 332-341.
- Bendjaballah, M., Shirazi-Adl, A., Zukor, D., 1995. Biomechanics of the human knee joint in compression: reconstruction, mesh generation and finite element analysis. *The knee* 2, 69-79.
- Chen, C.H., Gadikota, H.R., Hosseini, A., Kozanek, M., Van de Velde, S.k., Gill, T., Li, G., 2011. Tibiofemoral kinematics during the stance phase of gait in the normale and ACL defecient knees. *57th Annual Meeting of Orthopaedic Research Society*. Long Beach USA.
- Coleman, J.L., Widmyer, M.R., Leddy, H.A., Spritzer, C.E., Moorman, C.T., DeFrate, L.E., 2011. An In Vivo Tricompartmental Analysis of Diurnal Strains in Articular Cartilage of the Human Knee. *57th Annual Meeting of Orthopaedic Research Society*. Long Beach USA.

- De Leva, P., 1996. Adjustments to Zatsiorsky-Seluyanov's segment inertia parameters. *Journal of Biomechanics* 29, 1223-1230.
- Delp, S.L., Anderson, F.C., Arnold, A.S., Loan, P., Habib, A., John, C.T., Guendelman, E., Thelen, D.G., 2007. OpenSim: open-source software to create and analyze dynamic simulations of movement. *Biomedical Engineering, IEEE Transactions on* 54, 1940-1950.
- Donahue, T.L.H., Hull, M., 2002. A finite element model of the human knee joint for the study of tibio-femoral contact. *Journal of Biomechanical Engineering* 124, 273.
- Engh, G.A., 2003. The difficult knee: severe varus and valgus. *Clinical Orthopaedics and Related Research* 416, 58.
- Grood, Suntay, W.J., 1983. A joint coordinate system for the clinical description of three-dimensional motions: application to the knee. *Journal of Biomechanical Engineering* 105, 136.
- Hillman, 2003. *Interactive Functional Anatomy*, , London.
- Hunt, Smith, R.M., Torode, M., Keenan, A.M., 2001. Inter-segment foot motion and ground reaction forces over the stance phase of walking. *Clinical Biomechanics* 16, 592-600.
- Hurwitz, D.E., Sumner, D.R., Andriacchi, T.P., Sugar, D.A., 1998. Dynamic knee loads during gait predict proximal tibial bone distribution. *Journal of Biomechanics* 31, 423-430.
- Kim, H.J., Fernandez, J.W., Akbarshahi, M., Walter, J.P., Fregly, B.J., Pandy, M.G., 2009. Evaluation of predicted knee joint muscle forces during gait using an instrumented knee implant. *Journal of Orthopaedic Research* 27, 1326-1331.
- Koo, S., Rylander, J.H., Andriacchi, T.P., 2011. Knee joint kinematics during walking influences the spatial cartilage thickness distribution in the knee. *Journal of Biomechanics*.
- Kutzner, I., Heinlein, B., Graichen, F., Bender, A., Rohlmann, A., Halder, A., Beier, A., Bergmann, G., 2010. Loading of the knee joint during activities of daily living measured in vivo in five subjects. *Journal of Biomechanics* 43, 2164.
- Lin, Y.C., Walter, J.P., Banks, S.A., Pandy, M.G., Fregly, B.J., 2010. Simultaneous prediction of muscle and contact forces in the knee during gait. *Journal of Biomechanics* 43, 945-952.

- Mason, J., Leszko, F., Johnson, T., Komistek, R., 2008. Patellofemoral joint forces. *Journal of Biomechanics* 41, 2337-2348.
- Mesfar, W., Shirazi-Adl, A., 2005. Biomechanics of the knee joint in flexion under various quadriceps forces. *The knee* 12, 424-434.
- Mesfar, W., Shirazi-Adl, A., 2006. Knee joint mechanics under quadriceps-hamstrings muscle forces are influenced by tibial restraint. *Clinical Biomechanics* 21, 841-848.
- Mesfar, W., Shirazi-Adl, A., 2008. Knee joint biomechanics in open-kinetic-chain flexion exercises. *Clinical Biomechanics* 23, 477-482.
- Moglo, K., Shirazi-Adl, A., 2005. Cruciate coupling and screw-home mechanism in passive knee joint during extension-flexion. *Journal of Biomechanics* 38, 1075-1083.
- Neptune, R., Zajac, F., Kautz, S., 2004. Muscle force redistributes segmental power for body progression during walking. *Gait & Posture* 19, 194-205.
- Sakai, N., Luo, Z.P., Rand, J.A., An, K.N., 1996. Quadriceps forces and patellar motion in the anatomical model of the patellofemoral joint. *The knee* 3, 1-7.
- Sharma, L., Lou, C., Cahue, S., Dunlop, D.D., 2000. The mechanism of the effect of obesity in knee osteoarthritis: the mediating role of malalignment. *Arthritis & Rheumatism* 43, 568-575.
- Shelburne, K.B., Pandy, M.G., Anderson, F.C., Torry, M.R., 2004. Pattern of anterior cruciate ligament force in normal walking. *Journal of Biomechanics* 37, 797-805.
- Shelburne, K.B., Torry, M.R., Pandy, M.G., 2005. Muscle, ligament, and joint-contact forces at the knee during walking. *Medicine & Science in Sports & Exercise* 37, 1948.
- Shelburne, K.B., Torry, M.R., Pandy, M.G., 2006. Contributions of muscles, ligaments, and the ground reaction force to tibiofemoral joint loading during normal gait. *Journal of Orthopaedic Research* 24, 1983-1990.
- Shirazi, R., Shirazi-Adl, A., 2009a. Analysis of partial meniscectomy and ACL reconstruction in knee joint biomechanics under a combined loading. *Clinical Biomechanics* 24, 755-761.
- Shirazi, R., Shirazi-Adl, A., 2009b. Computational biomechanics of articular cartilage of human knee joint: Effect of osteochondral defects. *Journal of Biomechanics* 42, 2458-2465.

- Shirazi, R., Shirazi-Adl, A., Hurtig, M., 2008. Role of cartilage collagen fibrils networks in knee joint biomechanics under compression. *Journal of Biomechanics* 41, 3340-3348.
- Taylor , K.A., Cutcliffe , H.C., Queen, R.M., Terry, M.E., Utturkar, G.M., Spritzer, C.E., Garrett, W.E., DeFrate, L.E., 2011. Measurement of In Vivo ACL Elongation During Gait. . *57th Annual Meeting of Orthopaedic Research Society*. Long Beach USA.
- Thambyah, A., 2007. Contact stresses in both compartments of the tibiofemoral joint are similar even when larger forces are applied to the medial compartment. *The knee* 14, 336-338.
- Zhao, D., Banks, S.A., Mitchell, K.H., D'Lima, D.D., Colwell, C.W., Fregly, B.J., 2007. Correlation between the knee adduction torque and medial contact force for a variety of gait patterns. *Journal of Orthopaedic Research* 25, 789-797.

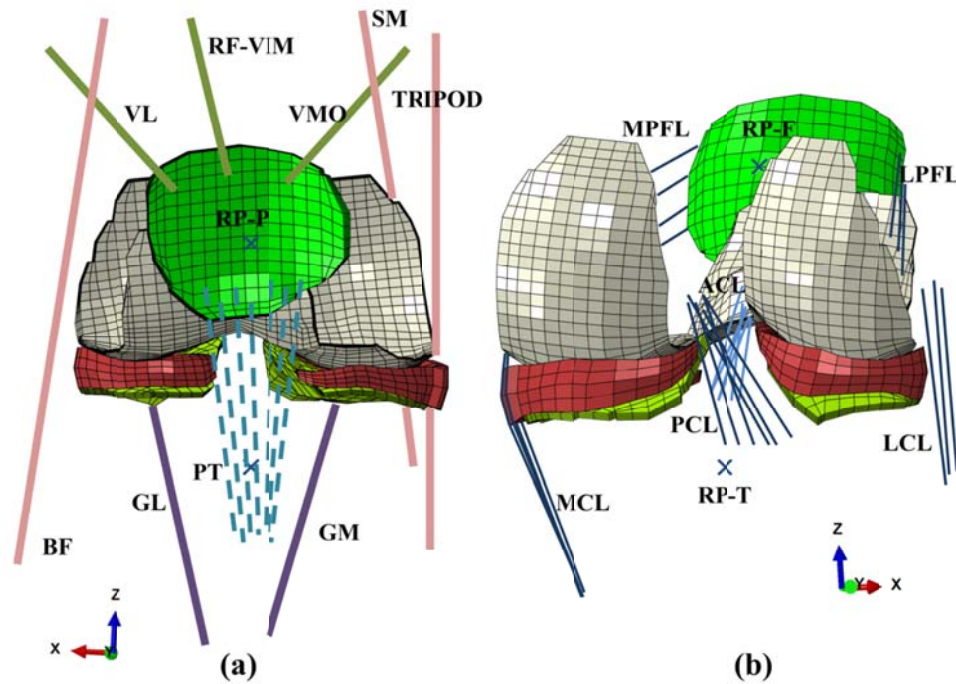


Figure 3-1: Knee joint FE model; tibiofemoral (TF) and patellofemoral (PF) cartilage layers, menisci, patellar Tendon (PT), quadriceps, hamstrings and gastrocnemius muscles (a), TF and PF cartilage layers, menisci and joint ligaments (b). Crosses indicate the reference points (RP) representing rigid bony structures that are not shown. Quadriceps components are vastus medialis obliquus (VMO), rectus femoris (RF), vastus intermedius medialis (VIM), and vastus lateralis (VL). Hamstring components include biceps femoris (BF), semimembranous (SM), and the TRIPOD made of Sartorius (SR), gracilis (GR), and semitendinosus (ST). Gastrocnemius components are gastrocnemius medial (GM) and gastrocnemius lateral (GL). Tibialis posterior and Soleus muscles of the ankle joint are not shown. Joint ligaments include lateral patellofemoral (LPFL), medial patellofemoral (MPFL), anterior cruciate (ACL), posterior cruciate (PCL), lateral collateral (LCL), and medial collateral (MCL).

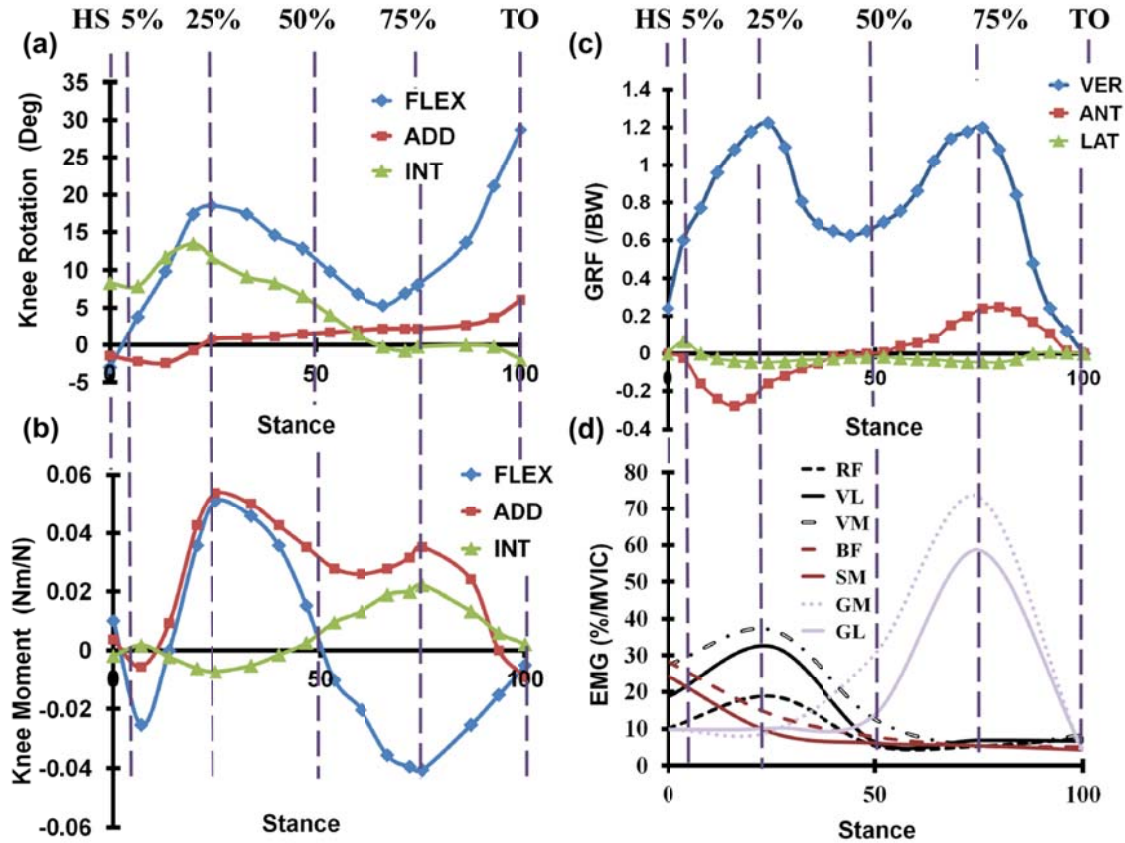


Figure 3-2: Knee joint rotations (a) and moments (b) reported as mean of asymptomatic subjects during the stance phase of gait (Astephen et al., 2008a) as well as vertical, anterior, and lateral ground reaction force components (c) reported during the stance phase of gait on asymptomatic subjects (Hunt et al., 2001), and mean normalized surface EMG data (d) recorded in 7 different knee joint muscles (Astephen, 2007). For muscle abbreviations, see the caption of Fig. 1. Six instances corresponding to beginning (heel strike, HS 0%), 5%, 25%, 50%, 75% and end (toe off, TO 100%) of the stance phase are indicated. Note that moments and forces are normalized to the BW=606.6 N of the female subject.

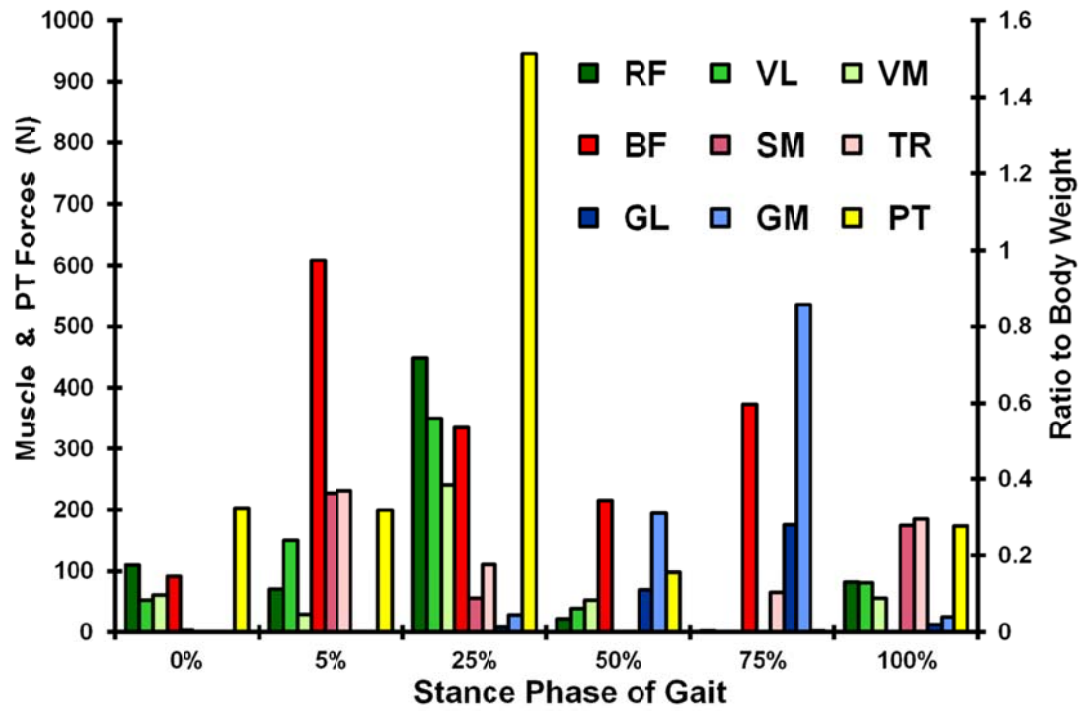


Figure 3-3: Predicted Muscle and TP forces at different stance phases (see Fig. 1 caption for muscle abbreviations). Ratios to body weight are given on the right axis.

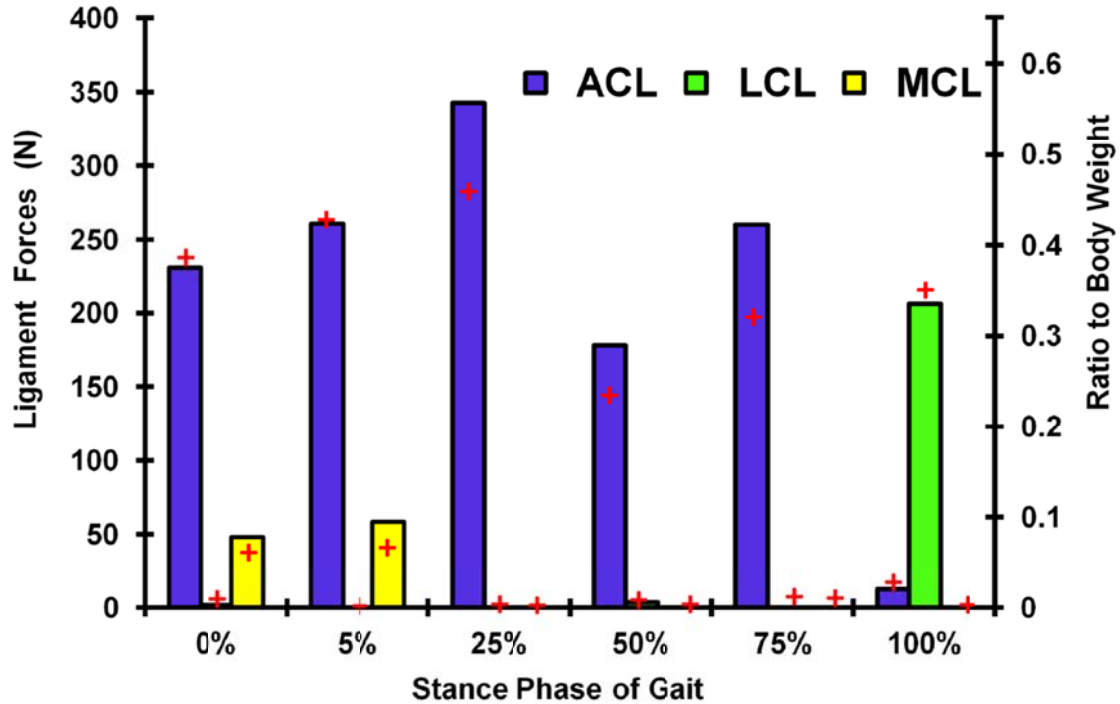


Figure 3-4: Predicted Ligaments forces at different stance phases (see Fig. 1 caption for ligaments abbreviations). (+) Results found in the model with less-refined mesh and isotopic representation of cartilage layers. Ratios to body weight are given on the right axis.

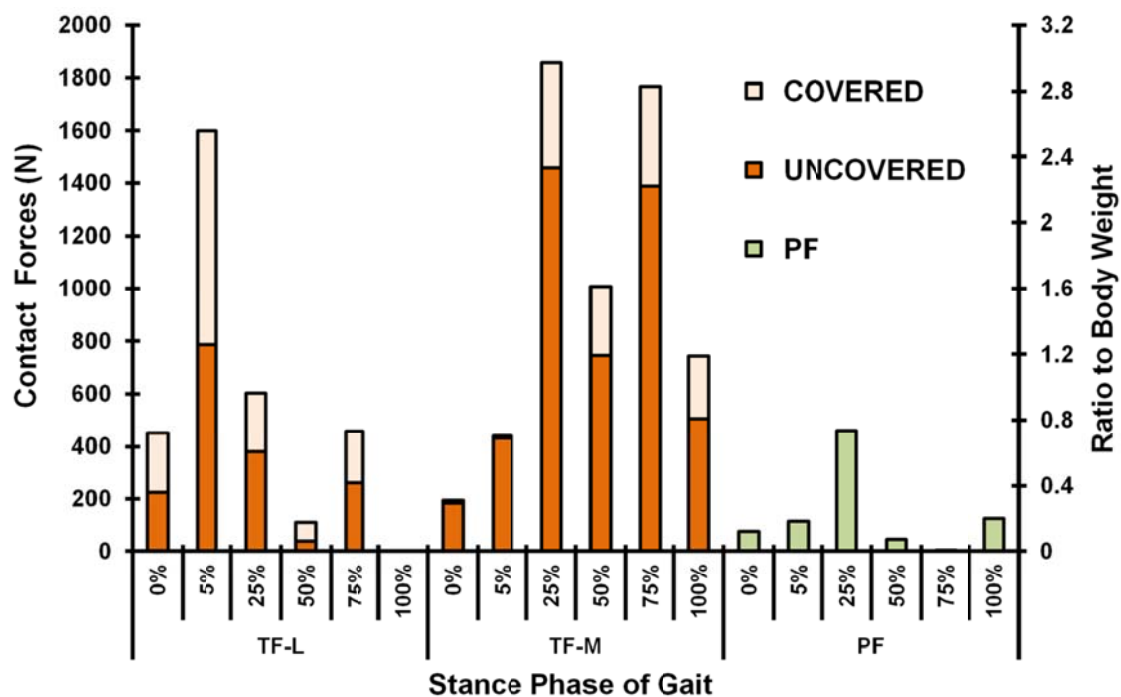


Figure 3-5: Predicted total TF (covered: via menisci, uncovered: via cartilage, M: medial plateau, L: lateral) and PF contact forces at different stance phases. Ratios to body weight are given on the right axis.

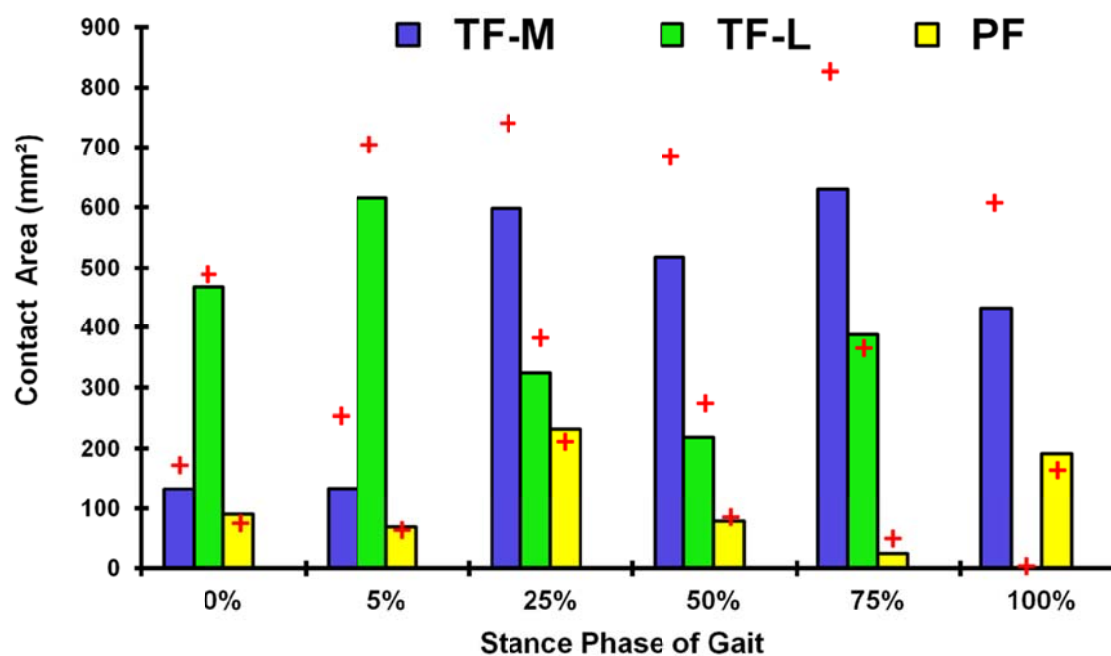


Figure 3-6: Predicted total TF (M: Medial and L: Lateral) and PF contact areas at different stance phases. (+) Results found in the model with less-refined mesh and isotropic representation of cartilage layers.

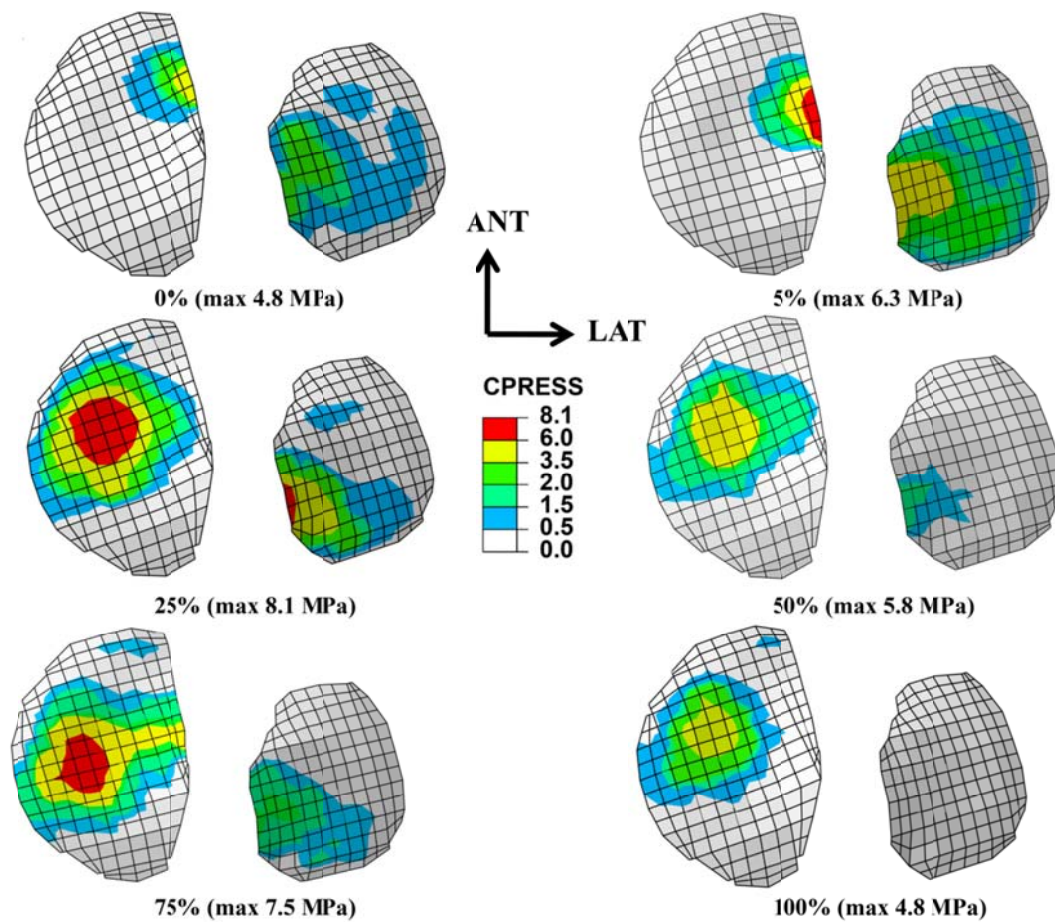


Figure 3-7: Predicted contact pressure at articular surface of lateral and medial tibial plateaus at different stance phases. Note that a common legend is used for ease in comparisons.

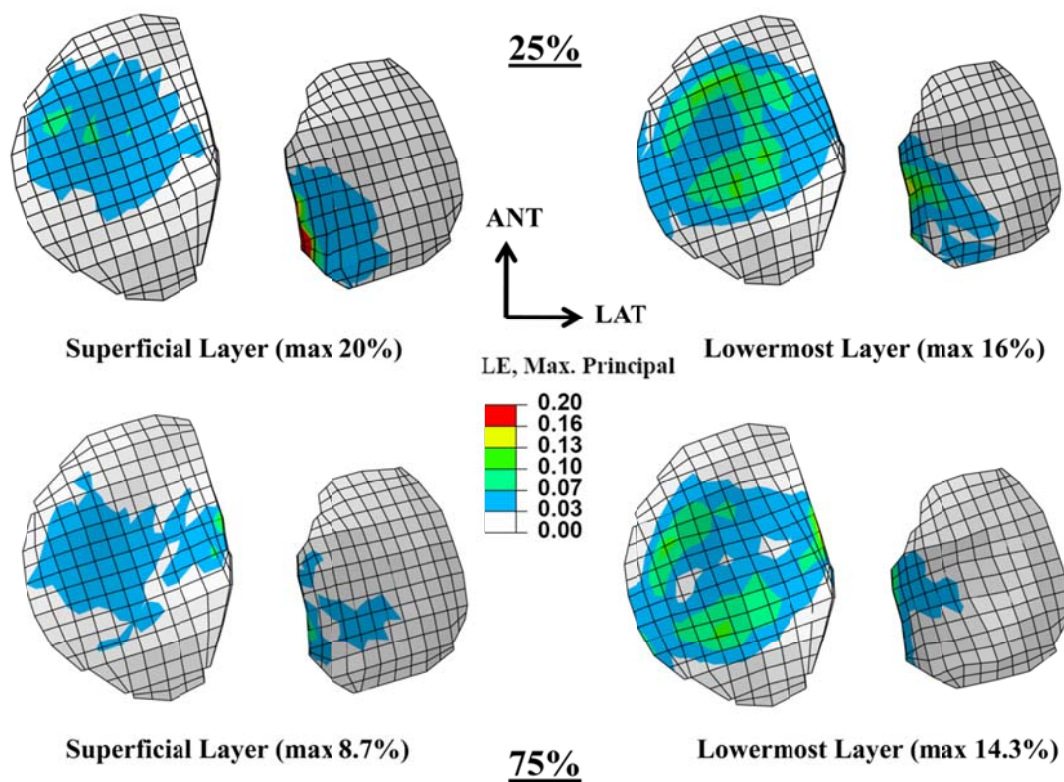


Figure 3-8: Maximum (tensile) principal strain in solid matrix at the superficial and lowermost layers of lateral and medial tibial cartilage at 25% and 75% stance phases. Note that a common legend is used for ease in comparisons.

**CHAPITRE 4 ARTICLE 2: CONSIDERATION OF EQUILIBRIUM
EQUATIONS AT THE HIP JOINT ALONGSIDE THOSE AT THE KNEE
AND ANKLE JOINTS HAS MIXED EFFECTS ON KNEE JOINT
RESPONSE DURING GAIT**

Adouni, M; Shirazi-Adl, A

Division of Applied Mechanics, Department of Mechanical Engineering
École Polytechnique, Montréal, Québec, Canada

Article published in
Journal of Biomechanics 2013
Volume 46, Issue 03, Pages 619-624.

Keywords: Gait, Knee Joint, Hip Joint, Finite element, Muscle Forces, Ligaments, Optimization, Cartilage, Contact

4.1 Abstract

Accurate estimation of muscle forces during daily activities such as walking is critical for a reliable evaluation of loads on the knee joint. To evaluate knee joint muscle forces, the importance of the inclusion of the hip joint alongside the knee and ankle joints when treating the equilibrium equations remains yet unknown. An iterative kinematics-driven finite element model of the knee joint that accounts for the synergy between passive structures and active musculature is employed. The knee joint muscle forces and biomechanical response are predicted and compared with our earlier results that did not account for moment equilibrium equations at the hip joint. This study indicates that inclusion of the hip joint in the optimization along the knee and ankle joints only slightly ($<10\%$) influences total forces in quadriceps, lateral hamstrings and medial hamstrings. As a consequence, even smaller differences are found in predicted ligament forces, contact forces/areas, and cartilage stresses/strains during the stance phase of gait. The distribution of total forces between the uni- and bi-articular muscle components in quadriceps and in lateral hamstrings, however, substantially alter at different stance phases.

4.2 Introduction

In various recreational and occupational activities, external as well as gravitational and inertial forces generate moments at the knee joint that are partly resisted by muscles crossing the joint. Estimation of these muscle forces and joint internal loads during the gait have been the focus of many studies (Anderson and Pandy, 2001; Andriacchi et al., 2009; Besier et al., 2009; Delp et al., 2007; Hurwitz et al., 1998; Kim et al., 2009; Neptune et al., 2004; Shelburne et al., 2004; Zajac et al., 2003). Recent works using instrumented knee implants in patients during gait demonstrate that, as a consequence of muscle activities, each tibiofemoral (TF) joint experiences compression forces much greater than the subject total body weight (Kim et al., 2009; Kutzner et al., 2010; Winby et al., 2009; Zhao et al., 2007). Accurate evaluation of load transmission and joint response is critical in effective prevention, treatment and rehabilitation of joint disorders. Due to technical difficulties, limitations and invasiveness of in vivo and in vitro measurements, model studies are recognized as viable complementary tools to attain these goals.

Due to inherent complexities, earlier model studies have often made a number of simplifying assumptions such as neglecting the passive resistance in supporting external loads, simulating cartilage and menisci with linear homogeneous properties, or considering limited number of muscles. Despite the requirement to consider external moments in all three planes as emphasized at the hip joint by Eng and Winter (1995), the system equilibrium equations at the knee joint are often limited to the sagittal plane (Anderson and Pandy, 2001; Besier et al., 2009; Kim et al., 2009; McGowan et al., 2009; Messier et al., 2011; Neptune et al., 2004; Shelburne et al., 2005, 2006). In such cases, the knee passive structures are supposed to support all the remaining out-of-sagittal plane loads with no contribution from muscles, an assumption that evidently casts doubt on the computed muscle forces (Lloyd and Buchanan, 2001). Due to the role of multi-articular muscles that contribute to the equilibrium equations at more than one joint, another concern relates to the need to include moment equations at the ankle and hip joints when computing muscle forces at the knee joint. The equations at the ankle, knee and hip joints have simultaneously been considered in earlier works (Anderson and Pandy, 2001; Delp et al., 2007). While neglecting the equilibrium in the frontal plane, analysis of the hip joint combined with the knee and ankle joints yielded greater recruitments in bi-articular muscles but nearly identical resultant hip contact forces (7% higher in average) when compared to results based on the hip joint alone (Frayssé et al., 2009). Similarly when analyzing the trunk biomechanics, the need to consider multi-level equilibrium equations at all spinal segments and not just a single one when attempting to evaluate trunk muscle forces has been emphasized especially under heavier tasks (Arjmand et al., 2007; Gagnon et al., 2011).

Recently using a detailed active-passive finite element (FE) model of the entire knee joint, we computed the joint muscle forces as well as contact areas/forces and tissue stresses/strains during the stance phase of gait (Adouni et al., 2012). The model accounted for the nonlinear depth-dependent cartilage and meniscus properties (Shirazi et al., 2008) and was driven by kinematics and kinetics collected on asymptomatic subjects during gait (Astéphen, 2007; Hunt et al., 2001). The FE model however satisfied the equilibrium conditions only at the ankle and knee joints without any consideration of moments at the hip joint; an assumption that may influence computed knee muscle forces and response. The current work is hence carried out with the objective to assess the effect of inclusion of hip moment equations along with those at the ankle and knee joints on estimated (uni- and bi-articular) muscle forces and internal stresses at the knee

joint. Both FE models, with and without hip moment equations, incorporate the same gait kinematics and kinetics data(Adouni et al., 2012). We hypothesize that the consideration of moment equations at the hip joint influences only the partitioning of forces between different components of hamstrings and quadriceps groups and not the total muscle forces in each of these groups. Moreover and as a consequence, ligament forces and contact areas/forces are minimally altered.

4.3 Methods

An iterative kinematics-driven FE model that accounts for the passive structures and active musculature of the knee joint is employed(Adouni et al., 2012). For the current study, it incorporates the hip as a 3D spherical joint crossed by 27 distinct muscles (Fig. 3.1). The FE knee model includes rigid bony structures (femur, tibia, patella) and their cartilages layers, menisci, six principals ligaments (ACL, PCL, LCL, MCL, MPFL, LPFL), patellar tendon PT, quadriceps (4 components), hamstring (6 components), gastrocnemius (2 components) as well as the tibialis posterior and soleus. Nonlinear depth-dependent composite articular cartilages and menisci consist of networks of collagen fibers embedded in non-fibrillar matrices(Adouni et al., 2012; Shirazi et al., 2008). The joint ligaments are modeled with nonlinear material properties and initial pre-strains (Mesfar and Shirazi-Adl, 2005).

Each muscle is simulated in the model as a force vector with an unknown axial force. The Q angle model ($Q = 14^\circ$; (Sakai et al., 1996)) is used for quadriceps muscles; orientations relative to the femoral axis in frontal/sagittal planes are: RF-VIM $0^\circ/4^\circ$ anteriorly, VL 22° laterally/ 0° and VMO 41° medially/ 0° . Orientations for hamstrings muscles relative to the tibial axis, respectively for BF (BFLH, BFSH), SM, and TRIPOD (GA,SR,ST) are taken (Aalbersberg et al., 2005) as 11.8° medially, 7° laterally, and 7.1° medially in the frontal plane whereas 0° , 16.1° , and 18.7° posteriorly in the sagittal plane. Gastrocnemius fascicles are parallel to the tibial axis in the sagittal plane while oriented (GM) 5.3° medially or (GL) 4.8° laterally in the frontal plane (Delp et al., 2007; Hillman, 2003). Tibialis posterior/Soleus are oriented $5.3^\circ/4.1^\circ$ laterally and $1.0^\circ/4^\circ$ anteriorly relative to the tibial axis(Delp et al., 2007). The orientations of the remaining hip muscles are taken from Delp et al. (2007).

Muscle forces at each instance of stance phase are computed using static optimization with moment equilibrium equations as constraints (3 at the knee joint, 3 at the hip joint, and 1 at the ankle joint). Cost function of the sum of cubed muscle stresses of the entire lower extremity is used (Adouni et al., 2012; Arjmand and Shirazi-Adl, 2006). Since our model was constructed based on a female knee joint, a body weight of $BW=606.6$ N (61.9 kg) is considered (De Leva, 1996). Analyses are carried out at 6 time instances corresponding to 0% (heel strike), 5%, 25%, 50%, 75%, and 100% (toe-off) of stance phase (Adouni et al., 2012). At each period the femur is fixed in its instantaneous position while the tibia and patella are free except for the prescribed TF rotations. The hip/knee/ankle joint rotations/moments and ground reaction forces at foot are taken from the mean data of *in vivo* measurements on asymptomatic subjects during gait (Astéphen, 2007; Hunt et al., 2001). The location of resultant ground reaction force at each instant is determined so as to generate reported joint moments accounting for the leg/foot weight (29.78 N/7.98 N). Non-orthogonal local joint coordinate systems (Grood and Suntay, 1983) are considered in compliance with prescribed rotations (Astéphen, 2007).

At each stance period and subject to ground reaction forces and leg/foot weight, muscle forces at the hip, knee and ankle joints are predicted. This is done iteratively by counterbalancing required moments in deformed configurations at each step. These muscle forces are subsequently applied as additional external loads and the procedure is repeated (8-12 iterations) till convergence (unbalanced moments <0.1 Nm). Two additional cases are analyzed at 75% stance phase in which the GL and GM forces are estimated separately alongside tibialis posterior and soleus at the ankle joint and considered subsequently at the knee or hip + knee models as known external forces. Matlab (R2009a Optimization Toolbox, genetic algorithms) and ABAQUS 6.10.1 (Static analysis) commercial programs are used.

4.4 Results

Results of the earlier FE model neglecting hip moments (Adouni et al., 2012) are also presented for comparison. These results are however updated at 75% stance period to estimate both the ankle and knee muscle forces in a single optimization. In the current model, forces in quadriceps increased by an average of 4.1%. This increase peaked at 25% of stance phase with 2.4%, 5% and 8.9% in RF-VIM, VL, and VM respectively (Fig. 3.2). Forces in hamstrings also increased by an average of 10.4% though the most active component (BF) increased only by 5%

(Fig.2). With partitioning BF, RF-VIM, and TRIPOD into distinct components in the present model; RF-VIM muscles peaked at 25% with much larger activation in VIM (Fig. 3.3), BFLH reached its maximum of 345 N early at 5% stance phase and dropped thereafter whereas BFSH peaked at 75% phase (388 N, Fig. 3.3), and ST remained as the most active muscle in TRIPOD (Fig. 3.3).

Negligible differences were found in ligament forces with ACL force increasing by an average of 2.6% (Fig. 3.4). Knee medial and lateral contact forces/areas also increased by an average of 4.6% (Fig. 3.5). Contact pressures slightly increased at 25% and 75% (by 0.3MPa at peaks, Fig. 3.6). Patellofemoral contact force/pressure/area increased only slightly by averages of 3.4%/1.9%/3.06%, respectively.

4.5 Discussion

In continuation of our earlier work (Adouni et al., 2012), this study aimed to quantify the effect of the consideration of moment equations at the hip joint along with those at the knee and ankle joints on estimated muscle forces and internal stresses. Comparison of results indicate that satisfaction of hip equilibrium equations has relatively small increasing effect (<10%) on total forces in quadriceps, medial hamstrings, and lateral hamstrings muscle groups (Fig. 3.2) and to even smaller extent on contact forces/areas (Fig. 3.5), ligament forces (Fig. 3.4) and tissue-level stresses (Fig. 3.6). Nevertheless, partitioning of forces between uni- and bi-articular fascicles (i.e., BFSH and BFLH in lateral hamstrings, RF and VIM in quadriceps) alters substantially at different stance phases (Fig. 3.3). The bi-articular RF noticeably drops at 25% stance phase relegating the activity to uni-articular VIM muscle. On the other hand, the relative contribution of uni-articular BFSH and bi-articular BFLH at various stance phases significantly alter and that despite nearly identical total forces in two models.

The foregoing predictions of small changes in the contact forces but substantial changes in uni-articular and bi-articular knee muscle fascicles agree with similar findings at the hip joint (Frayssé et al., 2009). Qualitatively (i.e., trend-wise), the collected superficial EMG of BF during gait (Astéphen, 2007) closely agrees with the estimated forces in the BFLH (and not the BFSH) that is also a superficial muscle. Moreover, the substantial drop in RF activity associated with nearly equal increases in VIM activity corroborates well with EMG data (Astéphen, 2007; Sasaki

and Neptune, 2010) that show minimum EMG activity in the RF compared to the VL and VM components.

Large forces in lateral hamstrings suggest their importance in resisting knee adduction moment in the frontal plane and extension moment in the sagittal plane. The former contribution has however been unaccounted in earlier studies that limit the role of hamstrings to the sagittal plane (Anderson and Pandy, 2001; McGowan et al., 2009; Messier et al., 2011; Shelburne et al., 2004; Shelburne et al., 2005, 2006). Consideration of the hip as a 3D joint and the knee as a 1D joint likely adversely affects estimated muscle forces. It is also to be noted that the roles of BFLH and SR in the frontal plane reverse at the knee versus the hip joint.

Additional analyses at the 75% stance period demonstrate that the inclusion of the ankle joint in the optimization alongside either the knee joint or the hip and the knee joints has minimal effects on computed muscle forces and knee joint response when compared with the cases in which the GM and GL forces are initially evaluated at the ankle joint alone and then applied in the knee or hip + knee models as external forces (Adouni et al., 2012). Predicted muscle forces show negligible differences not exceeding 22 N in the knee model (e.g., GM force increases from 514 N to 536 N while GL force drops from 188 N to 175 N when the ankle is treated separately) or 28 N in the hip + knee model (e.g., GM force increases from 508 N to 536 N while GL force drops from 180 N to 175 N when the ankle is treated separately). It is noted that the separate consideration of the ankle joint by its exclusion from the optimization equation in the knee or the hip + knee models has a much lessor effect on results than that of the hip joint.

In summary, inclusion of moment equations at the hip joint alongside those at the knee and ankle joints has small increasing effects on total muscle forces in quadriceps and hamstrings groups and hence on internal knee joint stresses and strains. The partitioning between uni- and bi-articular components in RF-VIM and in BF, however, substantially alters resulting in better qualitative agreement with reported superficial EMG data. Extrapolation of current findings to joint conditions and activities with marked differences in input kinematics-kinetics should await future studies.

4.6 Acknowledgements

The work was supported by a grant from the Natural Sciences and Engineering Research Council of Canada (NSERC-Canada) and a scholarship from the University Mission of Tunisia in North America (MUTAN-Tunisia).

4.7 References

- Aalbersberg, S., Kingma, I., Ronsky, J.L., Frayne, R., van Dieen, J.H., 2005. Orientation of tendons in vivo with active and passive knee muscles. *Journal of Biomechanics* 38, 1780-1788.
- Adouni, M., Shirazi-Adl, A., Shirazi, R., 2012. Computational biodynamics of human knee joint in gait: From muscle forces to cartilage stresses. *Journal of Biomechanics* 45, 2149-2156.
- Anderson, F.C., Pandy, M.G., 2001. Dynamic optimization of human walking. *Journal of Biomechanical Engineering* 123, 381.
- Andriacchi, T.P., Koo, S., Scanlan, S.F., 2009. Gait mechanics influence healthy cartilage morphology and osteoarthritis of the knee. *The Journal of Bone and Joint Surgery. American volume*. 91, 95.
- Arjmand, N., Shirazi-Adl, A., 2006. Sensitivity of kinematics-based model predictions to optimization criteria in static lifting tasks. *Medical engineering & physics* 28, 504-514.
- Arjmand, N., Shirazi-Adl, A., Parnianpour, M., 2007. Trunk biomechanical models based on equilibrium at a single-level violate equilibrium at other levels. *European Spine Journal* 16, 701-709.
- Astephen, J.L., 2007. Biomechanical factors in the progression of knee osteoarthritis. *School of Biomedical Engineering*. Halifax, Dalhousie university.
- Besier, T.F., Fredericson, M., Gold, G.E., Beaupré, G.S., Delp, S.L., 2009. Knee muscle forces during walking and running in patellofemoral pain patients and pain-free controls. *Journal of Biomechanics* 42, 898-905.
- De Leva, P., 1996. Adjustments to Zatsiorsky-Seluyanov's segment inertia parameters. *Journal of Biomechanics* 29, 1223-1230.
- Delp, S.L., Anderson, F.C., Arnold, A.S., Loan, P., Habib, A., John, C.T., Guendelman, E., Thelen, D.G., 2007. OpenSim: open-source software to create and analyze dynamic simulations of movement. *Biomedical Engineering, IEEE Transactions on* 54, 1940-1950.

- Eng, J.J., Winter, D.A., 1995. Kinetic analysis of the lower limbs during walking: what information can be gained from a three-dimensional model? *Journal of Biomechanics* 28, 753-758.
- Fraysse, F., Dumas, R., Cheze, L., Wang, X., 2009. Comparison of global and joint-to-joint methods for estimating the hip joint load and the muscle forces during walking. *Journal of Biomechanics* 42, 2357-2362.
- Gagnon, D., Arjmand, N., Plamondon, A., Shirazi-Adl, A., Larivière, C., 2011. An improved multi-joint EMG-assisted optimization approach to estimate joint and muscle forces in a musculoskeletal model of the lumbar spine. *Journal of Biomechanics* 44, 1521–1529.
- Grood, Suntay, W.J., 1983. A joint coordinate system for the clinical description of three-dimensional motions: application to the knee. *Journal of Biomechanical Engineering* 105, 136.
- Hillman, 2003. *Interactive Functional Anatomy*, , London.
- Hunt, Smith, R.M., Torode, M., Keenan, A.M., 2001. Inter-segment foot motion and ground reaction forces over the stance phase of walking. *Clinical Biomechanics* 16, 592-600.
- Hurwitz, D.E., Sumner, D.R., Andriacchi, T.P., Sugar, D.A., 1998. Dynamic knee loads during gait predict proximal tibial bone distribution. *Journal of Biomechanics* 31, 423-430.
- Kim, H.J., Fernandez, J.W., Akbarshahi, M., Walter, J.P., Fregly, B.J., Pandy, M.G., 2009. Evaluation of predicted knee joint muscle forces during gait using an instrumented knee implant. *Journal of Orthopaedic Research* 27, 1326-1331.
- Kutzner, I., Heinlein, B., Graichen, F., Bender, A., Rohlmann, A., Halder, A., Beier, A., Bergmann, G., 2010. Loading of the knee joint during activities of daily living measured in vivo in five subjects. *Journal of Biomechanics* 43, 2164.
- McGowan, C., Kram, R., Neptune, R., 2009. Modulation of leg muscle function in response to altered demand for body support and forward propulsion during walking. *Journal of Biomechanics* 42, 850-856.
- Mesfar, W., Shirazi-Adl, A., 2005. Biomechanics of the knee joint in flexion under various quadriceps forces. *The knee* 12, 424-434.

- Messier, S., Legault, C., Loeser, R., Van Arsdale, S., Davis, C., Ettinger, W., DeVita, P., 2011. Does high weight loss in older adults with knee osteoarthritis affect bone-on-bone joint loads and muscle forces during walking? *Osteoarthritis and Cartilage* 19, 272-280.
- Neptune, R., Zajac, F., Kautz, S., 2004. Muscle force redistributes segmental power for body progression during walking. *Gait & Posture* 19, 194-205.
- Sakai, N., Luo, Z.P., Rand, J.A., An, K.N., 1996. Quadriceps forces and patellar motion in the anatomical model of the patellofemoral joint. *The knee* 3, 1-7.
- Sasaki, K., Neptune, R.R., 2010. Individual muscle contributions to the axial knee joint contact force during normal walking. *Journal of Biomechanics* 43, 2780-2784.
- Shelburne, K.B., Pandy, M.G., Anderson, F.C., Torry, M.R., 2004. Pattern of anterior cruciate ligament force in normal walking. *Journal of Biomechanics* 37, 797-805.
- Shelburne, K.B., Torry, M.R., Pandy, M.G., 2005. Muscle, ligament, and joint-contact forces at the knee during walking. *Medicine & Science in Sports & Exercise* 37, 1948.
- Shelburne, K.B., Torry, M.R., Pandy, M.G., 2006. Contributions of muscles, ligaments, and the ground reaction force to tibiofemoral joint loading during normal gait. *Journal of Orthopaedic Research* 24, 1983-1990.
- Shirazi, R., Shirazi-Adl, A., Hurtig, M., 2008. Role of cartilage collagen fibrils networks in knee joint biomechanics under compression. *Journal of Biomechanics* 41, 3340-3348.
- Winby, C., Lloyd, D., Besier, T., Kirk, T., 2009. Muscle and external load contribution to knee joint contact loads during normal gait. *Journal of Biomechanics* 42, 2294-2300.
- Zajac, F.E., Neptune, R.R., Kautz, S.A., 2003. Biomechanics and muscle coordination of human walking:: Part II: Lessons from dynamical simulations and clinical implications. *Gait & Posture* 17, 1-17.
- Zhao, D., Banks, S.A., Mitchell, K.H., D'Lima, D.D., Colwell, C.W., Fregly, B.J., 2007. Correlation between the knee adduction torque and medial contact force for a variety of gait patterns. *Journal of Orthopaedic Research* 25, 789-797.

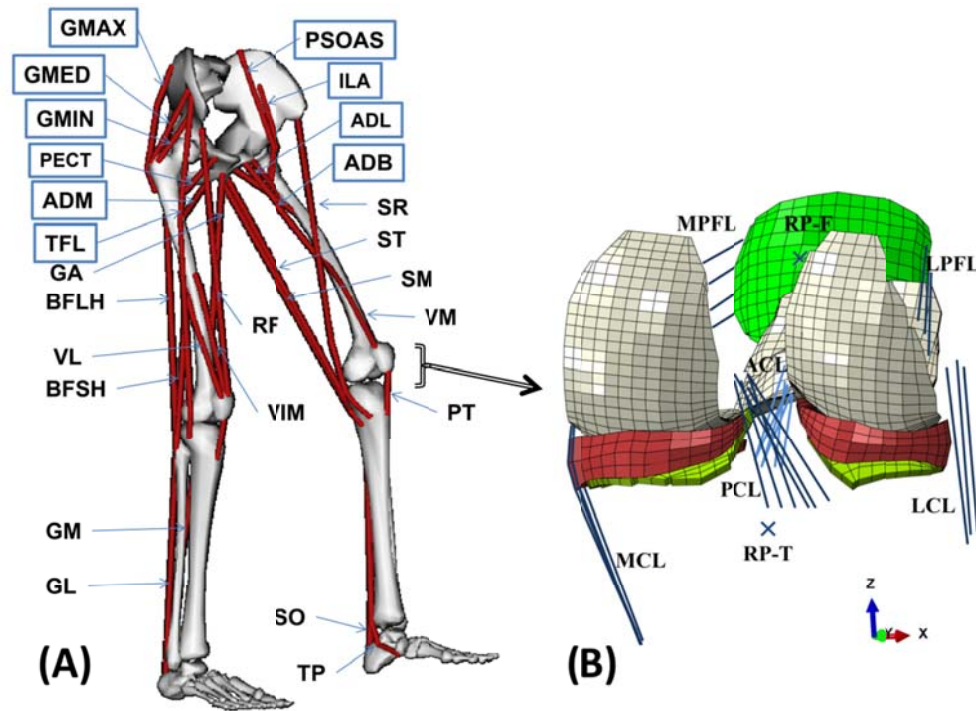


Figure 4-1: (A) Schematic diagram showing the 34 muscles incorporated into the lower extremity model (taken from OpenSim (Delp et al., 2007)), framed ones indicate muscles added in this study versus the earlier one (Adouni et al., 2012). Quadriceps components are vastus medialis obliquus (VMO), rectus femoris (RF), vastus intermedius (VIM), and vastus lateralis (VL). Hamstring components include biceps femoris long head (BFLH), biceps femoris short head (BFSH), semi membranous (SM), and the TRIPOD made of sartorius (SR), gracilis (GA), and semitendinosus (ST). Gastrocnemius components are gastrocnemius medial (GM) and gastrocnemius lateral (GL). Tibialis posterior (TP) and soleus (SO) muscles are uni-articular ankle muscles. Hip joint muscles (not all shown) include adductor, long (ADL), mag (3 components ADM) and brev (ADB); gluteus max (3 components GMAX), med (3 components GMED) and min (3 components GMIN); iliopsoas (PSOAS), quadriceps femoris; pectineus (PECT); tensor fascia lata (TFL); periformis. (B) Knee FE model; tibiofemoral (TF) and patellofemoral (PF) cartilage layers, menisci, patellar Tendon (PT). Joint ligaments include lateral patellofemoral (LPFL), medial patellofemoral (MPFL), anterior cruciate (ACL), posterior cruciate (PCL), lateral collateral (LCL), and medial collateral (MCL). Reference points (RP) for tibia and patella bony rigid bodies are also shown.

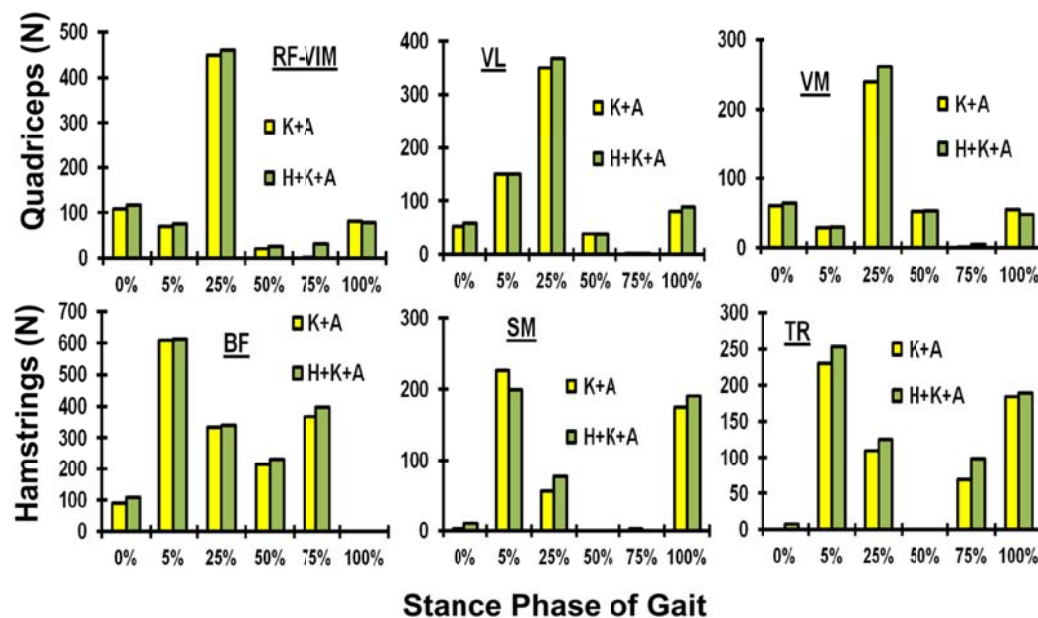


Figure 4-2: Predicted muscle forces at different stance phases. Earlier results (Adouni et al, 2012) accounting for the knee and ankle equations only (K + A) are also shown for comparison (see Fig. 1 for muscle abbreviations).

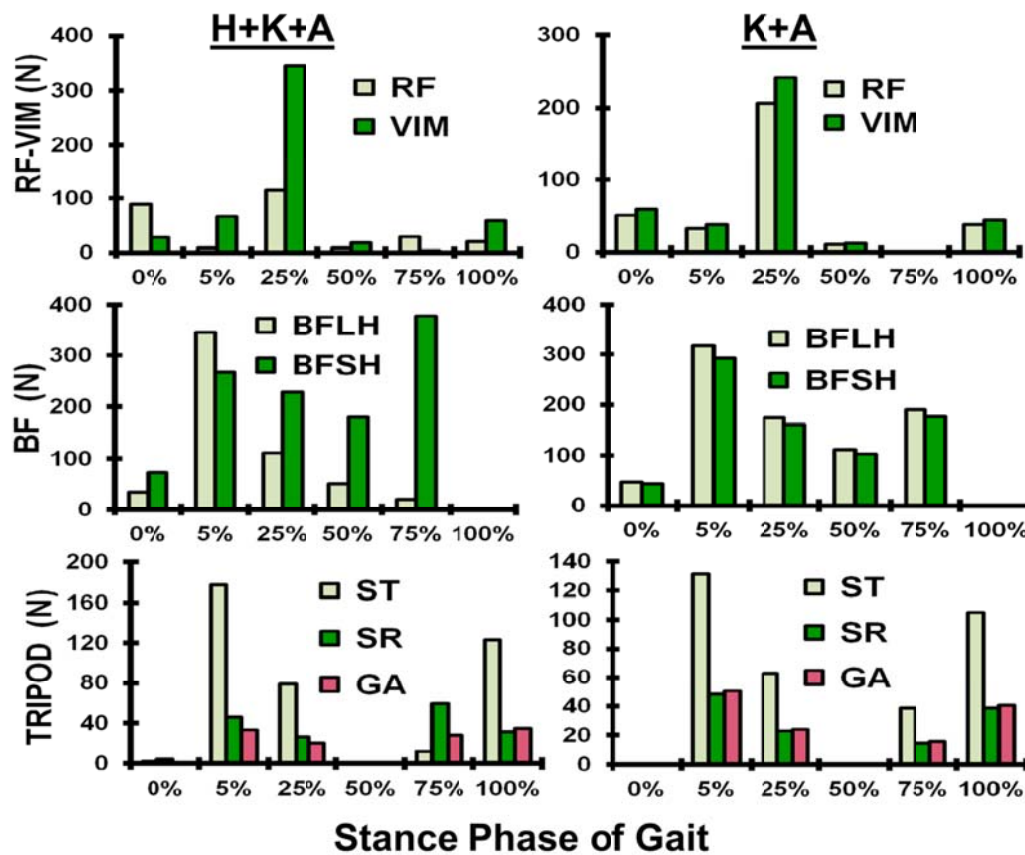


Figure 4-3: Predicted muscle forces in bi-articular (BFLH, RF, ST, SR, GA) and uni-articular (BFSH, VIM) components at different phases of stance. Earlier results (Adouni et al, 2012) accounting for the knee and ankle equations only (K + A) are also shown for comparison (see Fig. 1 for muscle abbreviations).

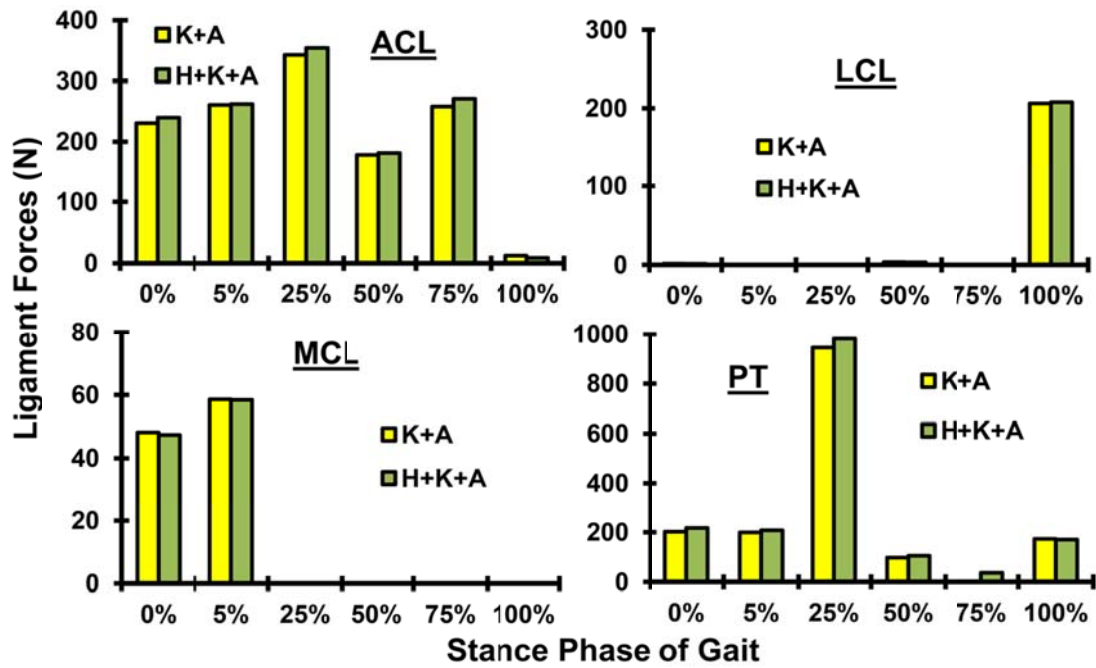


Figure 4-4: Predicted Ligament forces at different stance phases. Earlier results (Adouni et al, 2012) accounting for the knee and ankle equations only (K + A) are also shown for comparison (see Fig. 1 for ligament abbreviations).

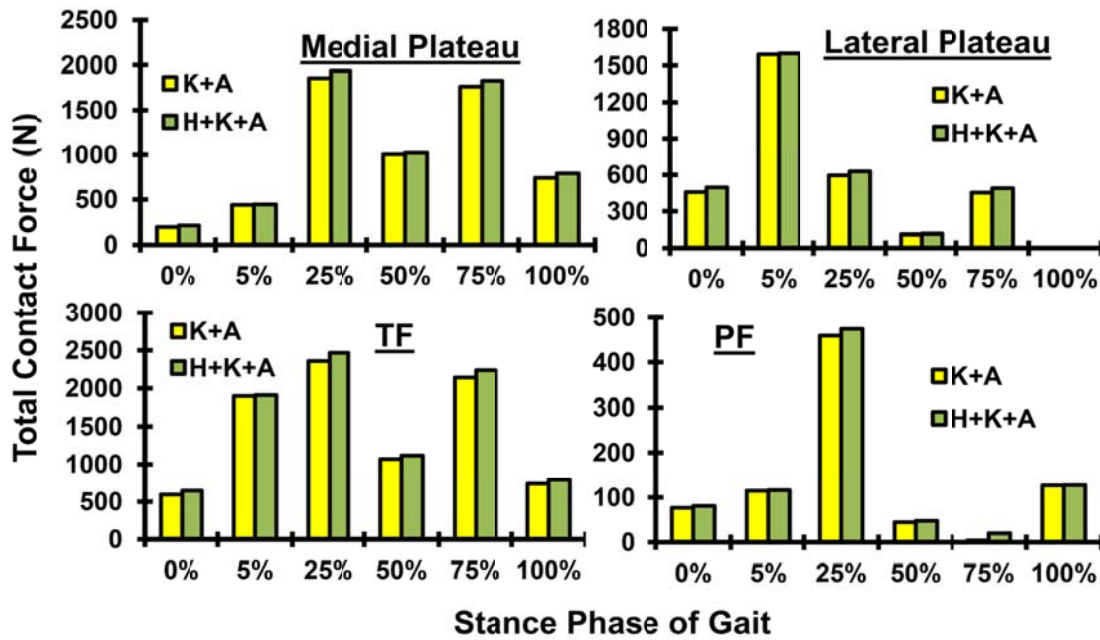


Figure 4-5: Predicted total TF (as well as individual components at medial and lateral plateaus) and PF contact forces. Earlier results (Adouni et al, 2012) accounting for the knee and ankle equations only (K + A) are also shown for comparison.

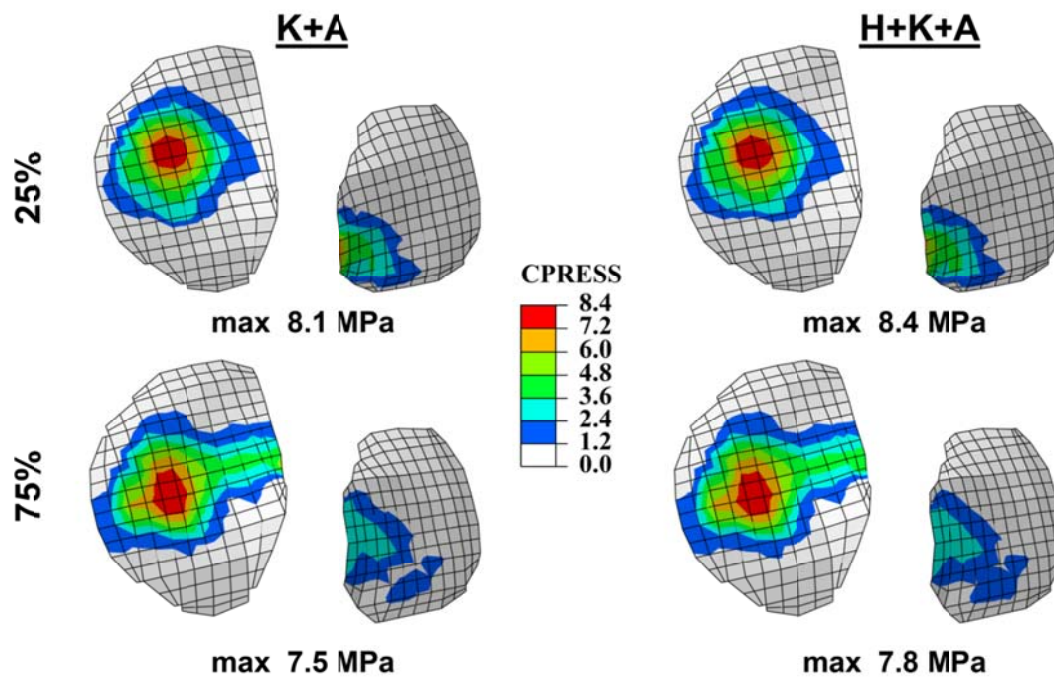


Figure 4-6: Predicted contact pressure at articular surfaces of lateral and medial tibial plateaus at 25% and 75% of stance phase. Earlier results (Adouni et al, 2012) accounting for the knee and ankle equations only (K + A) are also shown for comparison. Note that a common legend is used for ease in comparisons.

**CHAPITRE 5 ARTICLE 3: EVALUATION OF KNEE JOINT MUSCLE
FORCES AND TISSUE STRESSES-STRAINS DURING GAIT IN
SEVERE OA VERSUS NORMAL SUBJECTS**

Adouni, M; Shirazi-Adl, A

Division of Applied Mechanics, Department of Mechanical Engineering

École Polytechnique, Montréal, Québec, Canada

Article published in

Journal of Orthopaedic Research 2014

Volume 32, Issue 01, Pages 69-87.

Keywords: Gait, Biomechanical model, Knee osteoarthritis, Muscle forces, Cartilage

5.1 Abstract

Osteoarthritis (OA) is the leading cause of pain and disability in the elderly with the knee being the most affected weight bearing joint. We used a musculoskeletal biomechanical model of the lower extremity including a detailed validated knee joint finite element model to compute lower extremity muscle forces and knee joint stresses-strains during the stance phase of gait. The model is driven by gait data on OA patients and results are compared with those of the same model driven by data on normal controls. Additional analyses are performed with altered cartilage-menisci properties to evaluate the effects of deteriorations during OA. In OA patients compared to normal subjects, muscle forces dropped nearly at all stance periods except the mid-stance. Force in the anterior cruciate ligament remained overall the same. Total contact forces-stresses decreased by about 25%. Alterations in properties due to OA had negligible effects on muscle forces but increased contact areas and cartilage strains and reduced contact pressures. Reductions in contact stresses and increases in tissue strains and transfer of load via menisci are partly due to the altered kinetics-kinematics of gait and partly due to deteriorations in cartilage-menisci properties in OA patients.

5.2 Introduction

Due to the pain, disability and direct-indirect costs involved, joint osteoarthritis (OA) has become a major public health concern. Knee is the site most frequently affected among lower extremity joints (Oliveria et al., 1995). The dramatic increase in the number of knee replacement operations (as a remedy at the advanced stages of OA) in the recent years especially among the younger patients is alarming (Losina et al., 2012). With the ageing population and obesity epidemic along with the expectation to remain physically as active at elder ages, the problem is expected to deteriorate. There is hence an urgent need for adequate interventions to better understand, control and reduce the associated risk factors (Murphy et al., 2008). Though the pathomechanics of OA is not yet well understood, mechanical parameters are recognized to play an important role. To uncover biomechanical characteristics of knee OA initiation and progression, gait analyses have been carried out to quantify the ground reaction forces (GRF) as well as lower-extremity joint (i.e., ankle, knee and hip) rotations. Some have accordingly focused on the differences in gait response between asymptomatic and OA subjects at different stages in the development of the disease (Baliunas et al., 2002; Harding et al., 2012; Heiden et al., 2009;

Kaufman et al., 2001; Kumar et al., 2012a; Lewek et al., 2004). Apart from the kinematics, GRF and likely estimation of joint moments, these studies often do not compute muscle forces and hence the crucial internal joint loads which are essential for the subsequent prediction of stress-strain fields throughout soft tissues in general and articular cartilage in particular. Since direct in vivo measurements of muscle forces and tissue stresses are invasive and likely impossible, computational biomechanical modeling is recognized as a vital complementary tool to improve our knowledge of the joint response. Effective management of knee OA, from overall understanding to prevention and treatment modalities (including early attempts via focal repairs and osteotomies), is expected hence to benefit from the results of validated biomechanical model studies.

The stance phase of gait is considered to identify differences in kinematics-kinetics and muscle activation between asymptomatic subjects and OA patients (Astéphen et al., 2008a; Hunt et al., 2006; Zeni Jr and Higginson, 2009). Many have focused on the knee adduction moment as a surrogate measure of the medial load and associated OA (Zhao et al., 2007). Increases in the knee peak adduction moment in early stance have been indicated in severe OA patients when compared to controls (Lewek et al., 2004; Mündermann et al., 2005). In contrast, Astéphen et al. (2008a) reported a reduction in the peak adduction moment in early stance phase. Smaller knee flexion rotations during the stance phase accompanied with diminished both peak flexion moment in early stance and peak extension moment in late stance have been recorded in patients with knee OA (Astéphen et al., 2008a; Hubley-Kozey et al., 2009). Heiden et al. (2009) report however greater peak knee flexion during early stance and little difference in the knee flexion-extension moments between OA patients and controls. Foregoing differences have partly been found to depend on the walking speed of OA and normal subjects (Astéphen et al., 2008a; Heiden et al., 2009; Mündermann et al., 2005; Zeni Jr and Higginson, 2009). In general, larger normalised muscle activation and co-contraction have been indicated in OA patients (Astéphen, 2007; Heiden et al., 2009; Hubley-Kozey et al., 2013; Schmitt and Rudolph, 2008; Zeni Jr and Higginson, 2009).

In addition to the foregoing global alterations in the joint kinematics-kinetics during gait, OA is a disease with complex etiologies affecting articular tissues of the joint. Morphological, structural and biomechanical deteriorations in different components of the articular cartilage and

supporting subchondral bone manifest themselves in OA primarily via softening, loss of fluid/swelling, fibrillation and destruction of cartilage as well as hardening in underlying bone. Earlier investigations have demonstrated substantial reductions in compressive and tensile mechanical properties (dynamic and equilibrium moduli) of the articular cartilage in OA joints compared to healthy ones (Knecht et al., 2006; Obeid et al., 1994). Articular cartilage thickness also diminishes in OA patients (Andriacchi et al., 2009). The joint environment is hence influenced in OA both at the macro level by alterations in joint kinematics-kinetics during gait and at the micro level via deteriorations in tissue properties. Though dependent on the OA condition and gait parameters, the relative effects of foregoing changes in overall active musculature and passive joint properties at different stages of OA on the joint response remain yet unknown.

Loads on the knee joint during gait has been measured *in vivo* using instrumented implants in patients after surgery (Kutzner et al., 2010). Data collected via such instrumented implants along with gait kinematics-kinetics have been employed in lower-extremity biomechanical models to estimate muscle forces and joint contact loads (Kim et al., 2009; Kumar et al., 2012b; Lin et al., 2010; Zhao et al., 2007). In addition, similar investigations have been performed in asymptomatic subjects using associated gait data (Mononen et al., 2013a, b; Shelburne et al., 2004; Shelburne et al., 2005). In continuation of our earlier studies on biodynamics of normal knee joints using a musculoskeletal finite element (FE) model of the lower extremity (Adouni et al., 2012; Shirazi and Shirazi-Adl, 2009a), this work was set to investigate the detailed biomechanics of the knee joint in subjects with severe OA during the stance phase of gait. The FE analyses are driven here by kinematics-kinetics collected during gait of subjects with severe OA (Astéphen, 2007; Hunt et al., 2001). In the model simulating gait of OA subjects, material properties of the articular cartilage layers and menisci are either left unchanged as in the model of the asymptomatic group or altered (i.e., reduced matrix and fibril moduli) to represent the disease. We hypothesize that (1) muscle activation levels and joint contact loads alter in OA subjects when compared with asymptomatic subjects and (2) alterations in material properties simulating tissue destruction affect contact stresses/areas and tissue stresses/strains but not the estimated muscle forces and joint loads.

5.3 Methods

5.3.1 Finite Elements Model

As described earlier,(Adouni et al., 2012) the hip and ankle joints are considered as 3D and 2D spherical joints crossed by 31 distinct muscles (27 around the hip and 4 around the ankle) respectively (Fig. 4.1). The knee joint FE model, reconstructed initially by using CT images of bony structures along with direct digitization of articular soft tissue bounding surfaces and ligament insertion points of a female cadaver specimen,(Bendjaballah et al., 1995) consists of three bony structures (tibia, patella, femur) and their articular cartilage layers, menisci, six principal ligaments (ACL, PCL, LCL, MCL in TF and MPFL, LPFL in PF), patellar tendon (PT), as well as quadriceps (4 components), hamstrings (6 components) and gastrocnemius (2 components) (see Fig. 4.1 for details).

Articular cartilage layers and menisci are modeled as depth-dependent composites of an isotropic bulk reinforced by networks of collagen fibrils. In menisci, collagen fibrils are primarily oriented in the circumferential direction within the bulk but with no preferred orientation on bounding surfaces. In the cartilage superficial zones, fibrils are oriented horizontally parallel to the surface whereas they become random in the transitional zone and then turn perpendicular in the deep zone anchoring into the subchondral bone. Membrane elements are used to simulate fibril networks in the superficial and deep zones while brick elements represent the transitional zone network (Shirazi and Shirazi-Adl, 2009a; Shirazi et al., 2008). Bony structures are simulated as rigid bodies due to their much higher stiffness (Donahue and Hull, 2002). Ligaments are each modeled by a number of uniaxial connector elements with different initial pre-strains, non-linear (tension-only) material properties, and initial cross-sectional areas of 42, 60, 18, 25, 99, 42.7 and 28.5 mm² for ACL, PCL, LCL, MCL, PT, MPFL, and LPFL, respectively (Mesfar and Shirazi-Adl, 2005, 2006a; Moglo and Shirazi-Adl, 2003b; Shirazi-Adl and Moglo, 2005).

Muscle fascicles are modeled by connector elements with orientations at full extension taken from the literature. The Q angle model ($Q = 14^\circ$),(Sakai et al., 1996) is used for quadriceps muscles; orientations relative to the femoral axis in frontal/sagittal planes are: RF-VIM $0^\circ/4^\circ$ anteriorly, VL 22° laterally/ 0° and VMO 41° medially/ 0° . Orientations for hamstrings muscles relative to the tibial axis, respectively for BF (BFLH, BFSH), SM, and TRIPOD (GA, SR, ST)

are taken(Aalbersberg et al., 2005) as 11.8° medially, 7° laterally, and 7.1° medially in the frontal plane whereas 0° , 16.1° , and 18.7° posteriorly in the sagittal plane. Gastrocnemius fascicles are parallel to the tibial axis in the sagittal plane while oriented (GM) 5.3° medially or (GL) 4.8° laterally in the frontal plane.(Delp et al., 2007; Hillman, 2003) Tibialis posterior/Soleus are oriented $5.3^\circ/4.1^\circ$ laterally and $1.0^\circ/4^\circ$ anteriorly relative to the tibial axis.(Delp et al., 2007) The orientations of the remaining hip muscles are taken from Delp et al.(2007) (see Fig. 4.1 for abbreviations).

5.3.2 Material Properties

Depth-dependent isotropic hyperelastic (Ogden-Compressible) material properties are considered for non-fibrillar solid matrix of cartilage layers with the elastic modulus varying linearly from 10 MPa at the surface to 18 MPa at the deep zone and a Poisson's ratio of 0.49 (Adouni et al., 2012). This model that was taken due to convergence difficulties was initially verified to yield global displacements and stresses/strains in different components almost identical to an earlier one having nearly-incompressible matrix with much lower moduli (~ 1 MPa) and higher Poisson's ratio (Shirazi et al., 2008). The matrix of menisci (apart from reinforcing nonlinear collagen fibrils in different locations/directions) was similarly (as a consequence of convergence problems) taken as isotropic with 10 MPa for the elastic modulus and 0.45 for the Poisson's ratio. To simulate their horns at tibial insertions, meniscus matrices are stiffened at a higher modulus of 18 MPa at both ends (~ 5 mm length) (Shirazi et al., 2008).

The collagen content in the menisci is 14% in the circumferential direction and 2.5% in the radial direction of the bulk region along with 12% in the outer surfaces at both directions. For cartilage collagen fibrils volume fractions, 15% is considered in the superficial region, 18% in the transitional region, and 21% in the deep zone. Thicknesses of these zones are, respectively, 15%, 22.5% and 62.5% of the total height at each point (Shirazi and Shirazi-Adl, 2009b; Shirazi et al., 2008).

To simulate deteriorations in articular cartilage layers and menisci associated with OA disease,(Knecht et al., 2006) apart from the foregoing properties used in the intact and reference OA models, three additional cases are analyzed at 5% and 50% stance phases:(OA+E) elastic modulus of the matrix and stiffness of the collagen fibrils in the cartilage layers are decreased by

25% to simulate a drop in the dynamic response; (OA+E+P) in addition to foregoing reductions in elastic moduli, here the Poisson's ratio of the cartilage layers are also reduced from 0.49 to 0.45 to simulate increases in compliance, compressibility and fluid loss; and finally (OA+M+C) combined drops in the elastic moduli (by 25%) and Poisson's ratio (to 0.45 in cartilage and 0.35 in menisci) are considered in both cartilage layers and menisci. Larger reductions were also attempted but aborted due to convergence problems.

5.3.3 Muscle Force Estimation

Since the number of equilibrium equations at each level (hip, knee and ankle) is less than the number of unknown muscle forces, an optimization approach is used at each iteration. Static optimization with moment equilibrium equations (3 at the knee joint, 3 at the hip joint and 1 at the ankle joint) (Eq.2) and inequality equations on muscle forces remaining positive and larger than their passive forces but smaller than the sum of their passive and maximum active forces (Eq.3) as constraints are used along with the cost function of the sum of cubed muscle stresses of the entire lower extremity (Eq.1) (Arjmand and Shirazi-Adl, 2006).

$$Cost\ Function = \sum_{i=1}^n \left(\frac{F_i}{PCSA_i} \right)^3 \quad (Eq.1)$$

$$\sum_{i=1}^n r_{ij} \times F_{ij} = M_j \quad (Eq.2)$$

$$F_{pi} \leq F_i \leq (F_{pi} + \sigma_{imax} \times PCSA_i) \quad (Eq.3)$$

With F_i , F_{pi} , r_{ij} , σ_{imax} , $PCSA_i$ being the force, passive force component, lever arms in different planes j , maximum stress and physiological cross-sectional areas of a muscle i (Delp et al., 2007), respectively. M_j are moments resisted by muscles, they are iteratively computed at the knee joint by the FE model and are reported (Astefhen, 2007) at the hip and ankle joints in accordance with gait kinematics.

5.3.4 Loading, Kinematics and Boundary Conditions

Iterative kinematics-driven FE analyses that account for the passive structures and active musculature of the knee joint are carried out at 6 time instances corresponding to HS (heel strike), 5%, 25%, 50%, 75%, and TO (toe-off) of stance phase (Fig. 4.2). At each period the femur is initially fixed in its instantaneous position reported in gait while the patella is completely free. The hip/knee/ankle joint rotations/moments are taken from the mean data of *in vivo* measurements on severe OA subjects during gait (Fig.2) (Astefan, 2007; Hunt et al., 2001). Due to small differences between the asymptomatic and severe OA subjects, (Gok et al., 2002; Zeni Jr and Higginson, 2009) GRFs are taken from the mean data measurements on normal subjects (Hunt et al., 2001). Since our model was constructed based on a female knee joint, a body weight of $BW=606.6\text{ N}$ (61.9 kg) is considered (De Leva, 1996). The location of resultant GRF at each instant is determined so as to generate reported joint moments (Astefan et al., 2008a). accounting for the leg/foot weights (29.78 N/7.98 N). Non-orthogonal local joint coordinate systems (Grood and Suntay, 1983) are considered in compliance with prescribed rotations/moments (Astefan et al., 2008a).

At each stance period and subject to GRFs and leg/foot weights, muscle forces at the hip, knee and ankle joints are predicted. This is done iteratively by counterbalancing required moments in deformed configurations at each step. These muscle forces are subsequently applied as external loads and the procedure is repeated (8-10 iterations) till convergence (unbalanced moments $<0.1\text{ Nm}$). Matlab (Optimization Toolbox, genetic algorithms) and ABAQUS 6.10.1 (Static analysis, SIMULIA, Providence, RI, USA) programs are used.

5.4 Results

In the reference OA case (under gait data of OA group but with intact material properties) and as compared to the intact case N, muscle forces in the lateral hamstrings (BFLH, BFSH) dropped except at 0% and 50% periods with their peak at the 5% period (Fig. 3). Results of earlier FE analyses for gait of the normal group (Adouni et al., 2012) (case N) are also presented herein for completeness and comparison. Except at the 50% period, medial hamstrings (SM, GR, ST and SR) decreased significantly (Fig. 4.3). Quadriceps forces substantially dropped at 25% period where they reached their peak but increased at 50% and 75% periods. Forces in

gastrocnemius fascicles increased by 27% at the 50% period but decreased by 18% at the 75% period (Fig. 4.3). Alterations in material properties in the OA group had negligible effects on muscle forces.

In the reference OA case, ACL force reached the peak of 342N at the 75% period and, in comparison to the intact case N, increased during the stance phase except at the 0% and 25% periods (Fig. 4.4). This force was affected slightly by changes in material properties. Forces in remaining ligaments were much smaller and decreased compared to the normal case N with peaks of 47N at HS in MCL and 80N at TO in LCL.

Large total TF contact forces transferred through medial/lateral plateaus, via covered and uncovered areas of articulation, were predicted that followed variations in muscle forces (Fig. 4.5). They were much larger in the medial plateau at 25% period and thereafter and peaked at 25% and 75% periods. Compared to the normal case N, contact forces in OA were lower except at the 50% stance period. Moreover, the proportion of load transmitted via menisci increased in OA case and continued to do so in cases simulating damaged material properties. The PF contact force dropped substantially at the 5%, 25% and HS periods but increased at the 50% and 75% periods due to changes in quadriceps forces in OA group. The TF and PF contact areas followed nearly the same trends as their respective contact forces. Changes in material properties in OA group had negligible effects on foregoing total contact forces but markedly increased the contact areas; for example at the 50% period, the total TF contact area on the medial plateau increased from 615 mm² in OA case to 698 mm² in OA+M+C case. As a consequence and in contrast, the average contact pressure noticeably dropped in OA cases especially with simulated OA material properties.

In OA case and compared to the normal case N, the peak tibial articular contact pressure decreased throughout the stance phase except at the 50% period (Fig. 4.6). The overall patterns in contact pressure distribution remained however the same. In accordance with the increases in contact areas, the peak contact pressure dropped in cases with deteriorated material properties (Fig. 4.7). The maximum tensile strain in the articular cartilage occurred at the deep layers in all cases. These values decreased in OA case when compared with the normal case N, except at the 50% period. In contrast to the contact pressures, maximum tensile strain however increased in cases with altered material properties (Fig. 8).

5.5 Discussion

This study investigated the changes in the knee mechanical environment during gait in the event of a severe OA. For this purpose, the distinct kinematics-kinetics of gait collected on asymptomatic and severe OA subjects (Astefan, 2007; Hunt et al., 2001) were used separately to drive a lower-extremity iterative kinematics-driven active-passive FE model during the stance phase of gait. The likely effects of OA disease on articular cartilage and menisci tissues were also sequentially incorporated in the model of OA group by reducing the elastic modulus and Poisson's ratio of the bulk and collagen fibrils at 5% and 50% periods. To our knowledge no previous study investigated the detailed knee joint passive-active response in gait of OA patients. Predictions confirmed the hypotheses that (1) muscle forces and joint response altered markedly during the stance phase in OA group as compared to the normal group and (2) changes in material properties in OA model influenced contact stresses-areas as well as tissue stresses-strains but not the muscle, total contact and ligament forces.

The GRF considered in this study was taken based on the mean measurements of normal subjects (Hunt et al., 2001). Studies that have investigated the differences between asymptomatic and OA subjects have indicated a relatively small reduction in the peak GRF in OA patients (Zeni Jr and Higginson, 2009). Hunt et al. (2006) argued, however, that the differences in the recorded external moments at the knee joint in OA patients are due to marked alterations in GRF lever arm and not in GRF magnitude itself. In addition, by using the reported joint moments estimated for OA subjects in gait (Astefan, 2007), we automatically accounted for likely alterations in GRF magnitude and lever arm as far as joint moments are concerned. Any changes in GRF absolute magnitude can hence only negligibly influence the forces at the foot considered in our model of the OA group and not the resulting joint moments.

In accordance with the marked reduction in the knee flexion moment/rotation during the early stance (Fig. 4.2), (Astefan, 2007; Hunt et al., 2001) quadriceps muscle forces dropped substantially for example from their peak of 1087 N in the normal group at the 25% period to 525 N in the OA case (Fig. 4.3a). This could appear as relative quadriceps avoidance in the early stance phase in OA patients. The quadriceps are also more efficient in generating flexion moments at smaller knee flexion angles present in the OA case (Mesfar and Shirazi-Adl, 2005). Foregoing trends in joint flexion moments reversed however later in stance resulting in

significantly greater quadriceps forces in OA model (Fig. 4.3). At TO (100% period) and despite slightly larger flexion moment, much smaller quadriceps forces were computed in OA model due likely to much lower forces in medial hamstrings (acting as antagonists in flexion).

Large forces in lateral hamstrings (Fig. 4.2b) were generated in direct response to the knee adduction moments (Astefphen et al., 2008a). In association with the joint moments, forces in lateral hamstrings (BFLH, BFSH) decreased in the OA model during the stance phase except at the HS and mid-stance periods. The latter increase is due to the augmented adduction moment often associated with severe-OA (Astefphen et al., 2008a; Kumar et al., 2012a; Lewek et al., 2004). Forces in medial hamstrings (SM, ST, SR and GA) decreased almost at all periods. Lower hip flexion moments in OA patients also acted to reduce forces in hamstrings at early stance. In conjunction with variations in the knee adduction moment and disappearance of the large extension moment at the 2nd half of the stance phase, forces in the lateral and medial hamstrings dropped after the mid-stance period. At the final period of stance, lateral hamstrings were completely unloaded which along with the negligible activity in the lateral gastrocnemius resulted in the transfer of the entire joint load via the medial compartment. This finding is in agreement with earlier studies indicating very small loads or none at all on the lateral compartment at the end of the stance phase (Hurwitz et al., 1998; Shelburne et al., 2005, 2006; Winby et al., 2009). The lateral unloading at mid-stance periods in some OA patients computed in an EMG-driven model is likely associated with larger adduction rotations in OA patients (Kumar et al., 2012b).

In both normal and OA subject groups and despite the substantial adduction moments on the knee joint, larger activity was predicted in the MG as compared to the LG (Fig. 4.3d). To counterbalance this antagonistic activity, large forces were estimated in lateral hamstrings. The deeper short-head component of biceps femoris was hence the one carrying most of the force in lateral hamstrings at 25 to 75% stance periods (Fig. 4.3d). It is to be noted that this activity in deeper lateral hamstrings is hardly detectable by surface EMG measurements.

Generally greater muscle activation and co-contraction levels have been recorded via superficial EMG in OA patients compared to normal subjects (Astefphen, 2007; Heiden et al., 2009; Hubley-Kozey et al., 2009; Hubley-Kozey et al., 2013; Lewek et al., 2004; Schmitt and Rudolph, 2008; Zeni Jr and Higginson, 2009). Here to qualitatively validate our predictions with

reported normalized EMG measurements corresponding to the same input data used in our models,(Astephen, 2007; Hubley-Kozey et al., 2009) the computed muscle forces and the normalized EMG measurements (in N and OA cases) were both normalized to their maximal recorded values during the stance phase of gait(Fig. 4.9). Overall, the predictions in absolute terms in normal and OA groups plus their relative variations matched the reported trends. Estimated values in both OA and normal groups were however consistently smaller than measurements at HS (Fig. 4.9) which may partly be due to the absence of coactivity in our FE models to enhance joint stability and control at HS. Moreover, it should be noted that the commonly used normalization of collected EMG data to their values recorded at isometric maximal voluntary exertion should be taken with extreme caution when applied in patients with severe OA as candidates for knee replacement operation. Pain avoidance in patients may reduce the peak muscle activity during maximum exertion attempts by about 50% when compared with healthy subjects (Thomas et al., 2008). Finally, errors anticipated in the superficial EMG measurements in larger and deeper muscles and in any attempt to correlate the normalized EMG magnitude and active muscle force are additional factors that call for caution in such (qualitative) comparisons.

Forces in ACL altered in accordance with changes in muscle activation in OA patients (Fig. 4.4).Due to the marked drop in hamstrings activity at the second half of the stance phase, ACL force substantially increased in OA group. With the significant reduction in quadriceps activation at 25% period, however, ACL force slightly decreased from 354N in the normal group to 328N in OA group. As expected and under all these conditions, PCL remained slack with no force. The decrease in the knee joint adduction angle at the terminal period of stance (TO) dropped LCL force from 206N in the normal subjects to 80N in OA model.

In accordance with changes in muscle activation patterns, the TF contact load increased only at the mid-stance in OA models when compared with the normal model (case N). Due to the substantial increases in contact areas in OA models at all instances, the mean and peak contact pressures on both tibial and femoral surfaces decreased in OA models at all periods except the mid-stance period when they slightly increased (2%) despite much larger contact forces. Medial compartment carried for the most part after the initial stance periods 70% to 100% of the total joint load which agrees with reported estimations (Kumar et al., 2012a; Kumar et al., 2012b). In

addition, any varus alignments in OA subjects (Kumar et al., 2012a; Kumar et al., 2012b) could further increase the foregoing medial share of joint loading. The disagreement with the estimation of equal lateral/medial load sharing by Mononen et al.(2013a, b) is due partly to their knee valgus orientation during the stance phase of gait.

Deteriorations in cartilage and menisci material properties in OA models did not influence muscle, contact and ligament forces but substantially increased the contact areas that further reduced mean and peak contact pressures. This effect was evident even in the mid-stance when despite larger contact forces, peak and mean contact pressures dropped substantially (Fig. 4.7). In parallel, the portion of contact load transmitted via the menisci increased in OA models. In contrast to contact pressures, destruction in material properties increased, as expected, the superficial and deep strains in cartilage layers of OA models (Fig. 4.8). Markedly larger strains at the deep zone at the subchondral junction are predicted (Fig. 4.8) that could be related to the existing stiffness gradient (Radin and Rose, 1986). This bone–cartilage junction is reported as the site of horizontal split fractures occurring in daily activities (Meachim and Bentley, 1978) and impact loads (Atkinson and Haut, 1995; Vener et al., 1992). These results are in satisfactory agreements with earlier FE model studies (Mononen et al., 2011; Mononen et al., 2012).

Results and discussion in the current work should be considered in light of some limitations. Co-activity in muscle exertions was not considered. Identical musculature (no atrophy) was also assumed in both OA and normal subjects. The material destruction expected in the course of OA (Andriacchi et al., 2009; Knecht et al., 2006) was simulated sequentially by reductions in matrix and fibril dynamic moduli and tissue compressibility. Larger reductions in moduli (Knecht et al., 2006) were attempted but aborted due to convergence problems in our simulations. The cartilage thickness in TF and PF joints were left unchanged in foregoing OA models. Identical lower-extremity geometry was used in this study for both groups. Current results and conclusions remain dependent on the measured kinematics-kinetics used as input data into our OA and normal models. Despite the existing disagreements in the literature on the effect of OA during gait, (Heiden et al., 2009) the results of Astephen.(2007) were taken here due to the large number of subjects in each group and completeness of rotations and moments at ankle, knee and hip joints in addition to the collected EMG values.

In summary, OA-associated alterations in rotations and moments at lower extremity joints recorded during gait influenced activation levels in lower extremity musculature as well as contact forces-stresses and stresses-strains in knee articular cartilage. Reductions in mean and peak contact stresses as well as increases in tissue strains and transfer of load via menisci are partly due to altered kinetics-kinematics of gait and partly due to deteriorations in cartilage material properties in OA patients.

5.6 Acknowledgements

The work is supported by a grant from the Natural Sciences and Engineering Research Council of Canada (NSERC-Canada).

5.7 References

- Aalbersberg, S., Kingma, I., Ronsky, J.L., Frayne, R., van Dieen, J.H., 2005. Orientation of tendons in vivo with active and passive knee muscles. *Journal of Biomechanics* 38, 1780-1788.
- Adouni, M., Shirazi-Adl, A., Shirazi, R., 2012. Computational biodynamics of human knee joint in gait: From muscle forces to cartilage stresses. *Journal of Biomechanics* 45, 2149-2156.
- Andriacchi, T.P., Koo, S., Scanlan, S.F., 2009. Gait mechanics influence healthy cartilage morphology and osteoarthritis of the knee. *The Journal of Bone and Joint Surgery. American volume.* 91, 95.
- Arjmand, N., Shirazi-Adl, A., 2006. Sensitivity of kinematics-based model predictions to optimization criteria in static lifting tasks. *Medical engineering & physics* 28, 504-514.
- Astephen, J.L., 2007. Biomechanical factors in the progression of knee osteoarthritis. *School of Biomedical Engineering*. Halifax, Dalhousie university.
- Astephen, J.L., Deluzio, K.J., Caldwell, G.E., Dunbar, M.J., 2008a. Biomechanical changes at the hip, knee, and ankle joints during gait are associated with knee osteoarthritis severity. *Journal of Orthopaedic Research* 26, 332-341.
- Atkinson, P.J., Haut, R.C., 1995. Subfracture insult to the human cadaver patellofemoral joint produces occult injury. *Journal of Orthopaedic Research* 13, 936-944.
- Baliunas, A., Hurwitz, D., Ryals, A., Karrar, A., Case, J., Block, J., Andriacchi, T., 2002. Increased knee joint loads during walking are present in subjects with knee osteoarthritis. *Osteoarthritis and cartilage/OARS, Osteoarthritis Research Society* 10, 573.
- Bendjaballah, M., Shirazi-Adl, A., Zukor, D., 1995. Biomechanics of the human knee joint in compression: reconstruction, mesh generation and finite element analysis. *The knee* 2, 69-79.
- De Leva, P., 1996. Adjustments to Zatsiorsky-Seluyanov's segment inertia parameters. *Journal of Biomechanics* 29, 1223-1230.

- Delp, S.L., Anderson, F.C., Arnold, A.S., Loan, P., Habib, A., John, C.T., Guendelman, E., Thelen, D.G., 2007. OpenSim: open-source software to create and analyze dynamic simulations of movement. *Biomedical Engineering, IEEE Transactions on* 54, 1940-1950.
- Donahue, T.L.H., Hull, M., 2002. A finite element model of the human knee joint for the study of tibio-femoral contact. *Journal of Biomechanical Engineering* 124, 273.
- Gok, H., Ergin, S., Yavuzer, G., 2002. Kinetic and kinematic characteristics of gait in patients with medial knee arthrosis. *Acta Orthopaedica Scandinavica* 73, 647-652.
- Grood, Sunta, W.J., 1983. A joint coordinate system for the clinical description of three-dimensional motions: application to the knee. *Journal of Biomechanical Engineering* 105, 136.
- Harding, G.T., Hubley-Kozey, C.L., Dunbar, M.J., Stanish, W.D., Astephen Wilson, J.L., 2012. Body mass index affects knee joint mechanics during gait differently with and without moderate knee osteoarthritis. *Osteoarthritis and Cartilage*.
- Heiden, T.L., Lloyd, D.G., Ackland, T.R., 2009. Knee joint kinematics, kinetics and muscle co-contraction in knee osteoarthritis patient gait. *Clinical Biomechanics* 24, 833-841.
- Hillman, 2003. *Interactive Functional Anatomy*, London.
- Hubley-Kozey, C.L., Hill, N.A., Rutherford, D.J., Dunbar, M.J., Stanish, W.D., 2009. Co-activation differences in lower limb muscles between asymptomatic controls and those with varying degrees of knee osteoarthritis during walking. *Clinical Biomechanics* 24, 407-414.
- Hubley-Kozey, C.L., Robbins, S.M., Rutherford, D.J., Stanish, W.D., 2013. Reliability of surface electromyographic recordings during walking in individuals with knee osteoarthritis. *Journal of Electromyography and Kinesiology*.
- Hunt, Birmingham, T.B., Giffin, J.R., Jenkyn, T.R., 2006. Associations among knee adduction moment, frontal plane ground reaction force, and lever arm during walking in patients with knee osteoarthritis. *Journal of Biomechanics* 39, 2213-2220.
- Hunt, Smith, R.M., Torode, M., Keenan, A.M., 2001. Inter-segment foot motion and ground reaction forces over the stance phase of walking. *Clinical Biomechanics* 16, 592-600.

- Hurwitz, D.E., Sumner, D.R., Andriacchi, T.P., Sugar, D.A., 1998. Dynamic knee loads during gait predict proximal tibial bone distribution. *Journal of Biomechanics* 31, 423-430.
- Kaufman, K.R., Hughes, C., Morrey, B.F., Morrey, M., An, K.-N., 2001. Gait characteristics of patients with knee osteoarthritis. *Journal of Biomechanics* 34, 907-915.
- Kim, H.J., Fernandez, J.W., Akbarshahi, M., Walter, J.P., Fregly, B.J., Pandy, M.G., 2009. Evaluation of predicted knee joint muscle forces during gait using an instrumented knee implant. *Journal of Orthopaedic Research* 27, 1326-1331.
- Knecht, S., Vanwanseele, B., Stüssi, E., 2006. A review on the mechanical quality of articular cartilage—Implications for the diagnosis of osteoarthritis. *Clinical Biomechanics* 21, 999-1012.
- Kumar, D., Manal, K.T., Rudolph, K.S., 2012a. Knee joint loading during gait in healthy controls and individuals with knee osteoarthritis. *Osteoarthritis and Cartilage*.
- Kumar, D., Rudolph, K.S., Manal, K.T., 2012b. EMG-driven modeling approach to muscle force and joint load estimations: Case study in knee osteoarthritis. *Journal of Orthopaedic Research* 30, 377-383.
- Kutzner, I., Heinlein, B., Graichen, F., Bender, A., Rohlmann, A., Halder, A., Beier, A., Bergmann, G., 2010. Loading of the knee joint during activities of daily living measured in vivo in five subjects. *Journal of Biomechanics* 43, 2164.
- Lewek, M.D., Rudolph, K.S., Snyder-Mackler, L., 2004. Control of frontal plane knee laxity during gait in patients with medial compartment knee osteoarthritis. *Osteoarthritis and Cartilage* 12, 745-751.
- Lin, Y.C., Walter, J.P., Banks, S.A., Pandy, M.G., Fregly, B.J., 2010. Simultaneous prediction of muscle and contact forces in the knee during gait. *Journal of Biomechanics* 43, 945-952.
- Losina, E., Thornhill, T.S., Rome, B.N., Wright, J., Katz, J.N., 2012. The dramatic increase in total knee replacement utilization rates in the United States cannot be fully explained by growth in population size and the obesity epidemic. *The Journal of Bone & Joint Surgery* 94, 201-207.

- Meachim, G., Bentley, G., 1978. Horizontal splitting in patellar articular cartilage. *Arthritis & Rheumatism* 21, 669-674.
- Mesfar, W., Shirazi-Adl, A., 2005. Biomechanics of the knee joint in flexion under various quadriceps forces. *The knee* 12, 424-434.
- Mesfar, W., Shirazi-Adl, A., 2006. Biomechanics of changes in ACL and PCL material properties or prestrains in flexion under muscle force-implications in ligament reconstruction. *Computer Methods in Biomechanics and Biomedical Engineering* 9, 201.
- Moglo, K., Shirazi-Adl, A., 2003b. On the coupling between anterior and posterior cruciate ligaments, and knee joint response under anterior femoral drawer in flexion: a finite element study. *Clinical Biomechanics* 18, 751-759.
- Mononen, M., Julkunen, P., Töyräs, J., Jurvelin, J., Kiviranta, I., Korhonen, R., 2011. Alterations in structure and properties of collagen network of osteoarthritic and repaired cartilage modify knee joint stresses. *Biomechanics and Modeling in Mechanobiology* 10, 357-369.
- Mononen, M., Mikkola, M., Julkunen, P., Ojala, R., Nieminen, M., Jurvelin, J., Korhonen, R., 2012. Effect of superficial collagen patterns and fibrillation of femoral articular cartilage on knee joint mechanics—A 3D finite element analysis. *Journal of Biomechanics* 45, 579-587.
- Mononen, M.E., Jurvelin, J.S., Korhonen, R.K., 2013a. Effects of Radial Tears and Partial Meniscectomy of Lateral Meniscus on the Knee Joint Mechanics during the Stance Phase of the Gait Cycle—A 3D Finite Element Study. *Journal of Orthopaedic Research*.
- Mononen, M.E., Jurvelin, J.S., Korhonen, R.K., 2013b. Implementation of a gait cycle loading into healthy and meniscectomised knee joint models with fibril-reinforced articular cartilage. *Computer Methods in Biomechanics and Biomedical Engineering*, 1-12.
- Mündermann, A., Dyrby, C.O., Andriacchi, T.P., 2005. Secondary gait changes in patients with medial compartment knee osteoarthritis: increased load at the ankle, knee, and hip during walking. *Arthritis & Rheumatism* 52, 2835-2844.
- Murphy, L., Schwartz, T.A., Helmick, C.G., Renner, J.B., Tudor, G., Koch, G., Dragomir, A., Kalsbeek, W.D., Luta, G., Jordan, J.M., 2008. Lifetime risk of symptomatic knee osteoarthritis. *Arthritis Care & Research* 59, 1207-1213.

- Obeid, E., Adams, M., Newman, J., 1994. Mechanical properties of articular cartilage in knees with unicompartmental osteoarthritis. *Journal of Bone & Joint Surgery, British Volume* 76, 315-319.
- Oliveria, S.A., Felson, D.T., Reed, J.I., Cirillo, P.A., Walker, A.M., 1995. Incidence of symptomatic hand, hip, and knee osteoarthritis among patients in a health maintenance organization. *Arthritis & Rheumatism* 38, 1134-1141.
- Radin, E.L., Rose, R.M., 1986. Role of subchondral bone in the initiation and progression of cartilage damage. *Clinical Orthopaedics and Related Research* 213, 34-40.
- Sakai, N., Luo, Z.P., Rand, J.A., An, K.N., 1996. Quadriceps forces and patellar motion in the anatomical model of the patellofemoral joint. *The knee* 3, 1-7.
- Schmitt, L.C., Rudolph, K.S., 2008. Muscle stabilization strategies in people with medial knee osteoarthritis: the effect of instability. *Journal of Orthopaedic Research* 26, 1180-1185.
- Shelburne, K.B., Pandy, M.G., Anderson, F.C., Torry, M.R., 2004. Pattern of anterior cruciate ligament force in normal walking. *Journal of Biomechanics* 37, 797-805.
- Shelburne, K.B., Torry, M.R., Pandy, M.G., 2005. Muscle, ligament, and joint-contact forces at the knee during walking. *Medicine & Science in Sports & Exercise* 37, 1948.
- Shelburne, K.B., Torry, M.R., Pandy, M.G., 2006. Contributions of muscles, ligaments, and the ground reaction force to tibiofemoral joint loading during normal gait. *Journal of Orthopaedic Research* 24, 1983-1990.
- Shirazi-Adl, A., Moglo, K., 2005. Effect of changes in cruciate ligaments pretensions on knee joint laxity and ligament forces. *Computer Methods in Biomechanics and Biomedical Engineering* 8, 17-24.
- Shirazi, R., Shirazi-Adl, A., 2009a. Analysis of partial meniscectomy and ACL reconstruction in knee joint biomechanics under a combined loading. *Clinical Biomechanics* 24, 755-761.
- Shirazi, R., Shirazi-Adl, A., 2009b. Computational biomechanics of articular cartilage of human knee joint: Effect of osteochondral defects. *Journal of Biomechanics* 42, 2458-2465.
- Shirazi, R., Shirazi-Adl, A., Hurtig, M., 2008. Role of cartilage collagen fibrils networks in knee joint biomechanics under compression. *Journal of Biomechanics* 41, 3340-3348.

- Thomas, J.S., France, C.R., Sha, D., Vander Wiele, N., 2008. The influence of pain-related fear on peak muscle activity and force generation during maximal isometric trunk exertions. *Spine* 33, E342-E348.
- Vener, M.J., Thompson, R.C., Lewis Jr, J.L., Oegema, T.R., 1992. Subchondral damage after acute transarticular loading: an in vitro model of joint injury. *Journal of Orthopaedic Research* 10, 759-765.
- Winby, C., Lloyd, D., Besier, T., Kirk, T., 2009. Muscle and external load contribution to knee joint contact loads during normal gait. *Journal of Biomechanics* 42, 2294-2300.
- Zeni Jr, J.A., Higginson, J.S., 2009. Differences in gait parameters between healthy subjects and persons with moderate and severe knee osteoarthritis: A result of altered walking speed? *Clinical biomechanics (Bristol, Avon)* 24, 372.
- Zhao, D., Banks, S.A., Mitchell, K.H., D'Lima, D.D., Colwell, C.W., Fregly, B.J., 2007. Correlation between the knee adduction torque and medial contact force for a variety of gait patterns. *Journal of Orthopaedic Research* 25, 789-797.

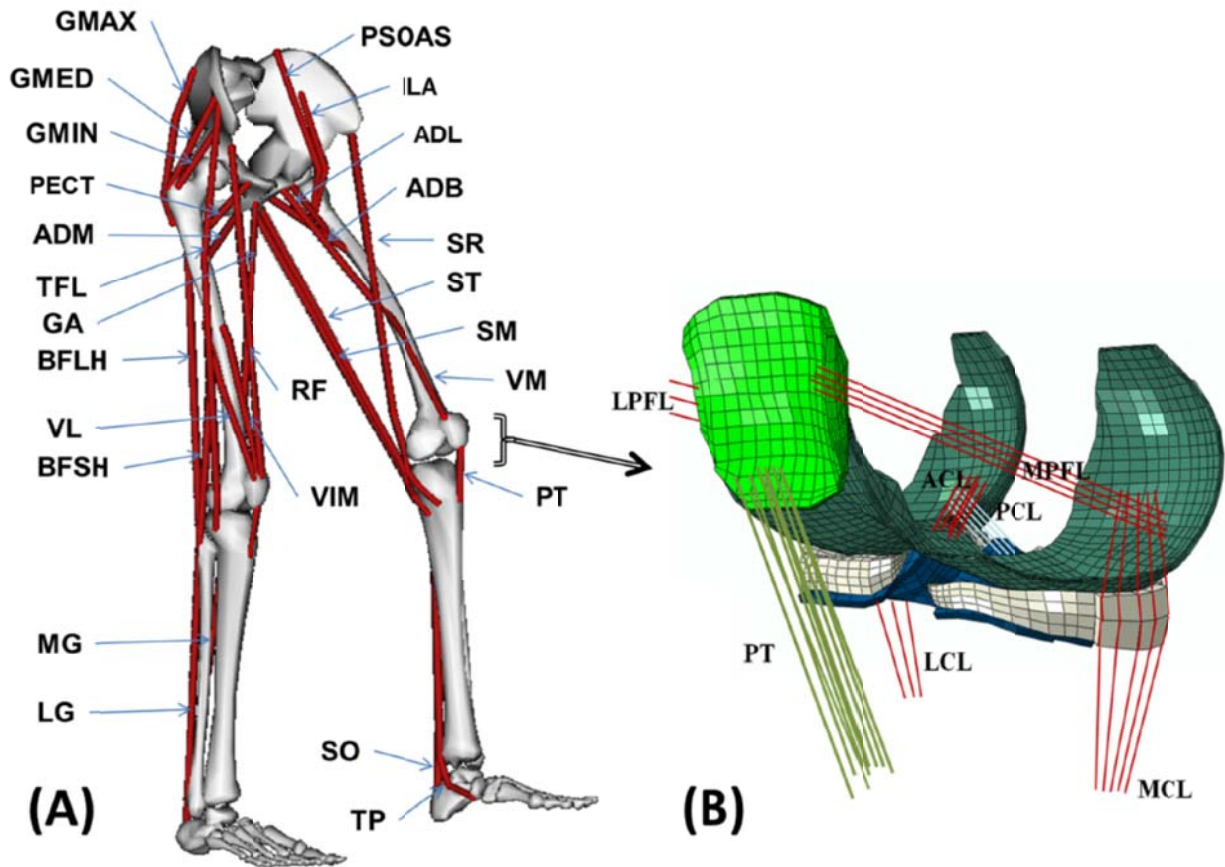


Figure 5-1: (A) Schematic diagram showing the 34 muscles incorporated into the lower extremity model (taken from OpenSim(Delp et al., 2007)). Quadriceps: vastus medialis obliquus (VMO), rectus femoris (RF), vastus intermedius medialis (VIM) and vastus lateralis (VL); Hamstrings: biceps femoris long head (BFLH), biceps femoris short head (BFSH), semimembranous (SM) and TRIPOD made of sartorius (SR), gracilis (GA) and semitendinosus (ST); Gastrocnemius: medial (MG) and lateral (LG). Tibialis posterior (TP) and soleus (SO) muscles are uni-articular ankle muscles. Hip joint muscles (not all shown) include adductor, long (ADL), mag (3 components ADM) and brev (ADB); gluteus max (3 components GMAX), med (3 components GMED) and min (3 components GMIN), iliacus (ILA), iliopsoas (PSOAS), quadriceps femoris, pectineus (PECT), tensor fascia lata (TFL), periformis. (B) Knee FE model; tibiofemoral (TF) and patellofemoral (PF) cartilage layers, menisci and patellar Tendon (PT). Joint ligaments: lateral/medial patellofemorals (LPFL/MPFL), anterior/posterior cruciates (ACL/PCL) and lateral collateral/medial collaterals (LCL/MCL).

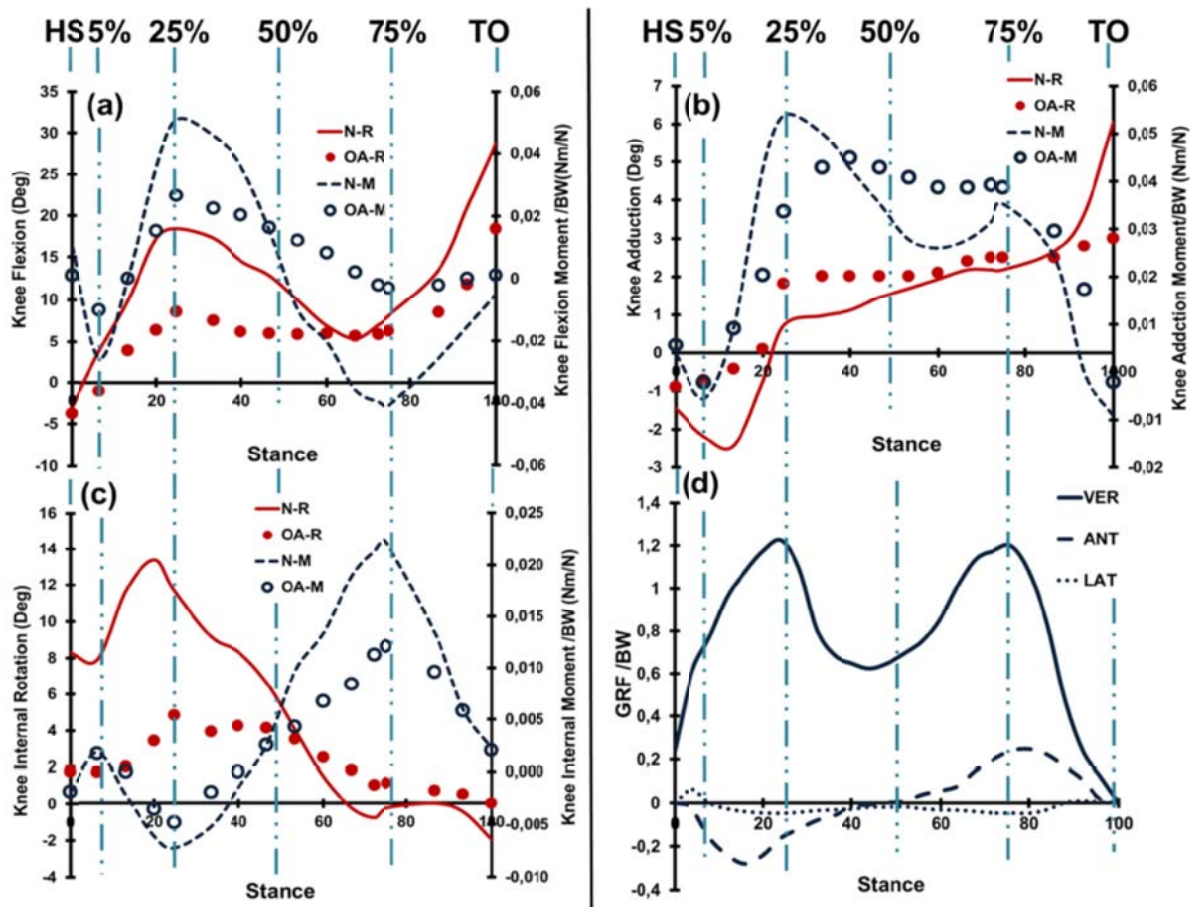


Figure 5-2: Knee joint rotations (R) and moments (M) reported as mean of asymptomatic (N) and severe OA (OA) subjects during the stance phase of gait. (Astrophen, 2007) (a) Flexion/Extension, (b) Adduction/Abduction and (c) Internal/External, (d) vertical, anterior and lateral GRF components. (Hunt et al., 2001) Six instances corresponding to beginning (heel strike, HS 0%), 5%, 25%, 50%, 75% and end (toe off, TO 100%) of the stance phase are indicated. Loads are normalized to the BW=606.6 N for the female subject of our FE model.

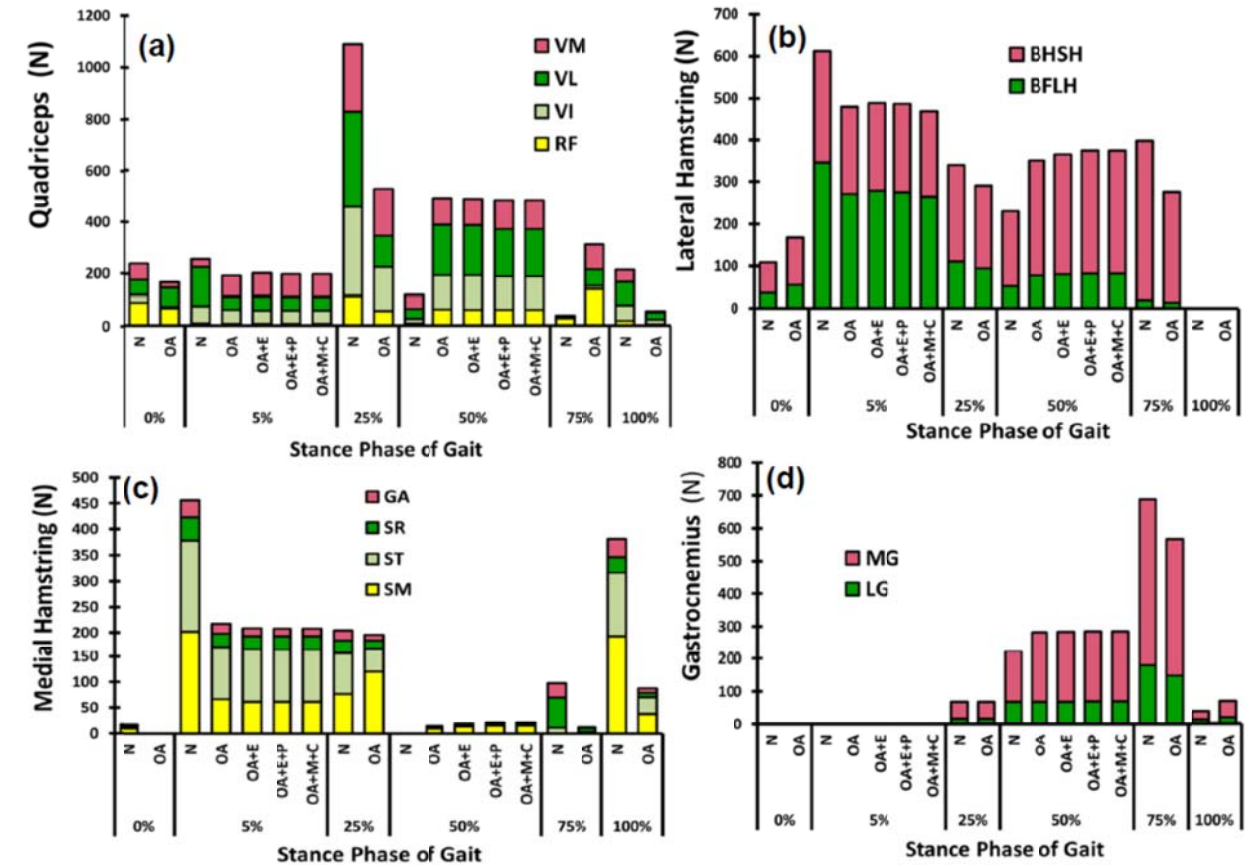


Figure 5-3: Muscle forces at different periods, (a) quadriceps, (b) lateral hamstring, (c) medial hamstring and (d)gastrocnemius.OA: SevereOA with intact material properties, N: results(Adouni et al., 2012)inasymptomatic subjects, OA+E, OA+E+P and OA+M+C present to different degrees the OA deterioration in cartilage and menisci roperties (see text).

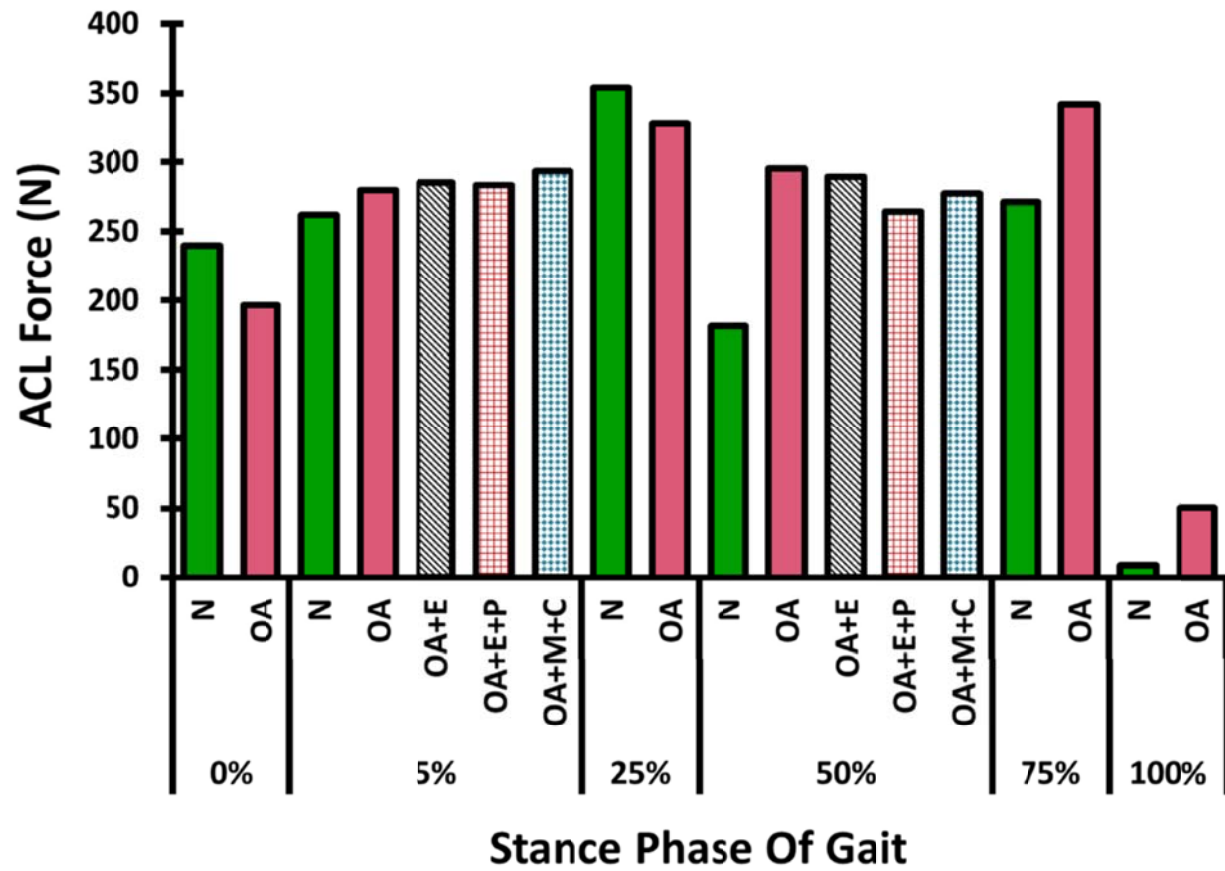


Figure 5-4: Predicted ACL forces at different stance periods (see caption of Fig.3).

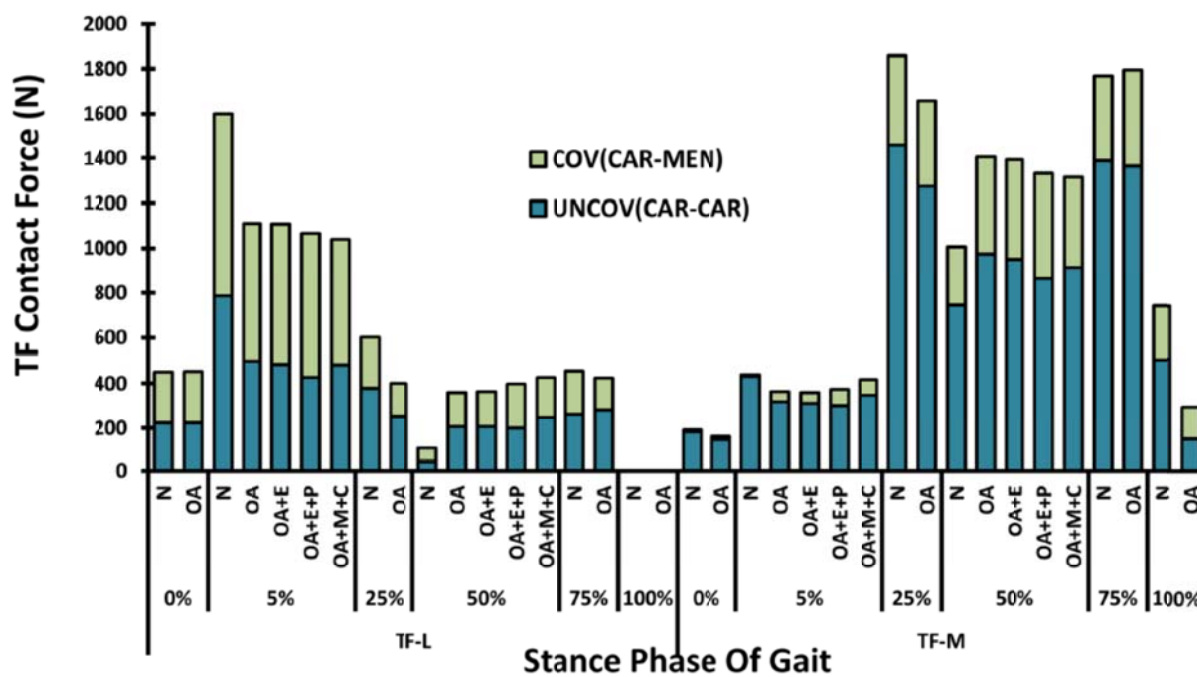


Figure 5-5: Predicted total TF contact forces (cov: via menisci, uncov: via cartilage, M: medial plateau, L: lateral) (See caption of Fig.3).

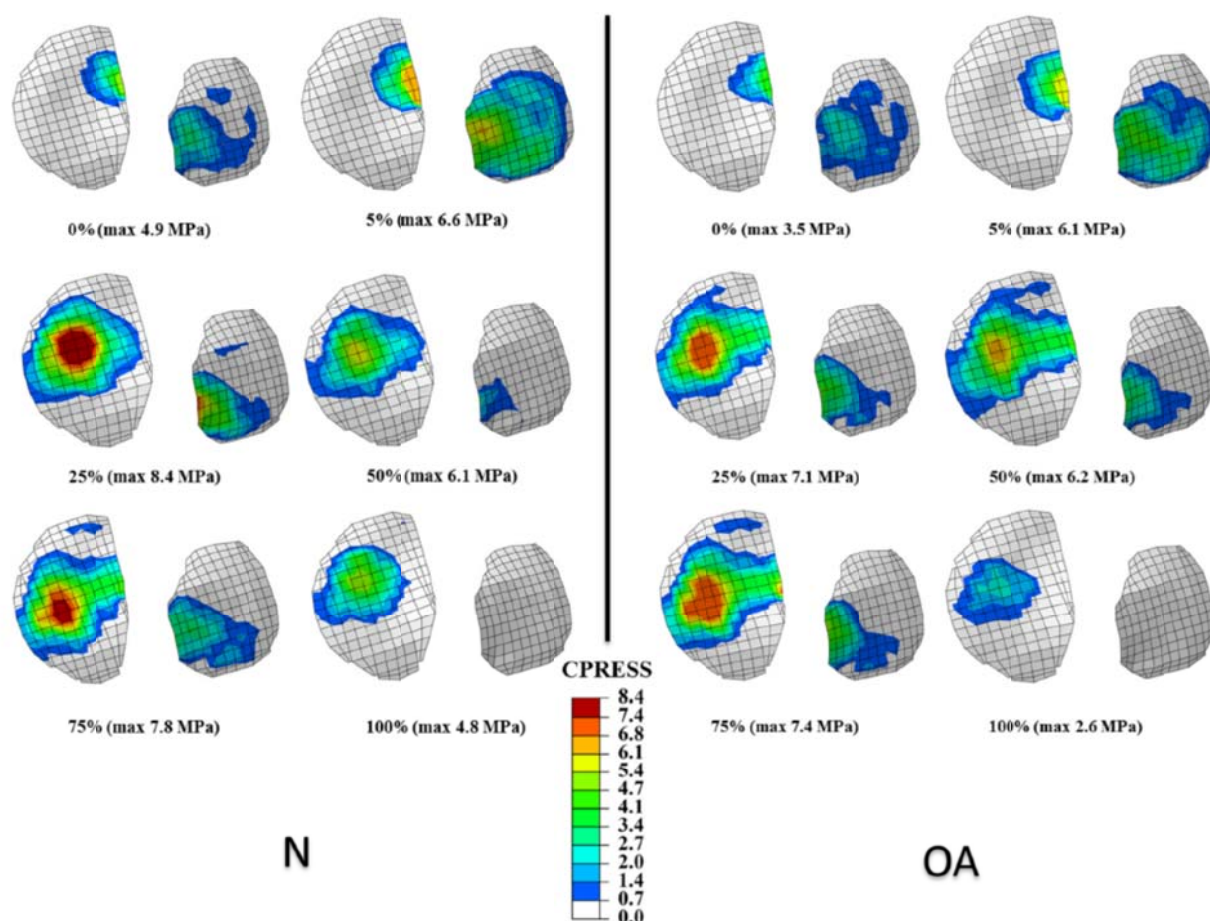


Figure 5-6: Predicted contact pressure distributions and max values at articular surfaces of tibial plateaus at different periods in normal and OA (with no change in material properties) models. Note that a common legend is used for ease in comparisons. The greater contact stresses on the medial plateau after 25% stance period and absence of articulation at the lateral plateau at TO are evident. Stresses are smaller in the OA model at all periods except at the mid-stance.

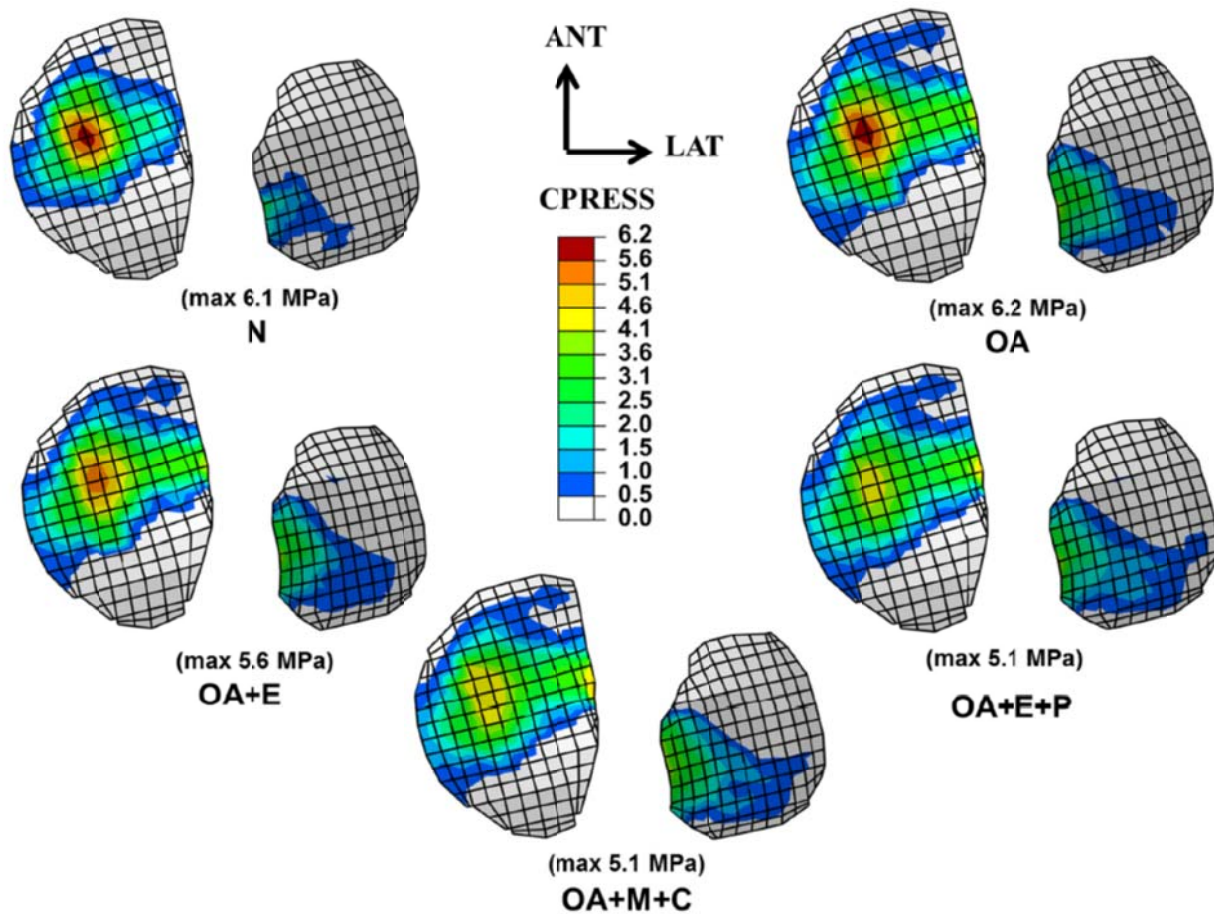


Figure 5-7: Predicted contact pressures distributions and max values at articular surfaces of tibial plateaus at the 50% of stance phase for normal and OA (with different material properties) models (see caption of Fig. 3). OA-associated deterioration in the articular tissues tends to increase contact areas and decrease contact pressures. Large stresses occur at the medial plateau on the cartilage-cartilage (uncovered) areas.

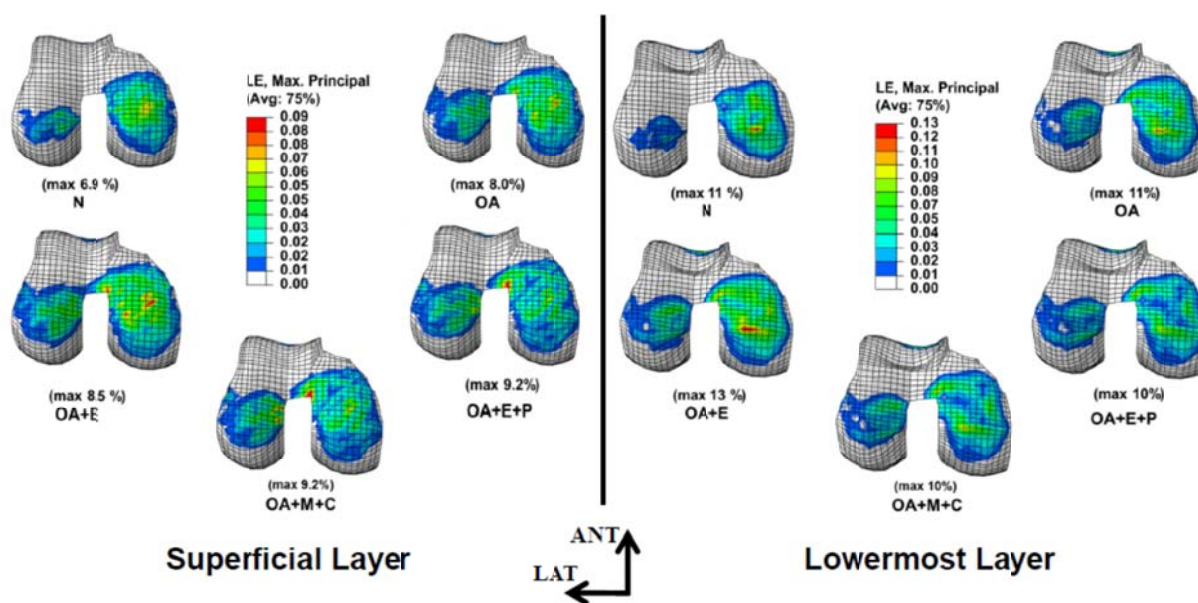


Figure 5-8: Maximum (tensile) principal strains distributions and max values at superficial and deep layers of femoral cartilage at the 50% stance phase for normal, OA (with different material properties) models (see caption of Fig. 3). Strains are much larger in the lower most layer compared to the superficial layer and on the medial condyle compared to the lateral one.

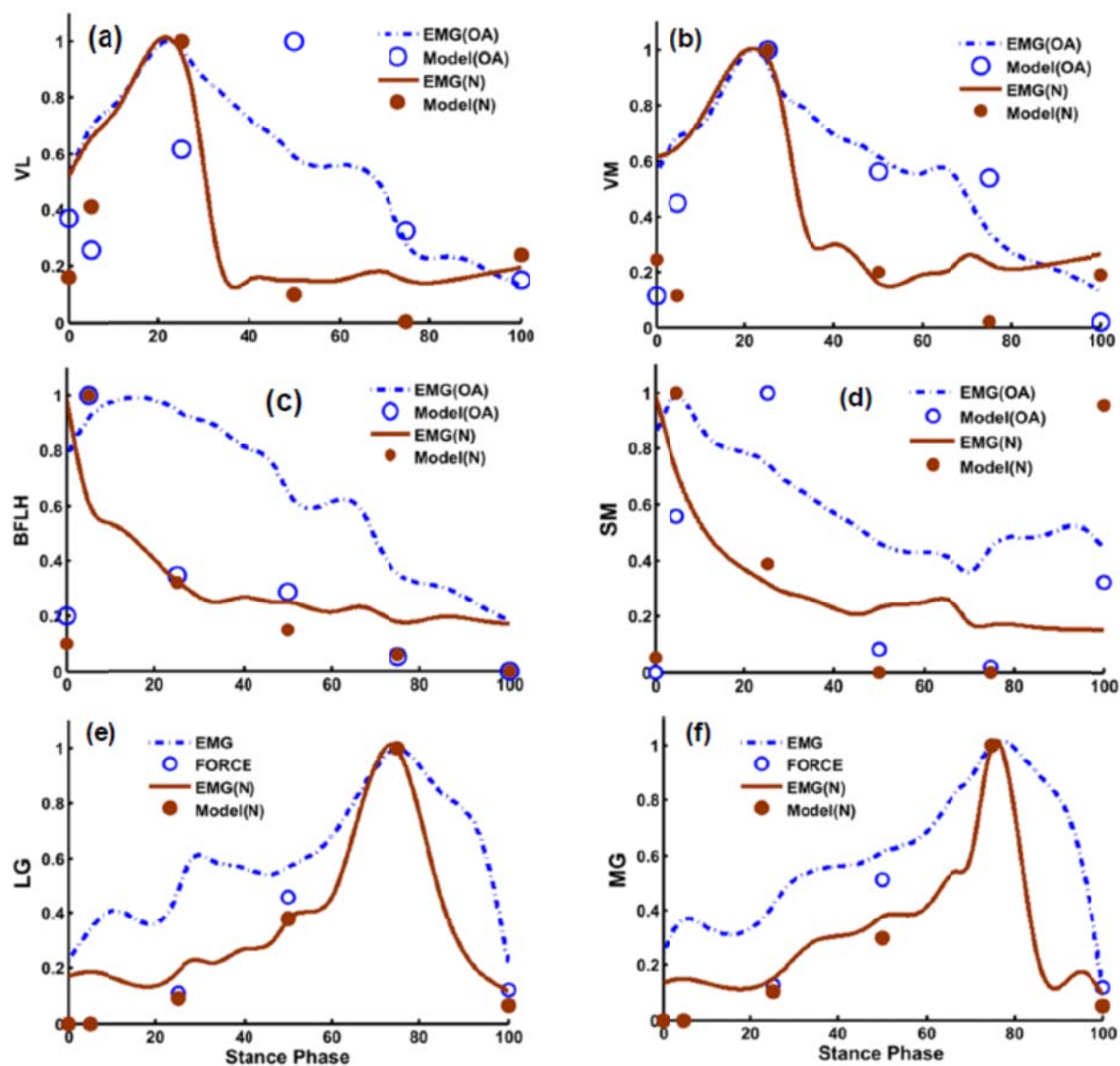


Figure 5-9: Ensemble averaged EMG (EMG)(Astephen, 2007; Hubley-Kozey et al., 2009) and estimated muscle forces (Model) normalised to their maximum values during the stance phase for various knee muscles.

**CHAPITRE 6 ARTICLE 4: PARTITIONING OF KNEE JOINT
INTERNAL FORCES IN GAIT IS DICTATED BY THE KNEE
ADDUCTION ANGLE AND NOT BY THE KNEE ADDUCTION
MOMENT**

Adouni, M; Shirazi-Adl, A

Division of Applied Mechanics, Department of Mechanical Engineering
École Polytechnique, Montréal, Québec, Canada

Article published in
Journal of Biomechanics, 2014
Volume 47, Issue 7, Pages 1696-1703

Keywords: Gait, Knee joint, Finite element method, Adduction rotation and moment, Medial contact force.

6.1 Abstract

Medial knee osteoarthritis is a debilitating disease. Surgical and conservative interventions are performed to manage its progression via reduction of load on the medial compartment or equivalently its surrogate measure, the external adduction moment. However, some studies have questioned a correlation between the medial load and adduction moment. Using a musculoskeletal model of the lower extremity driven by kinematics-kinetics of asymptomatic subjects at midstance of gait, we aim here to quantify the relative effects of changes in knee adduction rotation versus changes in adduction moment on the joint response and medial/lateral load partitioning. The reference adduction rotation of 1.6° is altered by $\pm 1.5^\circ$ to 3.1° and 0.1° or the knee reference adduction moment of 17 Nm is varied by $\pm 50\%$ to 25.5 Nm and 8.5 Nm. Quadriceps, hamstrings and tibiofemoral contact forces substantially increased as adduction rotation dropped and diminished as adduction rotation increased. The medial/lateral ratio of contact forces slightly altered by changes in the adduction moment but a larger adduction rotation increased the medial over lateral ratio from 8.8 to a whopping 90 while in contrast a smaller adduction rotation yielded a more uniform distribution. If the aim is to diminish the medial contact force irrespective of the lateral load, a drop of 1.5° in adduction rotation is much more effective by diminishing the medial load by 12% than reducing the adduction moment by 50% that only slightly (4%) decreases this load. Substantial role of changes in adduction rotation is due to the associated alterations in joint nonlinear passive resistance. These findings explain the poor correlation between knee adduction moment and tibiofemoral compartment loading during gait suggesting that the internal load partitioning is dictated by the joint adduction angle.

6.2 Introduction

Medial knee osteoarthritis (OA) is a common disease afflicting a large portion of population with a gloomy prognosis in our ageing and obese populations. The higher incidence in the medial compartment is likely associated with the greater compartmental load. Biomechanical model studies (Adouni and Shirazi-Adl, 2013; Adouni et al., 2012; Shelburne et al., 2005; Winby et al., 2009) and in vivo investigations with instrumented implants (Kim et al., 2009; Kutzner et al., 2010; Zhao et al., 2007) suggest that the major portion of tibiofemoral joint compression in gait is borne by the medial compartment. At various stages of OA pathology, surgical (e.g., osteotomy) and conservative (e.g., knee braces, shoe soles, gait modifications) interventions are

routinely carried out to manage its progression via reduction of loading on the medial compartment. The external knee adduction moment has often been considered as the surrogate measure of this medial load and a consistent marker for OA disease and severity (Andriacchi, 2013; Butler et al., 2007; Kinney et al., 2013; Sharma et al., 2000; Shelburne et al., 2008; Zhao et al., 2007). As such, it is considered as the primary parameter when evaluating the efficacy of different treatment modalities performed with the objective to diminish compartmental contact force. It is worth however to raise two important concerns here; one is that any alterations towards a valgus alignment may trigger OA initiation or progression process at the lateral compartment (Andriacchi, 2013; Felson et al., 2013; Sharma et al., 2001). The second point is that the internal load distribution is influenced not only by the external moments but also muscle forces crossing the joint and joint kinematics.

It is indeed conceivable to arrive at conditions in which larger adduction moments do not actually yield greater medial contact forces. In accordance, some recent *in vivo* studies using instrumented implants have questioned a direct association between the knee adduction moment and the medial load and qualified such correlation as poor to average (Meyer et al., 2013; Walter et al., 2010; Winby et al., 2013). Walter et al. (2010) have shown that gait modifications (medial thrust and walking pole) can significantly reduce knee adduction moment without producing equally important reductions in knee medial contact forces. To reduce knee medial loading, the foregoing study suggests minimizing alterations in the magnitude of knee flexion moment caused by gait modifications. Moreover, Meyer et al. (2013) demonstrated that external knee loads and EMG measures were not strong indicators of internal loads (medial and lateral contact forces) during gait activities. In addition, this investigation postulated that the external adduction moment was correlated more with the medial to total contact force ratio than with the medial contact force. Winby et al. (2013) also called for caution when inferring joint contact loads from external measures (i.e., loads and EMG). The mechanisms governing the association between the external loads on the knee joint and resulting load distribution within the joint remain hence unclear.

Adequate understanding of the role of various external parameters, being displacement or load dependent, is crucial in proper prevention and management of knee OA. The efficacy of prophylactic wedge insole interventions as a remedy for medial OA by reducing adduction

moment (Russell and Hamill, 2011) has been questioned as it influenced neither the adduction moment (Abdallah and Radwan, 2011; Nester et al., 2003; Schmalz et al., 2006) nor the medial contact forces estimated by an instrumented implant (Kutzner et al., 2011). Varus alignment has however been identified as a significant risk factor in medial OA (Sharma et al., 2001). A parameter that likely plays a crucial role in joint response and internal loading is the joint passive moment resistance. Ligaments, menisci, articular cartilage and contact forces are known to markedly contribute to the adduction passive moment-carrying capacity of the joint (Bendjaballah et al., 1997; Markolf et al., 1981; Marouane et al., 2013). Recently, Marouane et al. (2013) reported substantial passive resistance of the tibiofemoral joint against adduction moment that significantly increased with greater adduction rotation and compression force. The passive structures contribute both to the equilibrium of external moments thereby reducing muscle activation levels and to the stability by stiffening the joint (Markolf et al., 1981). Despite the strong sensitivity of the joint passive adduction resistance on the adduction rotation, joint rotations are either not measured or involve relatively large errors when estimated using motion analysis systems (Gorton III et al., 2009; Groen et al., 2012; Szczerbik and Kalinowska, 2011). Mean errors of up to 4.4° in adduction rotation were reported in gait when comparing intra-cortical pins versus skin markers (Benoit et al., 2005). Even with highly experienced testers, inter-tester differences of few degrees (2 to 6°) in peak rotations have been documented (Benoit et al., 2006; Leigh et al., 2013; Pohl et al., 2010). Such variations in adduction rotation could significantly (by few-fold) alter passive adduction moment of the tibiofemoral joint and as a consequence the muscle activity and internal load redistribution (Marouane et al., 2013).

Using a validated musculoskeletal model of the lower extremity including a detailed finite element (FE) model of the entire knee joint (Adouni and Shirazi-Adl, 2013) driven by reported kinematics-kinetics of asymptomatic subjects at midstance of gait (Astefhen, 2007; Hunt et al., 2001), we aim here to quantify the sensitivity of knee joint response when altering either the knee adduction rotation (by $\pm 1.5^\circ$) or the knee adduction moment (by $\pm 50\%$). Apart from the effects on muscle activation and ligament forces, attention is focused on the alterations in the contact forces on the medial and lateral compartments. It is hypothesized that the internal load partitioning is influenced primarily by changes in the adduction rotation as compared to changes in the adduction moment.

6.3 Methods

6.3.1 Finite Elements Model

An existing validated iterative kinematics-driven model that accounts for the active musculature of the lower extremity and detailed FE model of the knee joint is employed (Adouni and Shirazi-Adl, 2013; Adouni et al., 2012; Adouni and Shirazi-Adl, 2014). This model incorporates the hip and ankle respectively as 3D and 1D spherical joints crossed by a total of 31 distinct muscles (Fig. 5.1). The knee joint is represented by a complex nonlinear FE model consisting of bony structures (tibia, patella, femur), tibiofemoral (TF) and patellofemoral (PF) joints, major TF (ACL, PCL, LCL, MCL) and PF (MPFL, LPFL) ligaments, patellar tendon (PT), as well as quadriceps (4 distinct muscles), hamstrings (6 muscles), gastrocnemius (2 muscles) (see Fig. 5.1 caption). The bony structures are represented by rigid bodies due to their much higher stiffness (Donahue and Hull, 2002). Details on the musculature and knee joint ligaments (Fig. 5.1) are available elsewhere (Adouni and Shirazi-Adl, 2013, 2014) (Mesfar and Shirazi-Adl, 2005).

The depth-dependent fibrils networks at different regions of articular cartilage layers and menisci are considered. In superficial zones of femoral and tibial cartilage layers (15% of total thickness) as well as bounding surfaces of menisci, the collagen fibrils are simulated by membrane elements with uniform fibril distribution. In the transitional zone of femoral and tibial cartilage (22.5% of thickness) with random fibrils (i.e., no dominant orientations), continuum brick elements that take the principal strain directions as the material principal axes represent collagen fibrils. In the deep zones (62.5% of thickness), fibrils are modeled with vertical membrane elements similar to horizontal superficial ones while offering resistance only in their local fibril direction oriented initially normal to the subchondral junction. In the bulk region of each meniscus in between peripheral surfaces, collagen fibrils that are dominant in the circumferential direction are represented by membrane elements with local material principal axes defined in circumferential and radial directions. Thickness of membrane elements in different regions of cartilage and menisci is computed based on fibrils volume fraction in each zone. For cartilage, fibrils volume fractions of 15, 18 and 21% are considered in superficial, transitional and deep zones, respectively. In menisci, the collagen content is 14% in the circumferential direction and 2.5% in the radial direction of the bulk region along with 12% in

the outer surfaces at both directions (Shirazi and Shirazi-Adl, 2009b; Shirazi et al., 2008). The cartilage and menisci non-fibrillar matrices are simulated by continuum elements.

To study the short-term response of the joint, an elastic response (equivalent to a biphasic response) is taken with depth-dependent isotropic hyperelastic (Ogden-Compressible) material properties for the non-fibrillar solid matrix of cartilage with an elastic modulus varying linearly from 10 MPa at the surface to 18 MPa at the deep zone and a Poisson's ratio of 0.49. This model (considered here due to convergence difficulties) was initially verified to yield global displacements and stresses/strains almost identical to an earlier one having incompressible matrix with much lower moduli (~ 1 MPa) (Shirazi et al., 2008). The nearly incompressible hyperelastic model was initially also employed for the non-fibrillar menisci but due to convergence problems at contact areas, the matrix of menisci was represented, similar to our earlier studies (Mesfar and Shirazi-Adl, 2005), by a compressible elastic material with a Young's modulus of 10 MPa and a Poisson's ratio of 0.45.

6.3.2 Muscle Force Estimation

In each iteration, equilibrium equations are in the form of $\sum r \times f = M$ where r, f and M are respectively lever arms of muscles, unknown total muscle forces at the joint under consideration and associated required moments. To resolve the redundancy, optimization algorithm with the cost function of sum of cubed muscle stresses is employed along with inequality equations of muscle forces remaining positive but smaller than the maximum active forces (i.e. $0.6 \text{ MPa} \times \text{physiological cross-sectional areas, PCSA}$). Muscle force passive components are neglected here due to negligible changes expected in the muscle lengths.

6.3.3 Loading, Kinematics and Boundary Conditions

Analyses are carried out at the mid-stance period of gait. The femur is initially fixed in its instantaneous position reported in gait while the tibia and patella are completely free except for the prescribed TF rotations. The hip/knee/ankle joint rotations/moments and ground reaction forces at foot are taken from the mean data of *in vivo* measurements on asymptomatic subjects (Astefan et al., 2008a; Hunt et al., 2001). The location of resultant ground reaction force (GRF) at each instant is determined so as to generate reported joint moments (Astefan et al., 2008a)

accounting for the leg/foot weight (29.78 N/7.98 N). Since our model was constructed based on a female knee joint, a body weight of BW=606.6 N (61.9 kg) is considered (De Leva, 1996).

At mid-stance and subject to GRFs and leg/foot weight, muscle forces at the hip, knee and ankle joints are predicted iteratively by counterbalancing required moments in deformed configurations at each step. These muscle forces are subsequently applied as additional external loads and the procedure is repeated (8-10 iterations) till convergence (unbalanced moments <0.1 Nm). To investigate the effect of changes in the knee adduction rotation or moment on results, analyses are repeated under identical kinematics/kinetics except that the knee adduction angle or moment is altered one at a time; the reference adduction rotation of 1.6° is altered by $\pm 1.5^\circ$ to 3.1° and 0.1° ($R \pm 1.5$) or the knee reference adduction moment of 17 Nm is varied by $\pm 50\%$ to 25.5 Nm and 8.5 Nm ($M \pm 50\%$). These changes are chosen according to the reported variations in these quantities (Fig. 5.2) and errors in measurements (Benoit et al., 2006; Leigh et al., 2013; Pohl et al., 2010). Matlab (Optimization Toolbox, genetic algorithms) and ABAQUS 6.11.2 (SIMULIA, Providence, RI, USA) commercial programs are used.

6.4 Results

Changes in the adduction rotation or moment substantially altered muscle activations (Fig. 5.3). Forces in quadriceps increased by 77%, 65% and 22% and in R-1.5, M+50% and M-50% cases, respectively, but decreased by 26% in R+1.5 case; PT force followed similar trends reaching peak of 187N in R-1.5 case (Fig. 5.4). Forces in lateral hamstrings markedly diminished by 56% in R+1.5 and 85% in M-50% but reached its peak of 390 N in R-1.5 case. Medial hamstrings showed activity only in M-50% with minimal concurrent activity in lateral hamstrings. Forces in gastrocnemius muscles altered slightly in various cases.

Among ligaments, ACL force increased in all cases except in M-50% and reached its peak of 222N under larger adduction rotation (Fig. 5.4). The LCL force also substantially increased from 3N to its peak of 80N in R+1.5. The MCL and PCL remained unloaded throughout whereas PF ligaments resisted small forces (each <20 N) and altered negligibly in different cases.

Tibial contact forces (Fig. 5.5) remained larger always on the medial plateau and markedly increased on both plateaus with higher adduction moment but little changed with

smaller moment. Contact force on the lateral plateau hugely increased under smaller adduction rotation from 116N to 517N but almost disappeared when adduction rotation increased. The ratio of contact forces (medial over lateral) was found nearly unaffected by changes in moments but significantly increased with greater adduction rotation and diminished with smaller adduction rotation. Tibial contact areas followed nearly the same trends as contact forces; lateral contact area substantially increased by $\sim 320 \text{ mm}^2$ from R+1.5 to R-1.5 (Fig. 5.6). The PF contact force and area followed quadriceps forces and dropped only in R+1.5.

In accordance with the compartmental loads, contact pressures were much larger on the medial plateau (Fig. 5.7). A more uniform distribution was found when adduction rotation decreased (R-1.5). Maximum tensile strain in the articular cartilage occurred at the lowermost layer in all cases (Fig. 5.8). Maximum strains in the lateral plateau occurred at reduced adduction angle associated with a large contact force in this case (Fig. 5.5).

6.5 Discussion

The aim here was to investigate the effect of changes in knee external measures (adduction angle and adduction moment) on the joint response in general and medial/lateral load partitioning in particular. For this purpose, a lower-extremity musculoskeletal model accounting for passive-active structures (Adouni and Shirazi-Adl, 2013; Adouni et al., 2012) was analyzed while driven by reported kinematics/kinetics of gait at mid-stance (Astefphen, 2007; Hunt et al., 2001). Changes in the knee adduction angle substantially affected the knee passive moment resistance, forces in ACL/LCL ligaments, muscle activation, contact forces and medial/lateral partitioning. Under identical external moments, a 1.5° increase in the adduction rotation decreased the total contact force by 4% and almost unloaded the lateral compartment but increased the medial share slightly by 5%. A 1.5° drop in the adduction rotation, on the other hand, significantly increased total contact force by 20% and the lateral load by 346% but reduced the medial load by 12% resulting in a more uniform distribution of load on plateaus. The medial/lateral load ratio was hugely altered from 8.8 in the reference case to a whopping 90 or 1.7 as rotation respectively increased or decreased. With substantial alteration in the external adduction moment by 50% under identical joint rotations, the total/medial/lateral loads increased markedly by 21/18/50% with higher moment and decreased by only 3/4/-10% under lower

moment. The ratio of contact loads (medial over lateral) altered from 8.8 to 7 and 7.7 in these cases that are far smaller than those when adduction rotation was changed. These predictions confirm our hypothesis that the internal load distribution is influenced primarily by changes in the adduction rotation and not in the adduction moment.

In order to isolate the effects of changes in adduction rotation and adduction moment on the joint response, the input data at the mid-stance phase was altered one at a time. In this manner, the distinct effect of such alterations could be estimated without any confounding effects. The relative magnitude of predictions could have altered had another instance of gait been simulated but the conclusions would remain the same. The same applies to alterations in model geometry and material properties. Moreover, despite the fact that the changes in adduction rotation by $\pm 1.5^\circ$ covers the range of values reported in earlier studies (Fig. 5.2) and that 50% change in the adduction moment is relatively large (Fig. 5.2), the extent of differences computed here would as expected alter had we chosen other values. It has been reported that decreased knee adduction moments brought about by gait modifications could be coupled with increases in the knee flexion moment (Kinney et al., 2013; Meyer et al., 2013; Walter et al., 2010). We did not consider any concurrent changes in flexion moment or rotation.

Changes in the knee adduction rotation ($R \pm 1.5$) substantially altered knee muscle activations at mid-stance of gait. Forces in lateral hamstrings (primarily in BFSH) substantially dropped with larger adduction rotation ($R + 1.5$) but increased with smaller adduction rotation. These alterations are due to variations in the passive moment contribution of the knee joint that plays a significant role in the joint equilibrium in the frontal plane (Lloyd and Buchanan, 2001). This trend as adduction rotation increases also explains the electromyography (EMG) silence in lateral hamstrings reported during late stance (Astephen et al., 2008a; Besier et al., 2009; Shelburne et al., 2006; Winby et al., 2009). Due to the antagonism of these muscles with quadriceps in the sagittal plane, similar trends occurred in quadriceps; similar to lateral hamstrings quadriceps forces dropped with larger adduction rotation and increased with smaller adduction rotation (Fig. 5.3). The medial hamstrings remained silent irrespective of the adduction rotations considered. Had larger adduction rotations been applied here, activity in hamstrings would rise to overcome the passive resistance of the joint in excess of the external adduction moment. Forces in lateral hamstrings were linearly proportional to the external adduction

moment; a trend that concurred with the fact that the passive moment resistance of the joint remained nearly unchanged at a fixed adduction rotation.

The crucial role of the knee passive resistance in the response becomes more evident when the differences between the applied moments (i.e, via inverse dynamics) and the portion resisted by muscles are evaluated in the frontal plane. This difference is indicative of the passive contribution reaching adduction moments of 8, 0 and 14 Nm in the Ref, R-1.5 and R+1.5 cases, respectively. These dramatic changes in the passive moment contribution with the adduction rotation altered demands on muscle activities, joint response and internal loads. In corroboration and under similar axial compression forces (1400 N), Marouane et al. (2013) reported an increase of 14 Nm in the TF passive adduction moment resistance as the adduction rotation increased by $\sim 1.4^\circ$. Lloyd and Buchanan (2001) estimated the contribution of muscles to the joint adduction moment at 11-14% which agrees with our $\sim 16\%$ under larger adduction rotation. This small value (Lloyd and Buchanan, 2001) has widely been used as an argument to overlook the role of muscles in equilibrium of the frontal plane and limit attention to the sagittal plane alone (Besier et al., 2009; Fraysse et al., 2009; Shelburne et al., 2004; Shelburne et al., 2005, 2006; Winby et al., 2009). This argument holds when the applied external adduction moment is almost entirely supported by the passive resistance of the joint which happens only at a specific adduction rotation and joint compression. Due to the strong dependency of joint passive adduction resistance on adduction rotation and compression (Marouane et al., 2013), the domain of validity of such models shifts as rotation and compression alter and is limited at each instance with the error growing as adduction rotations or moments deviate.

Forces in ligaments, especially ACL and LCL, also altered as a consequence of alterations in muscle activity and joint translations as adduction rotation or moment changed. In particular, LCL force markedly increased under greater adduction rotation (R+1.5) since collateral ligaments are the primary load-bearing structures in the frontal plane. The force in ACL also increased that is likely due to the substantial drop in lateral hamstrings activity despite a smaller drop in quadriceps activity. Force in ACL also increased as adduction rotation decreased (R-1.5) that is likely due to higher quadriceps activity (Mesfar and Shirazi-Adl, 2005; Shin et al., 2011). Increases in ACL and LCL forces as adduction rotation decreases is the main reason for greater

contact force on the medial compartment despite much smaller activities in both hamstrings and quadriceps in this case.

The knee adduction moment has frequently been used as a surrogate measure for the medial contact forces and hence a marker for OA disease and severity (Butler et al., 2007; Kinney et al., 2013; Shelburne et al., 2008; Zhao et al., 2007). Nonetheless, such association has been questioned by several studies (Meyer et al., 2013). The efficacy of insole interventions as a remedy for medial OA by reducing adduction moment (Russell and Hamill, 2011) has also been questioned not to correlate either with the adduction moment (Abdallah and Radwan, 2011; Nester et al., 2003; Schmalz et al., 2006) or the medial contact forces using an instrumented implant (Kutzner et al., 2011). Varus alignment has however been identified as a significant risk factor in medial OA (Sharma et al., 2001). Our findings here show that with 50% increase in the adduction moment, the medial load alters by <18% and the ratio of medial over lateral load alters by <20% (Fig. 5.5). Smaller respective values of 4% and 13% are found when the adduction moment reduces by 50%. Similarly, large changes in the knee adduction moment did not translate to similar changes in cartilage contact pressures. In agreement with Walter et al. (2010), these results clearly refute any meaningful correlation between adduction moment and internal load redistribution.

At the same time, changes in the adduction rotation by only 1.5° (from 1.6° in the reference case) had significant effects on the medial/lateral load partitioning; greater adduction rotation increased the load on the medial compartment and almost unloaded the opposite lateral compartment. A reverse trend was observed with smaller adduction rotation where a huge contact force was computed on the lateral plateau resulting in greater total contact force (20%) despite lower load on the medial compartment. As a consequence of increased contact area under smaller adduction rotation, peak pressure on the articular cartilage decreased by ~30%. Higher adduction angle recorded at late stance would further unload the lateral plateau likely causing the lift-off mechanism despite the existing abduction moment (Adouni and Shirazi-Adl, 2013; Adouni and Shirazi-Adl, 2014; Hurwitz et al., 1998). Mononen et al. (2013b) computed greater lateral compartment load during stance phase that is due to the knee abduction rotation considered.

Current results hence demonstrate that the relative inter-compartmental partitioning of contact loads is influenced mainly by changes in the adduction rotation. The effects of 1.5° alterations in rotation far exceeded those caused by 50% change in adduction moment (Fig. 5.5). Overall and based on current results, if a more uniform distribution of contact loads between medial and lateral plateaus are sought; alignment of the joint should be adjusted towards a more neutral varus-valgus involving very small adduction-abduction rotations. Any deviation from this position loads one plateau at the expense of unloading the other. Here a larger adduction rotation increased the medial over lateral ratio from 8.8 to a whopping 90 while in contrast a smaller adduction rotation yielded a more uniform distribution. On the other hand, if the aim is to diminish the medial contact force irrespective of the lateral load, once again reducing the adduction rotation by 1.5° is much more effective by diminishing the load by 12% than reducing the adduction moment by 50% that only slightly (4%) decreases the medial load. The present findings emphasize also the importance of accurate recording of the knee joint adduction/abduction rotation in various activities.

Finally, changes in the knee adduction angle substantially affects the moment resistant capacity of knee passive structures, activation level in all muscles crossing the joint, contact forces and partitioning between compartments. An increase in the adduction rotation almost unloaded the lateral compartment and increased medial share while a decrease therein generated large load on the lateral compartment but a smaller load on the medial one. Alterations in external adduction moment had smaller effects. These findings explain the poor correlation between knee adduction moment and tibiofemoral compartment loading in gait suggesting that the internal load partitioning is dictated mainly by the joint adduction rotation. This has important consequences in therapeutic interventions aiming to diminish load on the medial compartment.

6.6 Acknowledgement

The work is supported by a grant from the Natural Sciences and Engineering Research Council of Canada (NSERC-Canada).

6.7 References

- Abdallah, A.A., Radwan, A.Y., 2011. Biomechanical changes accompanying unilateral and bilateral use of laterally wedged insoles with medial arch supports in patients with medial knee osteoarthritis. *Clinical Biomechanics* 26, 783-789.
- Adouni, M., Shirazi-Adl, A., 2013. Consideration of equilibrium equations at the hip joint alongside those at the knee and ankle joints has mixed effects on knee joint response during gait. *Journal of Biomechanics* 46, 619-624.
- Adouni, M., Shirazi-Adl, A., Shirazi, R., 2012. Computational biodynamics of human knee joint in gait: From muscle forces to cartilage stresses. *Journal of Biomechanics* 45, 2149-2156.
- Adouni, M., Shirazi-Adl, A., 2014. Evaluation of knee joint muscle forces and tissue stresses-strains during gait in severe OA versus normal subjects. *Journal of Orthopaedic Research* 32, 69-78.
- Andriacchi, T.P., 2013. Valgus alignment and lateral compartment knee osteoarthritis: A biomechanical paradox or new insight into knee osteoarthritis? *Arthritis & Rheumatism* 65, 310-313.
- Astephen, J.L., 2007. Biomechanical factors in the progression of knee osteoarthritis. *School of Biomedical Engineering*. Halifax, Dalhousie university.
- Astephen, J.L., Deluzio, K.J., Caldwell, G.E., Dunbar, M.J., 2008a. Biomechanical changes at the hip, knee, and ankle joints during gait are associated with knee osteoarthritis severity. *Journal of Orthopaedic Research* 26, 332-341.
- Bendjaballah, M., Shirazi-Adl, A., Zukor, D., 1997. Finite element analysis of human knee joint in varus-valgus. *Clinical Biomechanics* 12, 139-148.
- Benoit, D.L., Ramsey, D.K., Lamontagne, M., Xu, L., Wretenberg, P., Renstrom, P., 2006. Effect of skin movement artifact on knee kinematics during gait and cutting motions measured in vivo. *Gait Posture* 24, 152-164.
- Besier, T.F., Fredericson, M., Gold, G.E., Beaupré, G.S., Delp, S.L., 2009. Knee muscle forces during walking and running in patellofemoral pain patients and pain-free controls. *Journal of Biomechanics* 42, 898-905.

- Butler, R.J., Marchesi, S., Royer, T., Davis, I.S., 2007. The effect of a subject-specific amount of lateral wedge on knee mechanics in patients with medial knee osteoarthritis. *Journal of Orthopaedic Research* 25, 1121-1127.
- De Leva, P., 1996. Adjustments to Zatsiorsky-Seluyanov's segment inertia parameters. *Journal of Biomechanics* 29, 1223-1230.
- Delp, S.L., Anderson, F.C., Arnold, A.S., Loan, P., Habib, A., John, C.T., Guendelman, E., Thelen, D.G., 2007. OpenSim: open-source software to create and analyze dynamic simulations of movement. *Biomedical Engineering, IEEE Transactions on* 54, 1940-1950.
- Donahue, T.L.H., Hull, M., 2002. A finite element model of the human knee joint for the study of tibio-femoral contact. *Journal of Biomechanical Engineering* 124, 273.
- Felson, D.T., Niu, J., Gross, K.D., Englund, M., Sharma, L., Cooke, T.D., Guermazi, A., Roemer, F.W., Segal, N., Goggins, J.M., Lewis, C.E., Eaton, C., Nevitt, M.C., 2013. Valgus malalignment is a risk factor for lateral knee osteoarthritis incidence and progression: findings from the Multicenter Osteoarthritis Study and the Osteoarthritis Initiative. *Arthritis & Rheumatism* 65, 355-362.
- Frayssé, F., Dumas, R., Cheze, L., Wang, X., 2009. Comparison of global and joint-to-joint methods for estimating the hip joint load and the muscle forces during walking. *Journal of Biomechanics* 42, 2357-2362.
- Gao, B., Zheng, N.N., 2010. Alterations in three-dimensional joint kinematics of anterior cruciate ligament-deficient and-reconstructed knees during walking. *Clinical Biomechanics* 25, 222-229.
- Gorton III, G.E., Hebert, D.A., Gannotti, M.E., 2009. Assessment of the kinematic variability among 12 motion analysis laboratories. *Gait & Posture* 29, 398-402.
- Groen, B., Geurts, M., Nienhuis, B., Duysens, J., 2012. Sensitivity of the OLGA and VCM models to erroneous marker placement: Effects on 3D-gait kinematics. *Gait & Posture* 35, 517-521.
- Hunt, Smith, R.M., Torode, M., Keenan, A.M., 2001. Inter-segment foot motion and ground reaction forces over the stance phase of walking. *Clinical Biomechanics* 16, 592-600.

- Hurwitz, D.E., Sumner, D.R., Andriacchi, T.P., Sugar, D.A., 1998. Dynamic knee loads during gait predict proximal tibial bone distribution. *Journal of Biomechanics* 31, 423-430.
- Kadaba, M.P., Ramakrishnan, H., Wootten, M., 1990. Measurement of lower extremity kinematics during level walking. *Journal of Orthopaedic Research* 8, 383-392.
- Kim, H.J., Fernandez, J.W., Akbarshahi, M., Walter, J.P., Fregly, B.J., Pandy, M.G., 2009. Evaluation of predicted knee joint muscle forces during gait using an instrumented knee implant. *Journal of Orthopaedic Research* 27, 1326-1331.
- Kinney, A.L., Besier, T.F., Silder, A., Delp, S.L., D'Lima, D.D., Fregly, B.J., 2013. Changes in in vivo knee contact forces through gait modification. *Journal of Orthopaedic Research* 31, 434-440.
- Kozanek, M., Hosseini, A., Liu, F., Van de Velde, S.K., Gill, T.J., Rubash, H.E., Li, G., 2009. Tibiofemoral kinematics and condylar motion during the stance phase of gait. *Journal of Biomechanics* 42, 1877-1884.
- Kutzner, I., Damm, P., Heinlein, B., Dymke, J., Graichen, F., Bergmann, G., 2011. The effect of laterally wedged shoes on the loading of the medial knee compartment-in vivo measurements with instrumented knee implants. *Journal of Orthopaedic Research* 29, 1910-1915.
- Kutzner, I., Heinlein, B., Graichen, F., Bender, A., Rohlmann, A., Halder, A., Beier, A., Bergmann, G., 2010. Loading of the knee joint during activities of daily living measured in vivo in five subjects. *Journal of Biomechanics* 43, 2164.
- Leigh, R.J., Pohl, M.B., Ferber, R., 2013. Does tester experience influence the reliability with which 3D gait kinematics are collected in healthy adults? *Physical Therapy in Sport*.
- Lloyd, D.G., Buchanan, T.S., 2001. Strategies of muscular support of varus and valgus isometric loads at the human knee. *Journal of Biomechanics* 34, 1257-1267.
- Markolf, K.L., Bargar, W.L., Shoemaker, S.C., Amstutz, H.C., 1981. The role of joint load in knee stability. *The Journal of bone and joint surgery. American volume* 63, 570.

- Marouane, H., Shirazi-Adl, A., Adouni, M., 2013. Knee joint passive stiffness and moment in sagittal and frontal planes markedly increase with compression. *Computer Methods in Biomechanics and Biomedical Engineering*, 1-12.
- Mesfar, W., Shirazi-Adl, A., 2005. Biomechanics of the knee joint in flexion under various quadriceps forces. *The knee* 12, 424-434.
- Meyer, A.J., D'Lima, D.D., Besier, T.F., Lloyd, D.G., Colwell, C.W., Jr., Fregly, B.J., 2013. Are external knee load and EMG measures accurate indicators of internal knee contact forces during gait? *Journal of Orthopaedic Research* 31, 921-929.
- Mononen, M.E., Jurvelin, J.S., Korhonen, R.K., 2013. Implementation of a gait cycle loading into healthy and meniscectomised knee joint models with fibril-reinforced articular cartilage. *Computer Methods in Biomechanics and Biomedical Engineering*, 1-12.
- Nester, C., Van Der Linden, M., Bowker, P., 2003. Effect of foot orthoses on the kinematics and kinetics of normal walking gait. *Gait & Posture* 17, 180-187.
- Pohl, M.B., Lloyd, C., Ferber, R., 2010. Can the reliability of three-dimensional running kinematics be improved using functional joint methodology? *Gait & Posture* 32, 559-563.
- Russell, E.M., Hamill, J., 2011. Lateral wedges decrease biomechanical risk factors for knee osteoarthritis in obese women. *Journal of Biomechanics* 44, 2286-2291.
- Schmalz, T., Blumentritt, S., Drewitz, H., Freslier, M., 2006. The influence of sole wedges on frontal plane knee kinetics, in isolation and in combination with representative rigid and semi-rigid ankle-foot-orthoses. *Clinical Biomechanics* 21, 631-639.
- Sharma, L., Lou, C., Cahue, S., Dunlop, D.D., 2000. The mechanism of the effect of obesity in knee osteoarthritis: the mediating role of malalignment. *Arthritis & Rheumatism* 43, 568-575.
- Sharma, L., Song, J., Felson, D.T., Cahue, S., Shamiyeh, E., Dunlop, D.D., 2001. The role of knee alignment in disease progression and functional decline in knee osteoarthritis. *JAMA: the journal of the American Medical Association* 286, 188-195.
- Shelburne, K.B., Pandy, M.G., Anderson, F.C., Torry, M.R., 2004. Pattern of anterior cruciate ligament force in normal walking. *Journal of Biomechanics* 37, 797-805.

- Shelburne, K.B., Torry, M.R., Pandy, M.G., 2005. Muscle, ligament, and joint-contact forces at the knee during walking. *Medicine & Science in Sports & Exercise* 37, 1948.
- Shelburne, K.B., Torry, M.R., Pandy, M.G., 2006. Contributions of muscles, ligaments, and the ground reaction force to tibiofemoral joint loading during normal gait. *Journal of Orthopaedic Research* 24, 1983-1990.
- Shelburne, K.B., Torry, M.R., Steadman, J.R., Pandy, M.G., 2008. Effects of foot orthoses and valgus bracing on the knee adduction moment and medial joint load during gait. *Clinical Biomechanics* 23, 814-821.
- Shin, C.S., Chaudhari, A.M., Andriacchi, T.P., 2011. Valgus plus internal rotation moments increase anterior cruciate ligament strain more than either alone. *Med Sci Sports Exerc* 43, 1484-1491.
- Shirazi, R., Shirazi-Adl, A., 2009. Computational biomechanics of articular cartilage of human knee joint: Effect of osteochondral defects. *Journal of Biomechanics* 42, 2458-2465.
- Shirazi, R., Shirazi-Adl, A., Hurtig, M., 2008. Role of cartilage collagen fibrils networks in knee joint biomechanics under compression. *Journal of Biomechanics* 41, 3340-3348.
- Szczerbik, E., Kalinowska, M., 2011. The influence of knee marker placement error on evaluation of gait kinematic parameters. *Acta of Bioengineering and Biomechanics* 13, 43-46.
- Walter, J.P., D'Lima, D.D., Colwell, C.W., Jr., Fregly, B.J., 2010. Decreased knee adduction moment does not guarantee decreased medial contact force during gait. *Journal of Orthopaedic Research* 28, 1348-1354.
- Winby, C., Gerus, P., Kirk, T., Lloyd, D., 2013. Correlation between EMG-based co-activation measures and medial and lateral compartment loads of the knee during gait. *Clinical Biomechanics* 28, 1014-1019.
- Winby, C., Lloyd, D., Besier, T., Kirk, T., 2009. Muscle and external load contribution to knee joint contact loads during normal gait. *Journal of Biomechanics* 42, 2294-2300.

- Zhang, L.-Q., Shiavi, R.G., Limbird, T.J., Minorik, J.M., 2003. Six degrees-of-freedom kinematics of ACL deficient knees during locomotion—compensatory mechanism. *Gait & Posture* 17, 34-42.
- Zhao, D., Banks, S.A., Mitchell, K.H., D'Lima, D.D., Colwell, C.W., Fregly, B.J., 2007. Correlation between the knee adduction torque and medial contact force for a variety of gait patterns. *Journal of Orthopaedic Research* 25, 789-797.

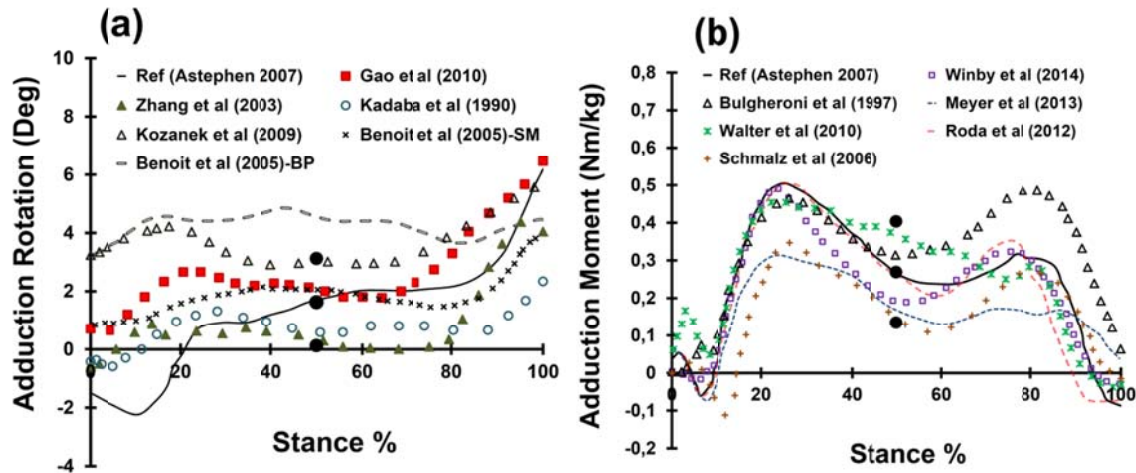


Figure 6-2: Knee joint adduction rotations (a) and moments (b) reported in the literature as mean of asymptomatic subjects during the stance phase of gait. The range of values for the data from our reference study (Astéphen, 2007) is also shown. Solid circle show the reference (Ref) and extreme values of $\text{Ref} \pm 1.5^\circ$ in rotation and $\text{Ref} \pm 50\%$ in moment. Note that moments are reported normalized to BW (Kg). Number of subjects used by Ref equal to 60 subjects (37 female and 23 male), 15 subjects for Gao et al.,(2010), 30 subjects (25 Female and 5 Male) for Zhang et al.,(2003), 40 subjects (28 Male and 12 Female) for Kadaba et al.,(1990), 8 subjects (6 Male and 2 Female) for Kozanek et al.,(2009), 8 subjects (Male) for benoit et al.,(2005)-SM (used skin marker) and BP (used Bone pin), 5 subjects for Bulgheroni et al.,(1997), 1 subject for Meyre et al.,(2013) and Walter et al., (2010), 28 subjects for Winby et al.,(2013), 10 subjects (6 Male and 4 Female) for Schmalz et al.,(2006) and finally 60 subjects for Roda et al.,(2012).

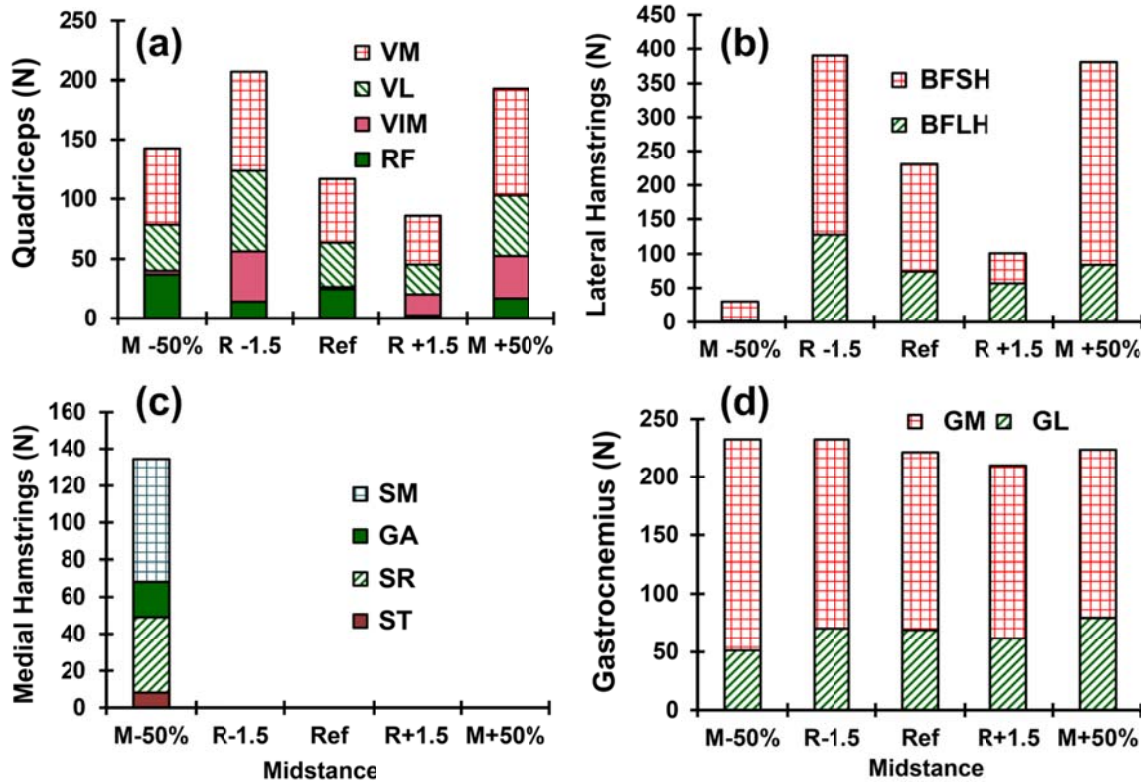


Figure 6-3: Predicted muscle forces at midstance of stance phase. (a) Quadriceps, (b) Lateral Hamstring, (c) Medial Hamstring and (d) Gastrocnemius. R ± 1.5 ; the reference adduction rotation of 1.6° is altered by $\pm 1.5^\circ$ to 3.1° and 0.1° or M $\pm 50\%$ the knee reference adduction moment of 17 Nm is varied by $\pm 50\%$ to 25Nm and 9Nm.

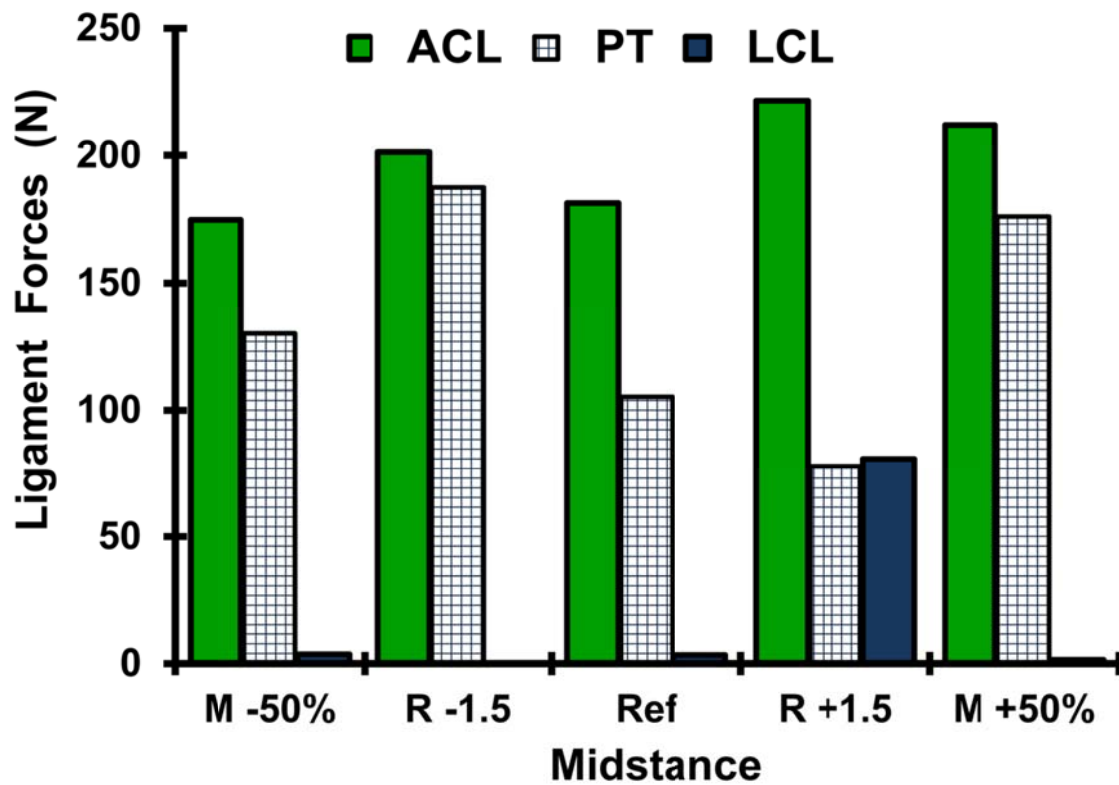


Figure 6-4: Predicted Ligament and patellar Tendon (PT) forces at 50% of stance phase (midstance). R ± 1.5 ; the reference adduction rotation of 1.6° is altered by $\pm 1.5^\circ$ to 3.1° and 0.1° or M $\pm 50\%$ the knee reference adduction moment of 17 Nm is varied by $\pm 50\%$ to 25Nm and 9Nm.

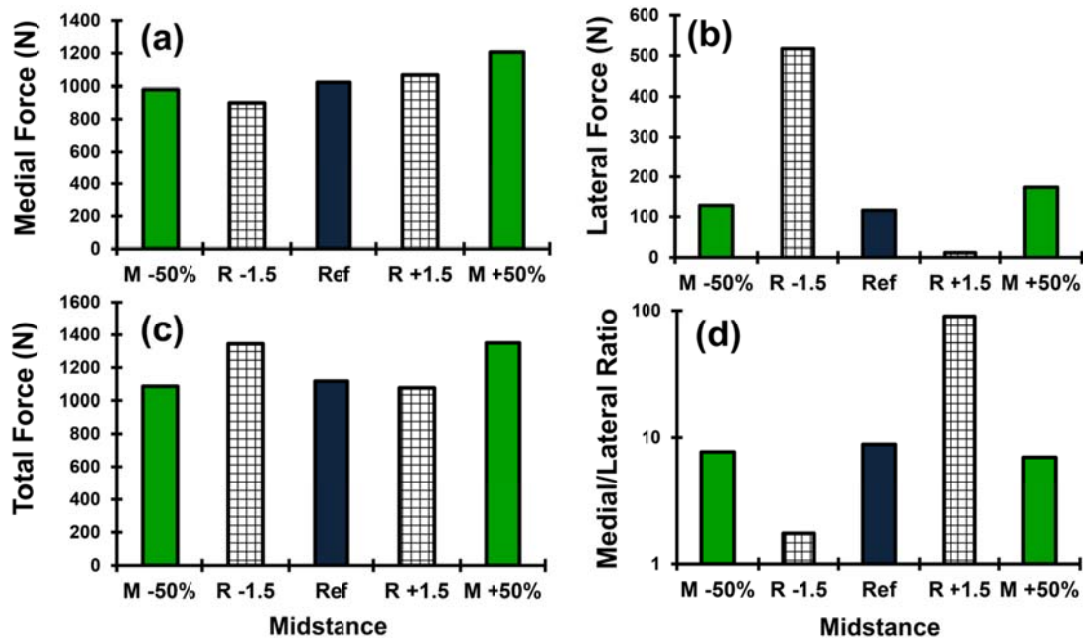


Figure 6-5: Predicted total TF (c) (as well as individual components at medial (a) and lateral (b) plateaus) and ratio medial to lateral forces (d). $R \pm 1.5$; the reference adduction rotation of 1.6° is altered by $\pm 1.5^\circ$ to 3.1° and 0.1° or $M \pm 50\%$ the knee reference adduction moment of 17 Nm is varied by $\pm 50\%$ to 25Nm and 9Nm.

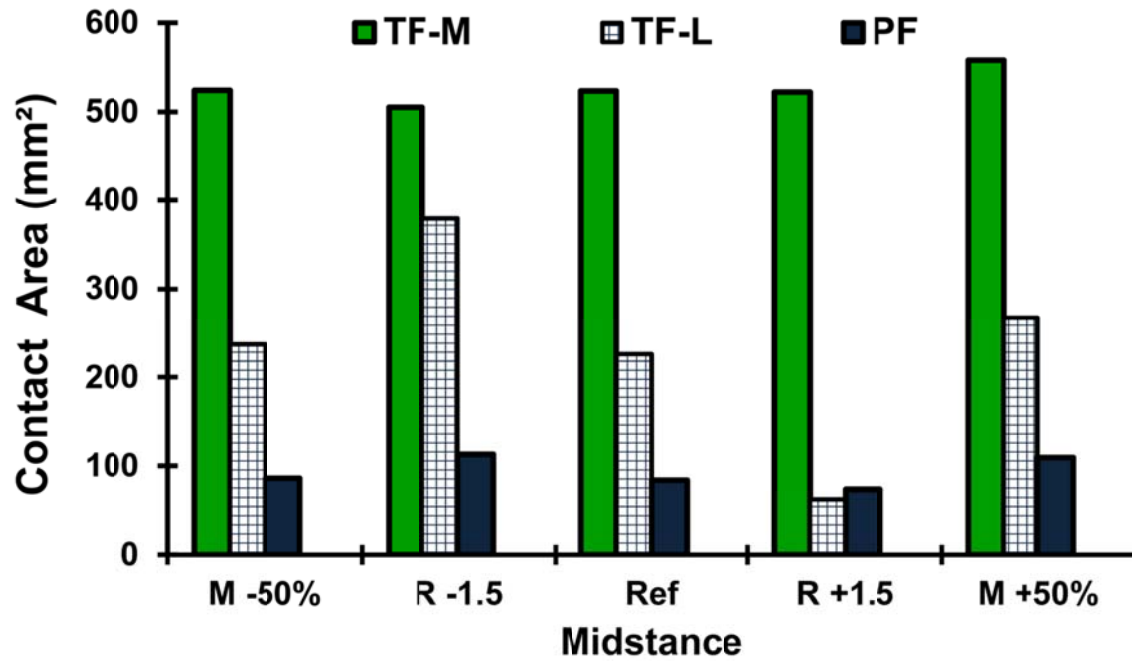


Figure 6-6: Predicted total TF (M: Medial and L: Lateral) and PF contact areas at midstance. R ± 1.5 ; the reference adduction rotation of 1.6° is altered by $\pm 1.5^\circ$ to 3.1° and 0.1° or M $\pm 50\%$ the knee reference adduction moment of 17 Nm is varied by $\pm 50\%$ to 25Nm and 9Nm.

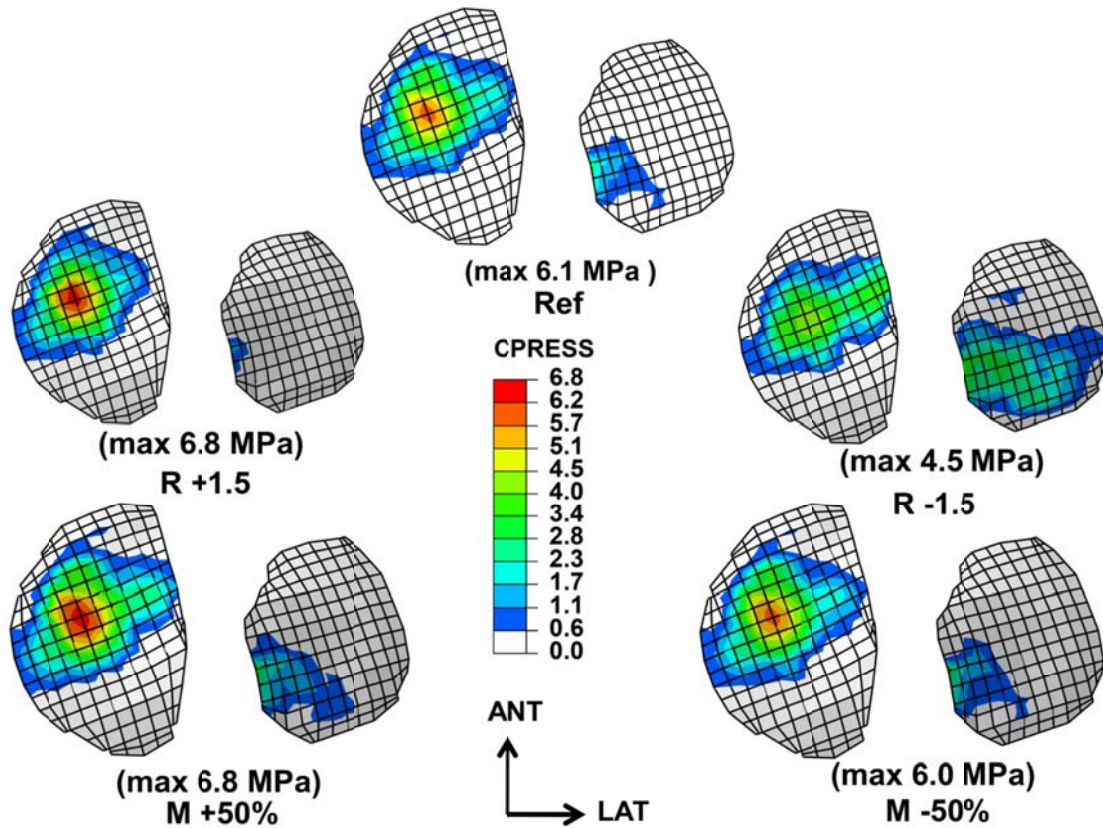


Figure 6-7: Predicted contact pressure at articular surface of lateral and medial tibial plateaus at midstance. $R \pm 1.5$; the reference adduction rotation of 1.6° is altered by $\pm 1.5^\circ$ to 3.1° and 0.1° or $M \pm 50\%$ the knee reference adduction moment of 17 Nm is varied by $\pm 50\%$ to 25Nm and 9Nm. Note that a common legend is used for ease in comparisons.

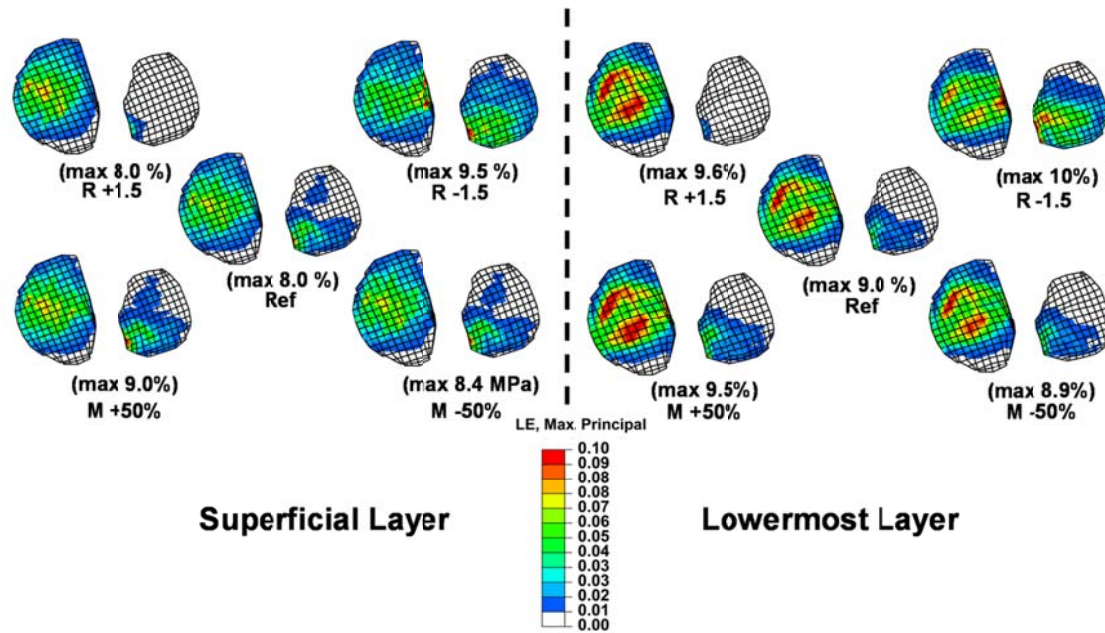


Figure 6-8: Maximum (tensile) principal strain in solid matrix at the superficial and lowermost layers of lateral and medial tibial cartilage at midstance. $R \pm 1.5$; the reference adduction rotation of 1.6° is altered by $\pm 1.5^\circ$ to 3.1° and 0.1° or $M \pm 50\%$ the knee reference adduction moment of 17 Nm is varied by $\pm 50\%$ to 25Nm and 9Nm. Note that a common legend is used for ease in comparisons.

**CHAPITRE 7 ARTICLE 5: GASTROCNEMIUS ACTS AS ACL
ANTAGONIST: ANALYSIS OF THE ROLE OF GASTROCNEMIUS
ACTIVATION ON KNEE BIOMECHANICS IN LATE STANCE AND IN
FLEXION**

Adouni, M; Shirazi-Adl, A; Marouane, H

Division of Applied Mechanics, Department of Mechanical Engineering

École Polytechnique, Montréal, Québec, Canada

Article submitted to

Computer Methods in Biomechanics and Biomedical Engineering, Février -2014

Keywords: Gastrocnemius, Gait, Knee Joint, Finite element, Muscle Forces, Anterior Cruciate Ligament, Cartilage, Contact

7.1 Abstract

Gastrocnemius is a premier muscle crossing the knee but its role in knee biomechanics and on the anterior cruciate ligament (ACL) remains less clear. The effect of changes in gastrocnemius force at late stance when it peaks on the knee joint response and ACL force was initially investigated using a lower extremity musculoskeletal model driven by gait kinematics-kinetics. The knee joint model under isometric contraction of gastrocnemius was subsequently analyzed at different flexion angles (0° - 90°). Changes in gastrocnemius force at late stance markedly influenced hamstrings forces. Gastrocnemius acted as ACL antagonist by substantially increasing its force. Simulations under isolated contraction of gastrocnemius confirmed these findings at all flexion angles. In particular, ACL force (anteromedial bundle) substantially increased with gastrocnemius activity at larger knee flexion angles. While hamstrings and gastrocnemius are both knee joint flexors, they play opposite roles in respectively protecting or loading ACL. Although the quadriceps is also recognized as antagonist of ACL, at larger joint flexion and in contrast to quadriceps, activity in gastrocnemius substantially increased ACL forces. The fact that gastrocnemius is an antagonist of ACL should help in effective prevention of ACL injuries, coping with an ACL injury and post ACL reconstruction periods.

7.2 Introduction

Gastrocnemius muscles along with hamstrings and quadriceps are the major lower extremity muscles that cross the human knee joint and in tandem with the knee passive articular-ligamentous structures resist the net external moments, control the movements and stabilize the joint under various activities. These functions become even more critical in the presence of commonly observed joint injuries for example the anterior cruciate ligament (ACL) ruptures and/or meniscal tears. Adequate understanding of the role of these muscles, acting single and combined, in the knee joint functional biomechanics is hence crucial in proper prevention and management of joint disorders as well as in performance enhancement programs. Analysis of the role of various active and passive structures and their interactions in the joint function and injuries can effectively be performed only when exploiting clinical, in vivo, in vitro and computational model studies altogether.

Mechanical function and injury of ACL have attracted a lot of attention due to its crucial role in the joint function and the high incidence of ACL rupture and replacement (Duncan et al., 2013). The influence of individual and combined activities in quadriceps and hamstrings on ACL loading at various flexion angles has accordingly been the focus of many studies (Draganich and Vahey, 1990; Dürselen et al., 1995; Li et al., 1999; Markolf et al., 2004; Mesfar and Shirazi-Adl, 2006b; Sakai et al., 1996; Singerman et al., 1995). Due to the anterior pull of the resultant muscle forces on the tibia, quadriceps as knee extensors act antagonistically by increasing ACL force at smaller flexion angles. In contrast, hamstrings as knee flexors and ACL agonists diminish ACL forces when acting alone or combined with quadriceps. The role of gastrocnemius on ACL loading on the other hand remains not as clear. Medial (MG) and lateral (LG) fascicles of gastrocnemius are among the premier leg flexor muscles at both ankle and knee joints. In vivo measurement of strain in the ACL-am (anteromedial bundle) of few anesthetized subjects has confirmed the antagonist role of gastrocnemius acting alone or combined with other muscle groups (Fleming et al., 2001). Using a 2D geometrical model, O'Connor (1993) computed high ACL forces over the entire knee flexion range when the gastrocnemius and quadriceps muscles were simultaneously active. In contrast, however, cadaver studies report on measurement of lower ACL-am strain at all flexion angles when the gastrocnemius activity is simulated (Dürselen et al., 1995; Lass et al., 1991). Greater and prolonged activity of gastrocnemius in ACL deficient knees during gait appears to be in line with the compensatory role of knee muscles to stabilize the joint by controlling joint laxity (Lass et al., 1991; Limbird et al., 1988).

The role of muscle activities and ground reaction forces on the knee joint response in gait has been the subject of various investigations (Kim et al., 2009; Neptune et al., 2004; Sasaki and Neptune, 2010; Shelburne et al., 2006; Winby et al., 2009; Zajac et al., 2002, 2003). Most of these works show a substantial activation level (peak of ~ 1.3 - 1.6 BW) in LG-MG muscles at post mid-stance phase. Estimation of such large forces in gastrocnemius muscle may partly be due to the lack of EMG recoding of deeper leg muscles such as the soleus that does not cross the knee joint and the negligence of the equilibrium equation in the frontal plane of the knee joint (Besier et al., 2009; Kim et al., 2009; Shelburne et al., 2004; Winby et al., 2009). In contrast to the gastrocnemius, the soleus muscle has been reported as an agonist of the ACL (Elias et al., 2003; Mokhtarzadeh et al., 2013). Computed large forces in the LG-MG could consequently overestimate ACL forces.

The current study was set to investigate the biomechanics of the knee joint under different gastrocnemius muscle activity levels. To attain this goal, we have initially analyzed the knee joint within a musculoskeletal model of the lower extremity at 75% of stance phase when LG-MG forces peak. For this purpose, the sensitivity of results (remaining muscle forces, knee joint response and ACL force) was analyzed while the force level in LG-MG was altered. In the second part, the detailed knee joint response was investigated at different flexion angles (0° - 90°) under isolated constant LG-MG force levels up to 1000 N acting as the sole external loads. The current study represents a direct continuation of our earlier works investigating the knee joint mechanics under quadriceps-hamstrings muscle forces (Mesfar and Shirazi-Adl, 2006b) and the biodynamic of the knee joint in gait (Adouni and Shirazi-Adl, 2013; Adouni et al., 2012; Adouni and Shirazi-Adl, 2014). We hypothesize that (1) alterations in LG-MG activation in late stance phase of gait markedly affect both the remaining joint muscle forces and ACL force and (2) isolated contraction of gastrocnemius increases ACL force at all flexion angles.

7.3 Methods

Details of the lower limb musculoskeletal model and non-linear kinematics-driven finite element (FE) algorithm have been presented elsewhere (Adouni and Shirazi-Adl, 2013; Adouni et al., 2012; Adouni and Shirazi-Adl, 2014; Shirazi et al., 2008) and are only briefly given here for the sake of completeness. The model consists of three joints structures (hip, knee and ankle). The hip and ankle joints are considered as spherical joints respectively with 3 and 1 rotational degrees-of-freedom and crossed by 27 and 4 distinct muscles (Fig. 6.1). The knee joint is represented in details as a deformable FE model consisting of three bony structures (tibia, patella, femur) and their articular cartilage layers, menisci, six principal ligaments (ACL, PCL, LCL, MCL, MPFL and LPFL), patellar tendon (PT), as well as quadriceps (4 components), hamstrings (6 components) and gastrocnemius (2 components) (see Fig. 6.1 for details).

Bony structures are simulated as rigid bodies due to their much higher stiffness (Donahue and Hull, 2002). Articular cartilage layers and menisci are modeled as depth-dependent composites of an isotropic bulk reinforced by networks of collagen fibrils. In menisci, collagen fibrils are primarily oriented in the circumferential direction within the bulk with no preferred orientation on bounding surfaces. In the cartilage superficial zones, fibrils are oriented horizontally parallel to the surface whereas they become random in the transitional zone and then

turn perpendicular in the deep zone anchoring into the subchondral bone. Membrane elements are used to simulate fibril networks in the superficial and deep zones while brick elements represent the transitional zone network (Shirazi and Shirazi-Adl, 2009a; Shirazi et al., 2008). Depth-dependent isotropic hyperelastic (Ogden-Compressible) material properties are considered for non-fibrillar solid matrix of cartilage layers with the elastic modulus varying linearly from 10 MPa at the surface to 18 MPa at the deep zone and a Poisson's ratio of 0.49 (Adouni et al., 2012). The matrix of menisci was represented, similar to our earlier studies (Bendjaballah et al., 1995; Mesfar and Shirazi-Adl, 2006b; Moglo and Shirazi-Adl, 2005), by an elastic material with a Young's modulus of 10 MPa and a Poisson's ratio of 0.45. The collagen content in menisci is 14% in the circumferential direction and 2.5% in the radial direction of the bulk region along with 12% in the outer surfaces at both directions. For cartilage collagen fibrils volume fractions, 15% is considered in the superficial region, 18% in the transitional region, and 21% in the deep zone. Thicknesses of these zones are, respectively, 15%, 22.5% and 62.5% of the total height at each point (Shirazi and Shirazi-Adl, 2009b; Shirazi et al., 2008).

Ligaments are each modeled by a number of uniaxial connector elements with different initial pre-strains, non-linear (tension-only) material properties and initial cross-sectional areas (Mesfar and Shirazi-Adl, 2005). The Q angle model (Sakai et al., 1996) ($Q = 14^\circ$; is used for quadriceps muscles; orientations relative to the femoral axis in frontal/sagittal planes are: RF-VIM $0^\circ/4^\circ$ anteriorly, VL 22° laterally/ 0° and VMO 41° medially/ 0° . Orientations for hamstrings muscles relative to the tibial axis, respectively for BF (BFLH, BFSH), SM, and TRIPOD (GA,SR,ST) are taken (Aalbersberg et al., 2005) as 11.8° medially, 7° laterally, and 7.1° medially in the frontal plane whereas 0° , 16.1° , and 18.7° posteriorly in the sagittal plane. Gastrocnemius fascicles are parallel to the tibial axis in the sagittal plane while oriented (MG) 5.3° medially and (LG) 4.8° laterally in the frontal plane (Delp et al., 2007; Hillman, 2003). Tibialis posterior/Soleus are oriented $5.3^\circ/4.1^\circ$ laterally and $1.0^\circ/4^\circ$ anteriorly relative to the tibial axis (Delp et al., 2007). The orientations of the remaining hip muscles are taken from Delp et al.(2007)

The hip/knee/ankle joint rotations/moments and ground reaction forces at foot during gait are based on reported in vivo measurements (Astefphen, 2007; Hunt et al., 2001). Analyses are performed at 75% of stance phase corresponding to maximum activation of the gastrocnemius

muscles during gait. Muscle forces are computed using static optimization with moment equilibrium equations as constraints (3 at the knee joint, 3 at the hip joint, and 1 at the ankle joint). Cost function of the sum of cubed muscle stresses of the entire lower extremity is used (Adouni et al., 2012; Arjmand and Shirazi-Adl, 2006). Since our model was constructed based on a female knee joint, a body weight of $BW=606.6\text{ N}$ (61.9 kg) is considered (De Leva, 1996). The femur is fixed in its instantaneous position while the tibia and patella are free except for the prescribed in vivo-based tibial rotations. The location of resultant ground reaction force is determined so as to generate reported joint moments accounting for the leg/foot weight ($29.78\text{ N}/7.98\text{ N}$). Non-orthogonal local joint coordinate systems (Grood and Suntay, 1983) are considered in compliance with prescribed rotations (Astéphen, 2007).

The Knee joint response is analyzed with updated muscle forces as external loads and iterations at deformed configurations continue till convergence is reached (8-10 iterations). To assess the sensitivity of gastrocnemius activation on knee joint response, the same analysis is repeated but the lever arm at the ankle and PCSA of the soleus muscle are changed to minimize or maximize estimated gastrocnemius activation forces (Yamaguchi et al., 1990). To compute the minimum activity level (case Min-G), soleus and gastrocnemius are given identical lever arms while increasing the PCSA of soleus by 20%. The maximum activity (case Max-G) is on the other hand evaluated by reducing (-20%) the lever arm and PCSA of soleus relative to the data taken from the literature (Delp et al., 2007) that corresponds to the reference condition (case Ref-G).

The second part of this study concentrates on the knee joint alone subject to constant LG-MG activation levels varying up to 1000 N and at different flexion angles (0° - 90°). Following the application of prestrains in ligaments and tibial flexion rotation with the femur fixed, the tibiofemoral joint is subject to incrementally increasing gastrocnemius forces (acting as external loads from 0 to 1000N). Forces in each component of gastrocnemius (LG, MG) are here assigned according to their relative PCSA. Since the joint flexion angle is prescribed, the required joint extensor/flexor moment under given muscle activation patterns is calculated at each step of the analysis. In order to investigate the effect on results of constraint on tibial rotations, additional cases are studied at 0° and 90° joint flexion angles with the joint fixed in varus/valgus rotation (V/V), internal/external rotation (I/E) or finally both rotations (V/V+I/E). At full extension, to

assess the sensitivity of results on the coordinates of LG-MG femoral footprints, the femoral insertions of both fascicles are also shifted by ± 4 mm in anterior-posterior or medial-lateral directions and analyses repeated. Matlab (R2009a Optimization Toolbox, genetic algorithms) and ABAQUS 6.10.1 (Static analysis) commercial programs are used.

7.4 Results

7.4.1 Gait Simulation

In the lower extremity musculoskeletal model, the LG/MG forces at 75% of stance phase were found to markedly alter from the reference case of 180N/508N (Adouni and Shirazi-Adl, 2013; Adouni et al., 2012) to either 119N/320N (case Min-G) or 235N/627N (case Max-G). The decrease in the gastrocnemius forces (Min-G) substantially increased forces in lateral and medial hamstrings but decreased the already small forces in quadriceps (Fig. 6.2). Reverse trends were computed when these LG-MG forces increased (Fig. 6.2). Tibiofemoral (TF) contact forces/areas/pressures were however slightly altered (Fig. 6.3). Forces in ACL significantly changed following the same trends as in LG-MG muscle forces (Fig. 6.3); they increased by 85% from Min-G to Max-G. Negligible differences were noted in forces in remaining joint ligaments.

7.4.2 Knee Joint Simulations

Isolated contraction of GL-GM (up to 1000N) in the joint with the femur fixed rotated the tibia internally from 10.3° external at full extension to 12.9° internal rotation at 90° flexion. This rotation changed to 3.2° and 7.0° at 0° and 90° flexion, respectively, when varus/valgus rotation was fixed. At full extension, a varus rotation of 2.2° was computed under 1000N gastrocnemius force that turned valgus (-1.6°) at 90° flexion. Fixed internal/external rotation changed the varus rotation at full extension to -0.3° and to 2.6° at 90° flexion. Tibial translations increased with greater gastrocnemius force and reached maximum of 2.3/3.9/3 mm at 90° flexion in the lateral/anterior/proximal directions. Changes in femoral insertions of LG-MG at full-extension had negligible effects on the knee joint kinematics at full extension.

Force in ACL reached its peak of 94 N under 500 N muscle force at full extension and of 174 N under 1000 N muscle force at 90° flexion (Fig. 6.4a). The effect of alteration in muscle force on ACL forces was markedly greater at larger flexion angles. Anteromedial and

poterolateral bundles of ACL followed distinct trends with joint flexion (Fig. 6.5). Constraints on rotations decreased ACL load at both 0° and 90° flexion except for the fixed internal/external rotation at 90° flexion (Fig. 6.4b). Due to the associated changes in anterior tibial translation, lateral or posterior shift in LG-MG femoral insertions slightly (<4%) decreased ACL force while medial or anterior shifts slightly increased (<5%) it. In contrast to ACL, PCL remained slack throughout flexion. For collateral ligaments, maximum LCL force of 89 N at full extension diminished with joint flexion and constraints on rotations while the peak MCL force of 40 N was computed at full extension with the varus/valgus rotation fixed.

The peak joint flexion moment occurred around mid-flexion angles reaching 15.5Nm and 31.2Nm at 40° under muscle forces of 500N and 1000N, respectively (Fig. 6.6). Constrained rotations had a negligible effect on these moments at 0° and 90° flexion. The effective lever arm of the joint estimated as the ratio of the joint moment to the corresponding muscle force followed the same trends as moments with the maximum value of 31.2 mm at 40° flexion (under both 500 N and 1000 N) and minimum of 23.2 mm at 90° flexion (under 1000 N force). The joint flexion moment, as expected, increased/decreased by less than 10% with the posterior/anterior shifts in muscle footprints while remaining almost unchanged during medial/lateral shifts.

Total tibiofemoral (TF) contact force decreased slightly with flexion, was always much greater at the medial plateau compared to the lateral one (Fig. 6.7) and was transmitted primarily through the uncovered areas (via cartilage-cartilage). The TF contact area reached also its maximum of 1000 mm² at full extension. In accordance with the compartmental loads, contact pressures were much larger on the medial plateau reaching peak of 4.3 MPa at 90° flexion (Fig. 6.8). Tensile strains were also larger in the medial cartilage reaching greater values at deep fibril networks (peak of 9% at 90°). At full extension, constraint on varus/valgus rotations resulted in larger contact forces on the lateral compartment. Effect of changes in femoral footprints of LG/MG muscles on contact forces/stresses was negligible (<1%).

7.5 Discussion

Following our earlier studies on mechanics of the knee joint under single/combined activations of quadriceps and hamstrings (Mesfar and Shirazi-Adl, 2006b) and on the biodynamics of the knee joint during the stance phase of gait (Adouni and Shirazi-Adl, 2013;

Adouni et al., 2012; Adouni and Shirazi-Adl, 2014), this work was performed to delineate the effect of different gastrocnemius activation levels on the knee joint biomechanics in general and ACL force in particular. For this purpose, both the lower extremity musculoskeletal model at 75% of stance phase when LG-MG activity peaks and the knee joint alone under isolated LG-MG muscle activity at different flexion angles were considered. Predictions confirmed the hypotheses that (1) alterations in gastrocnemius forces markedly changed quadriceps and hamstrings forces as well as ACL force at the late stance phase and (2) isolated contraction of gastrocnemius substantially increased ACL force at all flexion angles. This study therefore confirms that gastrocnemius muscles act as ACL antagonists during gait and in the knee joint at all flexion angles.

At the 75% of stance phase and under large net external extension and adduction moments at the knee joint (Astefphen, 2007), a 36% reduction in LG-MG forces from 180 N/508 N to 119 N/320 N (case Min-G) was compensated by additional activity in medial hamstrings and marked increase in bicep femoris (short head) force (Fig. 6.2). On the other hand, augmented gastrocnemius activation by 26% to 235 N/627 N (case Max-G) almost unloaded medial hamstrings while substantially decreasing bicep femoris (short head) force from 377N to 294N (Fig. 2). Quadriceps forces, albeit small, as well as contact forces/areas/pressures slightly increased in this case. These results corroborate earlier observations (Neptune et al., 2004; Sasaki and Neptune, 2010) that the gastrocnemius is a premier contributor in the joint moment resistance and hence joint loading at the late stance. In subjects with severe OA (Astefphen et al., 2008a; 2008b), reductions in quadriceps/hamstrings activity at early stance (associated with reduced knee flexion angle/torque) and in gastrocnemius activity at late stance (associated with the absence of knee extensor torque) serve to reduce joint loading (Adouni and Shirazi-Adl, 2014). Altering muscles coordination patterns to exploit functionally redundant muscles provides for an effective way to reduce loads on the joints.

At 75% period of stance with the knee at near full-extension, larger activations in gastrocnemius muscles generated greater tibial anterior force due directly to the pull of the muscle and indirectly via the added joint compression acting on a posteriorly sloped tibial plateau. With 36% reduction or 26% increase in LG-MG forces, ACL force markedly decreased from 271N to 178N or increased to 331N, respectively, following closely the trend in muscle

activation (Fig. 6.3). An effective mechanism to decrease ACL force and knee joint compression loading is hence to activate more the soleus rather than the gastrocnemius at the late stance in agreement with others (Neptune et al., 2001; Sasaki and Neptune, 2010). Estimation of much larger forces in gastrocnemius muscles in earlier studies (Besier et al., 2009; Kim et al., 2009; Shelburne et al., 2004; Winby et al., 2009) apparently due to the absent or limited contribution of soleus increased, similar to our model case Max-G, knee joint loading and ACL forces at late stance when compared to the reference case (Ref-G). The anterior pull of gastrocnemius, opposite to that of soleus, on the tibia during drop landing has also been indicated (Mokhtarzadeh et al., 2013). Smaller gastrocnemius/hamstrings (G/H) muscles activation ratio in ACL reconstructed knees versus intact knees during jump-cut maneuver could act to protect the graft by reducing ACL loading (Coats-Thomas et al., 2013). In accordance, ACL force decreased by 46% in our model when the G/H ratio diminished by 80% from Max-G to Min-G case. Moreover, in a similar study by Sanford et al.(2013) recording EMG in ACL intact and reconstructed subjects during stance, smaller gastrocnemius activation at the late stance in some ACL reconstructed subjects were found.

The foregoing antagonist role of gastrocnemius with ACL is also evident in the knee model alone under isolated activation of LG-MG muscles at all flexion angles (Fig. 6.4). At smaller flexion angles ($<40^\circ$), the ACL-pl carries the entire ACL force of 133 N under 1000 N muscle force. At larger flexion angles and with the drop in ACL-pl force, the ACL-am share slowly grows to its maximum at 90° of 90% at 157 N (Fig. 6.5). This redistribution of the load between ACL bundles with joint flexion is in agreement with earlier studies (Moglo and Shirazi-Adl, 2005; Woo et al., 1998). In contrast to ACL, gastrocnemius activation is computed here to protect PCL as it remains slack even at larger flexion angles. Current results support earlier findings of larger ACL strain when gastrocnemius is activated alone or combined with other muscles (Fleming et al., 2001; O'Connor, 1993) but disagrees with those reporting a drop in ACL-am strain and an increase in PCL strain under gastrocnemius activity (Dürselen et al., 1995). It is interesting to note that the joint kinematics and large ACL forces reported under axial compression forces (Banglmaier et al., 1999; Meyer and Haut, 2005, 2008) are similar to those in our model under isolated gastrocnemius forces that act to substantially increase joint compression in accordance with their orientation.

The joint flexion moment reached its maximum of 31.2Nm at 40° flexion and minimum of 23.2 Nm at 90° under 1000 N isolated gastrocnemius force. The efficiency or equivalent lever-arm of these muscles hence diminished at larger flexion. Under an isolated hamstrings force, this moment was found to monotonically increase with flexion demonstrating the efficiency of hamstrings at larger flexion angles (Mesfar and Shirazi-Adl, 2006b). In contrast, quadriceps were most efficient at near full extension (Mesfar and Shirazi-Adl, 2005). Under a unit muscle force and comparatively, however, quadriceps muscles are the most effective (with greatest lever-arm) at near full extension while hamstrings are most effective at 90° flexion.

In summary, while hamstrings and gastrocnemius are both knee joint flexors, they play opposite roles in respectively either protecting or loading ACL. Changes in gastrocnemius activity in gait substantially affected remaining muscle forces as well as forces in ACL. ACL force also increased in the knee joint at all flexion angles under isolated activity in gastrocnemius. Interestingly, ACL force substantially increased at larger flexion angles under isolated gastrocnemius activity, a trend that was not present even under quadriceps activity. The fact that gastrocnemius is an antagonist of ACL should hence help in effective prevention of and coping with ACL injury as well as rehabilitation after ACL reconstruction.

7.6 Acknowledgements

The work was supported by a grant from the Natural Sciences and Engineering Research Council of Canada (NSERC-Canada).

7.7 References

- Aalbersberg, S., Kingma, I., Ronsky, J.L., Frayne, R., van Dieen, J.H., 2005. Orientation of tendons in vivo with active and passive knee muscles. *Journal of Biomechanics* 38, 1780-1788.
- Adouni, M., Shirazi-Adl, A., 2013. Consideration of equilibrium equations at the hip joint alongside those at the knee and ankle joints has mixed effects on knee joint response during gait. *Journal of Biomechanics* 46, 619-624.
- Adouni, M., Shirazi-Adl, A., Shirazi, R., 2012. Computational biodynamics of human knee joint in gait: From muscle forces to cartilage stresses. *Journal of Biomechanics* 45, 2149-2156.
- Adouni, M., Shirazi-Adl, A., 2014. Evaluation of knee joint muscle forces and tissue stresses-strains during gait in severe OA versus normal subjects. *Journal of Orthopaedic Research* 32, 69-78.
- Arjmand, N., Shirazi-Adl, A., 2006. Sensitivity of kinematics-based model predictions to optimization criteria in static lifting tasks. *Medical engineering & physics* 28, 504-514.
- Astephen, J.L., 2007. Biomechanical factors in the progression of knee osteoarthritis. *School of Biomedical Engineering*. Halifax, Dalhousie university.
- Astephen, J.L., Deluzio, K.J., Caldwell, G.E., Dunbar, M.J., 2008a. Biomechanical changes at the hip, knee, and ankle joints during gait are associated with knee osteoarthritis severity. *Journal of Orthopaedic Research* 26, 332-341.
- Astephen, J.L., Deluzio, K.J., Caldwell, G.E., Dunbar, M.J., Hubley-Kozey, C.L., 2008b. Gait and neuromuscular pattern changes are associated with differences in knee osteoarthritis severity levels. *Journal of Biomechanics* 41, 868-876.
- Banglmaier, R., Dvoracek-Driksna, D., Oniang'o, T., Haut, R., 1999. AXIAL COMPRESSIVE LOAD RESPONSE OF THE 90 DEGREE FLEXED HUMAN TIBIOFEMORAL JOINT. In: Stapp Car Crash Conference Proceedings,
- Bendjaballah, M.Z., Shirazi-Adl, A., Zukor, D., 1995. Biomechanics of the human knee joint in compression: reconstruction, mesh generation and finite element analysis. *The Knee* 2, 69-79.

- Besier, T.F., Fredericson, M., Gold, G.E., Beaupré, G.S., Delp, S.L., 2009. Knee muscle forces during walking and running in patellofemoral pain patients and pain-free controls. *Journal of Biomechanics* 42, 898-905.
- Coats-Thomas, M.S., Miranda, D.L., Badger, G.J., Fleming, B.C., 2013. Effects of ACL reconstruction surgery on muscle activity of the lower limb during a jump-cut maneuver in males and females. *Journal of Orthopaedic Research* 31, 1890-1896.
- De Leva, P., 1996. Adjustments to Zatsiorsky-Seluyanov's segment inertia parameters. *Journal of Biomechanics* 29, 1223-1230.
- Delp, S.L., Anderson, F.C., Arnold, A.S., Loan, P., Habib, A., John, C.T., Guendelman, E., Thelen, D.G., 2007. OpenSim: open-source software to create and analyze dynamic simulations of movement. *Biomedical Engineering, IEEE Transactions on* 54, 1940-1950.
- Donahue, T.L.H., Hull, M., 2002. A finite element model of the human knee joint for the study of tibio-femoral contact. *Journal of Biomechanical Engineering* 124, 273.
- Draganich, L., Vahey, J., 1990. An in vitro study of anterior cruciate ligament strain induced by quadriceps and hamstrings forces. *Journal of Orthopaedic Research* 8, 57-63.
- Duncan, I.C., Kane, P.W., Lawson, K.A., Cohen, S.B., Ciccotti, M.G., Dodson, C.C., 2013. Evaluation of Information Available on the Internet Regarding Anterior Cruciate Ligament Reconstruction. *Arthroscopy: The Journal of Arthroscopic & Related Surgery*.
- Dürselen, L., Claes, L., Kiefer, H., 1995. The influence of muscle forces and external loads on cruciate ligament strain. *The American Journal of Sports Medicine* 23, 129-136.
- Elias, J.J., Faust, A.F., Chu, Y.-H., Chao, E.Y., Cosgarea, A.J., 2003. The Soleus Muscle Acts as an Agonist for the Anterior Cruciate Ligament An In Vitro Experimental Study. *The American Journal of Sports Medicine* 31, 241-246.
- Fleming, B.C., Renstrom, P.A., Ohlen, G., Johnson, R.J., Peura, G.D., Beynnon, B.D., Badger, G.J., 2001. The gastrocnemius muscle is an antagonist of the anterior cruciate ligament. *Journal of Orthopaedic Research* 19, 1178-1184.

- Grood, Suntay, W.J., 1983. A joint coordinate system for the clinical description of three-dimensional motions: application to the knee. *Journal of Biomechanical Engineering* 105, 136.
- Hillman, 2003. *Interactive Functional Anatomy*, , London.
- Hunt, Smith, R.M., Torode, M., Keenan, A.M., 2001. Inter-segment foot motion and ground reaction forces over the stance phase of walking. *Clinical Biomechanics* 16, 592-600.
- Kim, H.J., Fernandez, J.W., Akbarshahi, M., Walter, J.P., Fregly, B.J., Pandy, M.G., 2009. Evaluation of predicted knee joint muscle forces during gait using an instrumented knee implant. *Journal of Orthopaedic Research* 27, 1326-1331.
- Lass, P., Kaalund, S., Iefevre, S., Arendt-Nielsen, L., Sinkjæ, T., Simonsen, O., 1991. Muscle coordination following rupture of the anterior cruciate ligament: electromyographic studies of 14 patients. *Acta Orthopaedica* 62, 9-14.
- Li, G., Rudy, T., Sakane, M., Kanamori, A., Ma, C., Woo, S.L.Y., 1999. The importance of quadriceps and hamstring muscle loading on knee kinematics and in-situ forces in the ACL. *Journal of Biomechanics* 32, 395-400.
- Limbird, T.J., Shiavi, R., Frazer, M., Borra, H., 1988. EMG profiles of knee joint musculature during walking: changes induced by anterior cruciate ligament deficiency. *Journal of Orthopaedic Research* 6, 630-638.
- Markolf, K.L., O'Neill, G., Jackson, S.R., McAllister, D.R., 2004. Effects of applied quadriceps and hamstrings muscle loads on forces in the anterior and posterior cruciate ligaments. *The American Journal of Sports Medicine* 32, 1144.
- Mesfar, W., Shirazi-Adl, A., 2005. Biomechanics of the knee joint in flexion under various quadriceps forces. *The knee* 12, 424-434.
- Mesfar, W., Shirazi-Adl, A., 2006. Knee joint mechanics under quadriceps-hamstrings muscle forces are influenced by tibial restraint. *Clinical Biomechanics* 21, 841-848.
- Meyer, E.G., Haut, R.C., 2005. Excessive compression of the human tibio-femoral joint causes ACL rupture. *Journal of Biomechanics* 38, 2311-2316.

- Meyer, E.G., Haut, R.C., 2008. Anterior cruciate ligament injury induced by internal tibial torsion or tibiofemoral compression. *Journal of Biomechanics* 41, 3377-3383.
- Moglo, K., Shirazi-Adl, A., 2005. Cruciate coupling and screw-home mechanism in passive knee joint during extension–flexion. *Journal of biomechanics* 38, 1075-1083.
- Mokhtarzadeh, H., Yeow, C.H., Hong Goh, J.C., Oetomo, D., Malekipour, F., Lee, P.V.-S., 2013. Contributions of the Soleus and Gastrocnemius muscles to the anterior cruciate ligament loading during single-leg landing. *Journal of Biomechanics* 46, 1913-1920.
- Neptune, R., Zajac, F., Kautz, S., 2004. Muscle force redistributes segmental power for body progression during walking. *Gait & Posture* 19, 194-205.
- Neptune, R.R., Kautz, S., Zajac, F., 2001. Contributions of the individual ankle plantar flexors to support, forward progression and swing initiation during walking. *Journal of Biomechanics* 34, 1387-1398.
- O'Connor, J.J., 1993. Can muscle co-contraction protect knee ligaments after injury or repair? *Journal of Bone & Joint Surgery, British Volume* 75, 41-48.
- Sakai, N., Luo, Z.P., Rand, J.A., An, K.N., 1996. Quadriceps forces and patellar motion in the anatomical model of the patellofemoral joint. *The knee* 3, 1-7.
- Sanford, B.A., Williams, J.L., Zucker-Levin, A.R., Mihalko, W.M., 2013. Tibiofemoral Joint Forces during the Stance Phase of Gait after ACL Reconstruction. *Open Journal of Biophysics* 3, 277.
- Sasaki, K., Neptune, R.R., 2010. Individual muscle contributions to the axial knee joint contact force during normal walking. *Journal of Biomechanics* 43, 2780-2784.
- Shelburne, K.B., Pandy, M.G., Anderson, F.C., Torry, M.R., 2004. Pattern of anterior cruciate ligament force in normal walking. *Journal of Biomechanics* 37, 797-805.
- Shelburne, K.B., Torry, M.R., Pandy, M.G., 2006. Contributions of muscles, ligaments, and the ground reaction force to tibiofemoral joint loading during normal gait. *Journal of Orthopaedic Research* 24, 1983-1990.
- Shirazi, R., Shirazi-Adl, A., 2009a. Analysis of partial meniscectomy and ACL reconstruction in knee joint biomechanics under a combined loading. *Clinical Biomechanics* 24, 755-761.

- Shirazi, R., Shirazi-Adl, A., 2009b. Computational biomechanics of articular cartilage of human knee joint: Effect of osteochondral defects. *Journal of Biomechanics* 42, 2458-2465.
- Shirazi, R., Shirazi-Adl, A., Hurtig, M., 2008. Role of cartilage collagen fibrils networks in knee joint biomechanics under compression. *Journal of Biomechanics* 41, 3340-3348.
- Singerman, R., Berilla, J., Davy, D., 1995. Direct in vitro determination of the patellofemoral contact force for normal knees. *Journal of Biomechanical Engineering* 117, 8.
- Winby, C., Lloyd, D., Besier, T., Kirk, T., 2009. Muscle and external load contribution to knee joint contact loads during normal gait. *Journal of Biomechanics* 42, 2294-2300.
- Woo, S.L.Y., Fox, R.J., Sakane, M., Livesay, G.A., Rudy, T.W., Fu, F.H., 1998. Biomechanics of the ACL: measurements of in situ force in the ACL and knee kinematics. *The knee* 5, 267-288.
- Yamaguchi, G.T., Sawa, A.G.U., Moran, D.W., Fessler, M.J., Winters, J.M., 1990. A survey of human musculotendon actuator parameters. In: Springer-Verlag (Ed.) *Multiple Muscle Systems*. New York, Springer-Verlag, pp.717-773
- Zajac, F.E., Neptune, R.R., Kautz, S.A., 2002. Biomechanics and muscle coordination of human walking:: Part I: Introduction to concepts, power transfer, dynamics and simulations. *Gait & Posture* 16, 215-232.
- Zajac, F.E., Neptune, R.R., Kautz, S.A., 2003. Biomechanics and muscle coordination of human walking:: Part II: Lessons from dynamical simulations and clinical implications. *Gait & Posture* 17, 1-17.

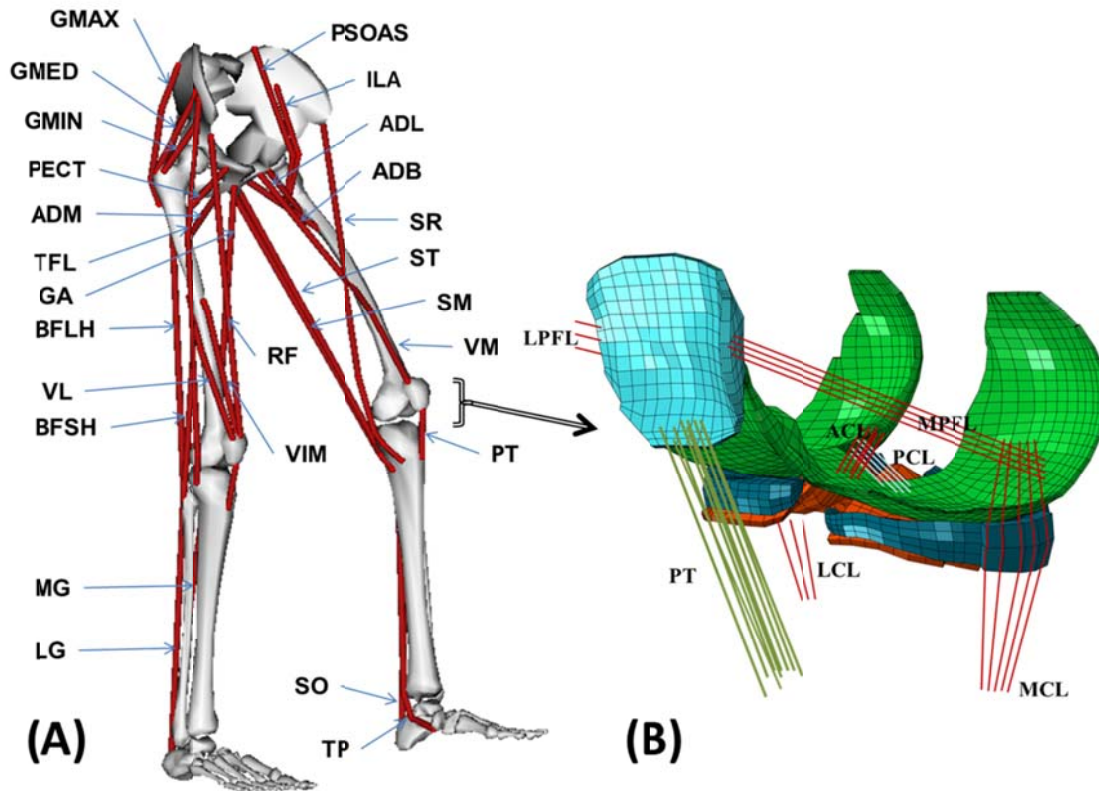


Figure 7-1: (A) Schematic diagram showing the 34 muscles incorporated into the lower extremity model (taken from OpenSim(Delp et al., 2007)). Quadriceps: vastus-medialis-obliquus (VMO), rectus femoris (RF), vastus-intermidus-medialis (VIM) and vastus-lateralis (VL); Hamstrings: biceps femoris long head (BFLH), biceps femoris short head (BFSH), sem-imembranous (SM) and TRIPOD made of sartorius (SR), gracilis (GA) and semitendinosus (ST); Gastrocnemius: medial (MG) and lateral (LG). Tibialis posterior (TP) and soleus (SO) muscles are uni-articular ankle muscles. Hip joint muscles (not all shown) include adductor, long (ADL), mag (3 components ADM) and brev (ADB); gluteus max (3 components GMAX), med (3 components GMED) and min (3 components GMIN), iliacus (ILA), iliopsoas (PSOAS), quadriceps femoris, pectineus (PECT), tensor facia lata (TFL), periformis. (B) Knee FE model; tibiofemoral (TF) and patellofemoral (PF) cartilage layers, menisci and patellar Tendon (PT). Joint ligaments: lateral/medial patellofemorals (LPFL/MPFL), anterior/posterior cruciates (ACL/PCL) and lateral collateral/medial collaterals (LCL/MCL).

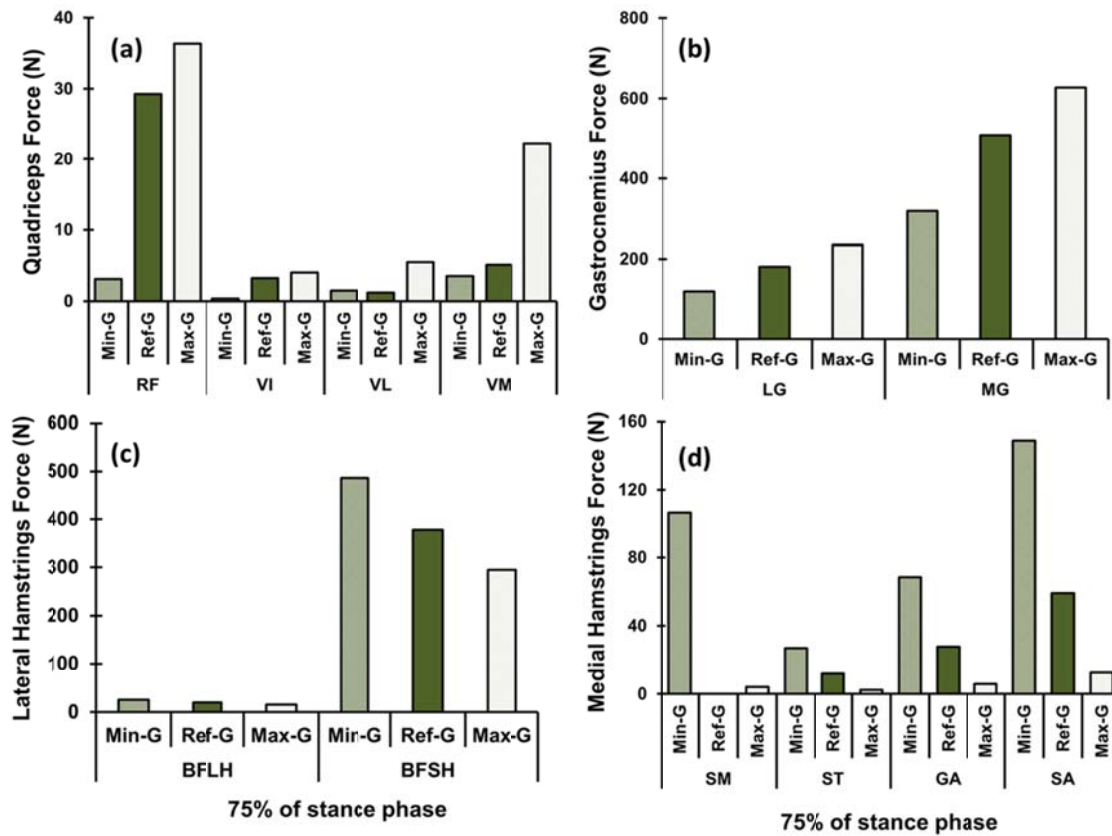


Figure 7-2: Predicted muscle forces at 75% of stance phase. (a) Quadriceps, (b) Gastrocnemius, (c) Lateral Hamstring and (d) Medial Hamstring. Min-G: minimum activation of gastrocnemius muscle, Ref-G: reference activation of gastrocnemius muscle. Max-G: maximum activation of gastrocnemius muscle.

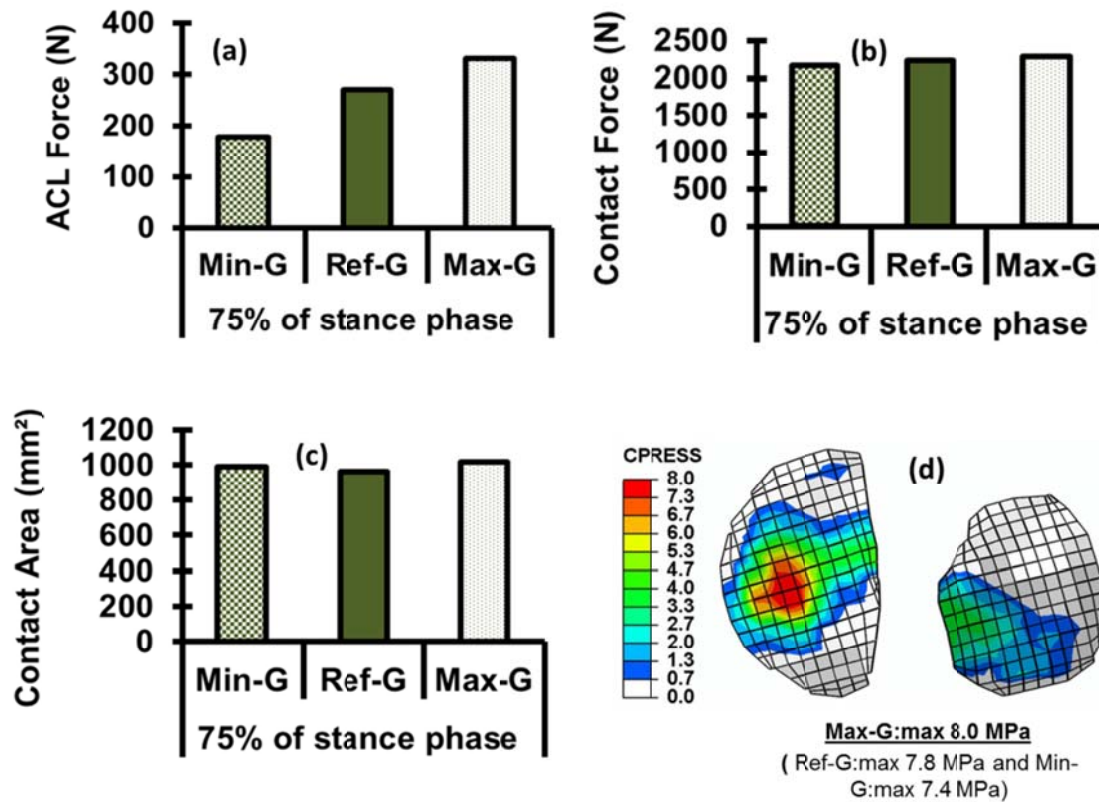


Figure 7-3: Predicted knee joint forces at 75% of stance phase. (a)Anterior cruciate ligament (ACL) force, (b)Total contact force, (c) Total contact area and (d) contact pressure. Min-G: minimum activation of gastrocnemius muscle, Ref-G: reference activation of gastrocnemius muscle. Max-G: maximum activation of gastrocnemius muscle.

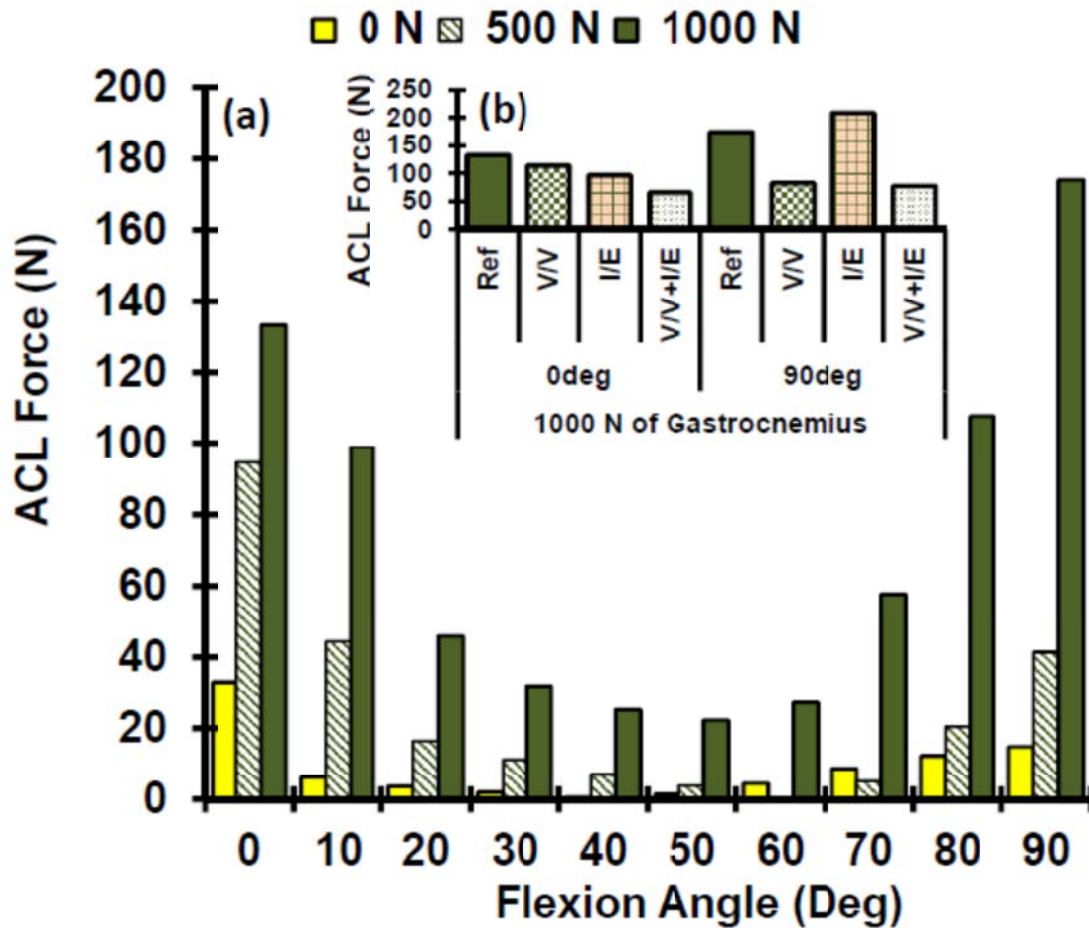


Figure 7-4: (A) Computed force in anterior cruciate ligament (ACL) at different flexion angles and under isolated gastrocnemius force of 0N, 500N and 1000N. (B) ACL force under gastrocnemius force of 1000N at 0° and 90° in the cases Ref: reference case with free coupled rotations, V/V: varus/valgus fixed, I/E: internal/external fixed, V/V+I/E: constrained coupled rotations.

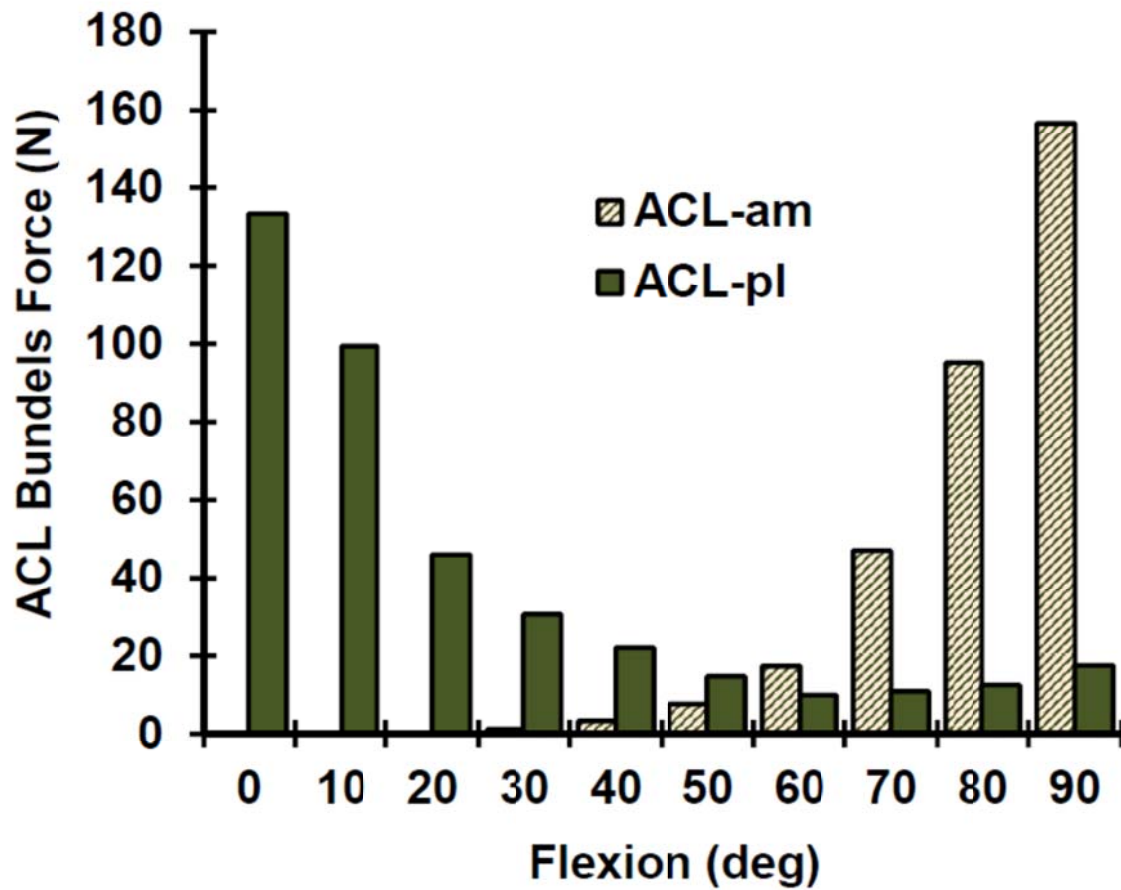


Figure 7-5: Computed force in ACL bundles at different flexion angles and under isolated gastrocnemius force of 1000N. ACL-am; anteromedial bundle and ACL-pl; posterolateral bundle.

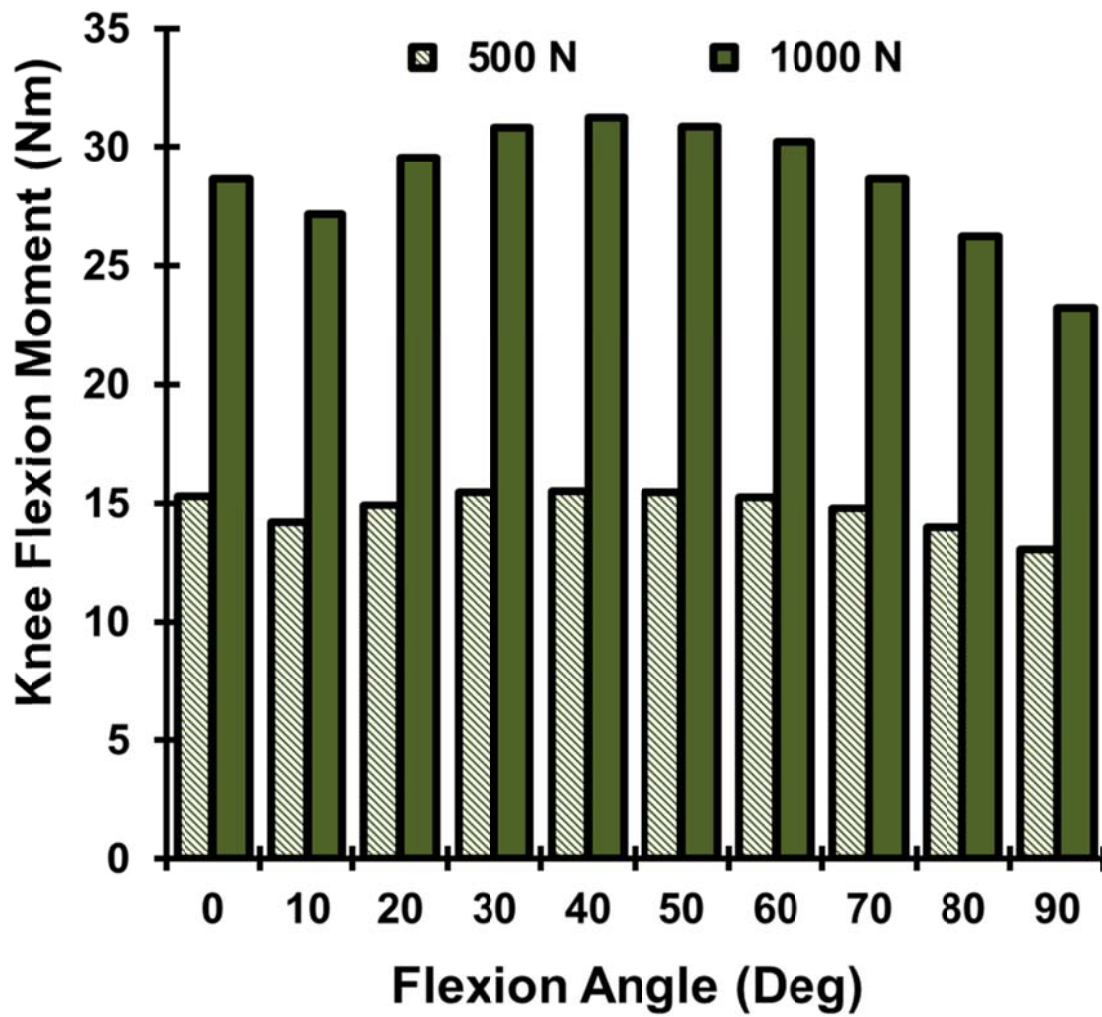


Figure 7-6: Flexor joint moment on the tibia under gastrocnemius forces of 500 N and 1000 N at different flexion angles.

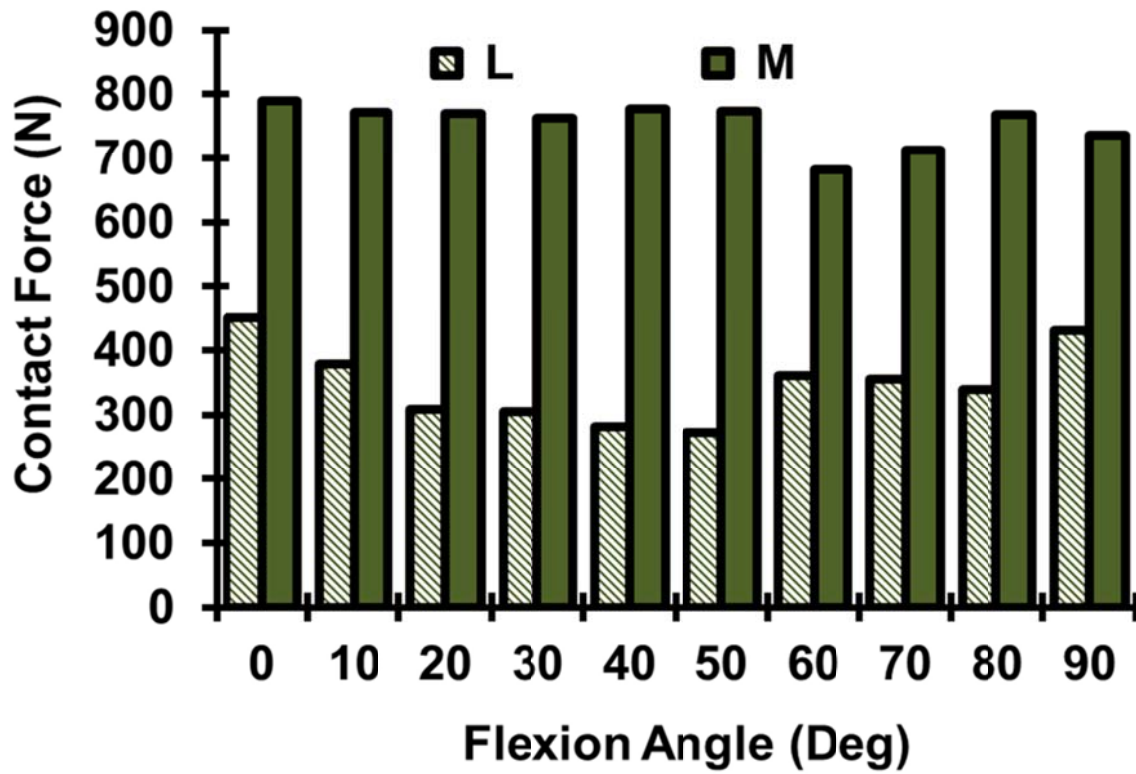


Figure 7-7: Predicted total TF (M: Medial and L: Lateral) contact forces at different flexion angles and under gastrocnemius forces of 1000 N.

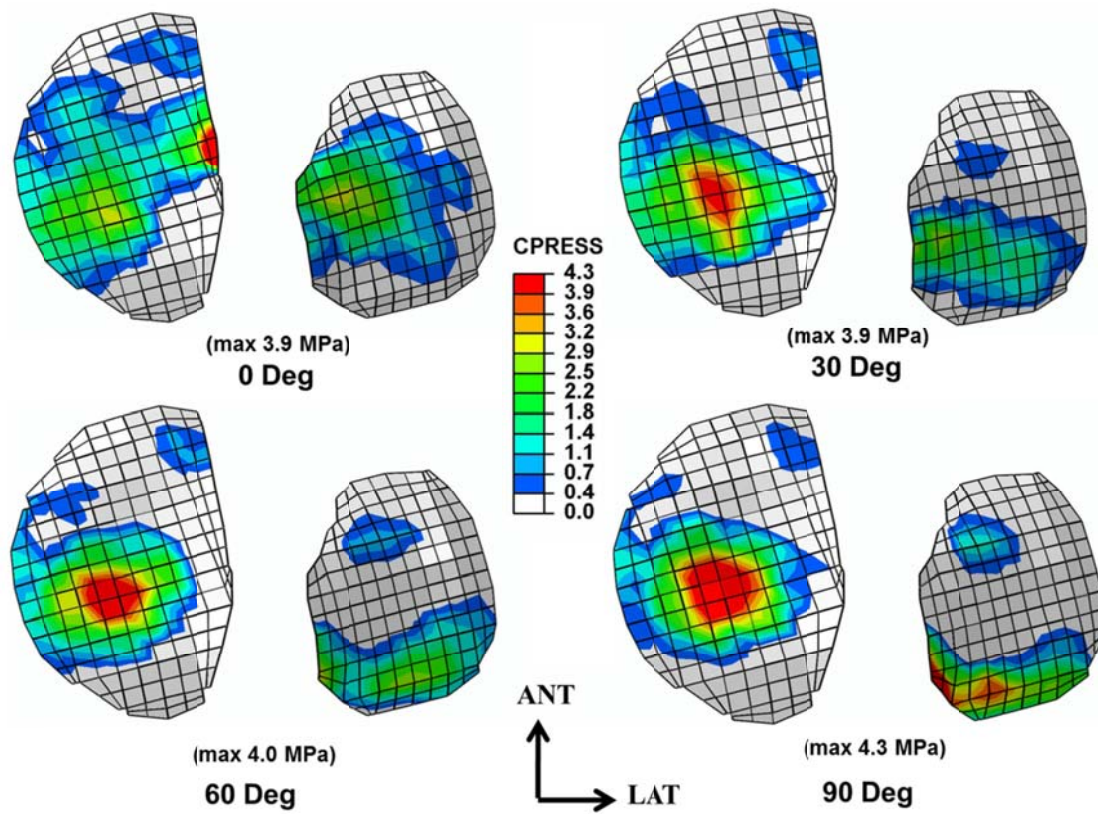


Figure 7-8: Predicted contact pressure at articular surface of lateral and medial tibial plateaus at different flexion angles and undergastrocnemius force of 1000 N. Note that a common legend is used for ease in comparisons.

CHAPITRE 8 DISCUSSION

8.1 Généralités

Dans le but d'analyser la réponse complète du genou humain durant la phase d'appui de la marche en présence des éléments moteurs, à savoir les muscles qui agissent directement ou indirectement, un modèle musculosquelettique du membre inférieur a été développé. Ce modèle considère l'articulation de la hanche et de la cheville comme un joint rigide sphérique en 3D et 2D respectivement. L'articulation du genou a été simulée par un joint déformable qui tient compte de tous les paramètres passifs. Ce modèle, développé initialement par Bendjaballah et al.(1995), a été reconstruit d'un cadavre d'un spécimen femelle. Suite aux travaux de Moglo et Shirazi-Adl.(2003a, 2003b, 2005), ce modèle a subi des améliorations par l'addition de mécanisme extenseur et les muscles fléchisseurs dans les travaux de Mesfar et Shirazi-Adl.(2005). Dernièrement, ce modèle a été raffiné par Shirazi et al.(2008). L'ensemble du modèle est constitué par trois structures osseuses (fémur, tibia, rotule) ainsi que leurs cartilages articulaires, des ménisques, quatre ligaments fémorotibiaux (deux croisés, deux latéraux), deux ligaments fémoro-patellaires (ailerons rotuliens interne et externe), le tendon rotulien et l'ensemble de tous les muscles entourant l'articulation de genou.

Le modèle développé a été utilisé afin d'effectuer des analyses élasto-statiques non linéaires du genou humain durant la phase d'appui de la marche sous les contraintes de données cinématiques et cinétiques produites par l'analyse de la marche à cadence normale sur deux types de sujets; des sujets sains et des sujets atteints par l'ostéoarthrite sévère. Cette étude a été effectuée par le groupe de Deluzio.(Astephen, 2007), (Astephen, 2007) et Hunt et al.(2001). Deux techniques d'optimisation (globale et locale) ont été considérées au début de ces études pour tester la précision de notre prédiction. Le modèle a servi aussi pour effectuer des études paramétriques consistant à étudier l'influence de l'altération de forces musculaires de jumeau à pleine activation (75% de phase d'appui) et en flexion normale de 0° à 90° sur la réponse globale du genou et particulièrement le ligament croisé antérieur (LCA). La variation de la rotation et du moment appliquée au joint de genou dans le plan frontal, servant à détecter la relation entre ces paramètres externes et la répartition de charge sur les deux plateaux du tibia, a fait aussi l'objet de certaines analyses.

8.2 Évaluation du modèle

8.2.1 Comportements structurel et mécanique

Dans ce modèle, les articulations de la hanche et de la cheville ont été considérées comme des joints simplement sphériques rigides (rotule). Cette hypothèse est en accord avec la plupart des travaux étudiés sur la marche humaine (Astephen, 2007; Besier et al., 2009; Erdemir et al., 2007; Neptune et al., 2004; Shelburne et al., 2004; Winby et al., 2009; Zajac et al., 2002; Zhao et al., 2007), spécifiquement, les travaux de références considérés au départ pour accomplir nos simulations. Ce choix de la modélisation est dû à l'absence des géométries réelles des jointures de la hanche et de la cheville qui sont reliées directement à notre modèle principal de l'articulation du genou et aussi l'intérêt spécifique à la réponse biomécanique du joint du genou. En ce qui concerne l'articulation de genou, une représentation du corps rigide a été considérée pour chacune des structures osseuses : tibia, fémur et rotule, ce qui offre une précision et un temps plus efficace dans une analyse non linéaire. Ce choix est dû à leur rigidité qui est plus grande par rapport à celle des tissus mous (Donahue and Hull, 2002). Ce choix est aussi justifié vu qu'on n'est pas à la recherche de l'état de déformations dans les structures osseuses. Chaque structure osseuse a été représentée par un nœud primaire (point de référence, PR), situé au centre, et par un ensemble de système de coordonnées local qui tourne avec le corps rigide.

La représentation du cartilage articulaire (ou sa matrice) et de la matrice méniscale par des matériaux élastiques demeure admissible du moment qu'on s'intéresse à la réponse à court terme de la structure. Dans une version simplifiée et non-raffinée du modèle, les couches articulaires du cartilage couvrant les corps rigides osseux sont considérées élastiques isotropes homogènes (Mesfar and Shirazi-Adl, 2005). Ce modèle a eu un raffinement extensif pour les couches de cartilages et les ménisques (Shirazi et al., 2008). Ces raffinements permettent l'incorporation des réseaux fibreux de collagènes aux différentes régions tout au long de la profondeur de cartilages articulaires, en respectant la variation de propriétés matérielles et structurelles du cartilage articulaire. Un comportement composite est assigné pour les cartilages articulaires dans le modèle raffiné où la matrice a été considérée comme un matériau hétérogène isotrope hyper-élastique compressible ce qui est équivalent à un matériau bi-phasique (poroélastique) à court terme (période transitoire) (Shirazi et al., 2008). Un module d'élasticité à l'équilibre de matrice solide du cartilage articulaire a été choisi comme suit: 10, 12, 14 et 18 MPa

en déplaçant respectivement de la surface articulaire jusqu'à la couche la plus basse sous-jacent l'os sous-chondral (Adouni et al., 2012). L'épaisseur des éléments membrane dans les différentes régions du cartilage a été calculée en fonction de la fraction volumique des fibrilles dans chaque zone. Ces fractions volumiques de 15%, 18% et 21% ont été estimées dans la zone superficielle, la zone de transition et la zone profonde respectivement. Ces estimations ont été en fonction de propriétés des tissus signalées en tension (Shirazi and Shirazi-Adl, 2005, 2009a, b; Shirazi et al., 2008) et la courbe de contrainte-déformation du collagène de type II qui représente 70% de la résistance de collagène type I (Shirazi and Shirazi-Adl, 2005). Ces estimations sont en conformité avec l'augmentation rapportée dans la teneur en collagène le long de la profondeur (Julkunen et al., 2008).

La matrice du ménisque (indépendamment de renfort fibres non linéaires de collagène dans les deux directions circonférentielles et radiales) est également prise comme isotrope avec 10 MPa pour le module élastique et 0.45 pour le coefficient de poisson pour les deux modèles. De la même façon que les cartilages articulaires les fibres de collagène ont été employées pour renforcer la structure du ménisque qui sont de type I et leurs répartitions sont basées essentiellement sur la fraction volumique caractéristique de chaque zone constituant le ménisque: le modèle non raffiné de fractions volumiques est de 7% pour les couches superficielles (radiale et circonférentielle) et 14% pour les couches profondes (seulement circonférentielles) (Fithian et al., 1990; Whipple et al., 1984). Une petite modification apportée pour ces valeurs dans le modèle raffiné, telle que 2.5% comme fraction volumique additionnelle dans la zone profonde radialement et une diminution de la fraction volumique de la zone superficielle par 2% (Proctor et al., 1989; Skaggs et al., 1994). Ces propriétés des matériaux conduisent à des résultats globalement similaires dans différentes composantes de déformations et de contraintes pour les deux modèles raffiné et non raffiné (Shirazi et al., 2008).

Les différents ligaments constituant le modèle du genou sont modélisés avec des éléments connecteurs non-linéaires uni-axiaux. Les comportements mécaniques de chaque ligament et du tendon rotulien et leurs élongations initiales associées ont été obtenus de la littérature (Atkinson et al., 2000; Butler et al., 1986; Moglo and Shirazi-Adl, 2003a, 2003b, 2005; Stäubli et al., 1999). Il est à signaler que les élongations initiales représentent les précontraintes au niveau des ligaments et par conséquent, des précontraintes au niveau de l'articulation de genou. Des travaux antérieurs ont été effectués pour prouver le choix des élongations initiales et montrer

l'importance de prendre en compte ce paramètre sans le négliger dans les simulations numériques. La modélisation du tendon rotulien peut montrer une certaine limitation du fait qu'il n'y pas un contact établi entre le tendon et le cartilage du fémur à des grands angles de flexion (Matsuda et al., 1997). Cette dernière dépasse la limite de la rotation de flexion durant la phase d'appui de la marche humaine.

Les muscles représentent les forces qui sont appliquées au système dont leur direction varie en fonction de la rotation pour les joints rigides (hanche et cheville), alors que, en fonction de la rotation et de la translation pour le joint de genou. Des connecteurs uni-axiaux avec des forces constantes ont été employés pour simuler cet état de muscles. Les articulations du cartilage-cartilage au niveau du joint patellofémoral et tibiofémoral ainsi que les articulations ménisque-cartilage au joint tibiofémoral ont été simulées à l'aide d'un algorithme de contact *surface to surface* qui donne une bonne précision au niveau des éléments de contact.

8.3 Simulations.

8.3.1 Données cinématiques et cinétiques

Dans la première étape de ce travail, on a choisi les données cinématiques et cinétiques produites par l'analyse de la marche à cadence normale sur des sujets sains. Cette analyse a été effectuée par le groupe de Deluzio.(Astephen 2007), (Astephen, 2007) et Hunt et al. (2001). Les travaux de Astephen (2007) portent sur l'étude de la marche de 60 sujets sains n'ayant aucun historique de douleur ni d'interventions chirurgicales aux membres inférieurs. Ils ont été aussi testés pour : des maladies neuromusculaires, des antécédents de maladie cardio-vasculaires et d'accidents vasculaires cérébraux, aussi, pour tout autre trouble de la marche. L'objectif de cette étude était de constituer une base de données de référence et de comparer les sujets avec sévérité variable de l'ostéoarthrite du genou par rapport aux sujets asymptomatiques. Les données cinétiques et cinématiques des sujets, qui ont de l'ostéoarthrite sévère (60 sujets), ont été considérées dans la deuxième phase de notre étude. Par contre, l'étude de Hunt et al.,(2001) s'est concentrée sur les mouvements du pied et la force de réaction produite durant la marche à cadence normale avec le même type de sujets traités par Astephen et al.(2008a; 2008c). Ce choix est dû principalement aux disponibilités de toutes les données cinématiques et cinétiques décrivant le cycle de la marche et le nombre élevé de sujets considérés durant ces études.

8.3.2 Transformation du système d'axe

Un référentiel non orthogonal défini par Grood et Santy.(1983) est employé par Astephen et al.(2008a; 2008b) pour décrire la cinétique et la cinématique des articulations (genou, hanche, cheville) qui composent les membres inférieurs. La rotation flexion / extension est mesurée sur l'axe médial / latéral du segment proximal, la rotation interne / externe est mesurée sur l'axe proximal / distal du segment distal, et l'adduction / abduction a lieu autour de l'axe flottant (perpendiculaire aux axes de la flexion / extension et interne / externe) (Fig. 7.1).

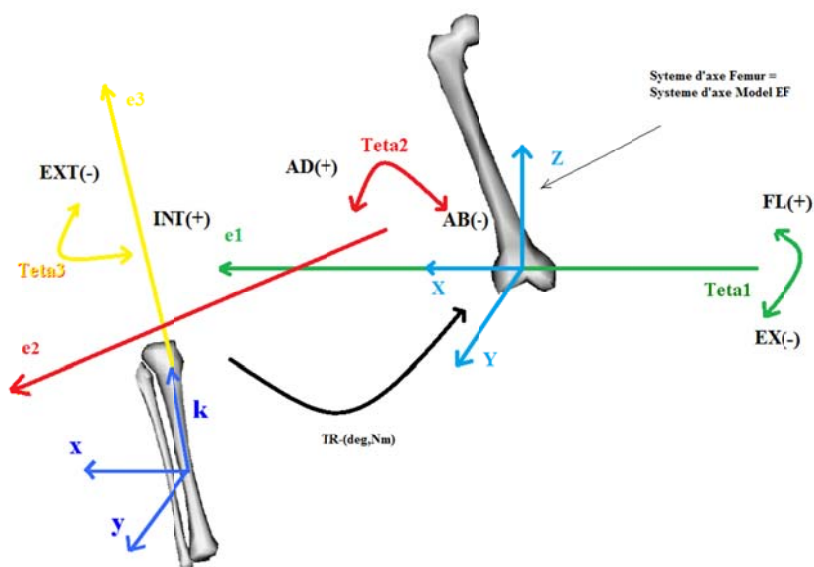


Figure 8-1: Référentiel non orthogonal défini par Grood et Santy.(1983), employé pour décrire la cinétique et la cinématique des articulations des membres inférieurs.

Une transformation est obligatoire pour définir les rotations de tibia par rapport au système d'axe global de notre modèle d'éléments finis (Assemblage ABAQUS). Cette transformation a pour base le chemin inverse suivi par Mesfar et Shirazi-Adl.(2005) pour trouver les rotations cliniques. En plus, il y a un besoin nécessaire qui est la transformation des moments donnés par rapport au système d'axe clinique non orthogonal au système d'axe global du modèle. Cette transformation est détaillée dans l'article de Grood et Santy.(1983).

8.3.3 Détermination des forces musculaires

L'objectif de cette partie de notre travail est l'estimation des forces musculaires par une technique d'optimisation en résolvant les équations d'équilibre (3 au niveau du genou, 3 au

niveau de la hanche et 1 au niveau de la cheville) obtenues à chaque niveau de la phase d'appui. Le minimum de la somme des contraintes musculaires cubique ($\min \sum \sigma^3$) a été considéré comme une fonction objective dans l'optimisation sous des contraintes d'inégalités obligeant les contraintes musculaires à demeurer supérieures aux contraintes passives (σ_p) et inférieures aux contraintes maximales ($0.6\text{MPa} + \sigma_p$) (Arjmand and Shirazi-Adl, 2006). Les composantes passives de forces musculaires sont négligées dans les simulations à cause de changements négligeables dans la longueur du muscle. La somme des contraintes musculaires au cube a été jugée appropriée pour prédire des résultats qui sont qualitativement en accord avec les mesures expérimentales de EMG (Arjmand and Shirazi-Adl, 2006). La valeur de 0,6 MPa, prise pour la contrainte maximale admissible dans les muscles, se trouve dans le milieu de gamme de valeurs trouvés dans la littérature (0,3-1,0 MPa (McGill and Norman, 1986)).

8.3.4 Simulations et études paramétriques

Les analyses actuelles sont exécutées dans des conditions aux rives les plus stables et les plus proches du cas réel pour différentes configurations durant la phase d'appui de la marche humaine. La première étape de chaque analyse consiste à placer l'articulation de genou dans sa position actuelle relativement au joint de la hanche. Le fémur est fixé tandis que le tibia et la rotule sont laissés complètement libres excepté les angles de tibia qui sont prescrits. Pour chaque analyse une configuration de référence est initialement produite à pleine extension en considérant la réponse du joint du genou sous l'action de pré-tensions ligamentaires (Mesfar and Shirazi-Adl, 2006a). Le tibia subit une action de rotation d'une manière successive à des nouvelles positions sur une plage de rotation définie durant la phase d'appui. À chaque position, on fixe les trois angles de rotations et on cherche alors les forces musculaires qui équilibrent le moment induit par les forces de poids et de réaction du pied, ce qui va tendre le moment au niveau du joint vers zéro après un nombre des itérations bien défini (entre 8 et 14 itérations). La détermination des forces musculaires est décrite précédemment dans la section de forces musculaires et ses calculs d'optimisations sont exécutés avec MATLAB[®] (the MathWorks Inc., Natick, MA, USA, version 2012). Puisque notre modèle d'éléments finis représente la géométrie d'un sujet femelle, les forces au centre de jambe et de pied sont prises égales à 29.3 N et 7.85N respectivement, (De Leva, 1996). Les analyses non linéaires sont exécutées en utilisant ABAQUS 6.10-12 (ABAQUS).

Les instants de la phase d'appui de la marche qui ont été choisis pour être analysés durant cette étude sont : l'instant de double appuis de réception (0%), 5%, 25% , 50%,75% et finalement l'instant de double appuis de propulsion (100%). Ce choix a été considéré suite à des variations dans les données de référence qui ont été utilisées comme point de départ pour nos analyses. Notre investigation initiale s'est concentrée sur la réponse du genou humain dans le cas de la marche à cadence normale pour des sujets sains et l'effet de l'optimisation globale et locale du membre inférieur. Ensuite, les mêmes étapes des analyses ont été considérées pour étudier l'effet de l'ostéoarthrite du genou sévère sur la réponse active et passive du genou. Un volet consiste à étudier la réponse du genou à 50% de la phase d'appui sous l'effet de changement de rotation et de moment dans le plan frontal. Ce dernier, comme un outil faiblement supporté dans la littérature, sert à minimiser le chargement supporté par le plateau tibial médial durant la phase d'appui de la marche. Finalement, le manque de clarté, à cause du faible nombre de études dans la littérature, nous a poussé à étudier la relation entre les muscles du jumeau et le ligament croisé antérieur (LCA) durant la marche et durant une contraction isolée de ce muscle sur le joint tibiofemoral en flexion.

8.4 Analyse des résultats

L'analyse, la comparaison et la discussion des résultats sont présentées dans les sections suivantes: les activités musculaires, les forces ligamentaires ainsi que le mécanisme de transfert de charge. Dans ce cadre, certains éléments doivent être pris en compte. En effet, la comparaison de nos prédictions avec d'autres travaux et l'évaluation du modèle dépendent de la variation de la géométrie des spécimens du genou et de la différence des comportements des matériaux. Elles dépendent aussi des méthodes expérimentales employées, des conditions aux rives et du choix du système de coordonnées.

8.4.1 Forces musculaires

Les forces musculaires dans la première partie de cette étude sont estimées en satisfaisant les équations des moments aux niveaux de la cheville et du genou. Nos prédictions des niveaux d'activation dans les muscles de quadriceps et les muscles *jumeau* corroborent de manière générale les données de la littérature (Besier et al., 2009; Lin et al., 2010; Neptune et al., 2004; Shelburne et al., 2005; Winby et al., 2009) et suivent les mêmes tendances que les activités EMG

mesurées par Astephen (2007) (Fig. 2.3). Les forces du *Ischio-jambiers* calculées atteignent leurs valeurs maximales à 5% de la phase d'appui, directement après le double appui de la réception (*heel strike*). Les activités EMG normalisées de *Ischio-jambiers* superficielles latérales et médiales (Astephen, 2007) sont également maximales au début de la phase d'appui et diminuent par la suite. Les mesures expérimentales d'EMG montrent une inactivité presque total de muscles du *Ischio-jambiers* à la phase de la propulsion (de 50% à 100% de phase d'appuis) et ceci est peu différent par-rapport à nos prédictions pour ces muscles. Des analyses supplémentaires à 75% de la phase d'appui négligent totalement la contribution du muscle de *Soléaire* à la résistance de la flexion de la cheville. Ces analyses montrent une baisse importante de l'activité de *Ischio-jambiers* latéral (*BF*) (de 381 N à 181 N) et une augmentation significative des forces dans les *jumeau* latéral et médial (de 710 N à 1512 N) ainsi que dans les forces de quadriceps (de 4 N à 299 N). Cette diminution de la force d'*Ischio-jambiers* latérale minimise massivement le désaccord entre nos prédictions et les mesures expérimentales d'EMG à la phase de propulsion. Les comparaisons entre les forces musculaires estimées et les données EMG enregistrées doivent, cependant, tenir compte de l'absence de co-activité dans le modèle afin de renforcer la stabilité et le contrôle du joint, le manque de considération des équations des moments de la hanche lors du calcul des forces musculaires du genou et finalement la limitation de mesure EMG aux composantes musculaires superficielles.

La plupart des études antérieures de l'articulation du genou lors de la marche a négligé la résistance passive du joint lors du calcul des forces musculaires (Shelburne et al., 2004; Shelburne et al., 2005, 2006). En effet, les ligaments ainsi que les ménisques et les surfaces articulaires contribuent aux moments passifs qui doivent augmenter en compression. Ces moments passifs ont tendance à supporter une partie des moments extérieurs nets et à réduire les forces musculaires nécessaires. Par la suite, une prédiction précise des forces musculaires doit passer par une quantification précise de la résistance passive du joint sous diverses forces de compression. Nos résultats montrent que les différences entre les moments appliqués (estimés par la dynamique inverse) et les moments résistés par les muscles à la solution de convergence finale indiquent une résistance passive du joint de genou en flexion, adduction et interne de 6.5, 9.0, et 2.1 Nm, respectivement, à 25% de la phase d'appui et de 5.2, 10.8, et 2.0 Nm à 75% de la phase d'appui.

Les muscles de l'articulation du genou qui traversent la hanche ou aussi les muscles poly-articulaire doivent également participer à des équations d'équilibres similaires à l'articulation de la hanche. Pour évaluer l'effet de la considération d'équations des moments de la hanche simultanément avec les équations des équilibres des articulations du genou et de la cheville sur les activités musculaires durant la phase d'appui de la marche, le modèle a été étendu pour tenir compte des muscles et des moments de l'articulation de la hanche (Astéphen et al., 2008a; Delp et al., 2007). Ceci représente un mode d'optimisation global de membre inférieur qui est différent par rapport au mode local ou semi-global considéré au début de ces analyses. Nos résultats ont montré des variations relativement faibles (<10%) dans les composantes totales des forces musculaires estimées lorsque l'articulation de la hanche est incluse. Mais, des changements importants dans la répartition des activités entre les composantes uni-articulaires et bi-articulaires des muscles du genou durant la phase d'appui ont été en accord avec les travaux de Fraysse et al., (2009). Qualitativement (c.-à-d. tendance), une claire amélioration dans l'accord entre nos prédictions et les activités EMG mesurées durant la marche a été trouvée (Astéphen, 2007). Cet accord était plus clair avec les composantes superficielles comme le *BFLH*, qui avait une réponse presque nulle à la fin de la phase d'appui. La majorité de forces dans les muscles du *hamstring* latéraux est transférée par la composante interne *BFSH* à la fin de la phase d'appui. De plus, la baisse importante de l'activité de *RF*, associée à une augmentation à peu près égale à l'activité de *VIM*, corrobore bien avec les données EMG (Astéphen, 2007; Sasaki and Neptune, 2010) qui montrent une activité EMG minimale dans la *RF* par rapport aux composantes *VL* et *VM*. À noter aussi, les grandes forces dans les muscles du *Ischio-jambiers* latéraux expliquent leur importance dans la résistance au moment d'adduction et au moment d'extension du joint de genou. Ce rôle a été négligé dans la majorité des travaux antérieurs par la limitation du rôle des *Ischio-jambiers* au plan sagittal (Anderson and Pandy, 2001; McGowan et al., 2009; Messier et al., 2011; Shelburne et al., 2004; Shelburne et al., 2005, 2006). Cette limitation a été considérée indirectement par la modélisation de joint de genou comme un joint à un seul degré de liberté dans le plan sagittal. D'où les forces musculaires estimées seront affectées.

Lorsqu'on a fait la comparaison entre nos prédictions de forces musculaires pour le cas de sujets asymptomatiques et les sujets atteints par l'ostéoarthrite sévère au niveau de l'articulation de genou, on a constaté que les activités musculaires diminuent durant la phase d'appui à l'exception de l'instant de séparation entre la phase de réception et propulsion (50% de la phase

d'appui). Conformément à la réduction remarquable de moment et de rotation au plan sagittal (flexion) durant la première partie de la phase d'appui (Astephen, 2007), les forces musculaires du quadriceps ont diminué sensiblement de leur pic de 1087 N dans le groupe normal à 525 N dans le cas OA à 25% de la phase d'appui (Fig. 4.3). Cela peut apparaître comme une minimisation d'activation de quadriceps au début de la phase d'appui qui a été souvent rapportée pour des patients souffrant de l'OA (Astephen et al., 2008a). En effet, Les quadriceps sont également plus efficaces pour contrebalancer des moments de flexion à des angles faibles de flexion et ceci en accord avec la tendance angulaire présentée pour le cas OA (Mesfar and Shirazi-Adl, 2005). Due à la légère augmentation du moment de flexion à 50% et 75% de la phase d'appui, les forces du quadriceps augmentent relativement par rapport au cas normal. Les muscles du *Ischio-jambiers* latéraux et médiaux ont diminué considérablement durant la phase d'appui à l'exception de l'instant 50%, ceci est en liaison directe avec la variation du moment d'adduction du genou et de la disparition de moment d'extension à la période de la propulsion de la phase d'appui. La réduction dans les moments de flexion de la hanche au début de la phase d'appui dans le groupe OA a agi comme un facteur supplémentaire à la minimisation de l'activité du *Ischio-jambiers*. Nos résultats des forces musculaires suivent presque les mêmes tendances que celles des activités EMG mesurées durant la marche pour des patients de l'ostéoarthrite sévère du genou (Astephen et al., 2008b; Hubley-Kozey et al., 2009).

Concernant l'effet du changement de l'angle et du moment d'adduction sur la réponse musculaire de joint du genou durant la marche, il a été limité à l'instant 50% de la phase d'appui. Ceci est dû aux problèmes de convergence rencontrés avec les autres instances étudiées précédemment. Les variations de la rotation de l'adduction du genou ($R \pm 1.5$) ont conduit à une modification substantielle des activations musculaires du genou à mi-appui de la marche (50% de la phase d'appui). Une augmentation de cette rotation a diminué sensiblement les activités de *Ischio-jambiers* latéraux (principalement le *BFSH*). Mais les forces dans ces muscles ont augmenté avec une plus petite rotation d'adduction. Ces modifications étant suite à des variations de la contribution du moment passif dans l'équilibre total de l'articulation du genou dans le plan frontal (Lloyd and Buchanan, 2001). La diminution massive des activités des muscles de *Ischio-jambiers* latéraux avec l'augmentation de l'angle d'adduction peut expliquer les réponses silencieuses de ces muscles rapportées dans plusieurs travaux dans la littérature (Astephen et al., 2008a; Besier et al., 2009; Shelburne et al., 2006; Winby et al., 2009). En raison de l'antagonisme

de ces muscles aux quadriceps dans le plan sagittal, des tendances similaires ont eu lieu dans les quadriceps. Les forces du quadriceps augmentent avec la diminution de l'angle d'adduction et diminuent avec l'augmentation de cet angle. Par contre, Les composantes médiales des muscles du *Ischio-jambiers* sont restées silencieuses indépendamment des rotations d'adduction considérées. En effet, une activité sera développée par les muscles du *Ischio-jambiers* si un plus grand angle d'adduction a été considéré durant cette analyse, ceci apparaîtra comme une réponse au dépassement du moment d'adduction externe par la résistance passive du joint de genou. Les forces latérales dans les muscles du *Ischio-jambiers* sont linéairement proportionnelles au moment d'adduction externe; une tendance qui est en accord avec le fait que le moment de résistance passive de l'articulation est pratiquement inchangé avec une rotation de l'adduction fixe.

Le rôle crucial de la résistance passive du genou dans la réponse active de joint devient plus clair lorsque les différences entre les moments appliqués (via dynamique inverse) et la partie résistée par les muscles ont été évalués dans le plan frontal. Cette différence représente un indicatif de la contribution passive qui atteint des moments d'adduction de 8, 0 et 14 Nm dans les cas de référence, avec une diminution et une augmentation de 1.5 degré, respectivement. Ceci représente une explication quantitative de changement dramatique des forces musculaires estimées sous l'effet de changement de l'angle d'adduction. Sous des forces de compression axiales similaires (1400N), Marouane et al. (2013) ont rapporté une augmentation de 14 Nm dans la résistance passive dans le plan frontal associé à une augmentation de la rotation d'adduction de $\sim 1,4^\circ$. Lloyd et Buchanan (2001) ont estimé la contribution des muscles au moment d'adduction à 11-14 %, ce qui est d'accord avec notre prédiction de ~ 16 % sous un angle plus élevé d'adduction. Cette petite valeur (Lloyd and Buchanan, 2001) a été largement utilisée comme argument pour négliger le rôle des muscles dans l'équilibre du plan frontal du joint et de limiter l'attention sur le plan sagittal seulement (Besier et al., 2009; Fraysse et al., 2009; Shelburne et al., 2005, 2006; Winby et al., 2009). Cet argument peut être considéré seulement lorsque le moment d'adduction externe appliqué est presque entièrement pris en charge par la résistance passive de l'articulation. Donc, ceci ne se produit que lors d'une rotation d'adduction et une compression spécifique. En raison de la forte dépendance de la résistance d'adduction passive à la rotation de l'adduction et de la force de compression du joint (Marouane et al., 2013), le domaine de validité de certains modèles est limitée par la précision considérée dans l'acquisition des données

cinématiques et cinétiques dans le plan frontal. Par contre, le changement du moment d'adduction par $\pm 50\%$ a altéré faiblement les différences ($< 1\text{Nm}$) entre les moments appliqués (via dynamique inverse) et la partie résistée par les muscles.

8.4.2 Forces ligamentaires

Une différence négligeable ($< 2\%$) dans les forces ligamentaires estimées par les deux approches de modélisation (cheville + genou et cheville + genou + hanche) qui sont considérées au début de cette analyse à cause de faibles différences dans les forces musculaires trouvés par les deux modes d'optimisation. Les angles faibles de flexion considérés durant cette étude (Astephen, 2007) au début de la phase d'appui conduisent presque à une égalité entre la force totale des muscles de quadriceps et la force de tendon rotulien avec un ratio presque constant le long de la période de réception qui est égale à ~ 0.95 . Ces forces de tendon rotulien, à leur tour, tirent le tibia en avant à cause de leur orientation antérieure. Cette translation tibiale augmente la force du ligament croisé antérieur (LCA) (Fig. 2.4). La diminution de la force de tendon rotulien, et par conséquent la force de cisaillement antérieur de joint, conduit à une diminution de force du LCA au milieu de la phase d'appui. L'augmentation considérable de l'activité des muscles de *jumeau*, en particulier à 75% de la phase d'appui, ont tendance à diminuer les forces du *Ischio-jambiers* et comme conséquence une augmentation de force du LCA. Ces résultats concordent bien avec des variations similaires rapportées dans des études antérieures (Shelburne et al., 2004; Shelburne et al., 2005, 2006). Comme prévu et dans ces conditions, le ligament croisé postérieur (LCP) reste mou le long de la phase d'appui. À la fin de la phase d'appui, et dû à un grand angle d'adduction associé avec un moment d'abduction, le ligament collatéral latéral a subi une charge élevée pour assurer la stabilité du joint dans le plan frontal (Fig. 2.4).

En ce qui concerne les variations des forces ligamentaires pour le cas OA, la force du LCA suit les modifications estimées dans les activités musculaires (Fig. 4.4). La diminution de forces des muscles de *Ischio-jambiers*, lors de la deuxième moitié de la phase d'appui, a augmenté considérablement la force dans le LCA. Une légère diminution dans cette force a été calculée au début de la phase d'appui et ceci est dû à la réduction significative de l'activation du quadriceps. Une réduction dans la rotation d'adduction et dans le moment d'abduction à la fin de la phase d'appui avec les sujets patients conduit à une diminution massive des forces de ligament

collatéral latéral. Une force très faible ou presque nulle a été déterminée pour le reste de ligaments constituant le joint de genou avec le cas OA.

Les forces de ligaments prédites, en particulier LCA et LCL, sont influencées par les changements de l'activité musculaire causés par l'altération de rotation et du moment dans le plan frontal par rapport à sa configuration de référence. La force de LCL augmente avec l'augmentation de l'angle d'adduction, ceci est expliqué par le fait que cette structure s'oppose à la rotation d'adduction (Grood and Hefzy, 1982; Kennedy et al., 1977; Markolf et al., 1976; Warren et al., 1974). La force du LCA augmente aussi avec l'augmentation de l'angle d'adduction à cause de l'importante baisse dans les activités des muscles du *Ischio-jambiers* malgré les diminutions estimées dans les activités des quadriceps. Par contre, la réduction de l'angle d'adduction augmente aussi la force du LCA qui est dû à l'accroissement des activités des quadriceps (Mesfar and Shirazi-Adl, 2005; Shin et al., 2011).

L'influence du changement dans l'activation des muscles du *jumeau* sur la force de LCA a montré que ces muscles agissent pour augmenter la translation antérieure du joint tibiofemoral et par la suite jouent le rôle d'un muscle antagoniste pour cette ligament. À 75% de la phase d'appui, lorsque les muscles de *jumeau* en plein activation et le joint de genou près de son extension complète, une augmentation dans son activité génère une force additionnelle de cisaillement antérieure sur le tibia. Cette force additionnelle est due directement à la traction du muscle et indirectement à la compression ajoutée sur le joint qui agit sur une pente tibiale orientée postérieurement. Avec 36 % de réduction ou 26% d'augmentation des forces de *jumeau*, la force du LCA a clairement diminué de 271 N à 178 N ou augmenté de 271 N à 331 N, respectivement, en suivant de près l'évolution de l'activation musculaire (Fig. 6.2).

Puisque la diminution de l'activation de *jumeau* a été achevée dans ces analyses par une augmentation de l'activité de *Soléaire*, un mécanisme efficace pour diminuer la force de LCA et la compression du joint du genou est d'activer de plus le *Soléaire* plutôt que les *jumeaux* à la fin de la phase d'appui. Ceci est en accord avec quelques travaux dans la littérature (Neptune et al., 2001). La limitation ou l'absence de la considération du muscle *Soléaire* dans le calcul d'équilibre de membre inférieur dans les études antérieures (Besier et al., 2009; Kim et al., 2009; Shelburne et al., 2004; Winby et al., 2009) a conduit à une surestimation dans la prédiction des

forces du jumeau qui entraînent par la suite une augmentation de chargements passifs du joint et spécifiquement une augmentation de forces prédites dans le LCA.

Une confirmation claire du rôle antagoniste du jumeau sur le LCA a été démontrée par une analyse additionnelle qui tient compte seulement d'une activation isolée de ces muscles sur le joint tibiofemoral durant la flexion (Fig. 6.5). À des angles de flexion faibles ($< 40^\circ$), la charge dans le LCA a été supportée entièrement par sa partie postéro-latérale (LCA-pl). Par contre, une augmentation de flexion du joint transfère mutuellement la charge entre la partie postéro-latérale et la partie antero-médiale (LCA-am) du LCA telle que à 90° de flexion la plupart de charge sur le LCA est supportée par LCA-am ($\sim 90\%$). Cette redistribution de la charge entre les faisceaux du LCA avec la flexion de l'articulation est en accord avec les études antérieures (Moglo and Shirazi-Adl, 2005; Woo et al., 1998). Contrairement au croisé antérieur, l'activation de jumeau décharge le ligament croisé postérieur. Par la suite, on peut considérer ces muscles comme des protecteurs pour ce ligament même à des grands angles de flexion. Nos résultats actuels soutiennent des résultats précédents qui montrent une augmentation de chargement sur le LCA associé avec une activation seule ou combinée avec d'autres muscles du *jumeau* durant la flexion (Fleming et al., 2001; O'Connor, 1993). Mais, ces résultats ne sont pas en accord avec les résultats qui mentionnent une baisse de déformation du LCA-am et une augmentation de déformation du LCP lorsque les force du jumeau augmentent (Dürselen et al., 1995).

8.4.3 Force, pression et aire de contact

Les efforts de contact ainsi que les contraintes et les déformations de cartilage sont influencés par les activités musculaires et les forces calculées dans les ligaments durant la phase d'appui de la marche. À cause du moment et de la rotation d'adduction de l'articulation, le compartiment médial transporte la partie majeure de compression durant la phase d'appui à l'exception de la période de réception entre 0% et 5% de la phase d'appui (Fig. 2.5). Ces forces, dans les deux plateaux, sont transmises principalement dans les zones non couvertes par des interfaces de cartilage-cartilage. La partition disproportionnée de la charge entre les compartiments de joint TF est corroborée par des travaux antérieurs (Andriacchi et al., 2009; Hurwitz et al., 1998; Kutzner et al., 2010; Neptune et al., 2004; Shelburne et al., 2006; Thambyah, 2007; Zhao et al., 2007). Par contre, des forces de contact, qui sont relativement faibles, sont calculées au niveau du joint PF qui est dû principalement aux faibles angles de

flexion de l'articulation au cours de la phase d'appui. D'autre part, la marche n'est pas une préoccupation majeure pour le joint patello-fémorale (Mason et al., 2008).

Suite à la répartition déséquilibrée de forces de contact entre les deux plateaux tibiaux, des contraintes et des déformations plus élevées ont été calculées sur le cartilage tibial médial associé avec un décalage postérieur dans la zone de contact durant la phase d'appui (Fig. 2.7; 2.8). Ces observations sont bien en accord avec celles des études de Koo et al., (2011) et Coleman et al., (2011) qui ont enregistré une diminution plus importante dans l'épaisseur du cartilage et grands mouvements postérieures sur le plateau médial par rapport au latéral lors de la marche. Il faut signaler aussi, des contraintes de traction relativement importantes calculées dans les fibres verticales profondes du cartilage médial sous la zone de contact. Les déformations de fibres verticales sont encore plus grandes par rapport à celles de fibres superficielles horizontales à la même région. Ceci montre encore le rôle crucial des réseaux de fibrilles profonds dans le support de charge externe du cartilage articulaire (Shirazi et al., 2008). Ces résultats peuvent expliquer l'observation fréquente de l'arthrite articulaire au niveau du compartiment médial de l'articulation de genou (Eng and Winter, 1995; Sharma et al., 2001).

Due aux changements cinématique, cinétique et activités musculaires, la force de contact TF a augmenté seulement au milieu de la phase d'appui pour le cas OA par rapport au cas normal. L'augmentation importante de l'aire de contact prédite avec le cas OA explique clairement la diminution de pression de contact moyenne et maximale à l'exception de la période 50% de la phase d'appui, où il y a une augmentation très faible de pression de contact (~2%) malgré l'augmentation significative de force de contact. Comme la force de contact pour le cas normal, le plateau médial continue aussi à supporter la majorité de charge transmise à travers le joint tibiofemoral par une portion variant de 70% à 100% à l'exception de période initiale de réceptions (Kumar et al., 2012a; Kumar et al., 2012b). Ces observations sont en accord avec les observations antérieures qui supportent que l'alignement varus peut causer une augmentation de chargement qui est transmis par le compartiment médial durant la marche (Kumar et al., 2012a; Kumar et al., 2012b). Le désaccord de nos prédictions avec l'estimation de la répartition équilibrée de charge entre les deux plateaux tibial trouvés par Mononen et al.(2013a, b) est dû probablement à la rotation d'abduction considérée au cours de la phase d'appui de la marche durant leur étude.

Les simulations de la détérioration de propriétés des matériaux du cartilage et de ménisques dans la modélisation de cas OA n'ont pas d'influence sur les forces musculaires, les forces de contact et les forces ligamentaires. Par contre, ces modifications ont sensiblement augmenté l'aire de contact dans le joint qui réduit d'avantage la pression du contact moyenne et maximale. Cet effet était clair au milieu de la phase d'appui lorsque la force de contact a augmenté et la pression du contact maximale et moyenne ont diminué (Fig. 4.6 ; 4.7). Au même moment, la partie de charge de contact transmise via les ménisques a augmentée avec la diminution de la rigidité de cartilage et des ménisques. Par contre, ce changement dans le comportement des matériaux du cartilage et des ménisques a augmenté significativement les déformations dans les couches superficielles et profondes du cartilage articulaire (Fig. 4.8). Des grandes déformations dans la zone profonde à la jonction sous-chondral ont été prédites (Fig. 4.8). Ces déformations sont liées au gradient de rigidité persistant dans cette zone (Radin and Rose, 1986). Cette jonction os-cartilage représente le site d'initiation de fractures horizontales qui se produit dans le cartilage articulaire durant les activités quotidiennes (Meachim and Bentley, 1978) ou sportives (Atkinson and Haut, 1995; Vener et al., 1992). Ces résultats sont en accord avec des études antérieures qui utilisent la méthode des éléments finis pour modéliser l'effet de OA sur la réponse biomécanique de joint du genou (Mononen et al., 2013a, b).

Lors des analyses de l'effet d'altération de cinématique et de cinétique du joint de genou au milieu de la phase d'appui, un changement dans la rotation de l'adduction de 1.5° a donné des effets importants sur la répartition de charge entre les deux plateaux qui constituent le joint tibiofemoral. Une grande rotation d'adduction a augmenté la charge sur le compartiment médial et a presque déchargé le compartiment latéral opposé. Une tendance inverse est observée avec une plus petite rotation d'adduction, où une force de contact énorme est calculée sur le plateau latéral qui entraîne une force de contact totale plus grande (+20 %), malgré la diminution de la force de contact sur le compartiment médial. Suite à l'augmentation de l'aire de contact et à la diminution de rotation d'adduction, la pression du contact maximale sur le cartilage articulaire a diminué de $\sim 30\%$. Ceci permet d'expliquer le décrochage du contact dans le plateau latéral rapporté antérieurement à la fin de la phase d'appui, malgré qu'il existe un moment d'abduction à cet instant (Adouni and Shirazi-Adl, 2013; Adouni and Shirazi-Adl, 2014; Hurwitz et al., 1998). Mononen et al., (2013b) sont les seuls dans la littérature qui ont calculé une charge plus élevée

dans le compartiment latéral par rapport à celle de médial au cours de la phase d'appui. Ceci est dû à la rotation élevée d'abduction considérée.

Les résultats actuels montrent donc que la répartition relative des charges de contact entre les compartiments tibial est principalement influencée par les changements dans la rotation de l'adduction. Les effets de modification de 1.5° en rotation dépassent d'une manière remarquable les effets causés par le changement de 50% dans le moment d'adduction (Fig. 5.5). Dans l'ensemble et sur la base des résultats actuels, si une distribution plus uniforme des charges de contact entre les deux plateaux médial et latéral est recherchée, l'alignement de l'articulation doit être ajusté à un varus-valgus plus neutre avec des très petites rotations d'adduction-abduction. Tout écart par rapport à cette position, un chargement ou un déchargement d'un plateau par rapport à l'autre se produit. Une augmentation importante du rapport de force du contact médial par rapport au latéral a été calculée (de ~ 8.8 à 90) avec l'augmentation de rotation d'adduction de 1.5° . Alors qu'au contraire, une diminution de rotation d'adduction a donné une distribution plus uniforme (de ~ 8.8 à 1.6). En outre, si le but est de diminuer l'effort de contact médial, indépendamment de la charge latérale, la réduction de la rotation de l'adduction de 1.5° est beaucoup plus efficace. Cette modification a réduit la charge sur le plateau médial de 12%, par contre la réduction du moment d'adduction de 50% a légèrement diminué la charge médiale de $\sim 4\%$. Les présents résultats soulignent également l'importance d'une acquisition précise de rotation adduction / abduction de l'articulation du genou dans diverses activités.

8.4.4 Modèle raffiné et non raffiné

La comparaison entre les prédictions du modèle simplifié moins raffiné et celle du modèle raffiné, qui tient compte des réseaux fibreux de collagènes aux différentes régions tout au long de la profondeur de cartilages articulaires en respectant la variation de propriétés des matériaux et structurelles du cartilage, démontre des changements négligeables dans les forces musculaires estimées ($< 0,02$ BW). Par contre, les forces ligamentaires, les contraintes et les aires de contact sont toutefois modifiées. La force du ligament croisé antérieur augmente de 68 N avec le modèle raffiné à 25% de la phase d'appui. Par contre, une diminution remarquable de $\sim 170 \text{ mm}^2$ de l'aire de contact dans le joint tibiofemoral a été achevée au même instant du calcul. Cette diminution a augmenté sensiblement la contrainte moyenne dans la jointure tibiofemoral de $\sim 0.5 \text{ MPa}$ à 25% de la phase d'appui. Les changements remarquables dans les aires et les contraintes de contact sont

naturellement dus au raffinement et à la présentation réaliste du cartilage lui-même. L'utilisation du modèle simplifié est donc justifiée lors de la recherche de la réponse globale et des forces musculaires puisque ce modèle est compté très efficace en terme de convergence et coût de calculs par rapport au modèle raffiné. Par exemple, une simulation pour un instant de la phase d'appui avec le modèle simplifié dure de 1 à 2 heures, alors qu'avec le modèle raffiné de 32 à 48 heures en utilisant un ordinateur qui possède 12CPU et 32GB de mémoire vive. Par contre, les futures simulations de troubles articulaires (c.-à-d. des lésions ligamentaires, des défauts du cartilage et de dégénérescences) justifient également l'utilisation du modèle détaillé du joint du genou.

8.4.5 Limitations des modèles

Notre modélisation présente certaines limitations du fait qu'il n'y a pas une considération de co-activités musculaires qui sont souvent nécessaire pour mieux contrôler les mouvements et stabiliser le joint, en particulier au moment de l'initiation de la réception de la phase d'appui. Aussi, la considération de co-activités musculaires peut causer une augmentation de forces musculaires prédites durant la phase d'appui et par conséquent un changement d'équilibre passif du joint du genou. Des géométries réelles et une modélisation réaliste de structures passives, constituant les joints de la cheville et de la hanche, peuvent améliorer nos prédictions. Des limitations causées par les problèmes de convergence telles que la non considération complète du comportement bi-phasique du joint du genou qui affecte la précision des prédictions seulement pour des analyses à long terme. Par contre, le comportement hyper-élastique compressible considéré dans notre étude a été validé auparavant par des études antérieures expérimentales et théoriques comme un alternatif fiable pour les analyses transitoires. La limitation sur des périodes spécifiques pour l'exécution des analyses comme les cas de simulations des détériorations de matériaux de cartilage et des ménisques, pour le cas OA ou aussi la limitation à 50% de la phase d'appui pour analyser l'effet du changement d'angle et du moment d'adduction sur la réponse biomécanique du joint, est due principalement aux problèmes de convergence.

La non considération des analyses dynamiques est dû principalement au manque de quelques données expérimentales complémentaires comme les vitesses linéaires et angulaires de mouvements de différents segments constituant le membre inférieur durant la marche. Mais à noter aussi que nos analyses statiques sont valides: ils tiennent compte de l'inertie du corps en

mouvement puisque les moments externes des joints sont évalués avec la méthode de dynamique inverse. Une modélisation spécifique du joint du genou qui doit être associée aux sujets considérés durant l'analyse expérimentale représente aussi une limitation. Il est nécessaire de mentionner que les altérations de données cinématiques/cinétiques, les propriétés des matériaux et structurelles ainsi que l'axe de flexion de l'articulation, qui ont été considérés dans cette étude, ont une influence sur les prédictions et ceci ne peut être quantifié que par des analyses de sensibilité adéquates (Daher et al . , 2010; Moglo et Shirazi -Adl , 2005).

CHAPITRE 9 CONCLUSION ET RECOMMANDATIONS

9.1 Conclusion

Le travail mené dans cette thèse représente une première dans l'élaboration d'un modèle numérique du membre inférieur assez complet constituant une approche adéquate et complémentaire aux études expérimentales des analyses de la marche humaine. En incorporant le modèle tibiofémoral validé de Shirazi (2008), développé à l'origine par Bendjaballah (1998), au modèle musculosquelettique de membre inférieur. On a donné naissance à un modèle qui tient compte de plusieurs facteurs d'influence sur l'articulation de genou. Ce modèle est contrôlé par des données expérimentales collectées durant l'analyse de la marche (Astépen, 2007). À travers ce modèle, des calculs itératifs ont permis de déterminer simultanément la réponse active et passive du joint de genou dans six périodes critiques de la phase d'appui de la marche humaine pour des sujets normaux et des sujets patients avec l'ostéoarthrite (OA) sévère. Ce modèle a été utilisé pour comprendre l'effet de l'optimisation globale et locale sur la réponse biomécanique de joint du genou, aussi pour détecter le mécanisme principal responsable sur la répartition de la force compartimentale dans le joint tibiofémoral durant l'activité de la marche et finalement pour vérifier la relation antagoniste de muscles de jumeau avec le ligament croisé antérieur. Les analyses élaborées ont abouti aux conclusions suivantes :

- Durant l'analyse de la marche normale, les muscles de quadriceps jouent un rôle très important dans l'équilibre de l'articulation de genou au début de la phase d'appui. Ils permettent de contrebalancer le moment de flexion généré par la force de réaction au sol et d'inertie durant la période de réception de la phase d'appui. Le muscle de *Ischio-jambiers* latéral suit de proche la variation de moment d'adduction. Le muscle de *jumeau* intervient d'une manière massive dans l'équilibre de l'articulation à la fin de la phase d'appui pour assurer une stabilité de membre inférieur durant la propulsion à travers le balancement du moment de flexion dorsale de la cheville et du moment d'extension du genou. Ces configurations musculaires entourant l'articulation du genou avec la cinématique considérée conduisent à une charge tibiofémorale déséquilibrée entre les deux plateaux. Cette charge a été transmise majoritairement par le plateau médial à l'exception de l'initiation de la période de réception de la phase d'appui. Une concentration claire de contrainte de contact sur le plateau médial a

été aussi observée ce qui permet de donner une explication sur le cas d'arthrite articulaire médiale fréquente chez l'être humain. La force dans le ligament croisé antérieur augmente avec l'augmentation de la force de quadriceps et de *jumeau* telle qu'elle atteint des valeurs maximales à 25% et 75% de la phase d'appui.

- Les considérations simultanées de tous les joints du membre inférieur dans les équations d'équilibres durant l'optimisation des forces musculaires (ou aussi l'optimisation globale) ont permis une détermination plus précise de répartitions des forces entre les différentes composantes de muscles poly-articulaires. Les forces prédites avec cette technique sont qualitativement plus proches des mesures électromyographiques que les forces prédites par la méthode d'optimisation locale. Par contre, une différence presque négligeable entre les deux techniques a été calculée dans la résultante de forces musculaires de chaque groupe entourant l'articulation. Par conséquent, on a eu une très faible différence dans les chargements passifs du joint.
- Les modifications dans les rotations et les moments aux articulations des membres inférieurs enregistrées au cours de la marche associée avec le cas OA influencent les niveaux d'activation de la musculature du membre inférieure, les forces, les contraintes du contact et aussi les contraintes et les déformations dans le cartilage articulaire du genou. Une diminution remarquable a été trouvée dans la force de quadriceps au début de la phase d'appui causée principalement par la diminution de moment et d'angle de flexion et ceci corrobore les anciennes observations de l'exclusion de l'activation de quadriceps dans la période de réception. Aussi une réduction importante dans l'activité de *Ischio-jambiers* et *jumeau* a été recodée à cause de la diminution dans le moment d'adduction et le moment d'extension durant la période de propulsion. Suite à cette diminution d'activité musculaire, une légère diminution de la force a été calculée pour le ligament croisé antérieur. Les réductions de contrainte moyenne et maximale du contact, l'augmentation des déformations de tissus cartilagineux et le transfert de charge via les ménisques sont partiellement dues au changement cinétique-cinématique de la marche et aux détériorations de propriétés des matériaux du cartilage dans le cas OA.
- Les variations de l'angle d'adduction du genou affectent considérablement la résistance passive du genou, le niveau d'activation dans tous les muscles entourant l'articulation, les forces de contact du joint et leur distribution entre les compartiments. Une augmentation de la

rotation d'adduction décharge presque le compartiment latéral et augmente la part du plateau médial. Alors, une baisse de rotation d'adduction a généré une charge importante sur le compartiment latéral et a diminué la charge du plateau médial. Par contre, les altérations du moment d'adduction externe ont des effets plus faibles sur le chargement compartimental. Ces résultats expliquent la faible corrélation entre le moment d'adduction de genou et le chargement de compartiment tibiofemorale en marche. Par conséquent, la répartition de charge interne est dictée principalement par la rotation d'adduction et non pas par le moment. Cela a des conséquences importantes dans les interventions thérapeutiques qui visent à diminuer la charge sur le compartiment médial

- Enfin, les *Ischio-jambiers* et les *jumeaux* sont deux fléchisseurs de l'articulation du genou. Ils jouent des rôles opposés respectivement soit dans la protection ou dans le chargement de ligament croisé antérieur. Les variations du niveau d'activité de *jumeau* durant la marche affectent sensiblement le reste des forces musculaires ainsi que les forces de ligament croisé antérieur. La force du ligament croisé antérieur a également augmentée dans tous les angles de flexion sous l'activité isolée du *jumeau*. Il est intéressant de mentionner que la force dans le ligament croisé antérieur a considérablement augmenté dans des grands angles de flexion suite à l'activité isolée du *jumeau*, la tendance qui n'est pas présente et même dans l'activité des quadriceps. En plus, le fait de savoir que le *jumeau* est un antagoniste de ligament croisé antérieur, peut contribuer à la prévention efficace des blessures post-opératoires durant la réhabilitation après une reconstruction de ce ligament.

Les résultats de ces analyses peuvent avoir de grands intérêts et peuvent être très prometteurs pour les cliniciens afin de planifier la réhabilitation.

9.2 Recommandations.

Dans notre modèle de membre inférieur, seul l'articulation de genou a été considérée comme une articulation complète qui tient compte de tous les paramètres d'influences passives et actives. Par contre, les autres articulations qui constituent le membre inférieur comme l'articulation de la hanche et de la cheville ont été modélisées comme des joints sphériques simples. Pour améliorer la précision dans ce sens de modélisation, il est souhaitable d'obtenir une modélisation plus concrète pour ces deux joints par la considération d'une géométrie réelle et un comportement déformable de leurs tissus mous. Aussi, avec l'amélioration des outils d'imagerie

par résonance magnétique, il est devenu plus facile et rapide de reconstruire un modèle complet de membre inférieur. Avec cet avancement technologique, la détermination de modèles spécifiques, pour des sujets contrôlés par les données cinématiques et cinétiques collectées pour les mêmes sujets durant l'analyse de la marche *in vivo*, permettra d'obtenir des résultats plus généraux couvrant un champ plus grand de comportement du joint de genou en particulier et du membre inférieur en général durant différentes activités humaines. Ces résultats pourront permettre de mettre en place un protocole plus sophistiqué de prévention efficace des blessures et de réadaptation post-opératoire.

La présente étude examine seulement la réponse instantanée (à court terme) de l'articulation du genou durant l'activité de la marche. La présence d'eau est simulée en utilisant une solution élastique équivalente. Tenir compte des propriétés poroélastiques des ménisques et du cartilage est sans doute la méthode la plus appropriée afin d'entamer des études dynamiques et d'impacts dans un large intervalle du temps et pour des vitesses assez élevées. Une telle considération pourra élargir les capacités de ce modèle pour résoudre divers problèmes liés à l'articulation du genou humain sous plusieurs types de sollicitations et de mouvements.

Tenir compte aussi de certaines conditions telles que l'étude de la réponse de l'articulation de genou en cas de coupure totale de ligament croisé antérieur durant l'activité de la marche est parmi les recommandations pour les futurs travaux. Étudier aussi l'effet des orientations postérieures de pente tibiale sur la réponse globale de l'articulation durant la marche pourra aussi faire le sujet des études à venir.

BIBLIOGRAPHIE

- Aalbersberg, S., Kingma, I., Ronsky, J.L., Frayne, R., van Dieen, J.H., 2005. Orientation of tendons in vivo with active and passive knee muscles. *Journal of Biomechanics* 38, 1780-1788.
- ABAQUS, T.E., version 6.10, 2010. Simulia, Providence, RI.
- Abdallah, A.A., Radwan, A.Y., 2011. Biomechanical changes accompanying unilateral and bilateral use of laterally wedged insoles with medial arch supports in patients with medial knee osteoarthritis. *Clinical Biomechanics* 26, 783-789.
- Adams, M.E., Billingham, M.E., Muir, H., 1983. The glycosaminoglycans in menisci in experimental and natural osteoarthritis. *Arthritis & Rheumatism* 26, 69-76.
- Adouni, M., Shirazi-Adl, A., 2009. Knee joint biomechanics in closed-kinetic-chain exercises. *Computer Methods in Biomechanics and Biomedical Engineering* 12, 661.
- Adouni, M., Shirazi-Adl, A., 2013. Consideration of equilibrium equations at the hip joint alongside those at the knee and ankle joints has mixed effects on knee joint response during gait. *Journal of Biomechanics* 46, 619-624.
- Adouni, M., Shirazi-Adl, A., Shirazi, R., 2012. Computational biodynamics of human knee joint in gait: From muscle forces to cartilage stresses. *Journal of Biomechanics* 45, 2149-2156.
- Adouni, M., Shirazi-Adl, A., 2014. Evaluation of knee joint muscle forces and tissue stresses-strains during gait in severe OA versus normal subjects. *Journal of Orthopaedic Research* 32, 69-78.
- Ahmed, A., Burke, D., 1983. In-Vitro of Measurement of Static Pressure Distribution in Synovial Joints—Part I: Tibial Surface of the Knee. *Journal of Biomechanical Engineering* 105, 216.
- Ahmed, A., Burke, D., Duncan, N., Chan, K., 1992. Ligament tension pattern in the flexed knee in combined passive anterior translation and axial rotation. *Journal of Orthopaedic Research* 10, 854-867.
- Ahmed, A., Burke, D., Hyder, A., 1987. Force analysis of the patellar mechanism. *Journal of Orthopaedic Research* 5, 69-85.

- Anderson, F.C., Pandy, M.G., 2001. Dynamic optimization of human walking. *Journal of Biomechanical Engineering* 123, 381.
- Andriacchi, T., Mikosz, R., Hampton, S., Galante, J., 1983. Model studies of the stiffness characteristics of the human knee joint. *Journal of Biomechanics* 16, 23-29.
- Andriacchi, T.P., 2013. Valgus alignment and lateral compartment knee osteoarthritis: A biomechanical paradox or new insight into knee osteoarthritis? *Arthritis & Rheumatism* 65, 310-313.
- Andriacchi, T.P., Dyrby, C.O., 2005. Interactions between kinematics and loading during walking for the normal and ACL deficient knee. *Journal of Biomechanics* 38, 293-298.
- Andriacchi, T.P., Koo, S., Scanlan, S.F., 2009. Gait mechanics influence healthy cartilage morphology and osteoarthritis of the knee. *The Journal of Bone and Joint Surgery. American volume*. 91, 95.
- Arjmand, N., Shirazi-Adl, A., 2006. Sensitivity of kinematics-based model predictions to optimization criteria in static lifting tasks. *Medical engineering & physics* 28, 504-514.
- Arjmand, N., Shirazi-Adl, A., Parnianpour, M., 2007. Trunk biomechanical models based on equilibrium at a single-level violate equilibrium at other levels. *European Spine Journal* 16, 701-709.
- Astephen, J.L., 2007. Biomechanical factors in the progression of knee osteoarthritis. *School of Biomedical Engineering*. Halifax, Dalhousie university.
- Astephen, J.L., Deluzio, K.J., Caldwell, G.E., Dunbar, M.J., 2008a. Biomechanical changes at the hip, knee, and ankle joints during gait are associated with knee osteoarthritis severity. *Journal of Orthopaedic Research* 26, 332-341.
- Astephen, J.L., Deluzio, K.J., Caldwell, G.E., Dunbar, M.J., Hubley-Kozey, C.L., 2008b. Gait and neuromuscular pattern changes are associated with differences in knee osteoarthritis severity levels. *Journal of Biomechanics* 41, 868-876.
- Astephen, J.L., Deluzio, K.J., Caldwell, G.E., Dunbar, M.J., Hubley-Kozey, C.L., 2008c. Biomechanical Mechanisms of Knee Osteoarthritis. In:

- Atkinson, P., Atkinson, T., Huang, C., Doane, R., 2000. A COMPARISON OF THE MECHANICAL AND DIMENSIONAL PROPERTIES OF THE HUMAN MEDIAL AND LATERAL PATELLOFEMORAL LIGAMENTS.
- Atkinson, P.J., Haut, R.C., 1995. Subfracture insult to the human cadaver patellofemoral joint produces occult injury. *Journal of Orthopaedic Research* 13, 936-944.
- Baliunas, A., Hurwitz, D., Ryals, A., Karrar, A., Case, J., Block, J., Andriacchi, T., 2002. Increased knee joint loads during walking are present in subjects with knee osteoarthritis. *Osteoarthritis and cartilage/OARS, Osteoarthritis Research Society* 10, 573.
- Banglmaier, R., Dvoracek-Driksna, D., Oniang'o, T., Haut, R., 1999. AXIAL COMPRESSIVE LOAD RESPONSE OF THE 90 DEGREE FLEXED HUMAN TIBIOFEMORAL JOINT. In: *Stapp Car Crash Conference Proceedings*,
- Beard, D., Soundarapandian, R., O'Connor, J., Dodd, C., 1996. Gait and electromyographic analysis of anterior cruciate ligament deficient subjects* 1. *Gait & Posture* 4, 83-88.
- Bendjaballah, M., Shirazi-Adl, A., Zukor, D., 1995. Biomechanics of the human knee joint in compression: reconstruction, mesh generation and finite element analysis. *The knee* 2, 69-79.
- Bendjaballah, M., Shirazi-Adl, A., Zukor, D., 1997. Finite element analysis of human knee joint in varus-valgus. *Clinical Biomechanics* 12, 139-148.
- Bendjaballah, M., Shirazi-Adl, A., Zukor, D., 1998. Biomechanical response of the passive human knee joint under anterior-posterior forces. *Clinical Biomechanics* 13, 625-633.
- Benoit, D.L., Ramsey, D.K., Lamontagne, M., Xu, L., Wretenberg, P., Renstrom, P., 2006. Effect of skin movement artifact on knee kinematics during gait and cutting motions measured in vivo. *Gait Posture* 24, 152-164.
- Besier, T.F., Fredericson, M., Gold, G.E., Beaupré, G.S., Delp, S.L., 2009. Knee muscle forces during walking and running in patellofemoral pain patients and pain-free controls. *Journal of Biomechanics* 42, 898-905.

- Beynnon, B., Yu, J., Huston, D., Fleming, B., Johnson, R., Haugh, L., Pope, M.H., 1996. A sagittal plane model of the knee and cruciate ligaments with application of a sensitivity analysis. *Journal of Biomechanical Engineering* 118, 227.
- Beynnon, B.D., Fleming, B.C., 1998. Anterior cruciate ligament strain in-vivo: a review of previous work. *Journal of Biomechanics* 31, 519-525.
- Blankevoort, L., Huiskes, R., 1991a. Ligament-bone interaction in a three-dimensional model of the knee. *J Biomech Eng* 113, 263-269.
- Blankevoort, L., Huiskes, R., 1996. Validation of a three-dimensional model of the knee. *Journal of Biomechanics* 29, 955-961.
- Blankevoort, L., Huiskes, R., De Lange, A., 1988. The envelope of passive knee joint motion. *Journal of Biomechanics* 21, 705-709, 711-720.
- Blankevoort, L., Kuiper, J., Huiskes, R., Grootenboer, H., 1991b. Articular contact in a three-dimensional model of the knee. *Journal of Biomechanics* 24, 1019-1031.
- Bouisset, S., 2002. *Biomécanique et physiologie du mouvement*, Elsevier Masson.
- Broom, N., Marra, D., 1986. Ultrastructural evidence for fibril-to-fibril associations in articular cartilage and their functional implication. *Journal of Anatomy* 146, 185.
- Brown, T.D., Shaw, D.T., 1984. In vitro contact stress distribution on the femoral condyles. *Journal of Orthopaedic Research* 2, 190-199.
- Buckwalter, J., Mankin, H., 1997. Articular cartilage: degeneration and osteoarthritis, repair, regeneration, and transplantation. *Instructional course lectures* 47, 487-504.
- Buff, H.U., Jones, L.C., Hungerford, D.S., 1988. Experimental determination of forces transmitted through the patello-femoral joint. *Journal of Biomechanics* 21, 17-23.
- Butler, D., Noyes, F., Grood, E., 1980. Ligamentous restraints to anterior-posterior drawer in the human knee. A biomechanical study. *The Journal of Bone and Joint Surgery* 62, 259.
- Butler, D.L., Kay, M.D., Stouffer, D.C., 1986. Comparison of material properties in fascicle-bone units from human patellar tendon and knee ligaments. *Journal of Biomechanics* 19, 425-432.

- Butler, R.J., Marchesi, S., Royer, T., Davis, I.S., 2007. The effect of a subject-specific amount of lateral wedge on knee mechanics in patients with medial knee osteoarthritis. *Journal of Orthopaedic Research* 25, 1121-1127.
- Chen, C.H., Gadikota, H.R., Hosseini, A., Kozanek, M., Van de Velde, S.k., Gill, T., Li, G., 2011. Tibiofemoral kinematics during the stance phase of gait in the normale and ACL defecient knees. *57th Annual Meeting of Orthopaedic Research Society*. Long Beach USA.
- Clarke, I., 1974. Articular cartilage: a review and scanning electron microscope study. II. The territorial fibrillar architecture. *Journal of Anatomy* 118, 261.
- Coats-Thomas, M.S., Miranda, D.L., Badger, G.J., Fleming, B.C., 2013. Effects of ACL reconstruction surgery on muscle activity of the lower limb during a jump-cut maneuver in males and females. *Journal of Orthopaedic Research* 31, 1890-1896.
- Coleman, J.L., Widmyer, M.R., Leddy, H.A., Spritzer, C.E., Moorman, C.T., DeFrate, L.E., 2011. An In Vivo Tricompartmental Analysis of Diurnal Strains in Articular Cartilage of the Human Knee. *57th Annual Meeting of Orthopaedic Research Society*. Long Beach USA.
- Crowninshield, R., Pope, M., Johnson, R., 1976. An analytical model of the knee. *Journal of Biomechanics* 9, 397-405.
- De Leva, P., 1996. Adjustments to Zatsiorsky-Seluyanov's segment inertia parameters. *Journal of Biomechanics* 29, 1223-1230.
- Delp, S.L., Anderson, F.C., Arnold, A.S., Loan, P., Habib, A., John, C.T., Guendelman, E., Thelen, D.G., 2007. OpenSim: open-source software to create and analyze dynamic simulations of movement. *Biomedical Engineering, IEEE Transactions on* 54, 1940-1950.
- Donahue, T.L.H., Hull, M., 2002. A finite element model of the human knee joint for the study of tibio-femoral contact. *Journal of Biomechanical Engineering* 124, 273.
- Draganich, L., Vahey, J., 1990. An in vitro study of anterior cruciate ligament strain induced by quadriceps and hamstrings forces. *Journal of Orthopaedic Research* 8, 57-63.

- Duncan, I.C., Kane, P.W., Lawson, K.A., Cohen, S.B., Ciccotti, M.G., Dodson, C.C., 2013. Evaluation of Information Available on the Internet Regarding Anterior Cruciate Ligament Reconstruction. *Arthroscopy: The Journal of Arthroscopic & Related Surgery*.
- Dürselen, L., Claes, L., Kiefer, H., 1995. The influence of muscle forces and external loads on cruciate ligament strain. *The American Journal of Sports Medicine* 23, 129-136.
- Elias, J.J., Faust, A.F., Chu, Y.-H., Chao, E.Y., Cosgarea, A.J., 2003. The Soleus Muscle Acts as an Agonist for the Anterior Cruciate Ligament An In Vitro Experimental Study. *The American Journal of Sports Medicine* 31, 241-246.
- Eng, J.J., Winter, D.A., 1995. Kinetic analysis of the lower limbs during walking: what information can be gained from a three-dimensional model? *Journal of Biomechanics* 28, 753-758.
- Engh, G.A., 2003. The difficult knee: severe varus and valgus. *Clinical Orthopaedics and Related Research* 416, 58.
- Erdemir, A., McLean, S., Herzog, W., van den Bogert, A.J., 2007. Model-based estimation of muscle forces exerted during movements. *Clinical Biomechanics* 22, 131-154.
- Essinger, J., Leyvraz, P., Heegard, J., Robertson, D., 1989. A mathematical model for the evaluation of the behaviour during flexion of condylar-type knee prostheses. *Journal of Biomechanics* 22, 1229-1241.
- Felson, D.T., Niu, J., Gross, K.D., Englund, M., Sharma, L., Cooke, T.D., Guermazi, A., Roemer, F.W., Segal, N., Goggins, J.M., Lewis, C.E., Eaton, C., Nevitt, M.C., 2013. Valgus malalignment is a risk factor for lateral knee osteoarthritis incidence and progression: findings from the Multicenter Osteoarthritis Study and the Osteoarthritis Initiative. *Arthritis & Rheumatism* 65, 355-362.
- Fleming, B.C., Renstrom, P.A., Ohlen, G., Johnson, R.J., Peura, G.D., Beynnon, B.D., Badger, G.J., 2001. The gastrocnemius muscle is an antagonist of the anterior cruciate ligament. *Journal of Orthopaedic Research* 19, 1178-1184.
- Frayssé, F., Dumas, R., Cheze, L., Wang, X., 2009. Comparison of global and joint-to-joint methods for estimating the hip joint load and the muscle forces during walking. *Journal of Biomechanics* 42, 2357-2362.

- Fukubayashi, T., Kurosawa, H., 1980. The contact area and pressure distribution pattern of the knee: a study of normal and osteoarthrotic knee joints. *Acta Orthopaedica* 51, 871-879.
- Fukubayashi, T., Torzilli, P., Sherman, M., Warren, R., 1982. An in vitro biomechanical evaluation of anterior-posterior motion of the knee. Tibial displacement, rotation, and torque. *The Journal of Bone and Joint Surgery* 64, 258.
- Gagnon, D., Arjmand, N., Plamondon, A., Shirazi-Adl, A., Larivière, C., 2011. An improved multi-joint EMG-assisted optimization approach to estimate joint and muscle forces in a musculoskeletal model of the lumbar spine. *Journal of Biomechanics* 44, 1521–1529.
- Gao, B., Zheng, N.N., 2010. Alterations in three-dimensional joint kinematics of anterior cruciate ligament-deficient and-reconstructed knees during walking. *Clinical Biomechanics* 25, 222-229.
- Gok, H., Ergin, S., Yavuzer, G., 2002. Kinetic and kinematic characteristics of gait in patients with medial knee arthrosis. *Acta Orthopaedica Scandinavica* 73, 647-652.
- Gorton III, G.E., Hebert, D.A., Gannotti, M.E., 2009. Assessment of the kinematic variability among 12 motion analysis laboratories. *Gait & Posture* 29, 398-402.
- Goss, B.C., Howell, S.M., Hull, M., 1998. Quadriceps load aggravates and roofplasty mitigates active impingement of anterior cruciate ligament grafts against the intercondylar roof. *Journal of Orthopaedic Research* 16, 611-617.
- Groen, B., Geurts, M., Nienhuis, B., Duysens, J., 2012. Sensitivity of the OLGA and VCM models to erroneous marker placement: Effects on 3D-gait kinematics. *Gait & Posture* 35, 517-521.
- Grood, Hefzy, M., 1982. An analytical technique for modeling knee joint stiffness—Part I: Ligamentous forces. *Journal of Biomechanical Engineering* 104, 330.
- Grood, Suntay, W.J., 1983. A joint coordinate system for the clinical description of three-dimensional motions: application to the knee. *Journal of Biomechanical Engineering* 105, 136.
- Guccione, A.A., Felson, D.T., Anderson, J.J., Anthony, J.M., Zhang, Y., Wilson, P., Kelly-Hayes, M., Wolf, P.A., Kreger, B.E., Kannel, W.B., 1994. The effects of specific medical

- conditions on the functional limitations of elders in the Framingham Study. *American Journal of Public Health* 84, 351-358.
- Harding, G.T., Hubley-Kozey, C.L., Dunbar, M.J., Stanish, W.D., Astephen Wilson, J.L., 2012. Body mass index affects knee joint mechanics during gait differently with and without moderate knee osteoarthritis. *Osteoarthritis and Cartilage*.
- Heegaard, J., Leyvraz, P., Curnier, A., Rakotomanana, L., Huiskes, R., 1995. The biomechanics of the human patella during passive knee flexion. *Journal of Biomechanics* 28, 1265-1279.
- Heegaard, J., Leyvraz, P., Hovey, C., 2001. A computer model to simulate patellar biomechanics following total knee replacement: the effects of femoral component alignment. *Clinical Biomechanics* 16, 415-423.
- Hefzy, M., Jackson, W., Saddemi, S., Hsieh, Y.F., 1992. Effects of tibial rotations on patellar tracking and patello-femoral contact areas. *Journal of biomedical engineering* 14, 329-343.
- Hefzy, M., Yang, H., 1993. A three-dimensional anatomical model of the human patello-femoral joint, for the determination of patello-femoral motions and contact characteristics. *Journal of biomedical engineering* 15, 289-302.
- Heiden, T.L., Lloyd, D.G., Ackland, T.R., 2009. Knee joint kinematics, kinetics and muscle co-contraction in knee osteoarthritis patient gait. *Clinical Biomechanics* 24, 833-841.
- Hillman, 2003. *Interactive Functional Anatomy*, , London.
- Höher, J., Vogrin, T.M., Woo, S.L., 1999. In situ forces in the human posterior cruciate ligament in response to muscle loads: a cadaveric study. *Journal of Orthopaedic Research* 17, 763-768.
- Holden, J.P., Chou, G., Stanhope, S.J., 1997. Changes in knee joint function over a wide range of walking speeds. *Clinical Biomechanics* 12, 375-382.
- Hsieh, H., Walker, P., 1976. Stabilizing mechanisms of the loaded and unloaded knee joint. *The Journal of Bone and Joint Surgery* 58, 87.

- Huang, A., Hull, M., Howell, S.M., 2003. The level of compressive load affects conclusions from statistical analyses to determine whether a lateral meniscal autograft restores tibial contact pressure to normal: a study in human cadaveric knees. *Journal of Orthopaedic Research* 21, 459-464.
- Huberti, H., Hayes, W., Stone, J., Shybut, G., 1984. Force ratios in the quadriceps tendon and ligamentum patellae. *Journal of Orthopaedic Research* 2, 49-54.
- Hubley-Kozey, C.L., Hill, N.A., Rutherford, D.J., Dunbar, M.J., Stanish, W.D., 2009. Co-activation differences in lower limb muscles between asymptomatic controls and those with varying degrees of knee osteoarthritis during walking. *Clinical Biomechanics* 24, 407-414.
- Hubley-Kozey, C.L., Robbins, S.M., Rutherford, D.J., Stanish, W.D., 2013. Reliability of surface electromyographic recordings during walking in individuals with knee osteoarthritis. *Journal of Electromyography and Kinesiology*.
- Hungerford, D.S., Barry, M., 1979. Biomechanics of the patellofemoral joint. *Clinical Orthopaedics and Related Research* 144, 9.
- Hunt, Birmingham, T.B., Giffin, J.R., Jenkyn, T.R., 2006. Associations among knee adduction moment, frontal plane ground reaction force, and lever arm during walking in patients with knee osteoarthritis. *Journal of Biomechanics* 39, 2213-2220.
- Hunt, Smith, R.M., Torode, M., Keenan, A.M., 2001. Inter-segment foot motion and ground reaction forces over the stance phase of walking. *Clinical Biomechanics* 16, 592-600.
- Hunter, W., 1742. Of the structure and diseases of articulating cartilages, by William Hunter, surgeon. *Philosophical Transactions* 42, 514-521.
- Hurwitz, D.E., Sumner, D.R., Andriacchi, T.P., Sugar, D.A., 1998. Dynamic knee loads during gait predict proximal tibial bone distribution. *Journal of Biomechanics* 31, 423-430.
- Inaba, H., Arai, M., Watanabe, W., 1990. Influence of the varus—valgus instability on the contact of the femoro tibial joint. *ARCHIVE: Proceedings of the Institution of Mechanical Engineers, Part H: Journal of Engineering in Medicine* 1989-1996 (vols 203-210) 204, 61-64.

- Ingman, A., Ghosh, P., Taylor, T., 1974. Variation of collagenous and non-collagenous proteins of human knee joint menisci with age and degeneration. *Gerontology* 20, 212-223.
- Julkunen, P., Wilson, W., Jurvelin, J.S., Rieppo, J., Qu, C.J., Lammi, M.J., Korhonen, R.K., 2008. Stress-relaxation of human patellar articular cartilage in unconfined compression: prediction of mechanical response by tissue composition and structure. *Journal of Biomechanics* 41, 1978-1986.
- Kadaba, M.P., Ramakrishnan, H., Wootten, M., 1990. Measurement of lower extremity kinematics during level walking. *Journal of Orthopaedic Research* 8, 383-392.
- Kålund, S., Sinkjær, T., Arendt-Nielsen, L., Simonsen, O., 1990. Altered timing of hamstring muscle action in anterior cruciate ligament deficient patients. *The American Journal of Sports Medicine* 18, 245.
- Kanamori, A., Sakane, M., Zeminski, J., Rudy, T.W., Woo, S.L.Y., 2000. In-situ force in the medial and lateral structures of intact and ACL-deficient knees. *Journal of orthopaedic science* 5, 567-571.
- Kaufman, K.R., Hughes, C., Morrey, B.F., Morrey, M., An, K.-N., 2001. Gait characteristics of patients with knee osteoarthritis. *Journal of Biomechanics* 34, 907-915.
- Kennedy, J., Hawkins, R., Willis, R., 1977. Strain gauge analysis of knee ligaments. *Clinical Orthopaedics and Related Research* 129, 225-229.
- Kim, H.J., Fernandez, J.W., Akbarshahi, M., Walter, J.P., Fregly, B.J., Pandy, M.G., 2009. Evaluation of predicted knee joint muscle forces during gait using an instrumented knee implant. *Journal of Orthopaedic Research* 27, 1326-1331.
- Kinney, A.L., Besier, T.F., Silder, A., Delp, S.L., D'Lima, D.D., Fregly, B.J., 2013. Changes in in vivo knee contact forces through gait modification. *Journal of Orthopaedic Research* 31, 434-440.
- Knecht, S., Vanwanseele, B., Stüssi, E., 2006. A review on the mechanical quality of articular cartilage—Implications for the diagnosis of osteoarthritis. *Clinical Biomechanics* 21, 999-1012.

- Koo, S., Rylander, J.H., Andriacchi, T.P., 2011. Knee joint kinematics during walking influences the spatial cartilage thickness distribution in the knee. *Journal of Biomechanics*.
- Kozanek, M., Hosseini, A., Liu, F., Van de Velde, S.K., Gill, T.J., Rubash, H.E., Li, G., 2009. Tibiofemoral kinematics and condylar motion during the stance phase of gait. *Journal of Biomechanics* 42, 1877-1884.
- Krause, W., Pope, M., Johnson, R., Wilder, D., 1976. Mechanical changes in the knee after meniscectomy. *The Journal of Bone and Joint Surgery* 58, 599.
- Kumar, D., Manal, K.T., Rudolph, K.S., 2012a. Knee joint loading during gait in healthy controls and individuals with knee osteoarthritis. *Osteoarthritis and Cartilage*.
- Kumar, D., Rudolph, K.S., Manal, K.T., 2012b. EMG-driven modeling approach to muscle force and joint load estimations: Case study in knee osteoarthritis. *Journal of Orthopaedic Research* 30, 377-383.
- Kurosawa, H., FUKUBAYASHI, T., NAKAJIMA, H., 1980. Load-bearing mode of the knee joint: physical behavior of the knee joint with or without menisci. *Clinical Orthopaedics and Related Research* 149, 283.
- Kutzner, I., Damm, P., Heinlein, B., Dymke, J., Graichen, F., Bergmann, G., 2011. The effect of laterally wedged shoes on the loading of the medial knee compartment-in vivo measurements with instrumented knee implants. *Journal of Orthopaedic Research* 29, 1910-1915.
- Kutzner, I., Heinlein, B., Graichen, F., Bender, A., Rohlmann, A., Halder, A., Beier, A., Bergmann, G., 2010. Loading of the knee joint during activities of daily living measured in vivo in five subjects. *Journal of Biomechanics* 43, 2164.
- Lafortune, M., Cavanagh, P., Sommer III, H., Kalenak, A., 1992. Three-dimensional kinematics of the human knee during walking. *Journal of Biomechanics* 25, 347-357.
- Lass, P., Kaalund, S., Iefevre, S., Arendt-Nielsen, L., Sinkjæ, T., Simonsen, O., 1991. Muscle coordination following rupture of the anterior cruciate ligament: electromyographic studies of 14 patients. *Acta Orthopaedica* 62, 9-14.

- Lawrence, R.C., Felson, D.T., Helmick, C.G., Arnold, L.M., Choi, H., Deyo, R.A., Gabriel, S., Hirsch, R., Hochberg, M.C., Hunder, G.G., 2008. Estimates of the prevalence of arthritis and other rheumatic conditions in the United States: Part II. *Arthritis & Rheumatism* 58, 26-35.
- Leigh, R.J., Pohl, M.B., Ferber, R., 2013. Does tester experience influence the reliability with which 3D gait kinematics are collected in healthy adults? *Physical Therapy in Sport*.
- Lewallen, D.G., Riegger, C.L., Myers, E.R., Hayes, W.C., 1990. Effects of retinacular release and tibial tubercle elevation in patellofemoral degenerative joint disease. *Journal of Orthopaedic Research* 8, 856-862.
- Lewek, M.D., Rudolph, K.S., Snyder-Mackler, L., 2004. Control of frontal plane knee laxity during gait in patients with medial compartment knee osteoarthritis. *Osteoarthritis and Cartilage* 12, 745-751.
- Li, G., Gill, T.J., DeFrate, L.E., Zayontz, S., Glatt, V., Zarins, B., 2002a. Biomechanical consequences of PCL deficiency in the knee under simulated muscle loads—an in vitro experimental study. *Journal of Orthopaedic Research* 20, 887-892.
- Li, G., Kozanek, M., Hosseini, A., Liu, F., Velde, S.K.V., Rubash, H.E., 2009. New fluoroscopic imaging technique for investigation of 6DOF knee kinematics during treadmill gait. *Journal of Orthopaedic Surgery and Research* 4, 1-5.
- Li, G., Rudy, T., Sakane, M., Kanamori, A., Ma, C., Woo, S.L.Y., 1999. The importance of quadriceps and hamstring muscle loading on knee kinematics and in-situ forces in the ACL. *Journal of Biomechanics* 32, 395-400.
- Li, G., Rudy, T.W., Allen, C., Sakane, M., Woo, S.L., 1998. Effect of combined axial compressive and anterior tibial loads on in situ forces in the anterior cruciate ligament: a porcine study. *Journal of Orthopaedic Research* 16, 122-127.
- Li, G., Zayontz, S., Most, E., DeFrate, L.E., Suggs, J.F., Rubash, H.E., 2004. In situ forces of the anterior and posterior cruciate ligaments in high knee flexion: an in vitro investigation. *Journal of Orthopaedic Research* 22, 293-297.
- Lieb, F.J., Perry, J., 1971. Quadriceps function: an electromyographic study under isometric conditions. *The Journal of Bone and Joint Surgery* 53, 749.

- Limbird, T.J., Shiavi, R., Frazer, M., Borra, H., 1988. EMG profiles of knee joint musculature during walking: changes induced by anterior cruciate ligament deficiency. *Journal of Orthopaedic Research* 6, 630-638.
- Lin, Y.C., Walter, J.P., Banks, S.A., Pandy, M.G., Fregly, B.J., 2010. Simultaneous prediction of muscle and contact forces in the knee during gait. *Journal of Biomechanics* 43, 945-952.
- Liu, W., Maitland, M.E., 2000. The effect of hamstring muscle compensation for anterior laxity in the ACL-deficient knee during gait. *Journal of Biomechanics* 33, 871-879.
- Lloyd, D.G., Buchanan, T.S., 2001. Strategies of muscular support of varus and valgus isometric loads at the human knee. *Journal of Biomechanics* 34, 1257-1267.
- Losina, E., Thornhill, T.S., Rome, B.N., Wright, J., Katz, J.N., 2012. The dramatic increase in total knee replacement utilization rates in the United States cannot be fully explained by growth in population size and the obesity epidemic. *The Journal of Bone & Joint Surgery* 94, 201-207.
- Maquet, P.G., Van De Berg, A.J., Simonet, J., 1975. Femorotibial weight-bearing areas. Experimental determination. *The Journal of Bone and Joint Surgery* 57, 766.
- Markolf, K., Mensch, J., Amstutz, H., 1976. Stiffness and laxity of the knee--the contributions of the supporting structures. A quantitative in vitro study. *The Journal of Bone and Joint Surgery* 58, 583.
- Markolf, K.L., Bargar, W.L., Shoemaker, S.C., Amstutz, H.C., 1981. The role of joint load in knee stability. *The Journal of bone and joint surgery. American volume* 63, 570.
- Markolf, K.L., Burchfield, D.M., Shapiro, M.M., Davis, B.R., Finerman, G.A.M., Slauterbeck, J.L., 1996. Biomechanical consequences of replacement of the anterior cruciate ligament with a patellar ligament allograft. Part I: insertion of the graft and anterior-posterior testing. *The Journal of Bone and Joint Surgery* 78, 1720.
- Markolf, K.L., O'Neill, G., Jackson, S.R., McAllister, D.R., 2004. Effects of applied quadriceps and hamstrings muscle loads on forces in the anterior and posterior cruciate ligaments. *The American Journal of Sports Medicine* 32, 1144.

- Markolf, K.L., Willems, M.J., Jackson, S.R., Finerman, G.A.M., 1998. In situ calibration of miniature sensors implanted into the anterior cruciate ligament. Part I: Strain measurements. *Journal of Orthopaedic Research* 16, 455-463.
- Marouane, H., Shirazi-Adl, A., Adouni, M., 2013. Knee joint passive stiffness and moment in sagittal and frontal planes markedly increase with compression. *Computer Methods in Biomechanics and Biomedical Engineering*, 1-12.
- Mason, J., Leszko, F., Johnson, T., Komistek, R., 2008. Patellofemoral joint forces. *Journal of Biomechanics* 41, 2337-2348.
- Matsuda, S., Ishinishi, T., White, S.E., Whiteside, L.A., 1997. Patellofemoral joint after total knee arthroplasty: effect on contact area and contact stress. *The Journal of Arthroplasty* 12, 790-797.
- McGill, S.M., Norman, R.W., 1986. Partitioning of the L4-L5 dynamic moment into disc, ligamentous, and muscular components during lifting. *Spine (Phila Pa 1976)* 11, 666-678.
- McGowan, C., Kram, R., Neptune, R., 2009. Modulation of leg muscle function in response to altered demand for body support and forward propulsion during walking. *Journal of Biomechanics* 42, 850-856.
- Meachim, G., Bentley, G., 1978. Horizontal splitting in patellar articular cartilage. *Arthritis & Rheumatism* 21, 669-674.
- Mesfar, W., Shirazi-Adl, A., 2005. Biomechanics of the knee joint in flexion under various quadriceps forces. *The knee* 12, 424-434.
- Mesfar, W., Shirazi-Adl, A., 2006a. Biomechanics of changes in ACL and PCL material properties or prestrains in flexion under muscle force-implications in ligament reconstruction. *Computer Methods in Biomechanics and Biomedical Engineering* 9, 201.
- Mesfar, W., Shirazi-Adl, A., 2006b. Knee joint mechanics under quadriceps-hamstrings muscle forces are influenced by tibial restraint. *Clinical Biomechanics* 21, 841-848.
- Mesfar, W., Shirazi-Adl, A., 2008a. Computational biomechanics of knee joint in open kinetic chain extension exercises. *Computer Methods in Biomechanics and Biomedical Engineering* 11, 55.

- Mesfar, W., Shirazi-Adl, A., 2008b. Knee joint biomechanics in open-kinetic-chain flexion exercises. *Clinical Biomechanics* 23, 477-482.
- Messier, S., Legault, C., Loeser, R., Van Arsdale, S., Davis, C., Ettinger, W., DeVita, P., 2011. Does high weight loss in older adults with knee osteoarthritis affect bone-on-bone joint loads and muscle forces during walking? *Osteoarthritis and Cartilage* 19, 272-280.
- Meyer, A.J., D'Lima, D.D., Besier, T.F., Lloyd, D.G., Colwell, C.W., Jr., Fregly, B.J., 2013. Are external knee load and EMG measures accurate indicators of internal knee contact forces during gait? *Journal of Orthopaedic Research* 31, 921-929.
- Meyer, E.G., Haut, R.C., 2005. Excessive compression of the human tibio-femoral joint causes ACL rupture. *Journal of Biomechanics* 38, 2311-2316.
- Meyer, E.G., Haut, R.C., 2008. Anterior cruciate ligament injury induced by internal tibial torsion or tibiofemoral compression. *Journal of Biomechanics* 41, 3377-3383.
- Mizuno, Y., Kumagai, M., Mattessich, S.M., Elias, J.J., Ramrattan, N., Cosgarea, A.J., Chao, E., 2001. Q angle influences tibiofemoral and patellofemoral kinematics. *Journal of Orthopaedic Research* 19, 834-840.
- Moglo, K., Shirazi-Adl, A., 2003a. Biomechanics of passive knee joint in drawer: load transmission in intact and ACL-deficient joints. *The knee* 10, 265-276.
- Moglo, K., Shirazi-Adl, A., 2003b. On the coupling between anterior and posterior cruciate ligaments, and knee joint response under anterior femoral drawer in flexion: a finite element study. *Clinical Biomechanics* 18, 751-759.
- Moglo, K., Shirazi-Adl, A., 2005. Cruciate coupling and screw-home mechanism in passive knee joint during extension-flexion. *Journal of Biomechanics* 38, 1075-1083.
- Mokhtarzadeh, H., Yeow, C.H., Hong Goh, J.C., Oetomo, D., Malekipour, F., Lee, P.V.-S., 2013. Contributions of the Soleus and Gastrocnemius muscles to the anterior cruciate ligament loading during single-leg landing. *Journal of Biomechanics* 46, 1913-1920.
- Mommersteeg, T., Blankevoort, L., Huiskes, R., Kooloos, J., Kauer, J., 1996a. Characterization of the mechanical behavior of human knee ligaments: a numerical-experimental approach. *Journal of Biomechanics* 29, 151-160.

- Mommersteeg, T., Huiskes, R., Blankevoort, L., Kooloos, J., Kauer, J., 1997. An inverse dynamics modeling approach to determine the restraining function of human knee ligament bundles. *Journal of Biomechanics* 30, 139-146.
- Mommersteeg, T., Huiskes, R., Blankevoort, L., Kooloos, J., Kauer, J., Maathuis, P., 1996b. A global verification study of a quasi-static knee model with multi-bundle ligaments*. *Journal of Biomechanics* 29, 1659-1664.
- Mononen, M., Julkunen, P., Töyräs, J., Jurvelin, J., Kiviranta, I., Korhonen, R., 2011. Alterations in structure and properties of collagen network of osteoarthritic and repaired cartilage modify knee joint stresses. *Biomechanics and Modeling in Mechanobiology* 10, 357-369.
- Mononen, M., Mikkola, M., Julkunen, P., Ojala, R., Nieminen, M., Jurvelin, J., Korhonen, R., 2012. Effect of superficial collagen patterns and fibrillation of femoral articular cartilage on knee joint mechanics—A 3D finite element analysis. *Journal of Biomechanics* 45, 579-587.
- Mononen, M.E., Jurvelin, J.S., Korhonen, R.K., 2013a. Effects of Radial Tears and Partial Meniscectomy of Lateral Meniscus on the Knee Joint Mechanics during the Stance Phase of the Gait Cycle—A 3D Finite Element Study. *Journal of Orthopaedic Research*.
- Mononen, M.E., Jurvelin, J.S., Korhonen, R.K., 2013b. Implementation of a gait cycle loading into healthy and meniscectomised knee joint models with fibril-reinforced articular cartilage. *Computer Methods in Biomechanics and Biomedical Engineering*, 1-12.
- More, R.C., Karras, B.T., Neiman, R., Fritschy, D., Woo, S.L.Y., Daniel, D.M., 1993. Hamstrings—an anterior cruciate ligament protagonist. *The American Journal of Sports Medicine* 21, 231.
- Mow, V., Kuei, S., Lai, W., Armstrong, C., 1980. Biphasic creep and stress relaxation of articular cartilage in compression: theory and experiments. *Journal of Biomechanical Engineering* 102, 73-84.
- Mündermann, A., Dyrby, C.O., Andriacchi, T.P., 2005. Secondary gait changes in patients with medial compartment knee osteoarthritis: increased load at the ankle, knee, and hip during walking. *Arthritis & Rheumatism* 52, 2835-2844.

- Murphy, L., Schwartz, T.A., Helmick, C.G., Renner, J.B., Tudor, G., Koch, G., Dragomir, A., Kalsbeek, W.D., Luta, G., Jordan, J.M., 2008. Lifetime risk of symptomatic knee osteoarthritis. *Arthritis Care & Research* 59, 1207-1213.
- Neptune, R., Zajac, F., Kautz, S., 2004. Muscle force redistributes segmental power for body progression during walking. *Gait & Posture* 19, 194-205.
- Neptune, R.R., Kautz, S., Zajac, F., 2001. Contributions of the individual ankle plantar flexors to support, forward progression and swing initiation during walking. *Journal of Biomechanics* 34, 1387-1398.
- Nester, C., Van Der Linden, M., Bowker, P., 2003. Effect of foot orthoses on the kinematics and kinetics of normal walking gait. *Gait & Posture* 17, 180-187.
- O'Connor, J.J., 1993. Can muscle co-contraction protect knee ligaments after injury or repair? *Journal of Bone & Joint Surgery, British Volume* 75, 41-48.
- Obeid, E., Adams, M., Newman, J., 1994. Mechanical properties of articular cartilage in knees with unicompartamental osteoarthritis. *Journal of Bone & Joint Surgery, British Volume* 76, 315-319.
- Oliveria, S.A., Felson, D.T., Reed, J.I., Cirillo, P.A., Walker, A.M., 1995. Incidence of symptomatic hand, hip, and knee osteoarthritis among patients in a health maintenance organization. *Arthritis & Rheumatism* 38, 1134-1141.
- Pandy, M.G., Shelburne, K.B., 1997. Dependence of cruciate-ligament loading on muscle forces and external load. *Journal of Biomechanics* 30, 1015-1024.
- Pena, E., Calvo, B., Martinez, M., Palanca, D., Doblaré, M., 2005. Finite element analysis of the effect of meniscal tears and meniscectomies on human knee biomechanics. *Clinical Biomechanics* 20, 498-507.
- Perron, M., Malouin, F., Moffet, H., McFadyen, B.J., 2000. Three-dimensional gait analysis in women with a total hip arthroplasty. *Clinical Biomechanics* 15, 504-515.
- Perry, J., 1992. Gait analysis: normal and pathological function. *Journal of Pediatric Orthopaedics* 12, 815.

- Piazza, S.J., 2006. Muscle-driven forward dynamic simulations for the study of normal and pathological gait. *Journal of NeuroEngineering and Rehabilitation* 3, 5.
- Pohl, M.B., Lloyd, C., Ferber, R., 2010. Can the reliability of three-dimensional running kinematics be improved using functional joint methodology? *Gait & Posture* 32, 559-563.
- Proctor, C., Schmidt, M., Whipple, R., Kelly, M., Mow, V., 1989. Material properties of the normal medial bovine meniscus. *Journal of Orthopaedic Research* 7, 771-782.
- Radin, E.L., Rose, R.M., 1986. Role of subchondral bone in the initiation and progression of cartilage damage. *Clinical Orthopaedics and Related Research* 213, 34-40.
- Ramaniraka, N., Terrier, A., Theumann, N., Siegrist, O., 2005. Effects of the posterior cruciate ligament reconstruction on the biomechanics of the knee joint: a finite element analysis. *Clinical Biomechanics* 20, 434-442.
- Reilly, D.T., Martens, M., 1972. Experimental analysis of the quadriceps muscle force and patello-femoral joint reaction force for various activities. *Acta Orthopaedica Scandinavica* 43, 126.
- Reithmeier, E., Plitz, W., 1990. A theoretical and numerical approach to optimal positioning of the patellar surface replacement in a total knee endoprosthesis. *Journal of Biomechanics* 23, 883-885, 887-892.
- Rose, J., Ralston, H., Gamble, J.G., 1994. Energetics of walking. *Human walking*, 45–72.
- Russell, E.M., Hamill, J., 2011. Lateral wedges decrease biomechanical risk factors for knee osteoarthritis in obese women. *Journal of Biomechanics* 44, 2286-2291.
- Sakai, N., Luo, Z.P., Rand, J.A., An, K.N., 1996. Quadriceps forces and patellar motion in the anatomical model of the patellofemoral joint. *The knee* 3, 1-7.
- Sanford, B.A., Williams, J.L., Zucker-Levin, A.R., Mihalko, W.M., 2013. Tibiofemoral Joint Forces during the Stance Phase of Gait after ACL Reconstruction. *Open Journal of Biophysics* 3, 277.
- Sasaki, K., Neptune, R.R., 2010. Individual muscle contributions to the axial knee joint contact force during normal walking. *Journal of Biomechanics* 43, 2780-2784.

- Schmalz, T., Blumentritt, S., Drewitz, H., Freslier, M., 2006. The influence of sole wedges on frontal plane knee kinetics, in isolation and in combination with representative rigid and semi-rigid ankle-foot-orthoses. *Clinical Biomechanics* 21, 631-639.
- Schmitt, L.C., Rudolph, K.S., 2008. Muscle stabilization strategies in people with medial knee osteoarthritis: the effect of instability. *Journal of Orthopaedic Research* 26, 1180-1185.
- Seedhom, B., Hargreaves, D., 1979. Transmission of the load in the knee joint with special reference to the role of the menisci Part II: experimental results, discussion and conclusions. *ARCHIVE: Engineering in Medicine 1971-1988 (vols 1-17)* 8, 220-228.
- Sharma, L., Lou, C., Cahue, S., Dunlop, D.D., 2000. The mechanism of the effect of obesity in knee osteoarthritis: the mediating role of malalignment. *Arthritis & Rheumatism* 43, 568-575.
- Sharma, L., Song, J., Felson, D.T., Cahue, S., Shamiyeh, E., Dunlop, D.D., 2001. The role of knee alignment in disease progression and functional decline in knee osteoarthritis. *JAMA: the journal of the American Medical Association* 286, 188-195.
- Shelburne, K.B., Pandy, M.G., Anderson, F.C., Torry, M.R., 2004. Pattern of anterior cruciate ligament force in normal walking. *Journal of Biomechanics* 37, 797-805.
- Shelburne, K.B., Torry, M.R., Pandy, M.G., 2005. Muscle, ligament, and joint-contact forces at the knee during walking. *Medicine & Science in Sports & Exercise* 37, 1948.
- Shelburne, K.B., Torry, M.R., Pandy, M.G., 2006. Contributions of muscles, ligaments, and the ground reaction force to tibiofemoral joint loading during normal gait. *Journal of Orthopaedic Research* 24, 1983-1990.
- Shelburne, K.B., Torry, M.R., Steadman, J.R., Pandy, M.G., 2008. Effects of foot orthoses and valgus bracing on the knee adduction moment and medial joint load during gait. *Clinical Biomechanics* 23, 814-821.
- Shin, C.S., Chaudhari, A.M., Andriacchi, T.P., 2011. Valgus plus internal rotation moments increase anterior cruciate ligament strain more than either alone. *Med Sci Sports Exerc* 43, 1484-1491.

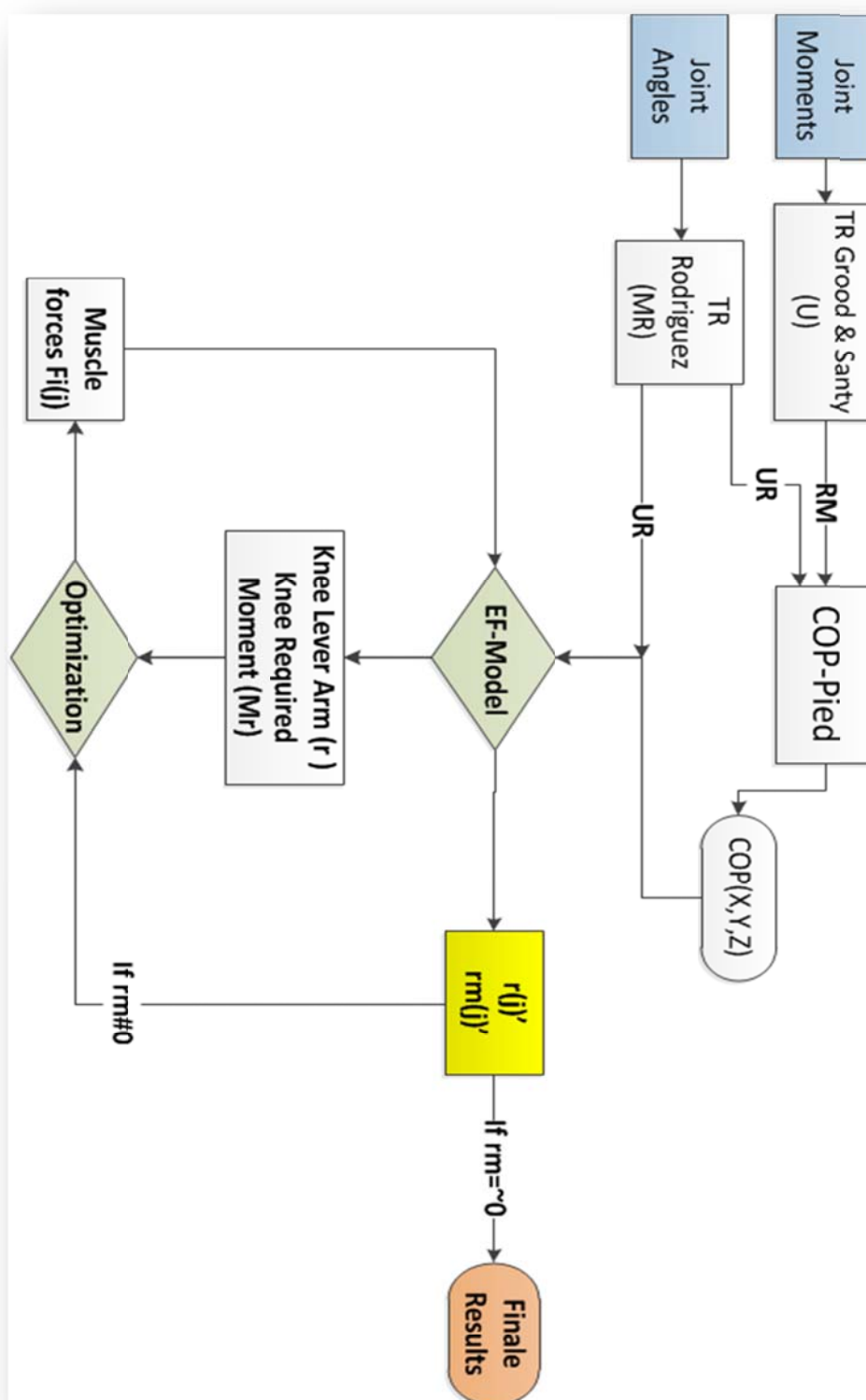
- Shirazi-Adl, A., Moglo, K., 2005. Effect of changes in cruciate ligaments pretensions on knee joint laxity and ligament forces. *Computer Methods in Biomechanics and Biomedical Engineering* 8, 17-24.
- Shirazi, R., Shirazi-Adl, A., 2005. Analysis of articular cartilage as a composite using nonlinear membrane elements for collagen fibrils. *Medical engineering & physics* 27, 827-835.
- Shirazi, R., Shirazi-Adl, A., 2009a. Analysis of partial meniscectomy and ACL reconstruction in knee joint biomechanics under a combined loading. *Clinical Biomechanics* 24, 755-761.
- Shirazi, R., Shirazi-Adl, A., 2009b. Computational biomechanics of articular cartilage of human knee joint: Effect of osteochondral defects. *Journal of Biomechanics* 42, 2458-2465.
- Shirazi, R., Shirazi-Adl, A., Hurtig, M., 2008. Role of cartilage collagen fibrils networks in knee joint biomechanics under compression. *Journal of Biomechanics* 41, 3340-3348.
- Shoemaker, S.C., Markolf, K., 1985. Effects of joint load on the stiffness and laxity of ligament-deficient knees. An in vitro study of the anterior cruciate and medial collateral ligaments. *The Journal of Bone and Joint Surgery* 67, 136.
- Shrive, N., O'CONNOR, J., Goodfellow, J., 1978. Load-bearing in the knee joint. *Clinical Orthopaedics and Related Research* 131, 279.
- Singerman, R., Berilla, J., Davy, D., 1995. Direct in vitro determination of the patellofemoral contact force for normal knees. *Journal of Biomechanical Engineering* 117, 8.
- Skaggs, D., Warden, W., Mow, V., 1994. Radial tie fibers influence the tensile properties of the bovine medial meniscus. *Journal of Orthopaedic Research* 12, 176-185.
- Spilker, R.L., Donzelli, P.S., Mow, V.C., 1992. A transversely isotropic biphasic finite element model of the meniscus. *Journal of Biomechanics* 25, 1027-1045.
- Stäubli, H.U., Schatzmann, L., Brunner, P., Rincón, L., Nolte, L.P., 1999. Mechanical tensile properties of the quadriceps tendon and patellar ligament in young adults. *The American Journal of Sports Medicine* 27, 27.
- Szczerbik, E., Kalinowska, M., 2011. The influence of knee marker placement error on evaluation of gait kinematic parameters. *Acta of Bioengineering and Biomechanics* 13, 43-46.

- Taylor , K.A., Cutcliffe , H.C., Queen, R.M., Terry, M.E., Utturkar, G.M., Spritzer, C.E., Garrett, W.E., DeFrate, L.E., 2011. Measurement of In Vivo ACL Elongation During Gait. . *57th Annual Meeting of Orthopaedic Research Society*. Long Beach USA.
- Terry, G.C., Hughston, J.C., Norwood, L.A., 1986. The anatomy of the iliopatellar band and iliotibial tract. *The American Journal of Sports Medicine* 14, 39.
- Thambyah, A., 2007. Contact stresses in both compartments of the tibiofemoral joint are similar even when larger forces are applied to the medial compartment. *The knee* 14, 336-338.
- Thomas, J.S., France, C.R., Sha, D., Vander Wiele, N., 2008. The influence of pain-related fear on peak muscle activity and force generation during maximal isometric trunk exertions. *Spine* 33, E342-E348.
- Van Eijden, T., Kouwenhoven, E., Verburg, J., Weijs, W., 1986. A mathematical model of the patellofemoral joint. *Journal of Biomechanics* 19, 219-223, 225-229.
- Vener, M.J., Thompson, R.C., Lewis Jr, J.L., Oegema, T.R., 1992. Subchondral damage after acute transarticular loading: an in vitro model of joint injury. *Journal of Orthopaedic Research* 10, 759-765.
- Walker, P.S., Erkiuan, M.J., 1975. The role of the menisci in force transmission across the knee. *Clinical Orthopaedics and Related Research* 109, 184.
- Walter, J.P., D'Lima, D.D., Colwell, C.W., Jr., Fregly, B.J., 2010. Decreased knee adduction moment does not guarantee decreased medial contact force during gait. *Journal of Orthopaedic Research* 28, 1348-1354.
- Wang, J.W., Kuo, K., Andriacchi, T., Galante, J., 1990. The influence of walking mechanics and time on the results of proximal tibial osteotomy. *The Journal of Bone and Joint Surgery* 72, 905.
- Warren, L.F., Marshall, J.L., Girgis, F., 1974. The prime static stabilizer of the medial side of the knee. *The Journal of Bone & Joint Surgery* 56, 665-674.
- Weidenhielm, L., Svensson, O., Broström, L., Mattsson, E., 1994. Adduction moment of the knee compared to radiological and clinical parameters in moderate medial osteoarthritis of the knee. In: 236

- Whittle, M.W., 1996. Clinical gait analysis: A review. *Human Movement Science* 15, 369-387.
- Winby, C., Gerus, P., Kirk, T., Lloyd, D., 2013. Correlation between EMG-based co-activation measures and medial and lateral compartment loads of the knee during gait. *Clinical Biomechanics* 28, 1014-1019.
- Winby, C., Lloyd, D., Besier, T., Kirk, T., 2009. Muscle and external load contribution to knee joint contact loads during normal gait. *Journal of Biomechanics* 42, 2294-2300.
- Woo, S.L.Y., Fox, R.J., Sakane, M., Livesay, G.A., Rudy, T.W., Fu, F.H., 1998. Biomechanics of the ACL: measurements of in situ force in the ACL and knee kinematics. *The knee* 5, 267-288.
- Yamaguchi G, A. Sawa, D. Moran, and, M.F., Winters, J., 1990. A survey of human musculotendon actuator parameters. IN Winters, J., Woo, a.S. (Eds.) *Multiple Muscle Systems*. New York
- Yamaguchi, G.T., Sawa , A.G.U., Moran , D.W., Fessler, M.J., Winters, J.M., 1990. A survey of human musculotendon actuator parameters. In: Springer-Verlag (Ed.) *Multiple Muscle Systems*. New York, Springer-Verlag, pp.717-773
- Yamaguchi, G.T., Zajac, F.E., 1989. A planar model of the knee joint to characterize the knee extensor mechanism. *Journal of Biomechanics* 22, 1-10.
- Yang, N.H., Canavan, P.K., Nayeb-Hashemi, H., Najafi, B., Vaziri, A., 2010. Protocol for constructing subject-specific biomechanical models of knee joint. *Computer Methods in Biomechanics and Biomedical Engineering* 13, 589-603.
- Yu, B., Stuart, M., Kienbacher, T., Growney, E., An, K., 1997. Valgus-varus motion of the knee in normal level walking and stair climbing. *Clinical Biomechanics* 12, 286-293.
- Zajac, F.E., Neptune, R.R., Kautz, S.A., 2002. Biomechanics and muscle coordination of human walking:: Part I: Introduction to concepts, power transfer, dynamics and simulations. *Gait & Posture* 16, 215-232.
- Zajac, F.E., Neptune, R.R., Kautz, S.A., 2003. Biomechanics and muscle coordination of human walking:: Part II: Lessons from dynamical simulations and clinical implications. *Gait & Posture* 17, 1-17.

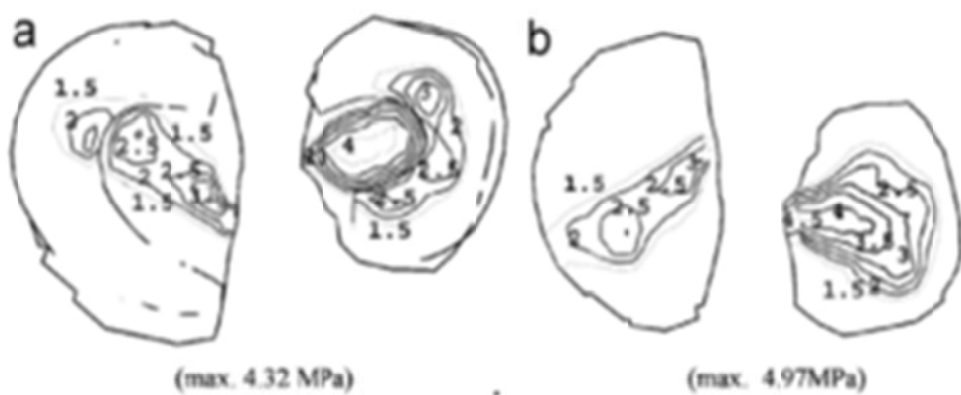
- Zeni Jr, J.A., Higginson, J.S., 2009. Differences in gait parameters between healthy subjects and persons with moderate and severe knee osteoarthritis: A result of altered walking speed? *Clinical biomechanics (Bristol, Avon)* 24, 372.
- Zhang, L.-Q., Shiavi, R.G., Limbird, T.J., Minorik, J.M., 2003. Six degrees-of-freedom kinematics of ACL deficient knees during locomotion—compensatory mechanism. *Gait & Posture* 17, 34-42.
- Zhao, D., Banks, S.A., Mitchell, K.H., D'Lima, D.D., Colwell, C.W., Fregly, B.J., 2007. Correlation between the knee adduction torque and medial contact force for a variety of gait patterns. *Journal of Orthopaedic Research* 25, 789-797.

ANNEXE 1 – Modèle itérative



ANNEXE 2 – Validation des propriétés matérielles

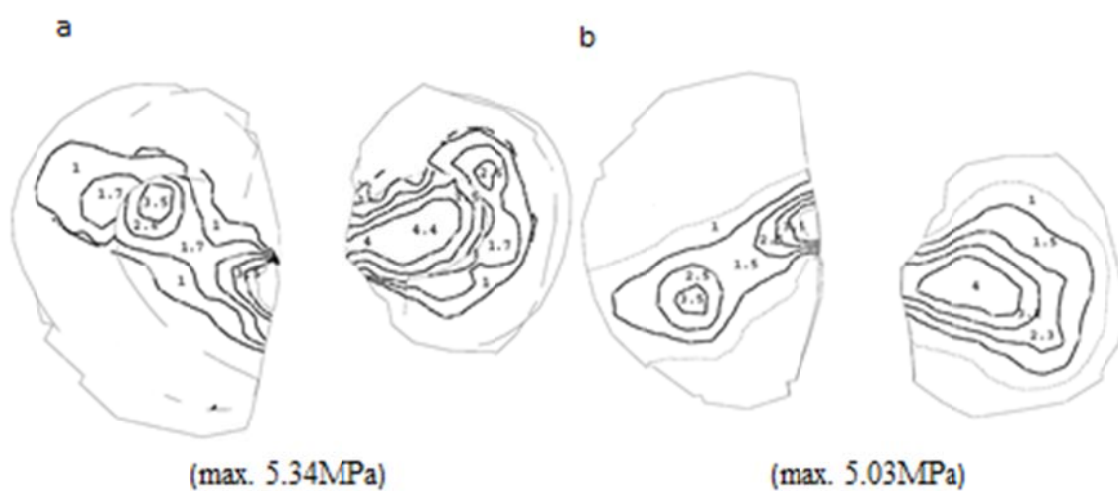
REF-2000N



(a)- Contact Pressure (MPa)

(b)-Pore Pressure (MPa)

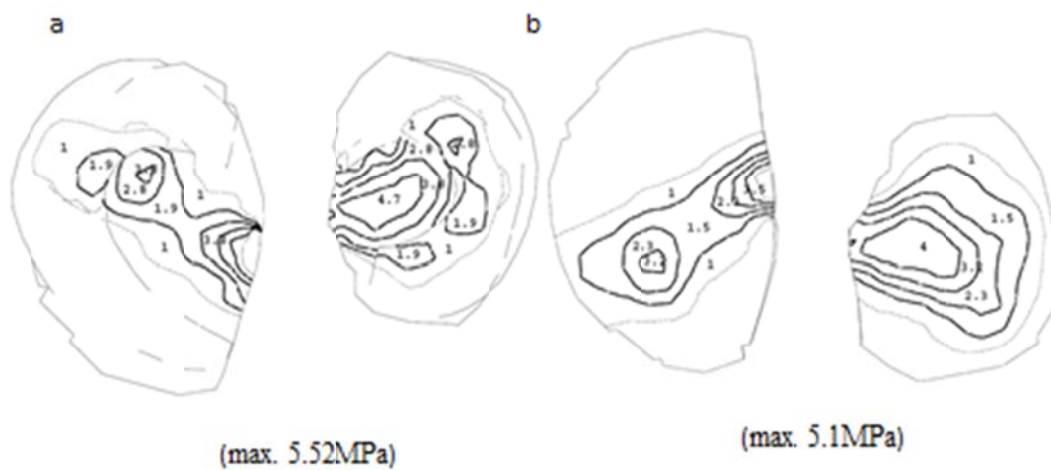
ELASTIQUE-2000N



(a)- Contact Pressure (MPa)

(b)-Pore Pressure (MPa)

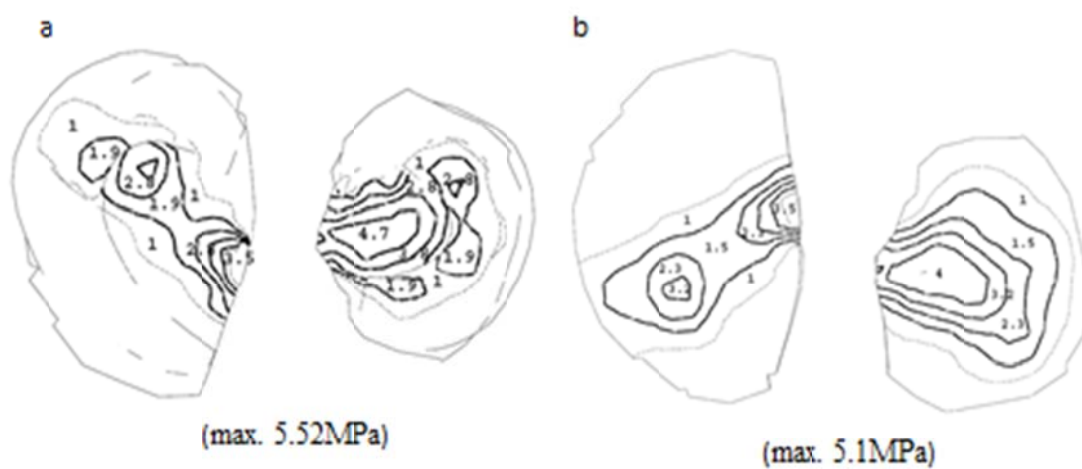
MIXTE-2000N



(a)- Contact Pressure (MPa)

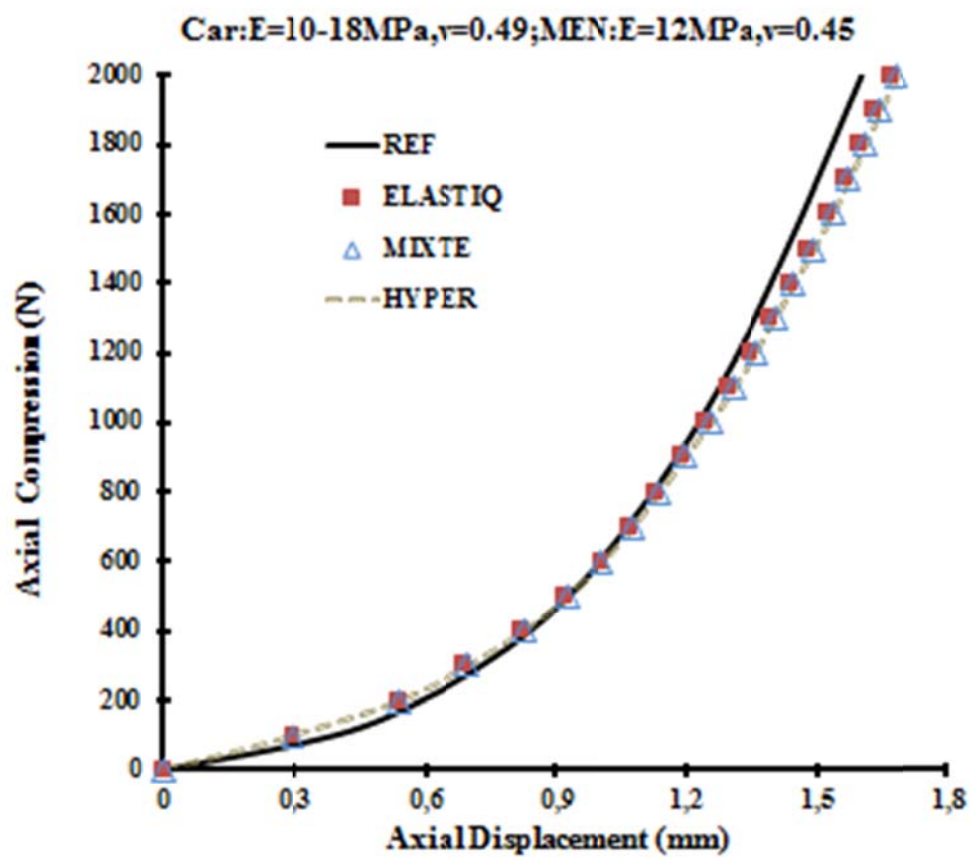
(b)-Pore Pressure (MPa)

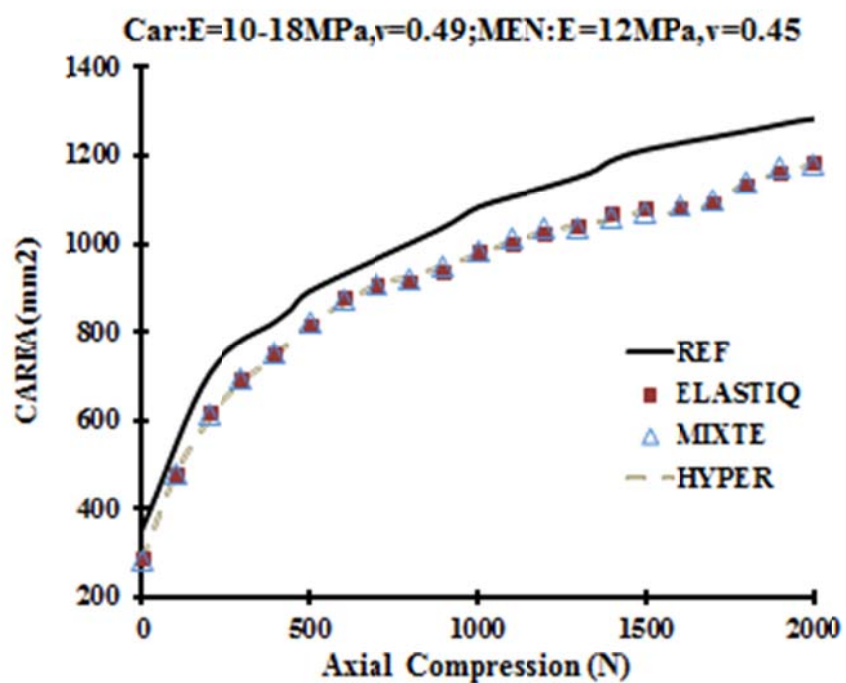
HYPER-2000N

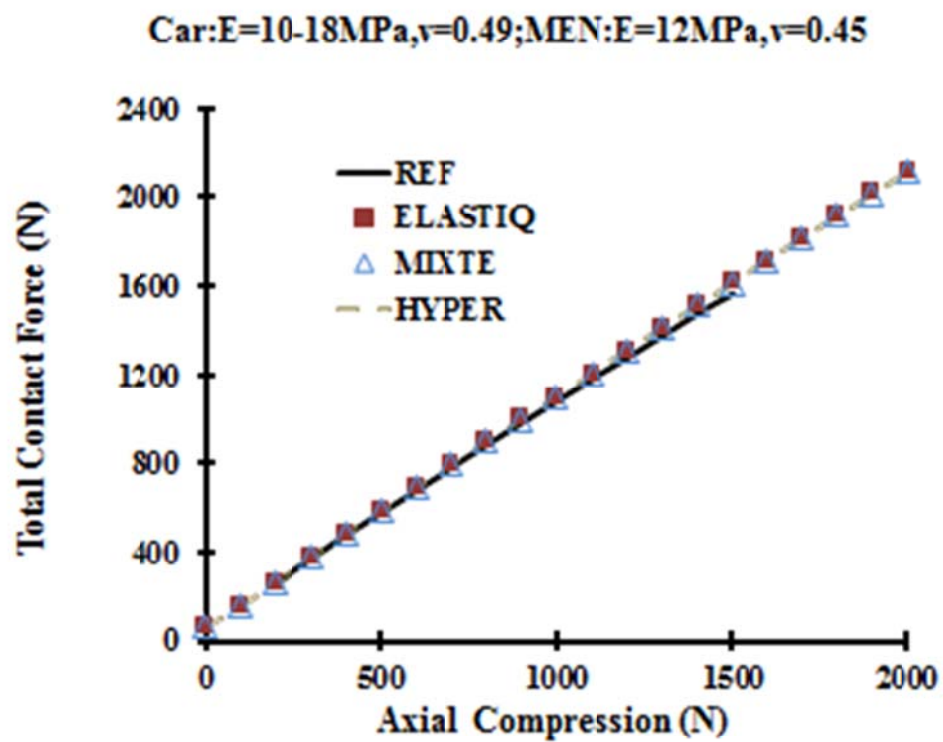


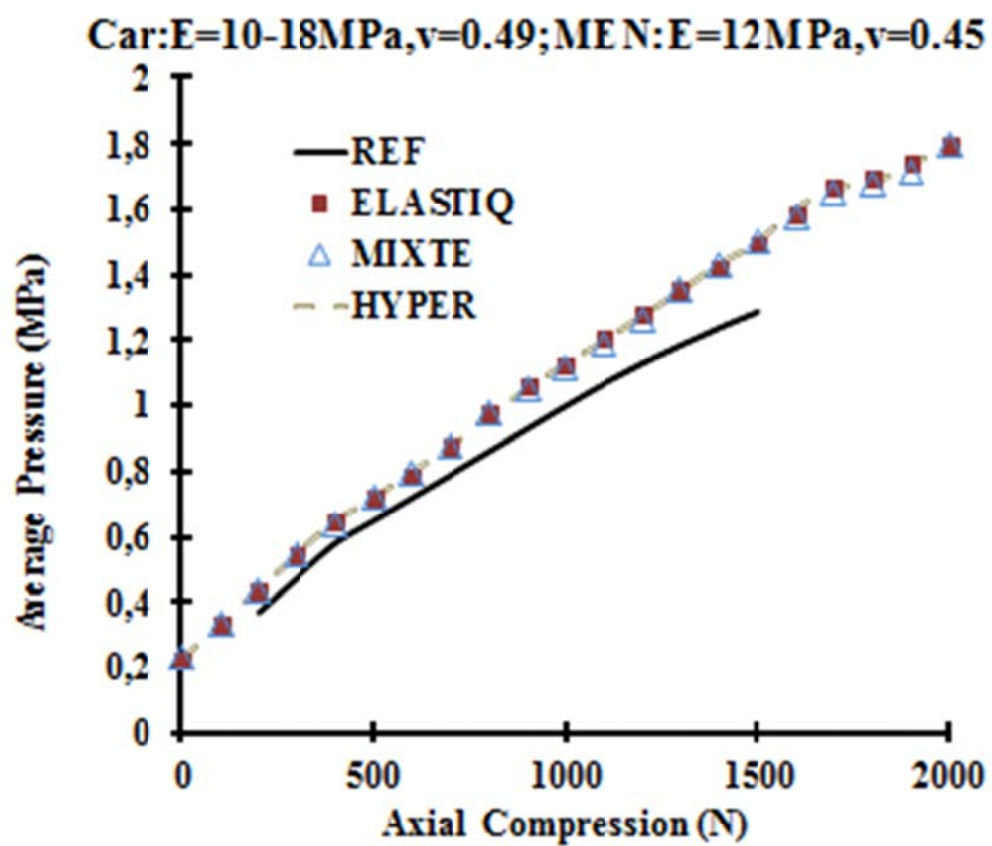
(a)- Contact Pressure (MPa)

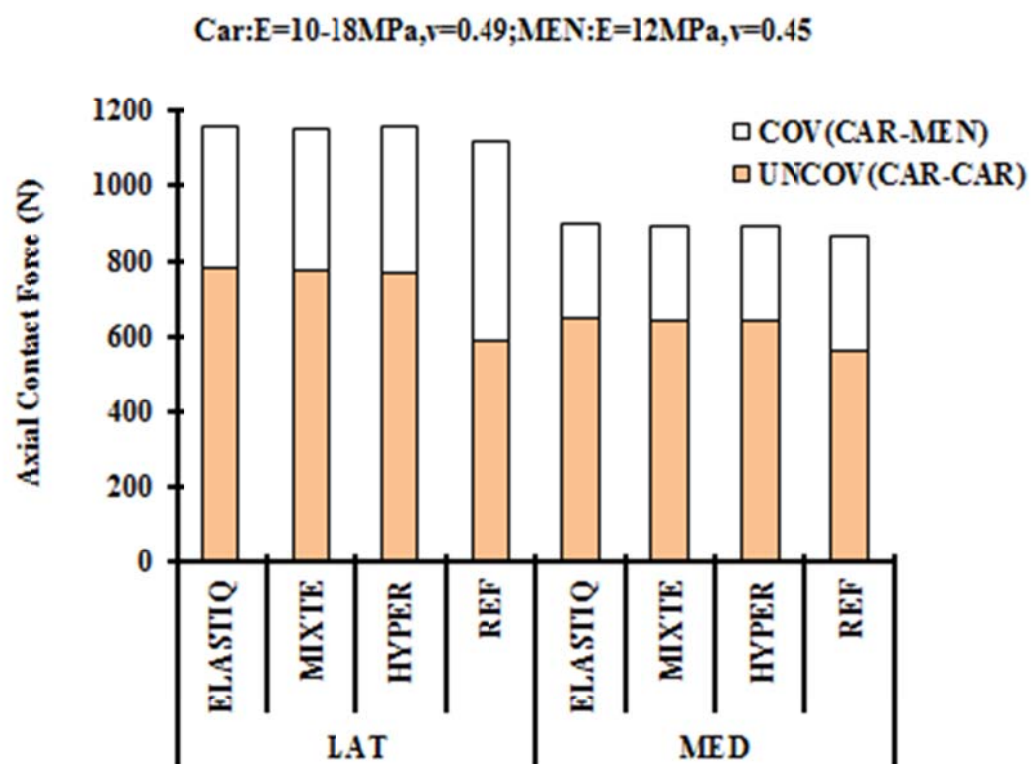
(b)-Pore Pressure (MPa)

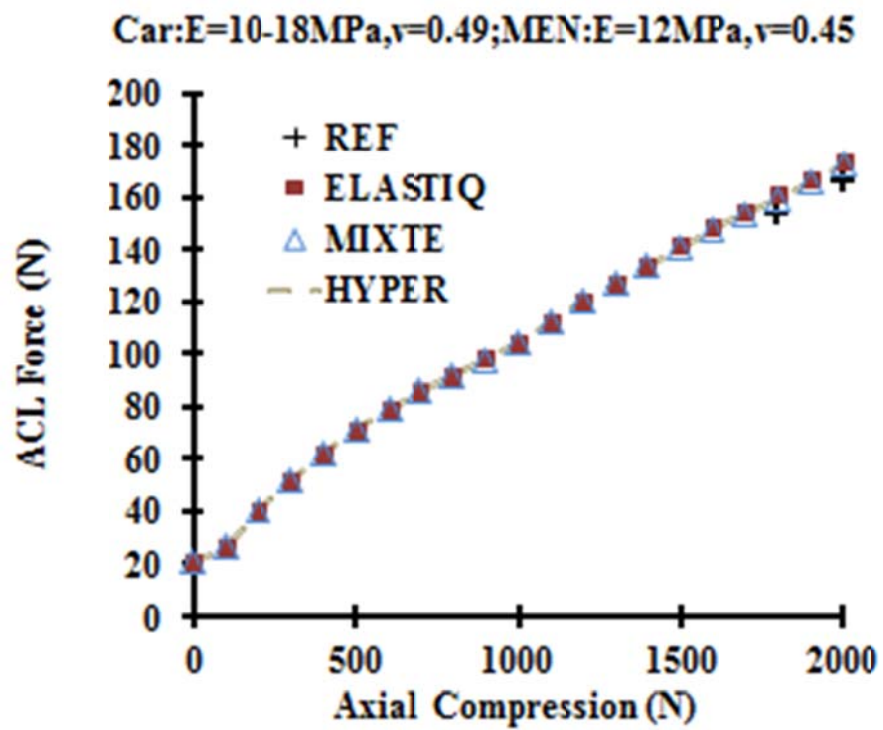


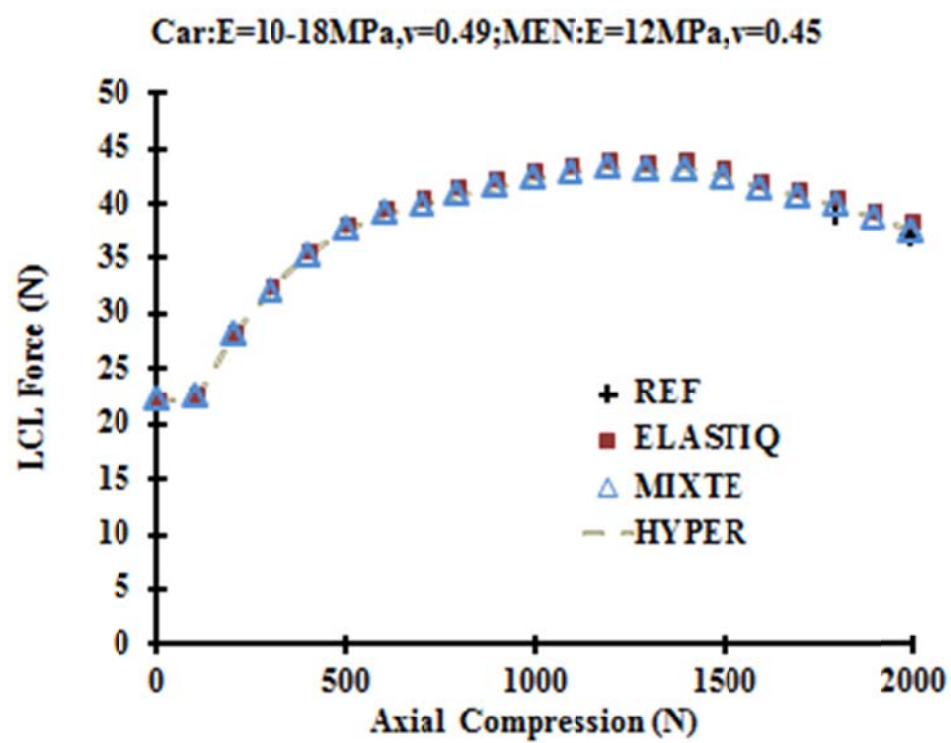


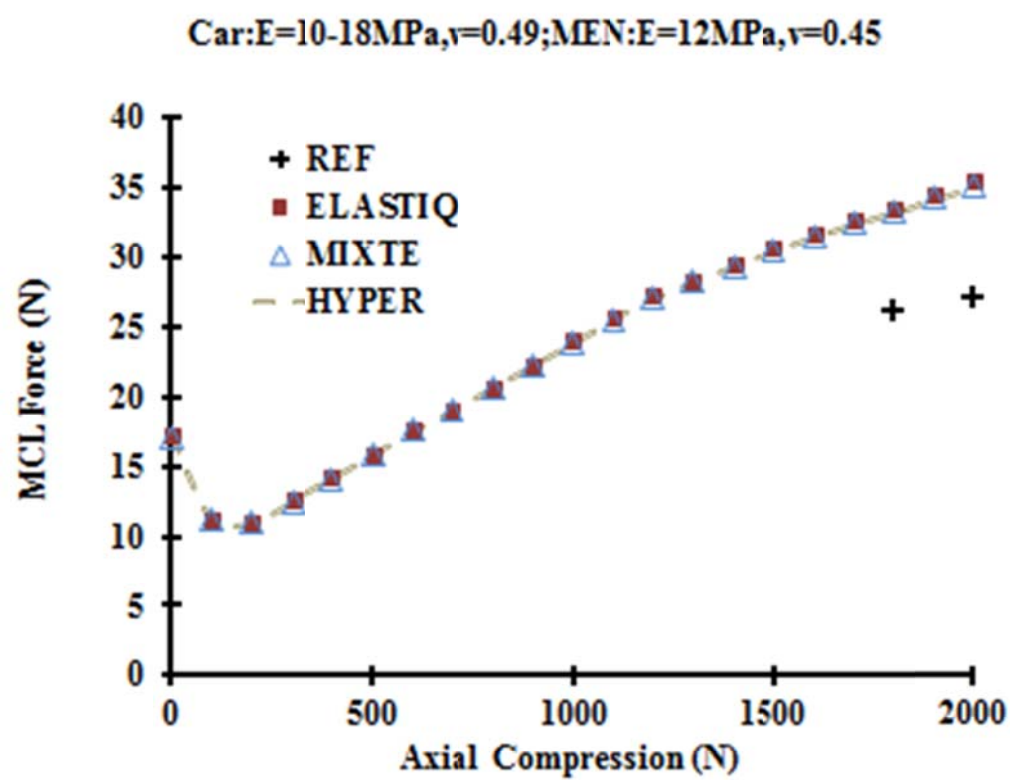


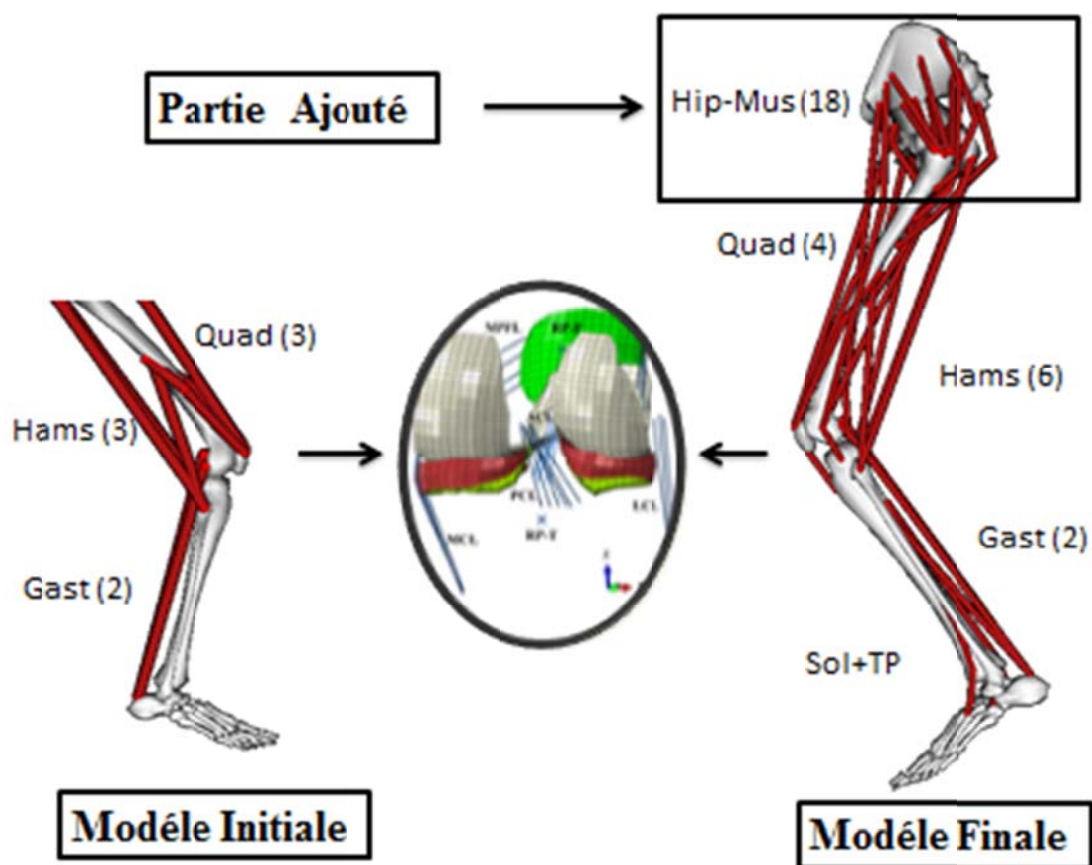


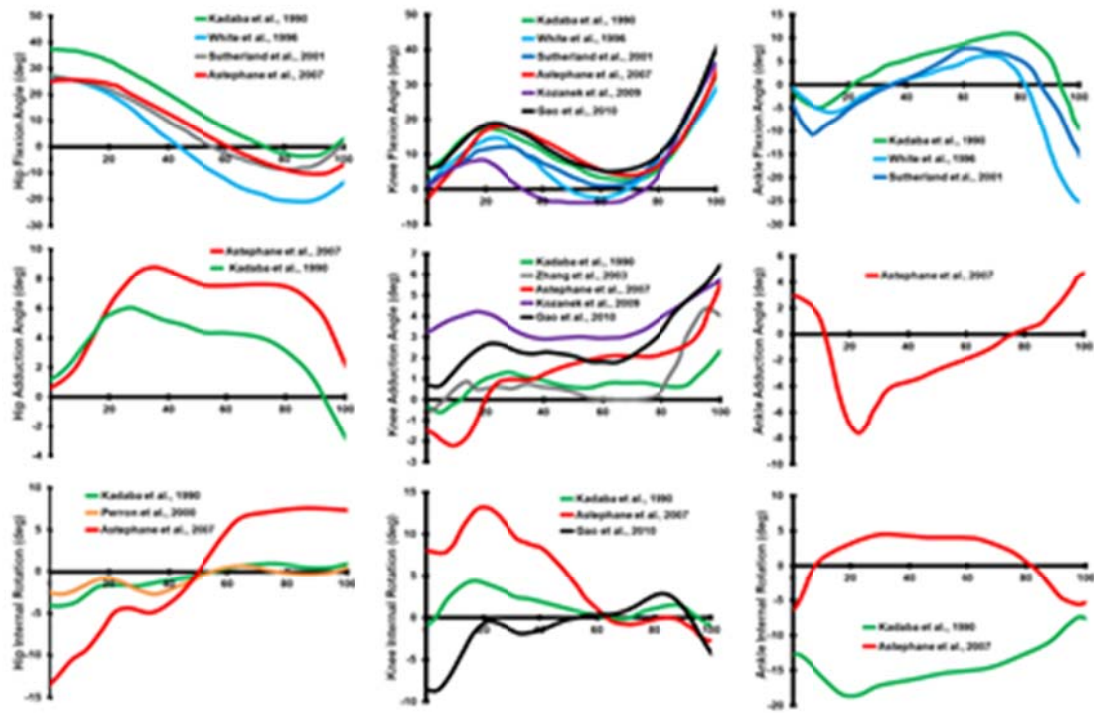




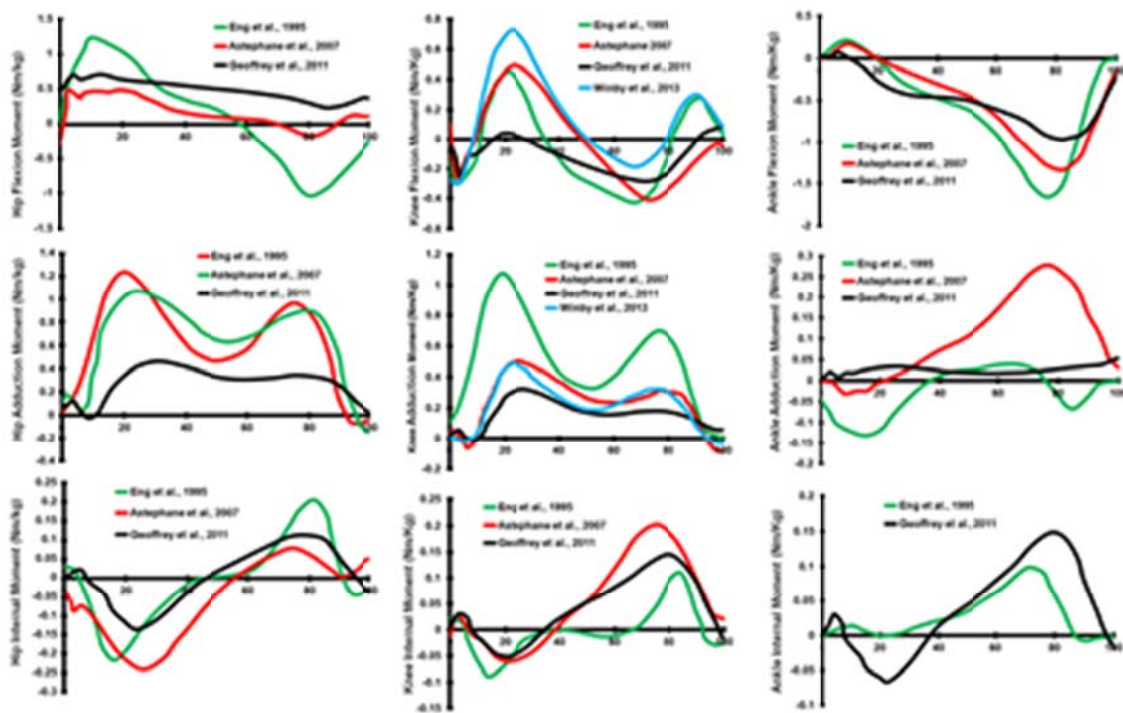




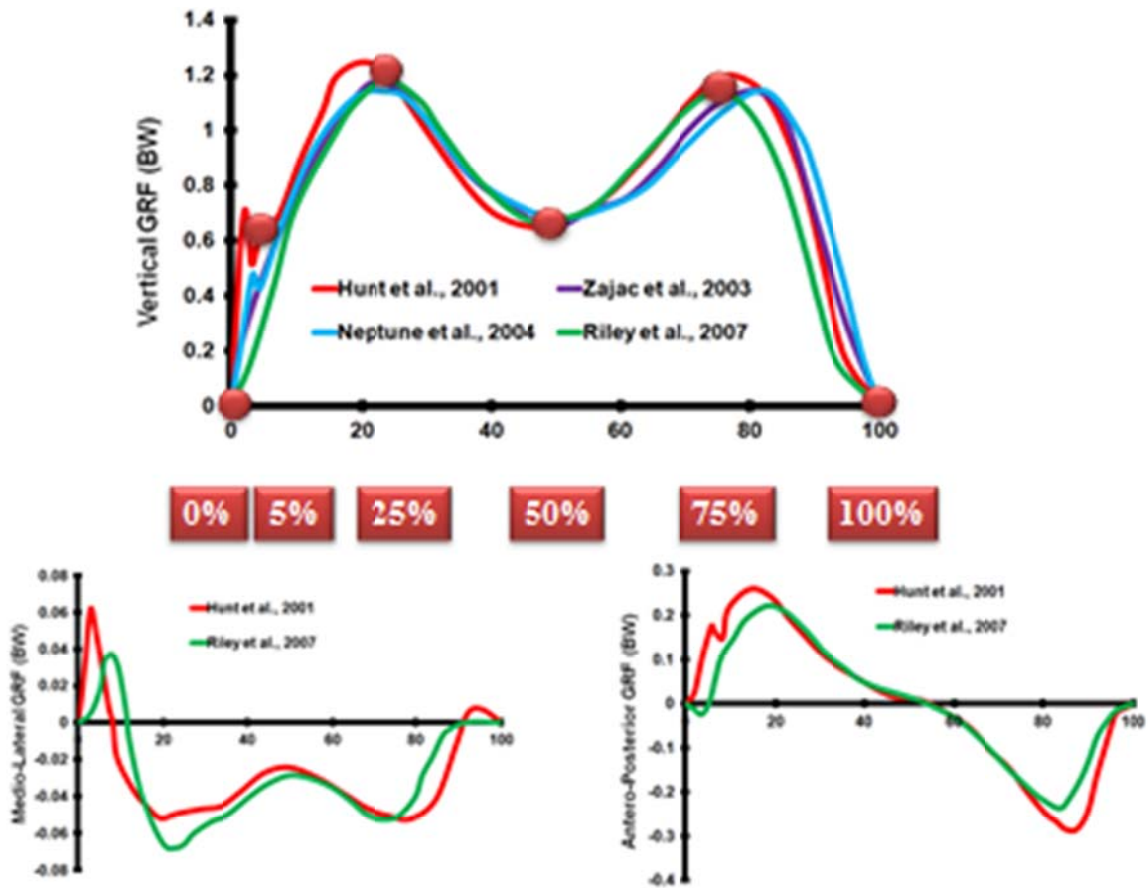




le travail utilisé comme input : **Astephane et al 2007**



le travail utilisé comme input : **Astephane et al 2007**



le travail utilisé comme input : **Hunt et al 2001**



$$[M_x] = \begin{pmatrix} \cos \alpha + (1 - \cos \alpha) n_1^2 & -n_1 \sin \alpha + (1 - \cos \alpha) n_1 n_2 & n_1 \sin \alpha + (1 - \cos \alpha) n_1 n_3 \\ n_2 \sin \alpha + (1 - \cos \alpha) n_1 n_2 & \cos \alpha + (1 - \cos \alpha) n_2^2 & -n_2 \sin \alpha + (1 - \cos \alpha) n_2 n_3 \\ -n_3 \sin \alpha + (1 - \cos \alpha) n_1 n_3 & n_3 \sin \alpha + (1 - \cos \alpha) n_2 n_3 & \cos \alpha + (1 - \cos \alpha) n_3^2 \end{pmatrix}$$

$$[U] = \begin{pmatrix} 1 & 0 & \cos \theta_2 \\ 0 & \cos \theta_1 & \sin \theta_1 \sin \theta_2 \\ 0 & -\sin \theta_1 & \cos \theta_1 \sin \theta_2 \end{pmatrix}$$